

2011

Synthesis and characterization of new conjugated materials based on benzobisazoles and their incorporation into electronic devices

Jared Franklin Mike
Iowa State University

Follow this and additional works at: <https://lib.dr.iastate.edu/etd>

 Part of the [Chemistry Commons](#)

Recommended Citation

Mike, Jared Franklin, "Synthesis and characterization of new conjugated materials based on benzobisazoles and their incorporation into electronic devices" (2011). *Graduate Theses and Dissertations*. 10394.
<https://lib.dr.iastate.edu/etd/10394>

This Dissertation is brought to you for free and open access by the Iowa State University Capstones, Theses and Dissertations at Iowa State University Digital Repository. It has been accepted for inclusion in Graduate Theses and Dissertations by an authorized administrator of Iowa State University Digital Repository. For more information, please contact digirep@iastate.edu.

**Synthesis and characterization of new conjugated materials based on benzobisazoles
and their incorporation into electronic devices**

by

Jared F. Mike

A dissertation submitted to the graduate faculty
in partial fulfillment of the requirements for the degree of
DOCTOR OF PHILOSOPHY

Major: Organic Chemistry

Program of Study Committee:
Malika Jeffries-EL, Major Professor
Aaron Sadow
Sumit Chaudhary
Yan Zhao
Mike Kessler

Iowa State University

Ames, Iowa

2011

TABLE OF CONTENTS

CHAPTER 1. General introduction.....	1
1.1 Dissertation Organization.....	1
1.2 Introduction to Organic Electronics	3
1.3 A Short Introduction to Benzobisoxazoles and Benzobisthiazoles.....	4
1.4 Characteristics Common to Organic Semiconductors.....	6
1.5 Conclusions.....	25
1.6 References.....	25
CHAPTER 2. An Efficient Synthesis of 2,6-Disubstituted Benzobisoxazoles: New Building Blocks for Organic Semiconductors.....	37
2.1 Abstract.....	37
2.2 Introduction.....	37
2.3 Experimental.....	39
2.4 Conclusions.....	44
2.5 Acknowledgement.....	44
2.6 References.....	44
2.7 Supporting information.....	46
CHAPTER 3. Facile Synthesis of 2,6-Disubstituted Benzobisthiazoles: Functional Monomers for the Design of Organic Semiconductors.....	71
3.1 Abstract.....	71
3.2 Introduction.....	71
3.3 Results and Discussion.....	72
3.4 Experimental Section.....	49
3.5 Discussion.....	76
3.6 Acknowledgement.....	78
3.7 References.....	78
3.8 Supporting information.....	79
CHAPTER 4. Synthesis and Characterization of Dialkoxy Substituted Poly(phenylenevinylene) Bezobisoxazoles.....	93
4.1 Abstract.....	93
4.2 Introduction.....	93
4.3 Experimental.....	95
4.4 Results and Discussion.....	98
4.5 Conclusions.....	103
4.6 Acknowledgements.....	103
4.7 References.....	103
4.8 Supporting information.....	106

CHAPTER 5. Synthesis, Characterization and Photovoltaic Properties of Poly(thiophenevinylene-alt-benzobisoxazole)s.....	111
5.1 Abstract.....	111
5.2 Introduction.....	112
5.3 Results and Discussion.....	113
5.4 Conclusions.....	123
5.5 Experimental Section.....	124
5.6 Acknowledgements.....	126
5.7 Notes and References.....	126
5.8 Supporting Information.....	131
CHAPTER 6. Efficient Synthesis of Benzobisazole Terpolymers Containing Thiophene and Fluorene.....	134
6.1 Abstract.....	134
6.2 Introduction.....	135
6.3 Results and Discussion.....	136
6.4 Conclusions.....	144
6.5 Experimental Section.....	145
6.6 Acknowledgement.....	149
6.7 Notes and References.....	150
6.8 Supporting Information.....	153
CHAPTER 7. The Synthesis of Benzobisazole Dithienoaryl polymers and their Photovoltaic Applications.....	174
7.1 Abstract.....	174
7.2 Introduction.....	174
7.3 Results and Discussion.....	177
7.4 Conclusions.....	185
7.5 Acknowledgement.....	185
7.6 Experimental.....	185
7.7 References.....	189
7.8 Supporting information.....	196
CHAPTER 8. General conclusions.....	218
8.1 Positional Functionalization.....	218
8.2 Synthesis of benzo[1,2- <i>d</i> ;5,4- <i>d'</i>] bithiazole.....	220
8.3 Small Molecules.....	221
8.4 Acknowledgements.....	223

CHAPTER 1

General Introduction

1.1 DISSERTATION ORGANIZATION

This thesis highlights work performed in the Jeffries-EL group concerning the synthesis of new materials for organic electronics. The focus will be on the enhanced synthesis of benzobisazoles, their subsequent incorporation into conjugated polymers for optoelectronic device fabrication. Chapter 1 is a general introduction that covers background information concerning organic semiconductors and their importance. Here are discussed details concerning structure-function relationships and device fabrication, with a specific focus on the inner workings of transistors, solar cells, and light emitting diodes.

Chapter 2 is a paper that was published in *Organic Letters* in 2008 that details the synthesis of two isomers of benzobisoxazole. The author of this dissertation performed the bulk of the synthetic work and elucidation of the final methodology reported in the paper as well a minor portion of the primary text and all of the supporting information. Drew Makowski synthesized the co-monomer for the polymer presented at the end of the work. Malika Jeffries-EL composed the bulk of the primary text.

Chapter 3 is a paper that was published in 2009 in *Journal of Organic Chemistry* concerning the synthesis of a variety of different benzobisthiazoles. The author performed most of the experimentation as well as drafting part of the SI and the experimental data. Jeremy Intemann synthesized the 1,4-diamino-2,5-benzenedithiol bishydrochloride used as a starting material. Malika Jeffries-EL drafted the final version of the text and SI.

Chapter 4 concerns the synthesis and analysis of benzobisoxazole polymers published in *Journal of Polymer Science: Part A: Polymer Chemistry* in 2010. The synthesis of phenylene containing benzobisoxazoles is covered along with their optoelectronic properties. The author of this dissertation performed the majority of

synthesis and analytical work along with compiling the supporting information. Drew Makowski synthesized the phenylene comonomers, and Tim Mauldin provided thermal decomposition and phase change data. Malika Jeffries-EL compiled the final manuscript.

Chapter 5 is a paper that was published in 2011 in *Physical Chemistry Chemical Physics* concerning the synthesis and function of poly(thiophenevinylene-*alt*-benzobisoxazole)s in organic solar cells. This chapter investigates the theoretical reasoning behind the quality of the synthesized polymer's performance in solar cells. The author of this dissertation carried out the polymer characterization and the majority of the synthesis work. Drew Makowski provided assistance in synthesis. Kanwar Nalwa and Daniel Putnam, working under the guidance of Sumit Chaudhary, fabricated photovoltaic devices out of the polymers. Aimee Tomlinson was responsible for theoretical calculations, and Malika Jeffries-EL compiled the manuscript.

Chapter 6 involves the synthesis of new single-bonded poly(benzobisazole)s. The author of this dissertation performed most of the synthetic and analytical work, wrote the supporting information, experimental information, and part of the final manuscript. Jeremy Intemann synthesized the fluorene comonomer. Min Cai and Teng Xiao, under the guidance of Drs. Joseph and Ruth Shinar produced and characterized the organic light emitting diodes from the polymers. Malika Jeffries-EL compiled and submitted the final draft of the paper.

The work in Chapter 7 involves further application of the benzobisoxazole and benzobisthiazole monomers synthesized in Chapter 6. This study explores the synthesis and photovoltaic device performance of six new donor/acceptor copolymers made from benzobisazole acceptor monomers and two donor comonomers. All of the synthetic work and analytical characterization of the polymers along was performed by the author. John Carr and Yuxing Chen, under the guidance of Sumit Chaudhary, fabricated organic solar cells from the polymers. Malika Jeffries-EL provided general conclusions and guidance.

Finally, Chapter 8 draws some general conclusions and discusses future synthesis and applications of benzobisazole containing conjugated organic molecules.

1.2 INTRODUCTION TO ORGANIC ELECTRONICS

Organic semiconductors (OSCs) have attracted much attention over the past few decades owing to their unique properties, which allow them to be included in a host of electronic device applications. There have been reports of conductivity in organic compounds as early as the 1950s.¹⁻⁴ However, the first major breakthroughs did not occur until the 1970s. In 2000, Alan J. Heeger, Alan G. McDiarmid and Hideki Shirakawa were awarded the Nobel Prize for their research of poly(acetylene) in the late 1970s, pioneering work in the field of organic electronics.^{5, 6} Since then, OSCs have been incorporated into any number of various electronic devices, including organic light-emitting diodes (OLEDs),^{7, 8} lasers,⁹ organic photovoltaics (OPVs),^{10, 11} non-linear optics (NLOs),¹² organic field effect transistors (OFETs),^{10, 13} batteries,^{14, 15} and sensors,^{16, 17} some of which have even been developed commercially.^{18, 19} Unfortunately, a major barrier to the introduction of organics into these areas has to do with inferior electrical properties as compared to traditional inorganic semiconductors. However, the goals of OSC technological development are not necessarily to exceed the performance of inorganics. Indeed, there is a great deal of promise in using combinations of the two.²⁰⁻²² OSCs offer new device functionalities (optical transparency, chemical response, lightweight) as well as a way to produce electronic materials at a lower cost.^{10, 23, 24}

Perhaps the most appealing part about using OSCs as opposed to traditional inorganic semiconductors comes from the synthetic diversity inherent in organic molecules. There are many different ways to alter the properties of OSCs through chemical synthesis, making them easily tunable to fit the needs of a device.^{25, 26} Additionally, most OSCs are cheaper to produce and process than inorganic semiconductors.²⁴ Whereas inorganics utilize vapor deposition under high vacuum and temperatures, many organics can be processed using “soft” techniques such as inkjet printing or spray coating allowing for large area and continuous application.^{27, 28} These advantages, coupled with a growing interest in OSCs as part of new technology drives research in the synthesis of new compounds and the study of their structure and function.

excellent mechanical properties, thermal stability, and oxidative stability, these materials exhibited interesting optical and electronic processes.⁴²⁻⁴⁵ The discovery of these polymers at this time led to them being among the first conjugated polymers to be well-studied.

It was discovered that PBO and PBZT, being very rigid and planar, both form liquid crystalline solutions leading to high ordering in the solid state.⁴⁶⁻⁴⁸ This excellent degree of order along with the electron deficient benzobisazole heterocycles gives these materials n-type conductivity in the solid state.⁴⁹⁻⁵¹ As such, they have been used as electron transport and emissive materials in OLEDs with promising results.⁵¹⁻⁵³ More recently, PBO was used as an absorber for OPVs.⁵⁴ Unfortunately, the polymer delivered very poor performance. Other derivatives where the phenylene has been replaced by a thiophene,⁵⁵⁻⁵⁷ vinylene,⁵⁸ or fluorene,⁵⁹ or others⁶⁰⁻⁶² have also been synthesized with mixed results.

The major issues with the utilization of benzobisazole rigid rod polymers come from their synthesis and processing conditions. These polymers require very hot temperatures (in excess of 200°C) in highly acidic media poly(phosphoric acid) in order to be synthesized and remain soluble after cooling.^{43, 63} Casting these polymers into films also requires dissolution in highly acidic media (conc. sulfuric acid, aluminum chloride in nitromethane).⁶³⁻⁶⁶ Once cast, it is then very difficult to remove trace acid, which leads to unintended doping. The presence of acidic impurities can hurt performance in organic electronic devices by interfering with charge and exciton transport. It should also be noted that these harsh conditions are not suitable for synthesizing polymers containing the benzo[1,2-*d*;4,5-*d'*] bisoxazole unit. The starting material for this isomer decomposes when subjected to the aforementioned conditions.

As benzobisazole polymers have been shown to be excellent materials in their own right, the major goal of the author's research was to devise methods to produce these polymers under milder conditions. In this way, new conjugated materials based on the three benzobisazoles in Figure 1.1 have been produced.⁶⁷⁻⁷¹ The use of mild conditions and incorporation of solubilizing alkyl chains opens the doors for this material as a useful synthon by vastly improving its usability and purity.

1.4 CHARACTERISTICS COMMON TO ORGANIC SEMICONDUCTORS

1.4.1 Basic structural characteristics.

From a chemical perspective, there are two primary structural aspects that give rise to the properties of OSCs, 1) a conjugated core or backbone and 2) various types solubilizing side chains. These two structural elements, controlled by chemical synthesis, have a substantial impact on the optoelectronic energy levels, nanoscale morphology, and bulk physical characteristics of these materials. The following section will serve to review the two common structural aspects and highlight their impact on the basic optoelectronic, solid-state and physical properties of OSCs. In this way, a basic understanding of the materials can be established before covering the more detailed aspects of their operating principles.

Some examples of common OSCs may be found in Figure 1.2. Note that there are two main structural types of organic semiconductors presented here – conjugated polymers (CPs), and small molecules. These are in addition to graphene and its related structures (*e.g.*, graphene, carbon nanotubes, pyrene), which are not shown. The chemical structures present in the figure represent only a small portion of the overall chemical diversity present in this class of materials. One of the advantages of OSCs is the near limitless capacity for synthetic design. There are many different ways to tune the properties of OSCs through chemical synthesis in order to fit the needs of a device. Since chemical structure is what ultimately determines a material's properties, it is possible to design materials with desirable properties through the study of structure-function relationships.

another result of these strong stacking interactions, macromolecular aromatic systems tend to be insoluble in most laboratory solvents, making them difficult to use and functionalize. All of the above properties can be tuned by changing the presence of functionality on and controlling the size and shape of a conjugated system.⁷²

Side Chains. The other primary structural characteristic prevalent in OSCs is the presence of side chains (represented as R groups in Figure 1.1). In the same way that conjugation serves primarily to give an OSC its semiconducting and optical characteristics, side chains primarily serve to modify the solid state morphology and physical properties of the conjugated system. In order to combat solubility issues, aromatic cores are synthesized to bear side chains of various lengths, functionalities, and levels of branching in order to break up π -stacking through steric bulk and favorable interactions with a solvent.⁷³⁻⁷⁵ It is even possible to synthesize side chains possessing an ionic group (e.g., sulfonate or ammonium functional groups) and an OSC can “self-dope.”⁷⁶ Nevertheless, solubility is still a common problem in the laboratory.

In addition to adding solubility, side chains reduce thermal transition temperatures; however, they have the same effect on thermal stability. Side chain diversity allows for materials to be soluble in different solvents, affecting their processability by altering how films form when they dry (drying time, solvent interactions).^{77, 78} In the solid state, the conjugated portions of OSCs tend to segregate from the alkyl portions, often giving rise to ordered solid state structures and liquid crystalline properties.^{79, 80} In blended films containing more than one material, immiscible side chains can be used to control phase segregation in the nanoscale morphology.^{81, 82} It is important to note that side chains can also negatively impact OSC performance. Particularly bulky side chains can push chains apart, reducing π -stacking and hence reducing electrical mobilities within the material.

All in all, the combination of these structural motifs - conjugation and side chains – affects an OSC on every level – molecular to nanoscale to bulk. By studying how molecular structure impacts the optoelectronic, morphological, and physical characteristics of OSCs, deductions can be made as to how new structures will function. In this way, material research is driven by the study of structure-function relationships

and the design of new materials and device architectures that better take advantage of the benefits of OSCs. Before moving on to device architectures, the following sections will cover the basic

1.4.2 Optoelectronic Properties

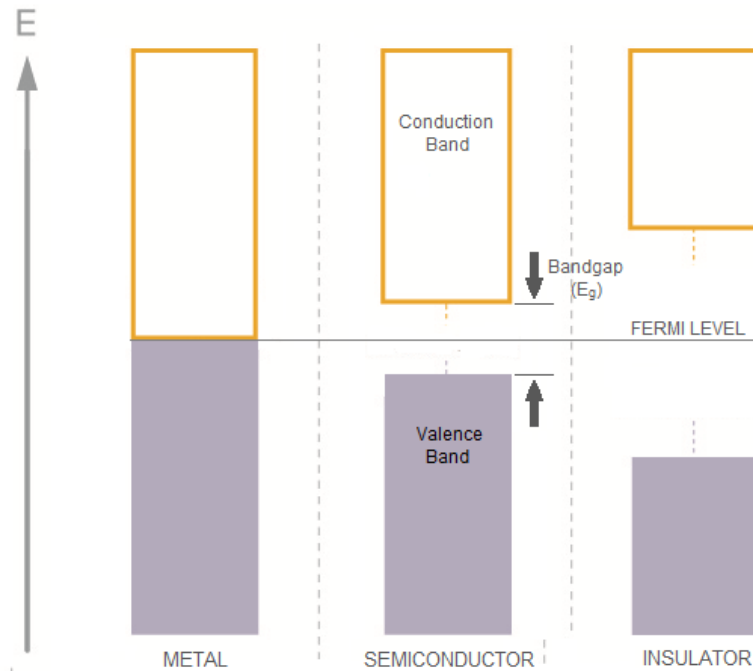


Figure 1.3. Band structure for different materials.

Semiconductors are in an intermediate state between an insulator and a metal (Figure 1.3). An insulator is a material with localized electronic structure and a prohibitively large bandgap, which is the difference between the lowest unoccupied molecular orbital (LUMO) and the highest occupied molecular orbital (HOMO). In other words, insulators have very stable structures and are relatively difficult to oxidize or reduce. Metals, on the other hand, have no bandgap, but rather possess partially filled bands. As such, electrons in metals are free to move about (completely delocalized) and are referred to as being a gas of electrons among a background of positive charge formed by atomic nuclei. Semiconductors are then materials possessing a narrow bandgap between the highest occupied states in the valence band and the lowest unoccupied states in the conduction band. These bands enable semiconductors to conduct electricity when charge carriers are

introduced either thermally, electrochemically, or optically.⁸³

Origin of Semiconducting Properties. As previously stated, conjugation is what gives rise to the semiconducting and absorptive/emissive properties of OSCs. CPs, in particular, have greatly extended conjugated systems owing to the large number of repeat units produced in their syntheses. Extended conjugation gives rise to two sets of energy levels corresponding to the conduction band and valence band of typical inorganic semiconductors.

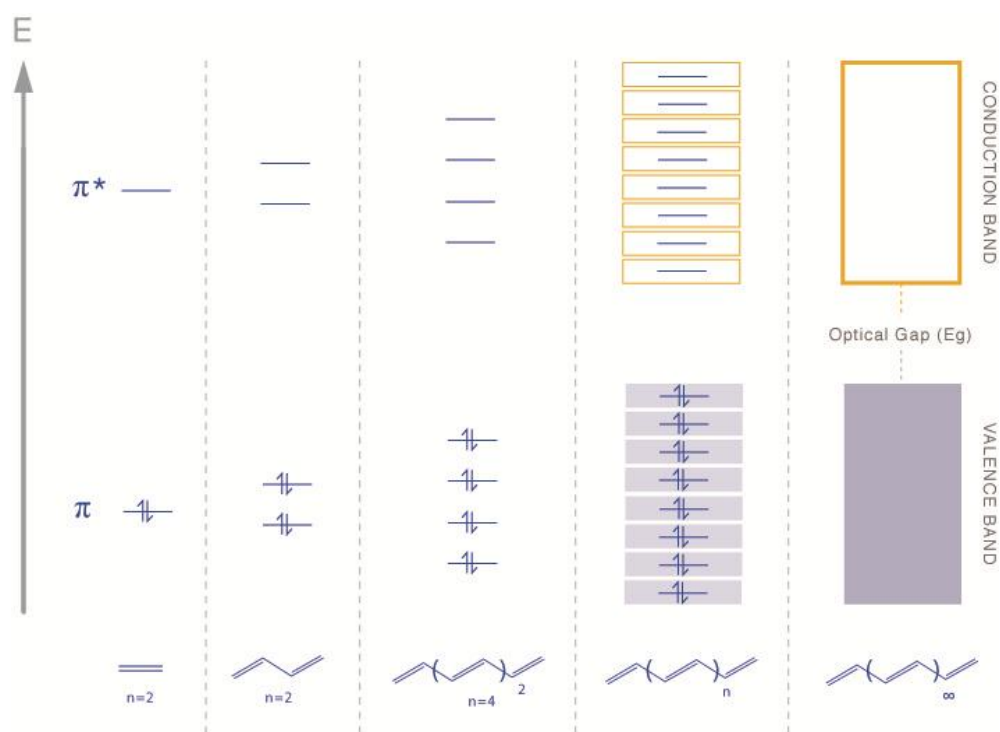


Figure 1.4. The origin of band structure in poly(acetylene).

Examining the case for poly(acetylene), starting with one ethene monomer unit (ethylene gas in this case), there are two energy levels as defined by the linear combination of the two atomic, unhybridized p -orbitals – the π -bond (HOMO) and the antibonding π^* -orbital (LUMO) (Figure 1.4). As more and more vinyl units are added to the chain, the number of orbitals involved in the π -system grows until, as a polymer, the orbital structure begins to resemble the analogous band structure of inorganic semiconductors.^{5, 84} For CPs, there are a set number of repeat units referred to as the

effective conjugation length that defines the point at which adding additional repeat units no longer affects the band structure of the material.⁸⁵⁻⁸⁷ The HOMO and LUMO correspond to the top of the valence band and bottom of the conduction band, respectively. Assuming a repeat unit of $(-CH-)_x$, these energy levels should converge to resemble the half-filled orbitals of metallic conductors, yet they do not. The energy is split due to Peierl's distortion, arising from the alternation of double and single bonds, and the repeat unit is better approximated as $(-CH=CH-)_x$.^{88, 89} The empty space in between those levels is referred to as the bandgap (1.5 eV for poly(acetylene)), with the Fermi level of the material sitting halfway between the two. Although there are similarities between the two, inorganic bands and organic "bands" do not conduct charge or interact with light in the same fashion.⁹⁰

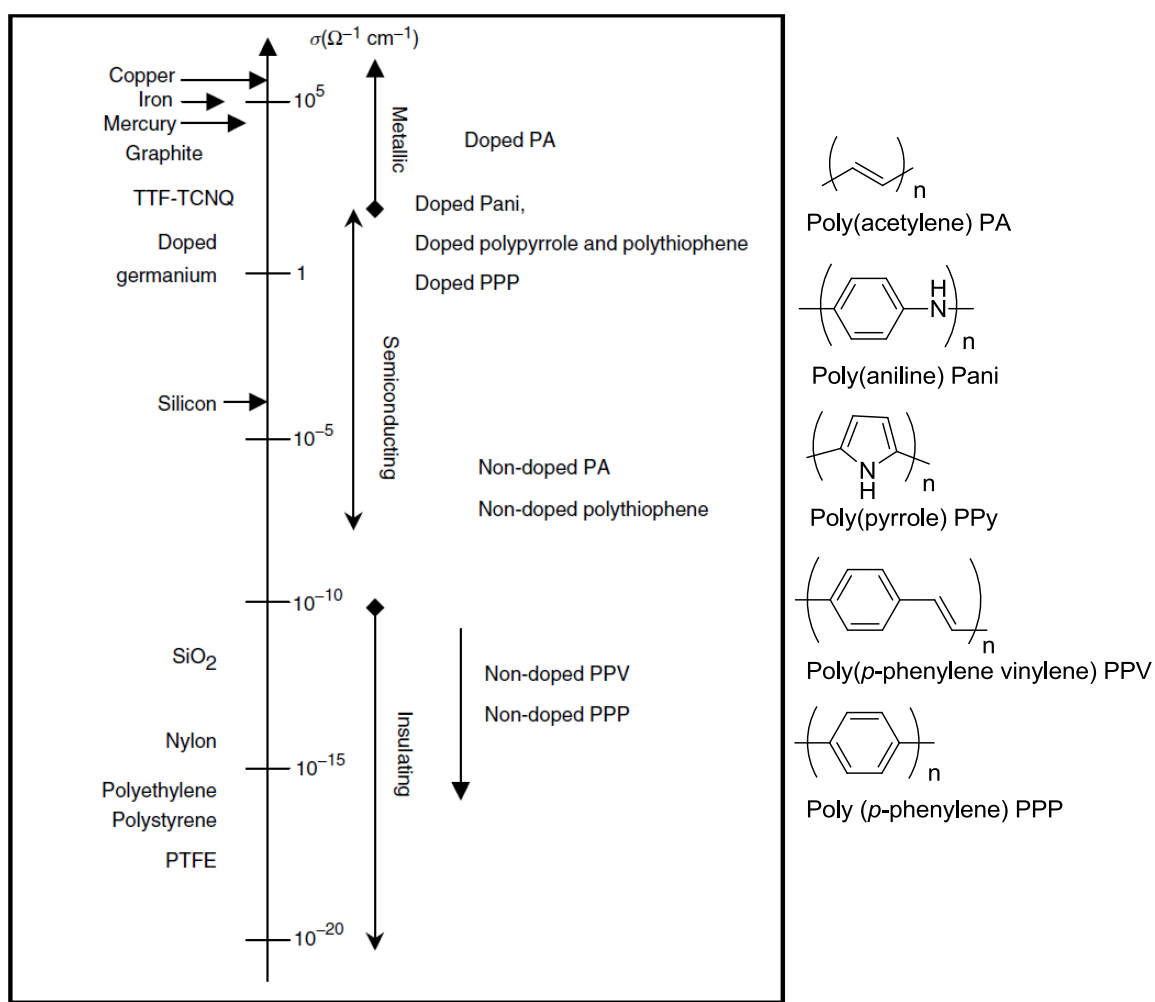


Figure 1.5. Conductivities of common materials.⁸⁴

In fact, semiconductors do not conduct in their native states, instead, free charge carriers must be introduced through doping. Doping in OSCs has led to conductivities approaching those of metals (Figure 1.5). Currently, the highest conductivity reported for an OSC is for stretch aligned chains of poly(acetylene) at approximately 80 kS/cm.⁹¹ Typical values for undoped CPs are much lower, ranging from about 10^{-9} to 10^{-4} S/cm.⁸⁴ Conductivity (σ) in CPs is defined by the relation:

$$\sigma = ne\mu_e + pe\mu_h$$

where n and p are the number of charge carriers (electrons or holes, respectively), e is the elementary charge in Coulombs, and μ_e and μ_h represent the mobilities of holes and electrons. The number of free charge carriers is affected by the doping density, while the mobility is affected by the mechanism of charge transport, the number and density of trap states, and the solid-state morphology.⁹²

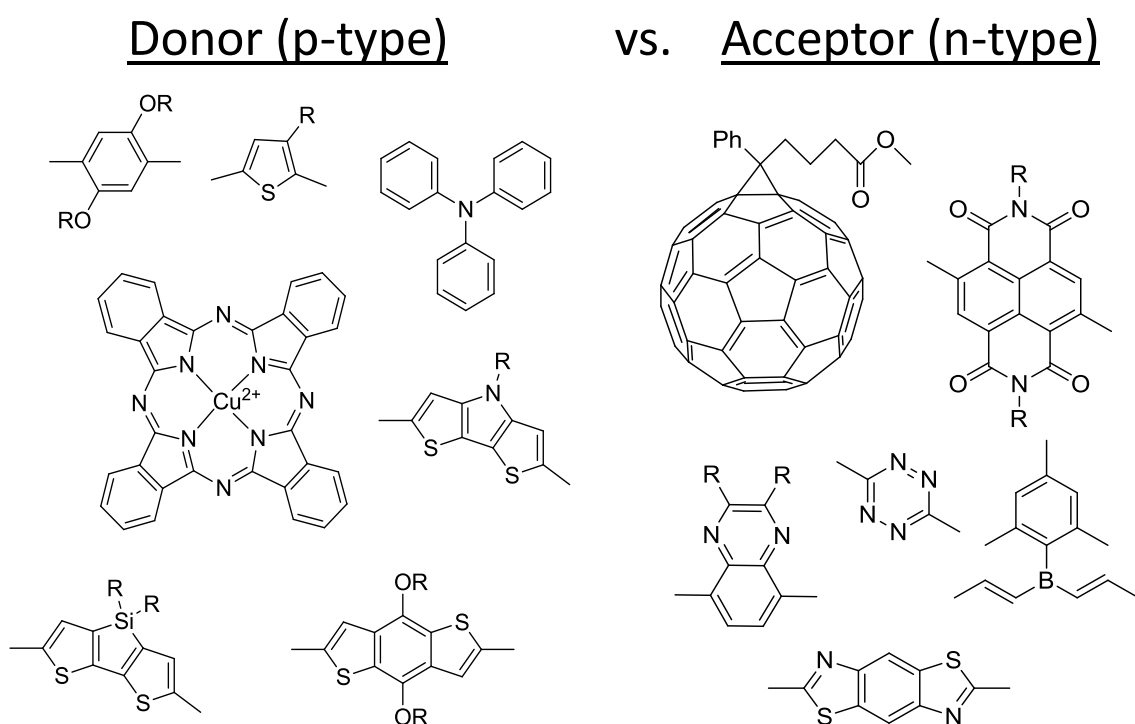


Figure 1.6. Examples of p-type and n-type conjugated systems. Many of these can commonly be found as monomer units in CPs.

There are two types of charge carriers in OSCs – electrons and holes. Determining whether a material is better at moving holes or electrons depends on how deep or shallow the HOMO and LUMO are. This is directly related to how well the organic structure is able to stabilize a cation or anion. Although there are no strict rules governing which material serves which function in a device, it is convenient to classify them into one of two categories – n-type and p-type – based upon whether it is better at conducting electrons or holes, respectively. In general, electron poor structures have lower LUMO values, while electron rich structures have higher HOMO values (Figure 1.6).^{26, 93} If the HOMO level is too high, it can impart oxidative instability on the material, especially in an oxygen rich atmosphere such as ours.

Dependent on the device, these properties can be tuned to suit the particular application for which they are designed.⁹⁴⁻⁹⁶ The HOMO and LUMO levels can be measured by voltammetric methods or through ultraviolet photoelectron spectroscopy. Knowing the positions of the energy levels allows for an understanding of how electrons will move in a system once it is pushed out of equilibrium into an excited state. The next section seeks to develop an understanding of how doping produces these excited states and how they relate to organic structure before describing how structure impacts charge transport and mobility.

Doping and Excited State Species. In silicon-based semiconductors, substitution is the primary method for doping wherein a Si atom in a crystal lattice is replaced with another element. This introduces new, allowed energy states within the band gap dependent on whether the dopant creates excess negative (n-type) or positive (p-type) charge carriers (electrons and holes, respectively).⁹⁷ For CPs, substitution doping does not result in new energy states due to bonding interactions; it merely results in the creation of new bands due to the linear combination of atomic orbitals. The incorporation of heteroatoms therefore serves to modify HOMO/LUMO values and solid-state structure (an incidentally useful property), but does not result in effective doping.⁷²

Instead of direct substitution, doping in CPs can be done electrochemically, either

through the incorporation of chemical oxidants (p-type) or reductants in the film (n-type), or through the application of an electrical potential. By measuring the potential required to oxidize or reduce a material, one can deduce the positions of the HOMO and LUMO levels, respectively, relative to vacuum.^{98, 99} Free charge carriers may also be introduced thermally (from excited states close to the conduction band edge, introduced in the next paragraph) and photochemically by exciting electrons into the conduction band directly through the absorption of photons. There are two factors to consider when doping – the appearance of new, excited electronic states within the bandgap region (which may or may not be occupied) and the physical reorganization of the structure through resonance to accommodate these new energy states.^{84, 100-102}

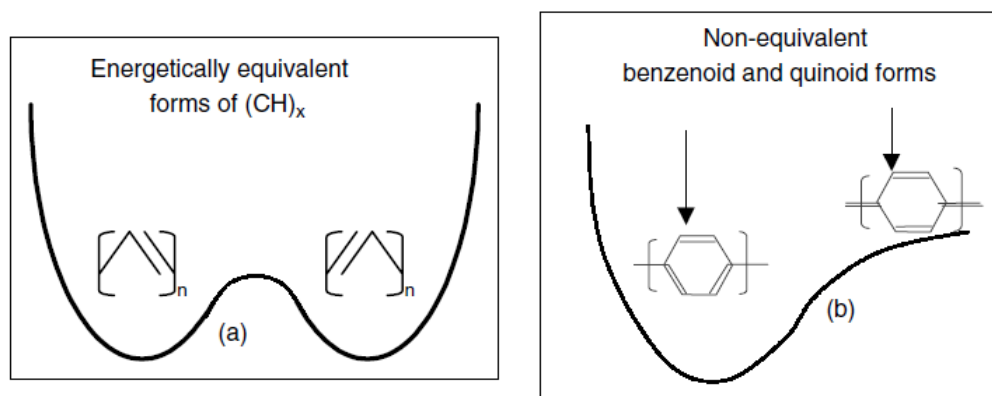


Figure 1.7. Degenerate states of poly(acetylene) (left) and non-degenerate states of poly(*p*-phenylene) (right).⁸⁴

The consequences of doping on the electronic structure depend on the degeneracy of the ground state. For poly(acetylene), there are two distinct resonance forms (A and B) of equal energy (Figure 1.7). An excited state, known as a soliton, serves as the boundary between the two degenerate phases.¹⁰⁰ Solitons are formed in soliton/antisoliton pairs which can annihilate upon recombination. Theoretical calculations have shown that the phase change from A to B is not abrupt, and instead the excited state is strongly coupled to the lattice and delocalized over approximately seven carbons.¹⁰³ Solitons can also be negatively or positively charged when they are formed.^{72, 101} These solitons result in the creation of a new subgap energy level (Figure 1.8). The occupancy of this new energy

level changes the position of the Fermi level and opens up new optically allowed transitions in the NIR range, altering the absorption spectrum of the CP.¹⁰⁴ It is also easier to thermally excite electrons when the doping density is high enough. Because of the degeneracy of the ground state and isolated nature of solitons, only one subgap energy level is created per soliton.⁷²

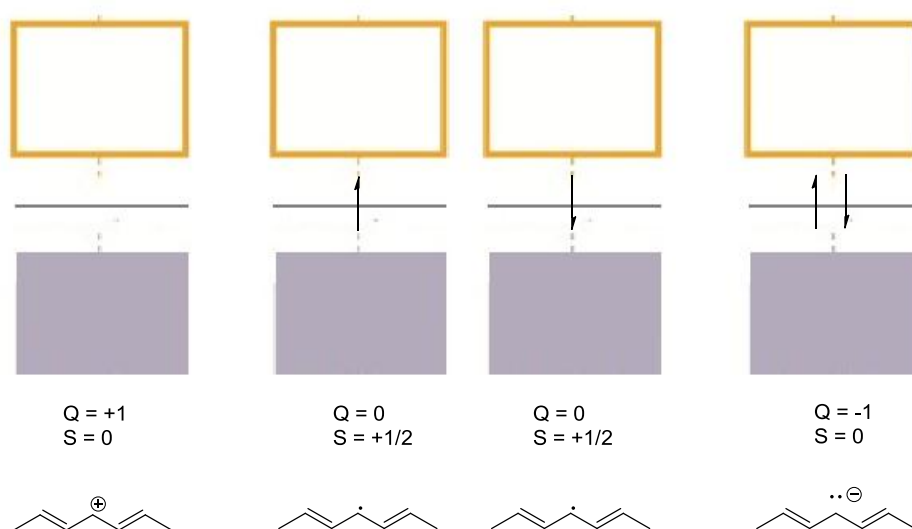


Figure 1.8. A positive soliton (left), neutral solitons (middle), and negative soliton (right) with corresponding charge and spin values.

However, it is the case that the great majority CPs do not have degenerate ground states. As an example, poly(*para*-phenylene) (Figure 1.7) possesses two resonance forms – benzenoid (low energy, aromatic) and quinoid (high energy, aromaticity is broken). Because of the non-degenerate ground state, isolated defect domains like solitons are energetically unfavorable as the quinoidal state is energetically unfavorable; a boundary between two degenerate states only exists in the close proximity of another defect. Instead of solitons, doping in CPs is described by polaron or bipolaron states.^{88, 100} Polarons are essentially radical cations (positive polarons) or radical anions (negative polaron) that are stabilized by resonance structure. Bipolarons are the same thing except that they consist of two positive charges (positive bipolaron) or two negative charges (negative bipolaron) closely bound. Polarons and bipolarons can be described as a

combination of two solitons (Figure 1.9). Said another way, a polaron is its own bound soliton/anti-soliton pair since the isolated soliton domains cannot exist.^{72, 89, 100, 105}

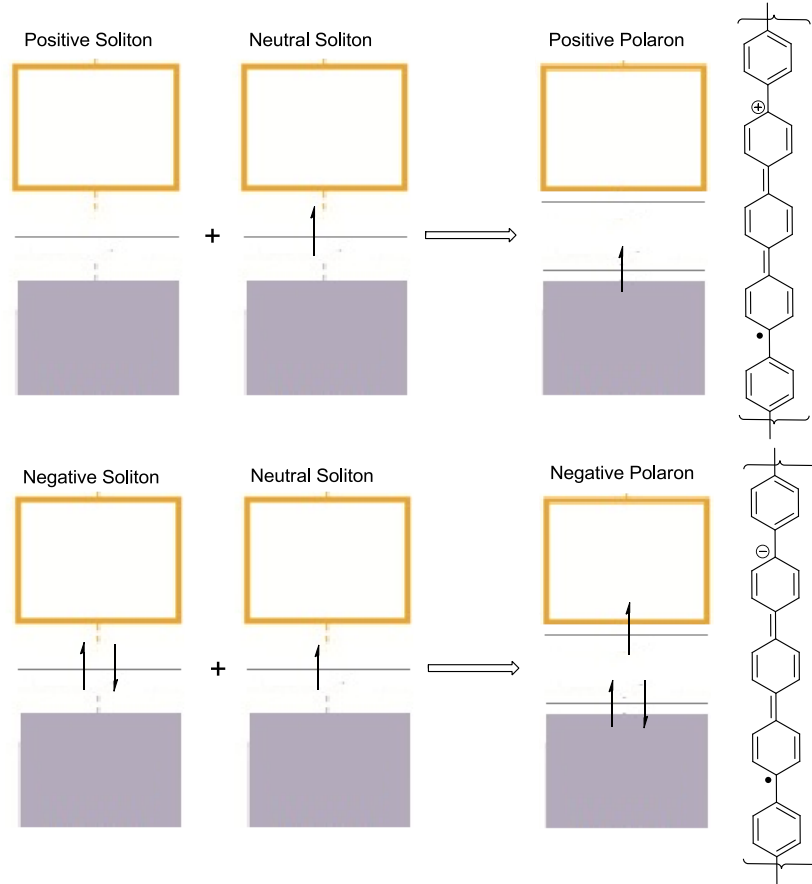


Figure 1.9. Depiction of a positive and negative polaron with the corresponding quinoidal structures to the right.

The formation of polarons and bipolarons results in the creation of two midgap states close to the band edges – one bonding, one anti-bonding.^{100, 106, 107} Theoretical studies have shown that polarons, like solitons, are delocalized and stabilized by resonance across several polymer repeat units. Just as in solitons, these new states open up new optical transitions, and, in heavily doped cases, the material begins to take on conductive properties. Unlike the case with solitons, however, the formation of two electronic states indicates that polarons are more coupled to structural alteration than solitons. In addition, the neutral excited state polaron is referred to as an exciton. A molecular exciton is a

stable excited state that is fundamentally different than just a neutral polaron.

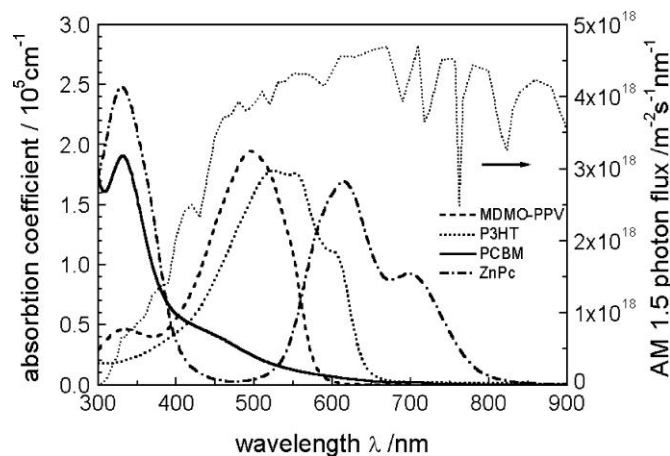


Figure 1.10. Depiction of the absorbances of some common conjugated materials in comparison to the solar spectrum. The amount of light absorbed is directly proportional to the amount of current generation in OPVs.¹⁰⁸

Conjugated materials tend to have very high extinction coefficients (on the order of $10^5 \text{ cm}\cdot\text{M}^{-1}$), and as a result, only thin films on the order of 100 nm are needed to absorb a large fraction of incident light (Figure 1.10).¹⁰⁸ When a photon with at least the energy of the bandgap is absorbed, it results in the formation of a bound electron-hole quasi-particle known as an exciton. Excitons may also be formed in organic molecules through polarized charge injection as occurs in OLEDs and through energy transfer processes (*e.g.*, Förster resonance energy transfer).^{102, 109} These neutral species are a fundamental aspect of semiconductors and central to the operation of both OLEDs and OPVs.

In inorganic semiconductors, weakly bound, Wannier excitons are formed that dissociate easily into free charge carriers in the presence of an applied field (Figure 1.11). This is because inorganic semiconductors are better at screening electric fields. Wannier excitons are not tightly bound, typically around 0.01 eV, and can be overcome by thermal energy at room temperature ($kT \sim 0.026 \text{ eV}$).^{92, 110} In organic molecules, however, Frenkel or molecular excitons are formed due to the relatively tight binding carbon exerts over its electrons. A molecular exciton's binding energy can be in excess of 0.5 eV, making them a relatively stable excited state.^{92, 111, 112}

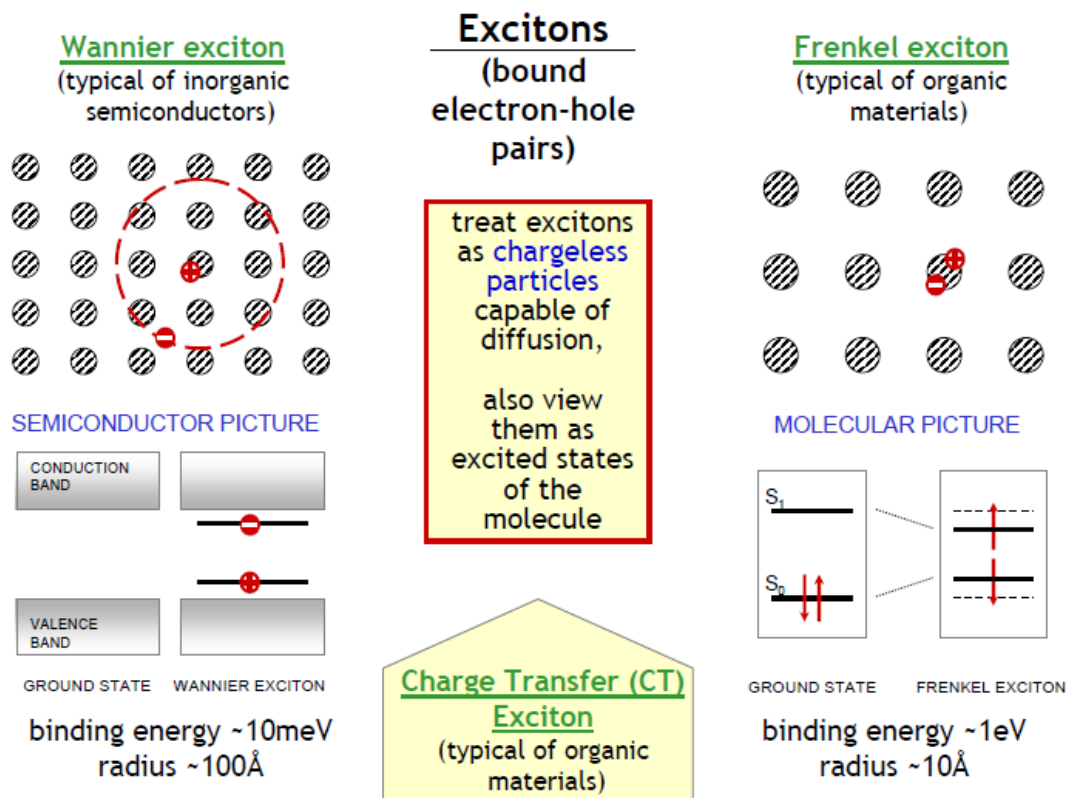


Figure 1.11. A diagram describing the differences and similarities of Wannier and Frenkel excitons.⁹²

The fate of an exciton depends on its local environment. Excitons are able to migrate along polymer chains, but as a neutral particle, they do not move under the influence of electric fields, but rather move under the effect of decreasing gap energy states. Unfortunately, little is actually known about exciton migration in CPs. Typical exciton diffusion lengths are on the order of 10 nm for most CPs in the solid state. Excitons in solution phase polymers have better exciton transport than in the solid state.¹¹³ When an exciton comes into close proximity (sub-nanometer to nanometer) of a change in energy levels, there is a chance for charge or energy transfer.^{102, 114} Without the influence of a separating potential, excitons can become trapped and will decay either thermally (non-radiatively) or via luminescence. Exciton quenching by thermal degradation is generally something to be avoided in devices. The fraction of luminescence or charge transfer events that occur per excitation event are referred to by their quantum efficiencies. High

luminescence quantum efficiencies in the solid state are desirable for the production of OLEDs,¹¹⁵ whereas the opposite is true of OPVs. In OPVs higher quantum efficiencies associated with exciton migration and dissociation are desired.¹¹⁶

The structurally coupled nature of excited states essentially determines how charge and energy is transported in CPs. The appearance of new subgap energy states and consequential altering of the Fermi level of the material are important considerations when designing devices.^{105, 106} Although there is still debate as to the exact nature of the excited states of CPs, especially excitons, what is important to consider from the perspective of a synthetic chemist is how basic polaronic band structure is involved in charge transport mechanisms and how changing the chemical structure affects these charge transfer mechanisms and hence the mobility of charges and energy.

1.4.3 Morphology and Mobility

Charge Transport and Mobility. Charge transport in OSCs, in general, is determined by a charge hopping mechanism. Charge hopping is an alternative transport mechanism to band transport. Instead of a very large charge delocalization that would allow the charge to move to another location through a band, many of the charges in CPs must “hop” from one chain to the next.¹¹⁷ Charge hopping is indicated by relatively low mobilities. Once polarons are formed, they travel according to the direction of the electric field (bulk and local) until they meet a defect or trap. Charge hopping occurs because CPs are packed chains of organic molecules, covalently bound in only one dimension, of finite length, and separated from one another by insulating side chains and empty space. Therefore, the direction of travel and the 3-dimensional arrangements of chains play important roles in transport. Traps and defects can be chemical dopants, impurities, kinks in the polymer chain, chain termination (or end group), or can even be an inherent part of the polymer (*i.e.*, the organic electronic structure is not conducive to charge transport). Additionally, the polaronic nature of charges means that stabilization of the quinoidal form through resonance structure is important to maintaining delocalization and good mobility.

Mobility can be variable by several orders of magnitude depending on whether charges are traveling parallel or perpendicular to the substrate (depending on the direction

of the field).¹¹⁸ Charges moving parallel to the substrate tend to move along polymer chains, whereas charges moving perpendicular must continually hop to new chains. CP chains can also be oriented face on with the surface or edge on, although this is possible to control to a degree by using surface treatments.^{119, 120} The packing at the surface sets up nucleation and therefore the packing for the rest of the thin film (a great majority of studies and devices focus on films ~50-100 nm in thickness). As a result of this anisotropic charge transport, it is important to make mobility comparisons using methods of measurement that match with the direction of charge transport in a device. For example, organic solar cells or light emitting diodes are constructed with a sandwich type structure where the charges move orthogonal to the surface, whereas in a transistor, they move parallel (Figure 1.12). It is just as important to use a method of mobility measurement that best mimics the direction of charge travel in a device for which the CP is being considered. Even so, correlations between mobility and device performance (especially in blend devices) are not always clear as this area of research is still developing.

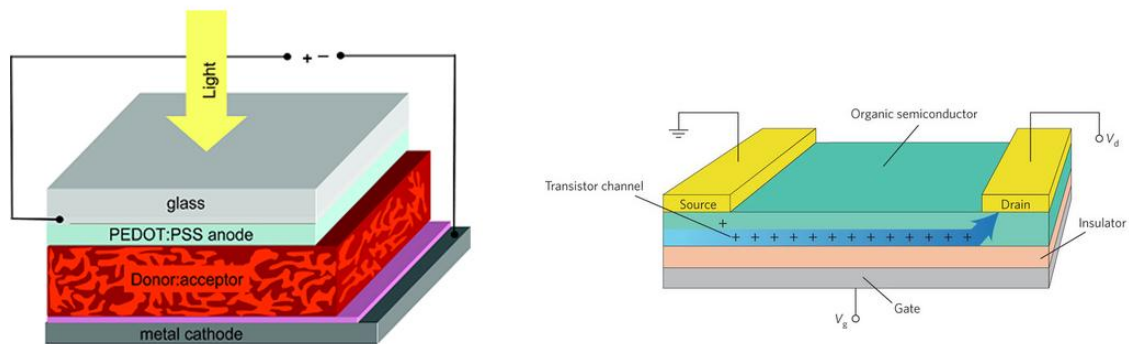


Figure 1.12. Examples of devices where the charge moves perpendicular to the surface (left, organic solar cell) or parallel (right, field effect transistor).

One of the major factors influencing charge transport is solid-state packing. Closer co-facial distances in adjacent CP chains allow for greater π -orbital overlap. The increased wavefunction mixing is similar to what is seen in the formation of stable

excimers.^{72, 90, 121} The mixing creates new subgap energy states that allow sharing of the polaron, leading to increased mobility. Good indicators of ordered packing of CPs in thin films are red-shifted absorption and fluorescence spectra as compared to those in solution. This can be seen when bulky branched side chains are used to impart better solubility but have the effect of decreasing mobility due to packing disruption. It is also why highly organized molecular crystals like pentacene or copper phthalocyanine have some of the highest mobilities of OSCs.^{122, 123}

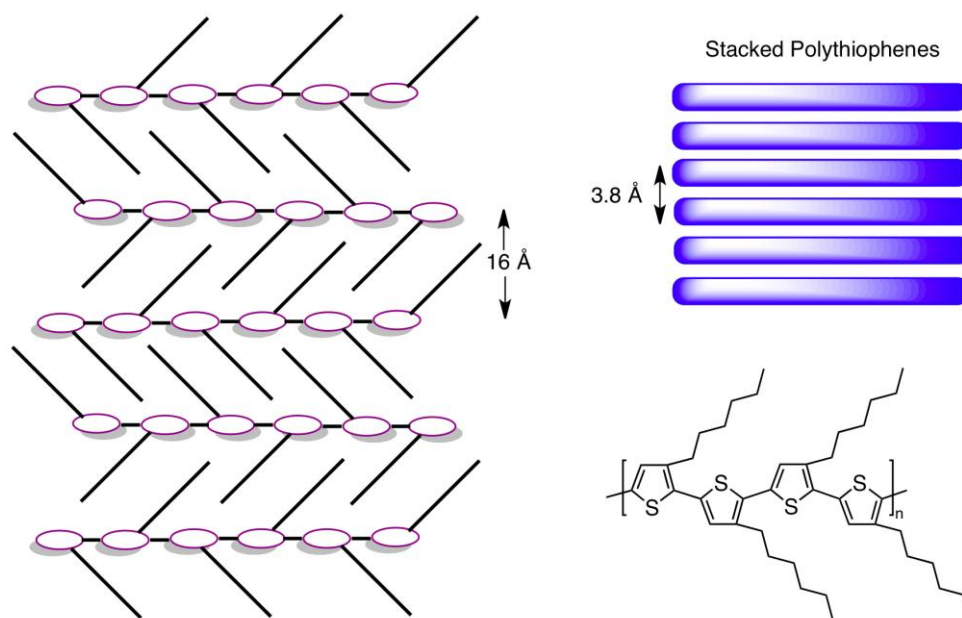


Figure 1.13. An illustration of the nature of regioregular packing found in poly(3-hexylthiophene) films.

In general, highly ordered, more crystalline systems tend to have the best charge transport, and researchers design systems to exploit this. Perhaps the largest impact on structural morphology is the organization of side chains in the solid state; however, this is mostly dependent on specific systems.^{124, 125} Regioregularity is ordered solid-state structuring wherein adjacent monomer units are all oriented in the same direction (Figure 1.13). When polymers can adopt a regioregular conformation, it results in better packing as well as helping to prevent twists in the polymer chain.¹²⁶⁻¹³² Twists in the polymer chain break up conjugation by decreasing the π -overlap of adjacent monomer repeat units. This results in a defect and a widening of the bandgap, affecting both optical

absorption and charge mobility.¹³³⁻¹³⁵ Even if polymers are not regioregular, designing them in order to minimize steric interaction between adjacent repeat units ensures better charge transfer characteristics.¹³⁶⁻¹³⁸ One way to do this is to lock rings together to form ladder-type structures or multicyclic ring systems (e.g. benzobisoxazole⁵¹, dithienosilole,¹³⁹⁻¹⁴¹ dithienopyrrole¹³⁷), preventing twisting of adjacent repeat units, although this can be difficult to do with CPs, there are some examples in the literature, nonetheless.¹⁴²⁻¹⁴⁴ Additionally, higher molecular weight polymer chains are desirable as they offer longer paths for charges to take.^{129, 137, 145-147} Interestingly, longer chains do not pack as well into highly ordered domains with well-defined phase boundaries, but this also means that charges are less likely to be trapped at the phase boundaries and are able to better migrate in the bulk of the material.¹²⁹

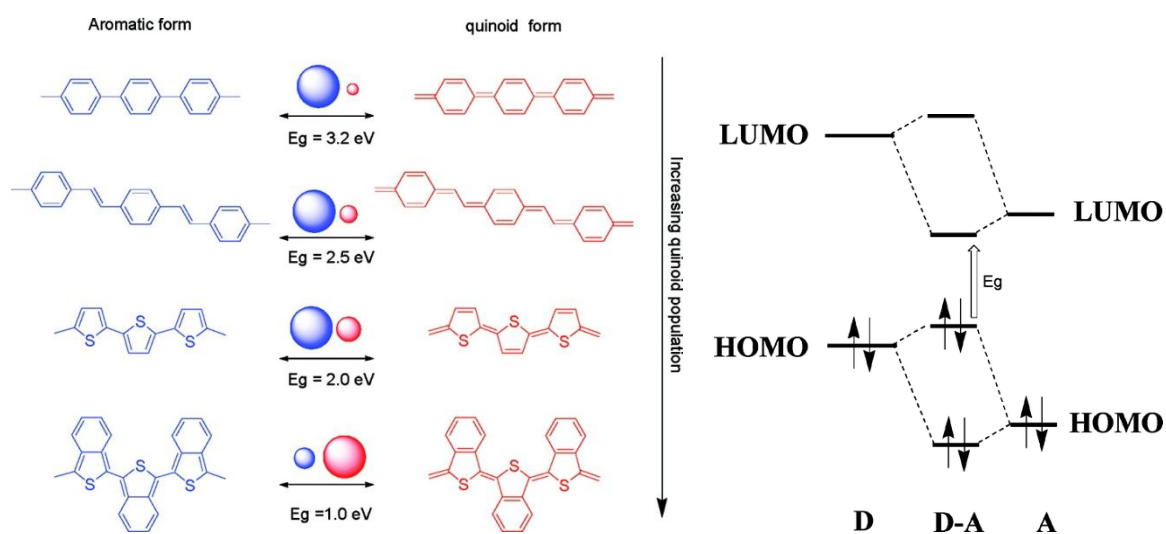


Figure 1.14. The stabilization of the quinoidal structure leads to lower bandgaps. This can be done through aromatization effects(left) or through the use of alternating DA units (right).²⁶

Inherent barriers to structural reorganization once charge is injected can impact the mobility.¹⁰² Resonance stabilization of the quinoidal structure to minimize reorganization energy is then a desired characteristic. The adoption of the quinoidal form results in breaking of aromaticity, but also an increase in the double bond nature of bonds that were originally single bonds and vice versa. Therefore, stabilization of the quinoidal structure

results in increased stiffness of the polymer chain, exhibiting similar utility to ladder structure (Figure 1.14).^{26, 148} The naphthothiophenes in the figure possess *ortho*-quinoidal benzene units that aromatize when excited. Depending on whether the charge carrier is a hole or electron, resonance stabilization can also be had through cation (alkoxy, amino, silyl) or anion (carbonyl, imino, nitro) stabilizing functionality, respectively. The use of functional groups in turn tunes the respective HOMO and LUMO levels.¹⁴⁹⁻¹⁵² Stabilization of the quinoidal form can also be accomplished through alternating donor-acceptor (DA) architecture. It is often the case for these types of systems that the HOMO resides on the donor portion of the molecule whereas the LUMO resides primarily on the acceptor portion.¹²⁴ Although the quinoidal form is stabilized for DA systems, they can have unprecedented effects of the mobility of electrons or holes, increasing the mobility of one, while decreasing the mobility of the other.¹⁵¹⁻¹⁵³ Incidentally, it should also be noted that stabilization of the quinoidal form also results in a decreased bandgap by both lowering the LUMO as well as increasing the HOMO, exhibiting an increasing tendency to stabilize both holes and electrons.^{106, 148}

Besides the impact of the chemical structure, the process of casting and forming a solid state film can greatly impact the morphology. Various mixtures of solvents and additives can drastically affect device performances, as can ratios of components in blend systems.^{154, 155} After a film is cast, annealing techniques can be used. Annealing involves heating polymer chains past their glass transition temperatures and allowing them to restructure themselves upon cooling.¹⁵⁶ Solvent annealing may also be used where a film (possibly heated) is exposed to solvent to partially redissolve the chains and allow them to restructure themselves.¹⁵⁷ In addition, other materials (*e.g.*, other CPs, TiO₂, fullerene) can also have an impact on the nanoscale morphology. Templating and nanolithography (using lasers or stamps, for example) can also be used in order to grant some type of structural order to a system.^{14, 158}

Doping, on the other hand, can increase disorder in the system.¹⁵⁹ Although conductivity may be increased through the introduction of more charge carriers, the reordering of the system around the dopants can decrease the prevalence of ordered solid-state structures that improve the mobility.^{160, 161} More trap states and deeper trap states

reduce mobility. Impurities produced during chemical synthesis can act as dopants, and should be removed before analyzing or using the material.^{162, 163} Usually, soxhlet purification is able to remove these impurities. Although not technically a chemical dopant or impurity, the end groups on CPs can act as trap sites.¹⁶⁴ For example, polymers made using Suzuki or Stille couplings can terminate with boronic esters or trialkylstannanes, respectively, which can act as impurities of sorts, distorting the potential at the end of the polymer chain. Fortunately, end-capping the polymer at the final stages of polymerization can be done by reaction with aryl halides (I, Br) followed by an aryl boronic acid.^{165, 166}

When considering device applications, controlling morphology is crucial to making high-efficiency devices. The function of morphology is to set up the chemicals (donor/acceptor, organic/inorganic) in such a way that desirable absorption, charge transfer and/or energy transfer events take place with as high efficiency as possible. Understanding what gives a material good mobility allows better molecular design. Although mobility is generally desirable, there are, however, other factors that must be taken into account before a good material is discovered. For example, it has been shown that branched side chains can actually increase the open circuit voltage (V_{oc}) for OPVs, boosting power conversion efficiency.¹⁶⁷ This illustrates the fact that there must also be balance among desirable properties in order to achieve optimal device characteristics.

1.5 CONCLUSIONS

Taking the above factors into consideration, there are four main determinants as to how well an OSC will perform in a device:

- Stability
 - Oxidative
 - Thermal
- Properly aligned energy levels
 - With other components
 - To give absorption or luminescence
- Good thin film morphological characteristics
 - OPV vs. OLED
 - Able to carry charge effectively
- Purity and Defects
 - End groups
 - Dopants

In summary, CPs, in general, form polaronic states when excited, either through chemical doping, optical excitation, or charge/energy transfer processes. This causes the appearance of subgap electronic states and the reorganization of the chemical bonding to incorporate the new states. The relative energies of excited states affects the position of the Fermi level. The Fermi level of the semiconductor is related to the way a material functions (*i.e.*, electron transport or hole transport) in an optoelectronic application when combined with other materials to make a device. Ultimately, the chemical structure of the material is what determines the optoelectronic properties – the solid-state structure, the values of the energy levels and the band structure before and after doping.

1.6 REFERENCES

(1) Naarmann, H. *Polymers, Electrically Conducting*, in *Ullmann's Encyclopedia of Industrial Chemistry*; Wiley-VCH Verlag GmbH & Co. KGaA: 2000.

- (2) McNeill, R.; Weiss, D.; Willis, D. *Australian Journal of Chemistry*, **1965**, 18(4), 477-486.
- (3) Bolto, B.; Weiss, D.; Willis, D. *Australian Journal of Chemistry*, **1965**, 18(4), 487-491.
- (4) Akamatu, H.; Inokuchi, H.; Matsunaga, Y. *Nature*, **1954**, 173(4395), 168-169.
- (5) Shirakawa, H.; Louis, E.J.; MacDiarmid, A.G.; Chiang, C.K.; Heeger, A.J. *J. Chem. Soc., Chem. Commun.*, **1977**, 16, 578-580.
- (6) Heeger, A.J. *Angewandte Chemie International Edition*, **2001**, 40(14), 2591-2611.
- (7) Grimsdale, A.C.; Leok Chan, K.; Martin, R.E.; Jokisz, P.G.; Holmes, A.B. *Chemical Reviews*, **2009**, 109(3), 897-1091.
- (8) Friend, R.H.; Gymer, R.W.; Holmes, A.B.; Burroughes, J.H.; Marks, R.N.; Taliani, C.; Bradley, D.D.C.; Santos, D.A.D.; Bredas, J.L.; Logdlund, M.; Salaneck, W.R. *Nature*, **1999**, 397(6715), 121-128.
- (9) Kozlov, V.G.; Parthasarathy, G.; Burrows, P.E.; Khalfin, V.B.; Wang, J.; Chou, S.Y.; Forrest, S.R. *Quantum Electronics, IEEE Journal of*, **2000**, 36(1), 18-26.
- (10) Facchetti, A. *Chemistry of Materials*, **2010**, 23(3), 733-758.
- (11) Kietzke, T. *Advances in OptoElectronics*, **2007**, Article ID 40285(15 pages).
- (12) Cho, M.J.; Choi, D.H.; Sullivan, P.A.; Akelaitis, A.J.P.; Dalton, L.R. *Progress in Polymer Science*, **2008**, 33(11), 1013-1058.
- (13) Dimitrakopoulos, C.D.; Mascaro, D.J. *IBM Journal of Research and Development*, **2001**, 45(1), 11-27.
- (14) Pan, L.; Qiu, H.; Dou, C.; Li, Y.; Pu, L.; Xu, J.; Shi, Y. *International Journal of Molecular Sciences*, **2010**, 11(7), 2636-2657.
- (15) Meyer, W.H. *Advanced Materials*, **1998**, 10(6), 439-448.
- (16) Crone, B.; Dodabalapur, A.; Gelperin, A.; Torsi, L.; Katz, H.E.; Lovinger, A.J.; Bao, Z. *Applied Physics Letters*, **2001**, 78(15), 2229-2231.
- (17) Someya, T.; Kato, Y.; Sekitani, T.; Iba, S.; Noguchi, Y.; Murase, Y.; Kawaguchi, H.; Sakurai, T. *Proceedings of the National Academy of Sciences of the*

United States of America, **2005**, 102(35), 12321-12325.

- (18) Loo, Y.-L.; McCulloch, I. *MRS Bulletin*, **2008**, 33(7), 653-705.
- (19) Bernius, M.T.; Inbasekaran, M.; O'Brien, J.; Wu, W. *Advanced Materials*, **2000**, 12(23), 1737-1750.
- (20) Heliotis, G.; Itskos, G.; Murray, R.; Dawson, M.D.; Watson, I.M.; Bradley, D.D.C. *Advanced Materials*, **2006**, 18(3), 334-338.
- (21) Hagfeldt, A.; Boschloo, G.; Sun, L.; Kloo, L.; Pettersson, H. *Chemical Reviews*, **2010**, 110(11), 6595-6663.
- (22) Kagan, C.R.; Mitzi, D.B.; Dimitrakopoulos, C.D. *Science*, **1999**, 286(5441), 945-947.
- (23) Kelley, T.W.; Baude, P.F.; Gerlach, C.; Ender, D.E.; Muiyres, D.; Haase, M.A.; Vogel, D.E.; Theiss, S.D. *Chemistry of Materials*, **2004**, 16(23), 4413-4422.
- (24) Forrest, S.R. *Nature*, **2004**, 428(6986), 911-918.
- (25) Kim, Y.-G.; Thompson, B.C.; Ananthkrishnan, N.; Padmanaban, G.; Ramakrishnan, S.; Reynolds, J.R. *Journal of Materials Research*, **2005**, 20(12), 3188-3198.
- (26) Cheng, Y.-J.; Yang, S.-H.; Hsu, C.-S. *Chemical Reviews*, **2009**, 109(11), 5868-5923.
- (27) Tsutsui, T.; Fujita, K. *Advanced Materials*, **2002**, 14(13-14), 949-952.
- (28) Krebs, F.C. *Sol. Energ. Mat. Sol. Cells*, **2009**, 93(4), 394-412.
- (29) Osman, A.M.; Khalil, Z.H.; Youssef, M.S.K. *Indian J. Chem., Sect. B FIELD Full Journal Title: Indian Journal of Chemistry, Section B: Organic Chemistry Including Medicinal Chemistry*, **1978**, 16B(10), 865-8.
- (30) Osman, A.M.; Khalil, Z.H. *J. Appl. Chem. Biotechnol. FIELD Full Journal Title: Journal of Applied Chemistry & Biotechnology*, **1975**, 25(9), 683-93.
- (31) Osman, A.M.; Mohamed, S.A. *Indian Journal of Chemistry*, **1973**, 11(9), 868-870.
- (32) Osman, A.M.; Mohamed, S.A. *United Arab Republic Journal of Chemistry*, **1971**, 14(5), 475-492.
- (33) Lozinskii, M.; Il'chenko, A. *Chemistry of Heterocyclic Compounds*, **2009**,

45(4), 376-399.

(34) Hegedus, L.S.; Odle, R.R.; Winton, P.M.; Weider, P.R. *Journal of Organic Chemistry*, **1982**, 47(13), 2607-13.

(35) Ishikawa, H.; Chen, Q.; Bin, Y.; Komatsu, K.; Matsuo, M. *J. Mater. Sci. FIELD Full Journal Title:Journal of Materials Science*, **2007**, 42(18), 7772-7779.

(36) Hunsaker, M.E.; Price, G.E.; Bai, S.J. *Polymer*, **1992**, 33(10), 2128-35.

(37) Wolfe, J.F. *Polym. Mater. Sci. Eng. FIELD Full Journal Title:Polymeric Materials Science and Engineering*, **1986**, 54, 99-101.

(38) Wolfe, J.F.; Arnold, F.E. *Macromolecules*, **1981**, 14, 909-915.

(39) Welsh, W.J.; Bhaumik, D.; Mark, J.E. *Macromolecules FIELD Full Journal Title:Macromolecules*, **1981**, 14(4), 947-50.

(40) Evers, R.C.; Arnold, F.E.; Helmeniak, T.E. *Macromolecules*, **1981**, 14, 925-930.

(41) Choe, E.W.; Kim, S.N. *Macromolecules*, **1981**, 14, 920-924.

(42) Wolfe, J.F. *Proceedings of SPIE-The International Society for Optical Engineering*, **1987**, 682(Mol. Polym. Optoelectron. Mater.: Fundam. Appl.), 70-76.

(43) Wolfe, J.F. *Polymeric Materials Science and Engineering*, **1986**, 54, 99-101.

(44) Bhaumik, D.; Mark, J.E. *Journal of Polymer Science, Polymer Physics Edition*, **1983**, 21(7), 1111-8.

(45) Osaheni, J.A.; Jenekhe, S.A. *Chemistry of Materials*, **1992**, 4(6), 1282-1290.

(46) Dobrolyubova, E.I.; Drushlyak, A.G.; Ivashchenko, A.V. *Mol. Cryst. Liq. Cryst. FIELD Full Journal Title:Molecular Crystals and Liquid Crystals*, **1990**, 191, 219-21.

(47) Tsai, T.T.; Arnold, F.E. *Polymer Preprints (American Chemical Society, Division of Polymer Chemistry)*, **1986**, 27(2), 221-2.

(48) Evers, R.C.; Dotrong, M. *Materials Research Society Symposium Proceedings*, **1989**, 134(Mater. Sci. Eng. Rigid-Rod Polym.), 141-152.

(49) Jenekhe, S.A.; de Paor, L.R.; Chen, X.L.; Tarkka, R.M. *Chemistry of Materials*, **1996**, 8(10), 2401-2404.

(50) Babel, A.; Jenekhe, S.A. *Journal of Physical Chemistry B*, **2002**, 106(24),

6129-6132.

- (51) Alam, M.M.; Jenekhe, S.A. *Chemistry of Materials*, **2002**, *14*(11), 4775-4780.
- (52) Huang, J.-W.; Bai, S.J. *Nanotechnology*, **2005**, *16*(8), 1406-1410.
- (53) Zhang, X.; Jenekhe, S.A. *Macromolecules*, **2000**, *33*(6), 2069-2082.
- (54) Huang, J.-W.; Bai, S.J. *Journal of Polymer Science, Part B: Polymer Physics*, **2007**, *45*(8), 988-993.
- (55) Chen, Y.; Wang, S.; Zhuang, Q.; Li, X.; Wu, P.; Han, Z. *Macromolecules*, **2005**, *38*(23), 9873-9877.
- (56) Promislow, J.H.; Preston, J.; Samulski, E.T. *Macromolecules*, **1993**, *26*(7), 1793-5.
- (57) Kang, J.-G.; Cho, H.-G.; Kang, S.K.; Park, C.; Lee, S.W.; Park, G.B.; Lee, J.S.; Kim, I.T. *J. Photochem. Photobiol., A FIELD Full Journal Title:Journal of Photochemistry and Photobiology, A: Chemistry*, **2006**, *183*(1-2), 212-217.
- (58) Wang, S.; Lei, H.; Guo, P.; Wu, P.; Han, Z. *European Polymer Journal*, **2004**, *40*(6), 1163-1167.
- (59) Liu, X.; Xu, X.; Zhuang, Q.; Han, Z. *Polymer Bulletin* **2008**, *60*(6), 765-774.
- (60) Tan, L.-S.; Srinivasan, K.R.; Bai, S.J. *Journal of Polymer Science, Part A: Polymer Chemistry*, **1997**, *35*, 1909-1924.
- (61) Joseph, W.D.; Mercier, R.; Prasad, A.; Marand, M.; McGrath, J.E. *Polymer*, **1993**, *35*, 866-869.
- (62) Yu, S.C.; Gong, X.; Chan, W.K. *Macromolecules*, **1998**, *31*(17), 5639-5646.
- (63) Hu, X.-D.; Jenkins, S.E.; Min, B.G.; Polk, M.B.; Kumar, S. *Macromolecular Materials and Engineering*, **2003**, *288*(11), 823-843.
- (64) Tashiro, K.; Yoshino, J.; Kitagawa, T.; Murase, H.; Yabuki, K. *Macromolecules*, **1998**, *31*(16), 5430-5440.
- (65) Roitman, D.B.; Wessling, R.A.; McAlister, J. *Macromolecules*, **1993**, *26*, 5174-5184.
- (66) Jenekhe, S.A.; Johnson, P.O.; Agarwal, A.K. *Macromolecules*, **1989**, *22*, 3216-3222.

- (67) Mike, J.F.; Nalwa, K.; Makowski, A.J.; Putnam, D.; Tomlinson, A.L.; Chaudhary, S.; Jeffries-El, M. *Physical Chemistry Chemical Physics*, **2011**, *13*(4), 1338-1344.
- (68) Mike, J.F.; Makowski, A.J.; Mauldin, T.C.; Jeffries-El, M. *Journal of Polymer Science Part A: Polymer Chemistry*, **2010**, *48*(6), 1456-1460.
- (69) Intemann, J.J.; Mike, J.F.; Cai, M.; Bose, S.; Xiao, T.; Mauldin, T.C.; Rogers, R.A.; Shinar, J.; Shinar, R.; Jeffries-El, M. *Macromolecules*, **2010**, *44*(2), 248-255.
- (70) Mike, J.F.; Makowski, A.J.; Jeffries-EL, M. *Organic Letters*, **2008**, *10*(21), 4915-4918.
- (71) Mike, J.F.; Inteman, J.J.; Ellern, A.; Jeffries-El, M. *Journal of Organic Chemistry*, **2010**, *75*(2), 495-497.
- (72) Skotheim, T.A.; Reynolds, J.R. *Handbook of conducting polymers*; 3rd ed / edited by Terje A. Skotheim and John Reynolds. ed London Boca Raton, Fla.: **2007**, (various pagings) p.
- (73) Egbe, D.A.M.; Roll, C.P.; Birkner, E.; Grummt, U.-W.; Stockmann, R.; Klemm, E. *Macromolecules*, **2002**, *35*(10), 3825-3837.
- (74) Brustolin, F.; Goldoni, F.; Meijer, E.W.; Sommerdijk, N.A.J.M. *Macromolecules*, **2002**, *35*(3), 1054-1059.
- (75) Yang, L.; Zhou, H.; You, W. *The Journal of Physical Chemistry C*, **2010**, *114*(39), 16793-16800.
- (76) Stokes, K.K.; Heuze, K.; McCullough, R.D. *Macromolecules*, **2003**, *36*(19), 7114-7118.
- (77) Carter, J.; Wehrum, A.; Dowling, M.C.; Cacheiro-Martinez, M.; Baynes, N.d.B. *Recent developments in materials and processes for ink jet printing high resolution polymer OLED displays*. **2003**. Seattle, WA, USA: SPIE.
- (78) Yang, H.; LeFevre, S.W.; Ryu, C.Y.; Bao, Z. *Applied Physics Letters*, **2007**, *90*(17), 172116-3.
- (79) Pal, S.; Nandi, A.K. *Macromolecules*, **2003**, *36*(22), 8426-8432.
- (80) Kohno, H.; Saitoh, F.; Mihara, T.; Koide, N. *Polymer Journal (Tokyo*,

Japan), **2003**, 35(12), 945-950.

- (81) Chen, J.; Cao, Y. *Accounts of Chemical Research*, **2009**, 42(11), 1709-1718.
- (82) Mozer, A.J.; Sariciftci, N.S. *Comptes Rendus Chimie*, **2006**, 9(5-6), 568-577.
- (83) Harrison, W.A. *Elementary Electronic Structure*; Revised ed World Scientific Publishing Company: **2004**, 860 p.
- (84) Moliton, A.; Hiorns, R.C. *Polymer International*, **2004**, 53(10), 1397-1412.
- (85) Klaerner, G.; Miller, R.D. *Macromolecules*, **1998**, 31(6), 2007-2009.
- (86) Rissler, J. *Chemical Physics Letters*, **2004**, 395(1-3), 92-96.
- (87) Wohlgenannt, M.; Jiang, X.M.; Vardeny, Z.V. *Physical Review B: Condensed Matter and Materials Physics*, **2004**, 69(24), 241204/1-241204/4.
- (88) Moliton, A. *Optoelectronics of Molecules and Polymers*; 1st ed Springer: **2005**, 529 p.
- (89) Brédas, J.E.; Chance, R.R.; Silbey, R. *Molecular Crystals and Liquid Crystals*, **1981**, 77, 319 - 332.
- (90) Brédas, J.L.; Calbert, J.P.; da Silva Filho, D.A.; Cornil, J. *Proceedings of the National Academy of Sciences*, **2002**, 99(9), 5804-5809.
- (91) Shirakawa, H.; Ikeda, S. *Synthetic Metals*, **1980**, 1(2), 175-84.
- (92) Pope, M.; Swenberg, C.E. *Electronic Processes in Organic Crystals and Polymers: 2nd Edition* Oxford University Press: **1999** p.
- (93) Zhang, Q.T.; Tour, J.M. *Journal of the American Chemical Society*, **1998**, 120(22), 5355-5362.
- (94) Burn, P.L.; Kraft, A.; Baigent, D.R.; Bradley, D.D.C.; Brown, A.R.; Friend, R.H.; Gymer, R.W.; Holmes, A.B.; Jackson, R.W. *Journal of the American Chemical Society*, **1993**, 115(22), 10117-24.
- (95) Peng, Q.; Park, K.; Lin, T.; Durstock, M.; Dai, L. *Journal of Physical Chemistry B*, **2008**, 112(10), 2801-2808.
- (96) McCullough, R.D.; Williams, S.P. *Journal of the American Chemical Society*, **1993**, 115, 11608-11609.
- (97) Sapoval, B.; Hermann, C. *Physics of semiconductors* Springer: **2003** p.
- (98) Macdiarmid, A.G.; Zheng, W. *MRS Bulletin*, **1997**, 22(6), 24.

- (99) Cardona, C.M.; Li, W.; Kaifer, A.E.; Stockdale, D.; Bazan, G.C. *Advanced Materials*, **2011**, 23(20), 2367-2371.
- (100) Bredas, J.L.; Street, G.B. *Accounts of Chemical Research*, **1985**, 18(10), 309-15.
- (101) Heeger, A.J.; Kivelson, S.; Schrieffer, J.R.; Su, W.P. *Reviews of Modern Physics*, **1988**, 60(3), 781.
- (102) Bredas, J.-L.; Beljonne, D.; Coropceanu, V.; Cornil, J. *Chemical Reviews*, **2004**, 104(11), 4971-5003.
- (103) Su, W.P.; Schrieffer, J.R.; Heeger, A.J. *Physical Review Letters*, **1979**, 42(25), 1698.
- (104) Feldblum, A.; Heeger, A.J.; Chung, T.C.; MacDiarmid, A.G. *The Journal of Chemical Physics*, **1982**, 77(10), 5114-5121.
- (105) Moliton, A.; Hiorns, R.C. *Polymer International*, **2004**, 53(10), 1397-1412.
- (106) Bredas, J.-L.; Beljonne, D.; Coropceanu, V.; Cornil, J. *Chemical Reviews (Washington, DC, United States)*, **2004**, 104(11), 4971-5003.
- (107) Bradley, D.D.C.; Colaneri, N.F.; Friend, R.H. *Synthetic Metals*, **1989**, 29(1), 121-127.
- (108) Gunes, S.; Neugebauer, H.; Sariciftci, N.S. *Chem. Rev.*, **2007**, 107(4), 1324-1338.
- (109) Şener, M.; Strümpfer, J.; Hsin, J.; Chandler, D.; Scheuring, S.; Hunter, C.N.; Schulten, K. *ChemPhysChem*, **2011**, 12(3), 518-531.
- (110) Atkins, P.; Paula, J.D. *Physical Chemistry* W H Freeman & Co: **2006** p.
- (111) Brédas, J.-L.; Cornil, J.; Heeger, A.J. *Advanced Materials*, **1996**, 8(5), 447-452.
- (112) Brazovskii, S.; Kirova, N. *Chemical Society Reviews*, **2010**, 39(7), 2453-2465.
- (113) Bardeen, C. *Science*, **2011**, 331(6017), 544-545.
- (114) Forest, S.R. *MRS Bulletin*, **2005**, 30, 28-32.
- (115) Konezny, S.J.; Rothberg, L.J.; Galvin, M.E.; Smith, D.L. *Applied Physics Letters*, **2010**, 97(14), 143305-3.

- (116) Park, S.H.; Roy, A.; Beaupre, S.; Cho, S.; Coates, N.; Moon, J.S.; Moses, D.; Leclerc, M.; Lee, K.; Heeger, A.J. *Nat Photon*, **2009**, 3(5), 297-302.
- (117) Zuppiroli, L.; Bussac, M.N.; Paschen, S.; Chauvet, O.; Forro, L. *Physical Review B: Condensed Matter and Materials Physics*, **1994**, 50(8), 5196-203.
- (118) Siddiqui, A.S.; Wilson, E.G. *Journal of Physics C: Solid State Physics*, **1979**, 12(20), 4237.
- (119) Sista, P.; Bhatt, M.P.; McCary, A.R.; Nguyen, H.; Hao, J.; Biewer, M.C.; Stefan, M.C. *Journal of Polymer Science Part A: Polymer Chemistry*, **2011**, 49(10), 2292-2302.
- (120) Salleo, A.; Chabinyc, M.L.; Yang, M.S.; Street, R.A. *Applied Physics Letters*, **2002**, 81(23), 4383-4385.
- (121) Cornil, J.; Beljonne, D.; Calbert, J.P.; Bredas, J.L. *Advanced materials*, **2001**, 13(14), 16.
- (122) Hains, A.W.; Liang, Z.; Woodhouse, M.A.; Gregg, B.A. *Chemical Reviews*, **2010**, 110(11), 6689-6735.
- (123) Nelson, S.F.; Lin, Y.Y.; Gundlach, D.J.; Jackson, T.N. *Applied Physics Letters*, **1998**, 72(15), 1854-1856.
- (124) Zhou, H.; Yang, L.; Xiao, S.; Liu, S.; You, W. *Macromolecules*, **2009**, 43(2), 811-820.
- (125) Lee, S.K.; Cho, S.; Tong, M.; Hwa Seo, J.; Heeger, A.J. *Journal of Polymer Science Part A: Polymer Chemistry*, **2011**, 49(8), 1821-1829.
- (126) Zhu, Y.; Alam, M.M.; Jenekhe, S.A. *Macromolecules*, **2003**, 36(24), 8958-8968.
- (127) Jeffries-El, M.; Laskowski, R.; Mitchell, M.H. *Polym. Prepr.*, **2008**, 49(2), 654-655.
- (128) Jeffries-El, M.; Zaiger, K.L.; McCullough, R. *Abstracts of Papers, 223rd ACS National Meeting, Orlando, FL, United States, April 7-11, 2002*, **2002**, PMSE-133.
- (129) Kline, R.J.; McGehee, M.D.; Kadnikova, E.N.; Liu, J.; Frechet, J.M.J.; Toney, M.F. *Macromolecules*, **2005**, 38(8), 3312-3319.
- (130) Loewe, R.S.; Khersonsky, S.M.; McCullough, R.D. *Advanced Materials*,

1999, 11(3), 250-258.

(131) McCullough, R.D. *Regioregular, Head-To-Tail Coupled Poly(3-alkylthiophene) and its Derivatives.*, in *Handbook of Conducting Polymers*; T.A. Skotheim, Elsenbaumer, Ronald L., Reynolds, John R., Editor; Marcell Dekker: **1998**, New York. p. 225-258.

(132) McCullough, R.D.; Jayaraman, M. *Journal of the Chemical Society, Chemical Communications*, **1995**(2), 135-6.

(133) Rasmussen, S.C.; Straw, B.D.; Hutchison, J.E. *Tuning the Extent of Conjugation in Processable Polythiophenes Through Control of Side Chain Density and Regioregularity*, in *Semiconducting Polymers*; American Chemical Society: **1999**. p. 347-366.

(134) Andersson, M.R.; Thomas, O.; Mammo, W.; Svensson, M.; Theander, M.; Inganäs, O. *Journal of Materials Chemistry*, **1999**, 9(9), 1933-1940.

(135) Hu, X.; Kumar, S.; Polk, M.B. *Macromolecules*, **1996**, 29(11), 3787-92.

(136) Amb, C.M.; Chen, S.; Graham, K.R.; Subbiah, J.; Small, C.E.; So, F.; Reynolds, J.R. *Journal of the American Chemical Society*, **2011**, 133(26), 10062-10065.

(137) Liu, J.; Zhang, R.; Sauve, G.; Kowalewski, T.; McCullough, R.D. *Journal of the American Chemical Society*, **2008**, 130(39), 13167-13176.

(138) Liu, Y.; Liu, Y.; Zhan, X. *Macromolecular Chemistry and Physics*, **2011**, 212(5), 428-443.

(139) Chen, H.-Y.; Hou, J.; Hayden, A.E.; Yang, H.; Houk, K.N.; Yang, Y. *Advanced Materials*, **2010**, 22(3), 371-375.

(140) Ohshita, J.; Kai, H.; Sumida, T.; Kunai, A.; Adachi, A.; Sakamaki, K.; Okita, K. *Journal of Organometallic Chemistry*, **2002**, 642(1-2), 137-142.

(141) Beaujuge, P.M.; Pisula, W.; Tsao, H.N.; Ellinger, S.; Müllen, K.; Reynolds, J.R. *Journal of the American Chemical Society*, **2009**, 131(22), 7514-7515.

(142) Chen, Z.; Amara, J.P.; Thomas, S.W.; Swager, T.M. *Macromolecules*, **2006**, 39(9), 3202-3209.

(143) Izuhara, D.; Swager, T.M. *Journal of the American Chemical Society*, **2009**, 131(49), 17724-17725.

- (144) Babel, A.; Jenekhe, S.A. *J. Am. Chem. Soc.*, **2003**, *125*, 13656-13657.
- (145) Koynov, K.; Bahtiar, A.; Ahn, T.; Cordeiro, R.M.; Horhold, H.-H.; Bubeck, C. *Macromolecules*, **2006**, *39*, 8692-8698.
- (146) Neef, C.J.; Ferraris, J.P. *Macromolecules*, **2000**, *33*, 2311-14.
- (147) Zen, A.; Saphiannikova, M.; Neher, D.; Grenzer, J.; Grigorian, S.; Pietsch, U.; Asawapirom, U.; Janietz, S.; Scherf, U.; Lieberwirth, I.; Wegner, G. *Macromolecules*, **2006**, *39*(6), 2162-2171.
- (148) Bredas, J.L. *The Journal of Chemical Physics*, **1985**, *82*(8), 3808-3811.
- (149) Horie, K.; Ushiki, H.; Winnik, F.M., in *Molecular Photonics*; Wiley-VCH Verlag GmbH: **2007**. p. 126.
- (150) Liu, M.S.; Jiang, X.; Liu, S.; Herguth, P.; Jen, A.K.Y. *Macromolecules*, **2002**, *35*(9), 3532-3538.
- (151) Demanze, F.; Yassar, A.; Garnier, F. *Macromolecules*, **1996**, *29*(12), 4267-4273.
- (152) Colladet, K.; Fourier, S.; Cleij, T.J.; Lutsen, L.; Gelan, J.; Vanderzande, D.; Nguyen, L.H.; Neugebauer, H.; Sariciftci, S.; Aguirre, A.; Janssen, G.; Goovaerts, E. *Macromolecules*, **2007**, *40*(1), 65-72.
- (153) Salzner, U. *Journal of Physical Chemistry B*, **2002**, *106*(36), 9214-9220.
- (154) Lee, J.K.; Ma, W.L.; Brabec, C.J.; Yuen, J.; Moon, J.S.; Kim, J.Y.; Lee, K.; Bazan, G.C.; Heeger, A.J. *Journal of the American Chemical Society*, **2008**, *130*(11), 3619-3623.
- (155) Peet, J.; Senatore, M.L.; Heeger, A.J.; Bazan, G.C. *Advanced Materials*, **2009**, *21*(14-15), 1521-1527.
- (156) Kim, Y.; Choulis, S.A.; Nelson, J.; Bradley, D.D.C.; Cook, S.; Durrant, J.R. *Applied Physics Letters*, **2005**, *86*(6), 063502/1-063502/3.
- (157) Jo, J.; Na, S.-I.; Kim, S.-S.; Lee, T.-W.; Chung, Y.; Kang, S.-J.; Vak, D.; Kim, D.-Y. *Advanced Functional Materials*, **2009**, *19*(15), 2398-2406.
- (158) Lee, J.I.; Cho, S.H.; Park, S.-M.; Kim, J.K.; Kim, J.K.; Yu, J.-W.; Kim, Y.C.; Russell, T.P. *Nano Letters*, **2008**, *8*(8), 2315-2320.
- (159) Winokur, M.; Moon, Y.B.; Heeger, A.J.; Barker, J.; Bott, D.C.; Shirakawa,

H. *Physical Review Letters*, **1987**, 58(22), 2329.

(160) Tashiro, K.; Kobayashi, M.; Kawai, T.; Yoshino, K. *Polymer*, **1997**, 38(12), 2867-2879.

(161) Osaheni, J.A.; Jenekhe, S.A.; Burns, A.; Du, G.; Joo, J.; Wang, Z.; Epstein, A.J.; Wang, C.S. *Macromolecules*, **1992**, 25(21), 5828-35.

(162) Abdou, M.S.A.; Lu, X.; Xie, Z.W.; Orfino, F.; Deen, M.J.; Holdcroft, S. *Chemistry of Materials*, **1995**, 7(4), 631-641.

(163) Katz, H.E.; Bao, Z.; Gilat, S.L. *Accounts of Chemical Research*, **2001**, 34(5), 359-369.

(164) Kim, Y.; Cook, S.; Kirkpatrick, J.; Nelson, J.; Durrant, J.R.; Bradley, D.D.C.; Giles, M.; Heeney, M.; Hamilton, R.; McCulloch, I. *J. Phys. Chem. C*, **2007**, 111(23), 8137-8141.

(165) Yang, X.; Yang, W.; Yuan, M.; Hou, Q.; Huang, J.; Zeng, X.; Cao, Y. *Synthetic Metals*, **2003**, 135-136, 189-190.

(166) Park, J.K.; Jo, J.; Seo, J.H.; Moon, J.S.; Park, Y.D.; Lee, K.; Heeger, A.J.; Bazan, G.C. *Advanced Materials*, **2011**, 23(21), 2430-2435.

(167) Szarko, J.M.; Guo, J.; Liang, Y.; Lee, B.; Rolczynski, B.S.; Strzalka, J.; Xu, T.; Loser, S.; Marks, T.J.; Yu, L.; Chen, L.X. *Advanced Materials*, **2010**, 22(48), 5468-5472.

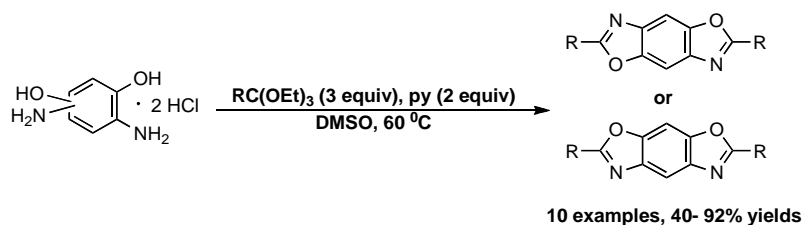
CHAPTER 2

**An Efficient Synthesis of 2,6-Disubstituted Benzobisoxazoles:
New Building Blocks for Organic Semiconductors**

Reproduced from *Organic Letters* **2008**, 10(21), 4915, with permission from American Chemical Society.
Copyright © 2011

Jared F. Mike, Andrew J. Makowski, and Malika Jeffries-EL*
Department of Chemistry, Iowa State University, Ames, IA 50011-3111

2.1 ABSTRACT



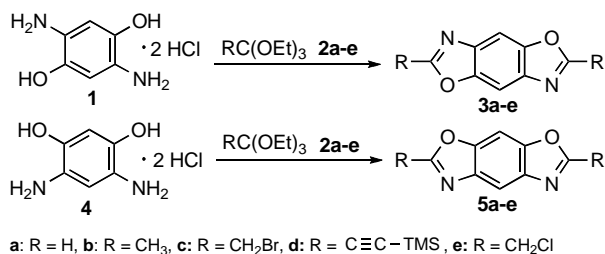
2,6-Disubstituted benzobisoxazoles have been synthesized by a highly efficient reaction of diaminobenzene diols with various orthoesters. The scope of this new reaction for the synthesis of substituted benzobisoxazoles has been investigated using four different orthoesters. The utility of these compounds as building blocks for the synthesis of conjugated polymers is demonstrated.

2.2 INTRODUCTION

Conjugated polymers and oligomers are of interest for use as organic semiconductors in applications such as thin-film transistors (TFTs),¹ light-emitting diodes (OLEDs),² and photovoltaic cells (PVCs).³ While there are a large number of π -conjugated small molecules, oligomers, and polymers which have been reported in the literature, the design and synthesis of new π -conjugated organic materials remains an important area of research. Of particular interest is the creation of materials with good electron transport

properties (n-type), which are less abundant in the literature than those with hole transport (p-type) properties.⁴ n-type materials with efficient electron transport are essential for improving the performance of TFTs, OLEDs, and PVCs and to enable other cost-effective applications such as complementary circuits.⁵

We are interested in developing benzobisoxazoles for their use as building blocks for novel organic semiconductors because conjugated small molecules and polymers based on benzobisoxazoles are well suited for use in organic semiconducting applications. These materials combine efficient electron transport, photoluminescence, and third-order nonlinear optical properties⁶ with excellent mechanical strength and thermal stability.⁷ Unfortunately, the fused benzobisoxazole ring system, the rodlike conformation of the resulting polymers, and efficient π -stacking between chains render fully conjugated poly(benzobisoxazoles) (PBOs) insoluble in aprotic solvents. As a result, PBOs are typically processed from acidic solvents, such as Lewis acid/nitromethane, methanesulfonic acid, trifluoromethanesulfonic acid, and sulfuric acid,⁸ which are impractical for use in device manufacturing.



Scheme 1. Synthesis of 2,6-Disubstituted Benzobisoxazoles

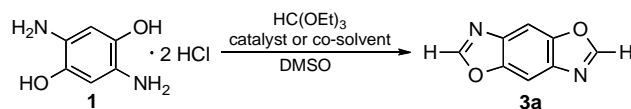
Generally, the solubility of π -conjugated materials can be improved through structural modification. In the case of small molecules and polymers containing the benzobisoxazole moiety, the synthesis is achieved by the high-temperature condensation of bis-*o*-aminophenols and aromatic diacids in the melt, in polyphosphoric acid (PPA), in phosphorus pentoxide/methanesulfonic acid, or in trimethylsilyl polyphosphate (PPSE)/*o*-dichlorobenzene.⁹ These conditions are rather harsh, thereby limiting the types of substituents that can be incorporated into the benzobisoxazole moiety. In this contribution, we report the synthesis of optoelectronic building blocks based on benzo[1,2-*d*;4,5-*d'*] bisoxazole (*trans*-BBO) (**3a-e**) and benzo[1,2-*d*;5,4-*d'*] bisoxazole

(*cis*-BBO) (**5a-e**) by the reaction of various orthoesters (**2a-e**) with 2,5-diaminoquinone (DAHQ) (**1**) and 4,6-diaminoresorcinol (DAR) (**4**), respectively (Scheme 1). In all cases, the target compounds have been obtained cleanly and in high yield. Using our strategy, we have synthesized several building blocks suitable for the synthesis of benzobisoxazole monomers.

2.3 RESULTS AND DISCUSSION

We rationalized that orthoesters could be used for the synthesis of benzobisoxazoles since they have been used for the synthesis of benzimidazoles, benzoxazoles, and benzothiazoles.¹⁰ The standard reaction conditions use 10 equiv of orthoester, which serves as both a reagent and the solvent, a catalytic amount of acid, and temperatures of 130 °C. Using the reaction of triethyl orthoformate and DAHQ as our model system, we first explored catalyst-free conditions, relying on the acid coordinated with the diamino-diol to catalyze the reaction (entry 1). This yielded *trans*-BBO 3a in 61% yield. When the reaction was performed under traditional conditions, using catalytic amounts of H₂SO₄, the target compound 3a was obtained in 65% yield (entry 3). While the yields were moderate in both cases, the product was contaminated with a significant amount of dark red oxidation products, complicating purification.

Due to the tendency of DAHQ (**1**) and DAR (**4**) to decompose at higher temperatures, we needed to reduce the reaction temperature. Furthermore, the use of such a large excess of orthoester is undesirable since the substituted orthoesters are costly. To reduce the need for excess orthoester, we used DMSO as a cosolvent since it can dissolve both DAHQ and DAR. We then explored the use of rare earth metal triflates as catalysts since they have been demonstrated to reduce reaction times and increase yields when used instead of traditional Lewis acid catalysts.¹¹ In the case of our model reaction, we found several effective catalysts as shown in Table 1. Interestingly, the Lewis acid catalysts do not work in the absence of the DMSO solvent. With the exception of Bi(OTf)₃ and Hf(OTf)₃, all of the metal triflates gave improved yields when compared to the traditional acid catalysts. The low reactivity of Bi(III) and Hf(III) may be attributed to their larger ionic radii.¹¹



entry	solvent	catalyst/ cosolvent	temp (°C)	time (h)	yield ^a (%)
1	none	none	130	5	61
2	DMSO	none	60	2.5	64
3	none	H ₂ SO ₄	130	2.5	65
4	DMSO	H ₂ SO ₄	130	1	64
5	DMSO	PTSA	110	4	71
6	DMSO	Bi(OTf) ₃	60	4	0
7	DMSO	Hf(OTf) ₃	60	4	36
8	DMSO	Eu(OTf) ₃	60	4	82
9	DMSO	Sc(OTf) ₃	60	4	82
10	DMSO	Y(OTf) ₃	60	4	81
11	none	Yb(OTf) ₃	60	4	0
12	DMSO	Yb(OTf) ₃	60	4	75
13	DMSO	Y(OTf) ₃ /Py	60	1	92 ^b
14	DMSO	Pyridine	45	1	78 ^b

^aStandard reaction conditions: substrate 1 M in DMSO, 10 equiv of ortho ester, 5 mol % catalyst, or py 2 equiv ^a Isolated yields. ^b 3 equiv of ortho ester.

Table 1. Investigation of the Effect of Catalyst on the Reaction of DAHQ (1) with Triethyl Orthoformate 2a^a

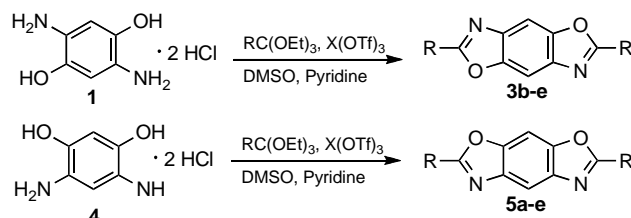
Unfortunately, we found that even with the addition of the DMSO the reaction yields significantly decreased when less than 10 equiv of orthoester was used. Moreover, we found that when the optimum reaction conditions, which were established for our model reactions, were used with ethyl orthobromoacetate^{12a} (2c) and trimethylsilyl ethyl

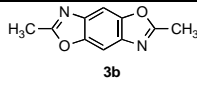
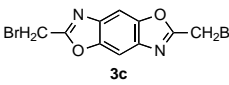
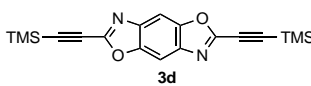
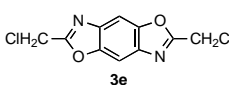
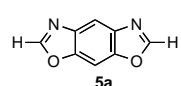
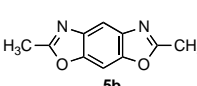
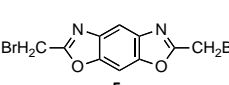
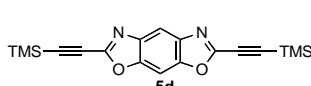
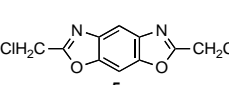
orthopropiolate^{12b} (**2d**), the yields of the target BBOs decreased. We rationalized that the substituted orthoesters were unstable to the current reaction conditions and set out to further improve our reaction conditions. We explored the use of pyridine as a cosolvent with DMSO since it has been reported that it improved the yields of orthoester reactions.¹³

This modification was fortuitous, and we were able to reduce the reaction temperatures and times while increasing the reaction yields. While it was previously reported that the addition of pyridine stabilizes the DMSO, we believe that this improvement is a result of the removal of the acid coordinated with the DAHQ and DAR, increasing their reactivity and preventing protic acid catalyzed decomposition of the orthoesters. Using yttrium triflate, the pure product **3a** was obtained in 91% yield after the addition of water to the reaction mixture and simple filtration (entry 13). In the absence of the catalyst, the product was obtained in 78% yield (entry 14). The advantages of this method are the fact that the reaction occurred at a lower temperature, preventing the formation of side products, and the desired product can be precipitated out from the reaction mixture, allowing for easy purification.

On the basis of the model reactions, we have determined the optimum reaction conditions to be: substrate 1 M in DMSO, 2 equiv of pyridine, 3 equiv of orthoester, and 5% Y(OTf)₃ for DAHQ or La(OTf)₃ for DAR. Using these conditions, we set out to investigate the scope of the reaction with respect to the orthoester (Table 2). We found that triethyl orthoacetate (**2b**) and trimethylsilyl ethyl orthopropiolate^{12b} (**2d**) could be employed to yield the corresponding BBOs in good yield. However, the reaction of triethyl orthobromoacetate (**2c**) only worked under traditional conditions, in the case of the transderivative, and failed to yield product in the case of the *cis* derivative. The inability to synthesize benzobisoxazole **3c** using **2c** and our modified reaction conditions is most likely due to the competing side reaction of the alkyl bromide of the orthoester with DMSO.¹⁴ Thus, we explored the use of triethyl orthochloroacetate (**2e**),^{12c} which is less prone to side reactions and gives good results using our reaction conditions. In all cases, the products can be purified by simple recrystallization, and this method can easily be scaled up to multigram quantities. Thus, by utilizing the corresponding orthoesters, we

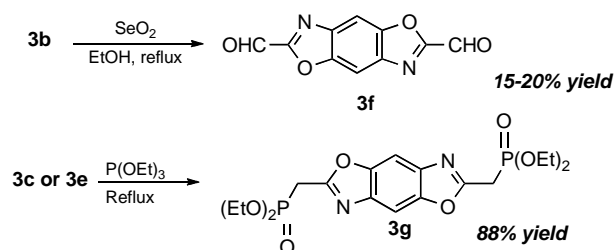
can incorporate methyl, bromomethyl, chloromethyl, and alkynyl groups into the BBO's. Compounds containing the latter three groups cannot be prepared using traditional approaches. Moreover, direct bromination of **3b** or **5b** also fails to yield **3c** and **5c**.



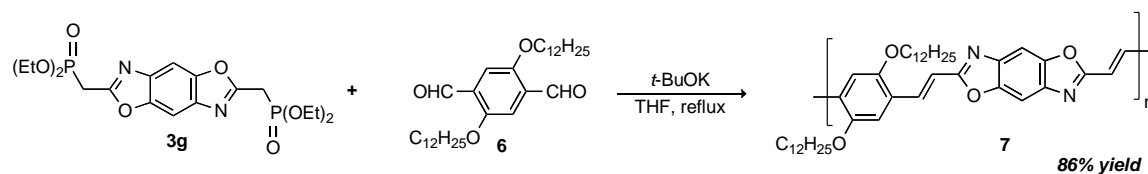
diamino diol	ortho ester	benzobisoxazole	% yield ^a
1	2b		86
1	2c		48 ^b
1	2d		67
1	2e		40
4	2a		91
4	2b		83
4	2c		0
4	2d		40
4	2e		73

^a Isolated yields. ^b Synthesized using standard conditions.

Table 2. Reaction of **1** and **4** With Various Orthoesters **2b–e**



Scheme 2. Synthesis of Benzobisoxazole Monomers



Scheme 3. Synthesis of Benzobisoxazole Polymer **7**

To demonstrate the utility of the new BBOs as building blocks for the synthesis of conjugated polymers, we first attempted the synthesis of monomer **3f**, by the oxidation of compound **3b** (Scheme 2). The reaction yields were very low (15-20%). Thus, we explored the synthesis of diphosphonate ester **3g**. Monomer **3g** can be synthesized by the Arbuzov reaction of **3c** or **3e** and triethylphosphite. The polymerization of monomer **3g** with 2,5-didodecyloxybenzaldehyde **6**¹⁵ by a Horner-Wadsworth-Emmons (HWE) olefination reaction produced a red polymer in 86% yield (Scheme 3). The resultant polymer was soluble in THF and chloroform, and the structure of the polymer was verified by ¹H NMR spectroscopy. Gel permeation chromatography (GPC) of the polymer showed a monomodal distribution with number average molecular weight (M_n) of 5672, and a PDI of 1.77, which corresponds to a number averaged degree of polymerization of approximately 8. We measured the emission and absorption spectra of the polymer in solution and found that the absorption maximum is 476 nm. The polymer exhibits green fluorescence with an emission maximum at 515 nm, which is blue-shifted from the photoluminescence of MEHPPV (ca. 600 nm).¹⁶ This represents the first synthesis of a PBO derivative which is soluble in aprotic organic solvents. We are currently working to optimize the reaction conditions to obtain a higher molecular weight polymer.

In summary, the reaction of orthoesters and DAHQ or DAR affords new 2,6-disubstituted benzobisoxazoles in good yields. Subsequent reactions can transform these compounds into monomers for the synthesis of novel polymers containing the electron-deficient benzobisoxazole moiety. Future efforts will focus on the synthesis of other monomers based on these materials, as well as device construction and evaluation of the electronic and optical properties of oligomers and polymers containing the benzobisoxazole moiety.

2.4 EXPERIMENTAL

Detailed descriptions of the synthetic and analytic methods are given in the Supporting information.

2.5 ACKNOWLEDGEMENT

M.J.E. would like to thank the 3M Foundation for a nontenured faculty grant. J.F.M. thanks the Department of Education for a GAANN fellowship. We thank Dr. Kamel Harrata and the Mass Spectroscopy Laboratory of Iowa State University (ISU) for analysis of our compounds and Dr. Tanay Kesharwani (ISU), Professor Gordon Miller (ISU), and Dr. Jesse Waldo (ISU) for helpful discussions regarding this work.

2.6 REFERENCES

- (1) (a) Mas-Torrent, M.; Rovira, C. *Chem. Soc. Rev.* **2008**, *37*, 827. (b) Usta, H.; Lu, G.; Facchetti, A.; Marks, T. J. *J. Am. Chem. Soc.* **2006**, *128*, 9034. (c) Kline, R. J.; McGehee, M. D.; Kadnikova, E. N.; Liu, J.; Frechet, J. M. J.; Toney, M. F. *Macromolecules* **2005**, *38*, 3312. (d) Dimitrakopoulos, C. D.; Malenfant, P. R. L. *Adv. Mater.* **2002**, *14*, 99.
- (2) (a) Tang, C. W.; VanSlyke, S. A. *Appl. Phys. Lett.* **1987**, *51*, 913. (b) Friend, R. H.; Gymer, R. W.; Holmes, A. B.; Burroughes, J. H.; Marks, R. N.; Taliani, C.; Bradley, D. D. C.; Dos Santos, D. A.; Bredas, J. L.; Logdlund, M.; Salaneck, W. R. *Nature* **1999**, *397*, 121.
- (3) (a) Thompson, B. C.; Frechet, J. M. J. *Angew. Chem. Int. Ed.* **2008**, *47*, 58. (b) Coakley, K. M.; McGehee, M. D. *Chem. Mater.* **2004**, *16*, 4533. (c) Scharber, M. C.;

Muehlbacher, D.; Koppe, M.; Denk, P.; Waldauf, C.; Heeger, A. J.; Brabec, C. J. *Adv. Mater.* **2006**, *18*, 789.

(4) (a) Cornil, J.; Bredas, J.-L.; Zaumseil, J.; Sirringhaus, H. *Adv. Mater.* **2007**, *19*, 1791. (b) Cravino, A. *Polym. Int.* **2007**, *56*, 943. (c) McNeill, C. R., Abrusci, A., Zaumseil, J., Wilson, R., McKiernan, M. J., Burroughes, J. H., Halls, J. J. M., Greenham, N. C., and Friend, R. H. *Appl. Phys. Lett.* **2007**, *90*, 193506/1. (c) Zhu, Y.; Alam, M. M.; Jenekhe, S. A. *Macromolecules* **2003**, *36*, 8958. (d) Babel, A.; Jenekhe, S. A. *J. Phys. Chem. B.* **2002**, *106*, 6129.

(5) (a) Kulkarni, A. P.; Tonzola, C. J.; Babel, A.; Jenekhe, S. A. *Chem. Mater.* **2004**, *16*, 4556. (b) Kietzke, T.; Egbe, D. A. M.; Horhold, H.- H.; Neher, D. *Macromolecules* **2006**, *39*, 4018 (c) Alam, M. M.; Jenekhe, S. A. *Chem. Mater.* **2004**, *16*, 4647.

(6) (a) Osaheni, J. A.; Jenekhe, S. A. *Macromolecules* **1994**, *27*, 739. (b) Osaheni, J. A.; Jenekhe, S. A. *Chem. Mater.* **1995**, *7*, 672. (c) Jenekhe, S. A.; Osaheni, J. A.; Meth, J. S.; Vanherzeele, H., *Chem. Mater.* **1992**, *4*, 683. (c) Reinhardt, B. A.; Unroe, M. R.; Evers, R. C. *Chem. Mater.* **1991**, *3*, 451.

(7) (a) Wolfe, J. F., *Encyclopedia of Polymer Science and Engineering*, John Wiley and Sons: New York, NY, 1988; Vol. 11, p 601. (b) Wolfe, J. F.; Loo, B. H.; Arnold, F. E., *Macromolecules* **1981**, *14*, 909.

(8) (a) Roberts, M. F.; Jenekhe, S. A., *Chem. Mater.* **1993**, *5*, 1744. (b) So, Y. H.; Heeschen, J. P. J. *Org. Chem.* **1997**, *62*, 3552.

(9) (a) Osman, A. M.; Mohamed, S. A. *Indian J. Chem.* **1973**, *11*, 868. (b) Osman, A. M.; Mohamed, S. A. *U.A.R.J. Chem.* **1971**, *14*, 475. (c) Imai, Y.; Itoya, K.; Kakimoto, M.-A. *Macromol. Chem. Phys.* **2000**, *201*, 2251. (d) Imai, Y.; Taoka, I.; Uno, K.; Iwakura, Y. *Makromol. Chem.* **1965**, *83*, 167. (e) So, Y. H.; Zaleski, J.; Murlick, C.; Ellaboudy, A. *Macromolecules* **1996**, *29*, 5229. (f) Kricheldorf, H. R.; Domschke, A. *Polymer* **1994**, *35*, 198.

(10) (a) Jenkins, G. L.; Knevel, A. M.; Davis, C. S., *J. Org. Chem.* **1961**, *26*, 274. (b) Jois, Y. H. R.; Gibson, H. W. J. *Heterocycl. Chem.* **1992**, *29*, 1365.

(11) (a) Wang, L.; Sheng, J.; Tian, H.; Qian, C. *Synth. Commun.* **2004**, *34*, 4265.

(b) Kobayashi, S.; Sugiura, M.; Kitagawa, H.; Lam, W. W. L. *Chem. Rev.* **2002**, *102*, 2227.

(12) (a) Beyerstedt, F.; McElvain, S. M. *J. Am. Chem. Soc.* **1937**, *59*, 1273. (b) Yamamoto, K.; Abrecht, S.; Scheffold, R. *Chimia* **1991**, *45*, 86. (c) Mylari, B. L.; Scott, P. J.; Zembrowski, W. J. *Synth. Commun.* **1989**, *19*, 2921.

(13) Dudgeon, C. D. Vogl, O., *J. Polym. Sci. Polym. Chem. Ed.* **1978**, *16*, 1831.

(14) (a) Nace, H.; Monagle, J. J. *J. Org. Chem.* **1959**, *24*, 1792. (b) Kornblum, N.; Jones, W. J.; Anderson, G. J. *J. Am. Chem. Soc.* **1959**, *81*, 4113.

(15) Liao, J.; Wang, Q. *Macromolecules* **2004**, *37*, 7061.

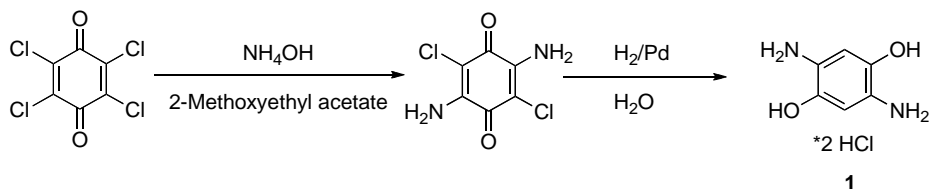
(16) Chen, S. H.; Su, A. C.; Chou, H. L.; Peng, K. Y.; Chen, S. A. *Macromolecules* **2004**, *37*, 167.

2.7 SUPPORTING INFORMATION

2.7.1 Experimental Section

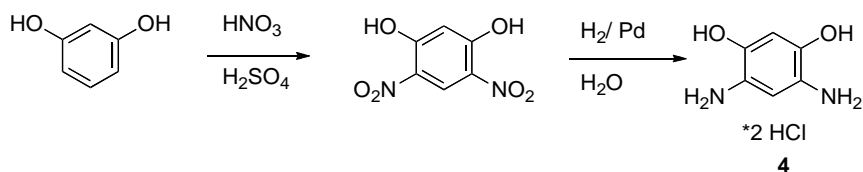
Materials and Equipment. Tetrahydrofuran was dried using an Innovative Technologies solvent purification system. Triethyl orthoformate **2a** and triethyl orthoacetate **2b** anhydrous DMSO and anhydrous pyridine were purchased from Aldrich. All other compounds were purchased from commercial sources and used without further purification. Deuterated solvents were obtained from Cambridge Isotope Laboratories, Inc. Nuclear magnetic resonance spectra were obtained on a Varian 400 MHz spectrometer (^1H at 400 MHz and ^{13}C at 100 MHz). All samples were referenced internally to residual protonated solvent and chemical shifts are given in δ relative to CHCl_3 . High resolution mass spectra were recorded on a Kratos MS50TC double focusing magnetic sector mass spectrometer using EI at 70 eV. Melting points were obtained using a Melt-temp melting point apparatus. GC-MS analysis was performed on a Shimadzu GC17A/ GC-MS QP5000 workstation. The GC column was a fused silica capillary column cross-linked with 5% phenylmethylsiloxane and Helium was the carrier gas. Gel permeation chromatography (GPC) measurements were performed on a Viscotek GPC Max 280 separation module equipped with three $5\mu\text{m}$ I-gel columns connected in series (guard, HMW, MMW and LMW) with a variable λ absorbance UV

detector, online viscometer and refractive index detector. Analyses were performed at 35 °C using THF as the eluent, and the flow rate was 1.0 μL/min. Calibration was based on polystyrene standards obtained from Viscotek. Fluorescence spectroscopy was performed on a Varian Cary Eclipse system and UV-Visible spectroscopy was performed on a Shimadzu UV-2101PC system. Both samples were in THF.



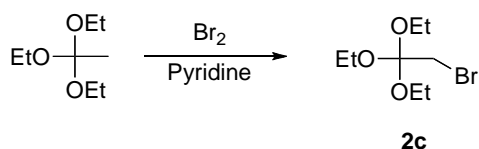
2,5-diamino-3,6-dichlorobenzoquinone. This compound was prepared in 91% yield according to the literature procedure, and used without further purification.¹

2,5-diaminohydroquinone bishydrochloride (1).¹ In a three-neck round bottom flask, (19.28 g, 93.61 mmol) of 2,5-diamino-3,6-dichlorobenzoquinone is stirred together with 1.2 g of 10% Pd on charcoal in 250 mL of water. To this is added 1 mL concentrated HCl. The air is purged by bubbling nitrogen through a gas inlet for 10 min. The gas inlet is then switched to hydrogen gas, which is bubbled through the mixture for 3 days at room temperature. The solution is then filtered to remove the catalyst and the filtrate is immersed in a cold bath (approx -30°C). 300 mL concentrated HCl is added to the solution and white solids begin to form in the flask. Once all the HCl has been added, the solution is placed in the freezer for several hours. When removed, the solids are filtered and washed with 50 mL cold ethanol followed by 200 mL diethyl ether. The solids were dried under vacuum to yield 16.47 g (82%) of 2,5-diaminohydroquinone bishydrochloride. Melting point: >260°C, with gradual darkening. ¹H NMR (DMSO-*d*₆) δ 4.45 (bs, 6H), 6.98 (s) 2H; ¹³C NMR δ 112.1, 119.1, 143.6.

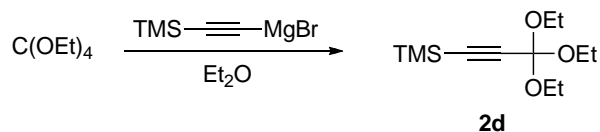


4,6-dinitroresorcinol. This compound was prepared in 46% yield according to the literature procedure.² ^1H NMR (DMSO- d_6) δ 1.3 (very broad, 2H), 6.69 (s, 1H), 8.58(s, 1H); ^{13}C NMR δ 106.5, 126.1, 129.4, 158.7.

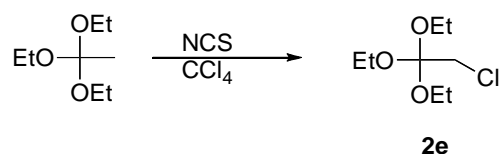
4,6-diaminoresorcinol bishydrochloride (4).³ In a three neck round bottom flask, 20.01 g (100 mmol) 4,6-dinitroresorcinol is suspended in 200 mL water with 1.3 g 10% Pd on charcoal to which is added 17 mL (210 mmol) concentrated HCl. The solution is purged with nitrogen for 10 min before switching to hydrogen. It is stirred for 3 days at room temperature. The reaction is then filtered to remove catalyst and the filtrate is treated with 300 mL concentrated HCl, added dropwise while being kept cold (approx -30°C). The pinkish solids are filtered, rinsed with 50 mL cold ethanol followed by 200 mL diethyl ether. The powder is dried under vacuum to yield 19.59 g (92%) of 4,6-diaminoresorcinol bishydrochloride. Melting point >260°C, with gradual darkening. ^1H NMR (DMSO- d_6) δ 4.5 (s, 6H), 6.68 (s, 1H), 7.31 (s, 1H); ^{13}C NMR δ 103.8, 110.1, 120.1, 152.1.



Triethyl orthobromoacetate 2c. This compound was prepared in 45 % yield according to the literature procedure.⁴ The product is distilled under reduced pressure to give 3 fractions. The 2nd fraction (110°-115°C), contains the purest product (90% pure by GC/MS). ^1H NMR (CDCl₃) δ 1.10 (t, 9H, $J=7$ Hz), 3.37 (s, 2H), 3.44 (q, 6H, $J=7\text{Hz}$); ^{13}C NMR δ 15.1, 30.3, 58.0, 112.1.



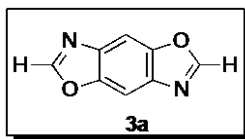
Trimethylsilyl triethyl orthopropiolate 2d. To a solution of ethyl magnesium bromide (prepared from reaction of 4.96 g (.204 mol) Mg and 22.23 g (.204 mol) ethyl bromide in 55 mL diethyl ether) is added 18.17 g (.185 mol) trimethylsilyl acetylene dissolved in 35 mL ether. The reaction is stirred for 1 hr at room temperature, then raised to reflux for 15 min before cooling back down to room temperature. Once cooled, a solution of 42.70 g tetraethyl orthocarbonate and 35 mL ether is added dropwise. After the addition is complete, the reaction is brought to reflux and allowed to stir overnight. The reaction is then poured into 300 mL of saturated aqueous NH_4Cl , and this is extracted four times with 250 mL diethyl ether. The combined ether layers are dried over Na_2SO_4 and the ether is removed by rotary evaporation to give a yellowish orange liquid. The liquid is distilled under vacuum from 60°- 65°C to yield 34.82 g (77%) of a colorless oil. (95% pure by GC/MS) ^1H NMR (CDCl_3) δ 0.14 (s, 9H), 1.17 (t, 9H), 3.62 (q, 6H); ^{13}C NMR δ 0.1, 15.1, 59.1, 89.0, 98.8, 108.6.



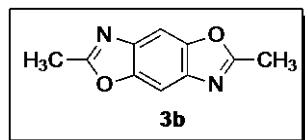
Triethyl orthochloroacetate 2e. This compound was prepared in 51% yield (93% pure by GC/MS), according to the literature procedure.⁵ ^1H NMR (CDCl_3) δ 1.09 (t, 9H, $J=7$ Hz), 3.56 (q, 6H, $J=7$ Hz); ^{13}C NMR δ 41.9, 57.9, 112.6.

2.7.2 Synthesis of Benzobisoxazoles via Orthoester Condensation.

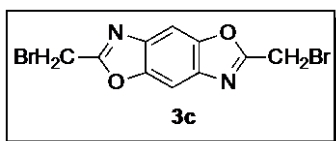
General method: A 1 M solution the diamino diol and pyridine (2 eq.) in DMSO is added via a syringe to the orthoester (3 eq.) a catalyst (5 mol %) in a round bottom flask. The reaction is stirred at 55 °C for 1 hour and then cooled. The reaction is diluted with water and the product collected by filtration. The resultant compounds can be further purified by recrystallization.



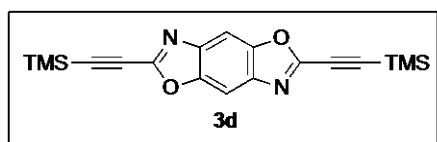
Benzo[1,2-*d*;4,5-*d'*]bisoxazole 3a.⁶ Recrystallization from benzene/ THF 1:1, afforded the product in 92% yield. Melting point 243-245°C, with gradual darkening. ¹H NMR (CDCl₃) δ 7.96 (s, 2H), 8.19 (s, 2H); ¹³C NMR δ 102.2, 139.0, 147.8, 154. HRMS (EI) calcd for C₈H₄N₂O₂ 160.02728, found 160.02757, deviation 1.8 ppm.



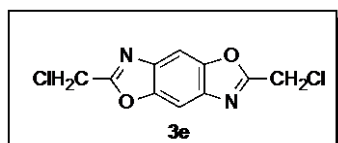
2,6-dimethyl benzo[1,2-*d*;4,5-*d'*]bisoxazole 3b. Recrystallization from heptanes afforded the product in 86 % yield. Melting point 188-190°C (lit mp. 191 °C).⁶ ¹H NMR (CDCl₃) δ 2.65 (s, 6H), 7.68 (s, 2H); ¹³C NMR δ 15.0, 100.4, 139.3, 148.5, 165.2. HRMS (EI) calcd for C₁₀H₈N₂O₂ 188.05858, found 188.05889, deviation 1.7 ppm.



2,6-(bis bromomethyl) benzo[1,2-*d*;4,5-*d'*]bisoxazole 3c. Prepared using 10 equiv. of ortho ester, and 1 drop of H₂SO₄. Recrystallization from MeOH/H₂O, afforded the product in 48% yield. Melting point 153-155°C. ¹H NMR (Acetone-*d*₆) δ 4.86 (s, 4H), 8.02 (s, 2H); ¹³C NMR δ 21.2, 101.9, 140.3, 148.9, 163.5. HRMS (EI) calcd for C₁₀H₆Br₂N₂O₂ 345.87755, found 345.87828, deviation 2.1 ppm.

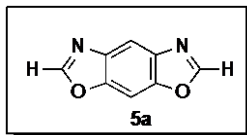


2,6-(bis trimethylsilyl ethynyl) benzo[1,2-*d*;4,5-*d'*]bisoxazole 3d. Recrystallization from heptanes/benzene afforded the product in 67% yield. Melting point 164°- 165°C ¹H NMR (CDCl₃) δ 0.32 (s, 18H), 7.79 (s, 2H); ¹³C NMR δ 0.5, 91.3, 101.6, 103.1, 140.3, 148.3, 148.5. HRMS (EI) calcd for C₁₈H₂₀N₂O₂Si₂ 352.10633, found 352.10706, deviation 2.1 ppm.

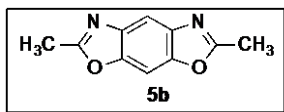


2,6-(bis chloromethyl) benzo[1,2-*d*;4,5-*d'*]bisoxazole 3e. Recrystallization from heptanes afforded the product in 40 % yield. Melting point 146-147 °C. ¹H NMR (CDCl₃) δ 4.78 (s, 4H), 7.87 (s, 2H); ¹³C NMR δ 36.6, 102.2, 139.8, 148.9, 162.7. HRMS (EI) calcd

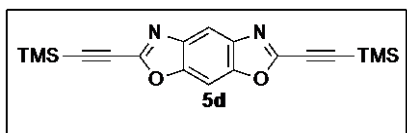
for $C_{10}H_6Cl_2N_2O_2$ 255.9806, found 255.9809, deviation 1.0 ppm.



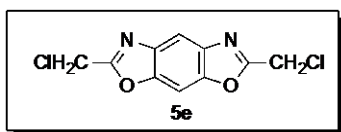
Benzo[1,2-*d*;5,4-*d'*]bisoxazole 5a. Recrystallization from THF/benzene afforded the product in 91% yield. Melting point 206-208°C. 1H NMR ($CDCl_3$) δ 7.79 (s, 1H), 8.16 (s, 3H); ^{13}C NMR δ 94.1, 111.5, 138.1, 148.5, 153.6. HRMS (EI) calcd for $C_8H_4N_2O_2$ 160.02728, found 160.02757, deviation 1.8 ppm.



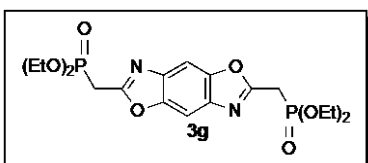
2,6-dimethyl benzo[1,2-*d*;5,4-*d'*]bisoxazole 5b. Recrystallization from heptane afforded the product in 83% yield. melting point 142-143°C (lit. mp. 143 °C).⁷ 1H NMR ($CDCl_3$) δ 2.62 (s, 6H), 7.52 (s, 2H), 7.82 (s, 2H); ^{13}C NMR δ 14.9, 92.8, 109.0, 138.9, 148.7, 164.5. HRMS (EI) calcd for $C_{10}H_8N_2O_2$ 188.05858, found 188.05889, deviation 1.7 ppm.



2,6-(bis trimethylsilyl ethynyl) benzo[1,2-*d*;5,4-*d'*]bisoxazole 5d. Recrystallization from heptane afforded the product in 40% yield. Melting point 186°-187°C. 1H NMR ($CDCl_3$) δ 0.31 (s, 18H), 7.61 (s, 1H), 8.00 (s, 1H); ^{13}C NMR δ 0.5, 91.2, 93.4, 102.8, 111.2, 139.1, 147.9, 149.2. HRMS (EI) calcd for $C_{18}H_{20}N_2O_2Si_2$ 352.10633, found 352.10706, deviation 2.1 ppm.

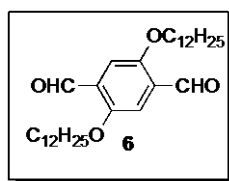


2,6-(bis chloromethyl) benzo[1,2-*d*;5,4-*d'*]bisoxazole 5e. Recrystallization from heptane afforded the product in 73% yield. Melting point 161-162 °C. 1H NMR ($CDCl_3$) δ 4.78 (s, 4H), 7.73 (s, 1H), 8.06 (s, 1H); ^{13}C NMR δ 36.5, 94.1, 111.6, 138.9, 149.6, 162.0. HRMS (EI) calcd for $C_{10}H_6Cl_2N_2O_2$ 255.9806, found 255.9804, deviation 0.9 ppm.



2,6-dimethyl benzo[1,2-*d*;4,5-*d'*]bisoxazole-diethylphosphonate Ester) 3g. Triethylphosphite (1.63

g, 9.8 mmol) and 2,6-(bis chloromethyl) benzo[1,2-*d*;4,5-*d'*]benzobisoxazole **3e**, (840 mg, 3.3 mmol) were heated to 150 °C for 4 h. The reaction was cooled and the crude product obtained as a solid. Recrystallization from xylenes affords the product in 94% yield. Melting point 145-146 °C. ¹H NMR (300 MHz, CDCl₃): δ 1.33 (t, 12H), 3.58 (d, 4H), 4.19 (m, 8H), 7.79 (s, 2H). ¹³C NMR δ 16.59, 16.65, 27.88, 29.27, 63.27, 63.34, 101.3, 139.6, 148.8, 160.2, 160.3. HRMS (EI) calcd for C₁₈H₂₆N₂O₈P₂ 460.11643, found 460.11761, deviation 2.6 ppm.



2,5-didodecyloxy-1,4-benzene dicarboxaldehyde 6 was synthesized in 26% yield, according to the literature procedure.⁸ Melting point 72-73 °C. ¹H NMR (300 MHz, CDCl₃): δ 0.877 (t, 6H), 1.26-1.54 (m 40H), 4.08 (t, 4H), 7.43 (s, 2H), 10.52 (s, 2H).

Synthesis of Polymer 7. Compound **3g** (370 mg, .80 mmol) and **2,5-didodecyloxy-1,4-benzene dicarboxaldehyde 6** (400 mg, .80 mmol) were dissolved in 15 mL of THF. Then a 1M solution of potassium *tert*-butoxide in THF (2 mL, 2.4 mmol) was added to the solution and the mixture and the solution was heated to reflux for 24 h to obtain a red solution. The solution was then precipitated in MeOH and filtered to obtain a red-orange solid. The resultant polymer was purified via Soxhlet extraction (MeOH, hexane and THF). Evaporation of the THF layer yielded the polymer, 0.256 g, 86% yield. ¹H-NMR (400 MHz, CDCl₃): δ 0.887 (m, CH₃-), 1.29 (br m, -(CH₂)₁₀-), 4.13 (br m, -OCH₂-), 7.39-7.46 (br m, Ar-H and vinylic peaks), 10.46 terminal aldehyde peak, 10.73 terminal P(=O)(OH)₂. UV-Vis (THF) λ_{max} = 476 nm. GPC: M_n = 5,672, M_w = 10,091, PDI = 1.77. Fluorescence (THF): λ_{em} = 515 nm (λ_{exc} = 476 nm).

2.7.3 References

- (1) Inbasekaran, M.; Strom, R. *OPPI Briefs* **1994**, *23*, 447-450.
- (2) Schmitt, R.J.; Ross, D.S.; Hardee, J.R.; Wolfe, J.F. *Journal of Organic Chemistry* **1988**, *53*, 5568-5569.
- (3) Wolfe, J.F.; Arnold, F.E. *Macromolecules*, **1981** *14*, 909-915.
- (4) Beyerstedt, F.; McEkvain, S.M. *Journal of the American Chemical Society*

1937, 59, 1273-1275.

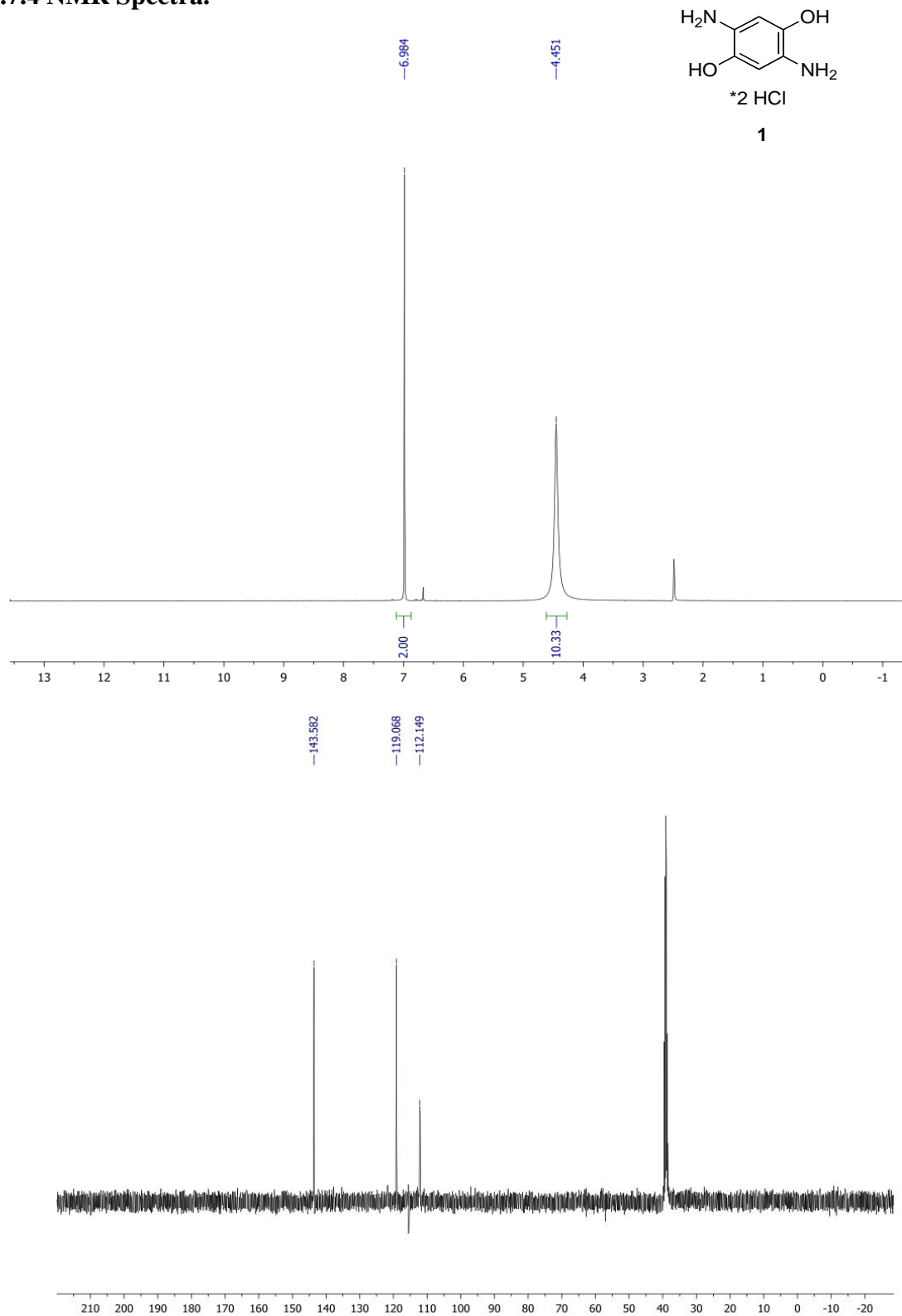
(5) Mylari, B.L.; Scott, P.J.; Zembrowski, W.J. *Synthetic Communications* **1989**, 19(16), 2921-2924.

(6) Osman, A.M.; Mohamed, S.A. *Indian Journal of Chemistry* **1973**, 11(9), 868-870.

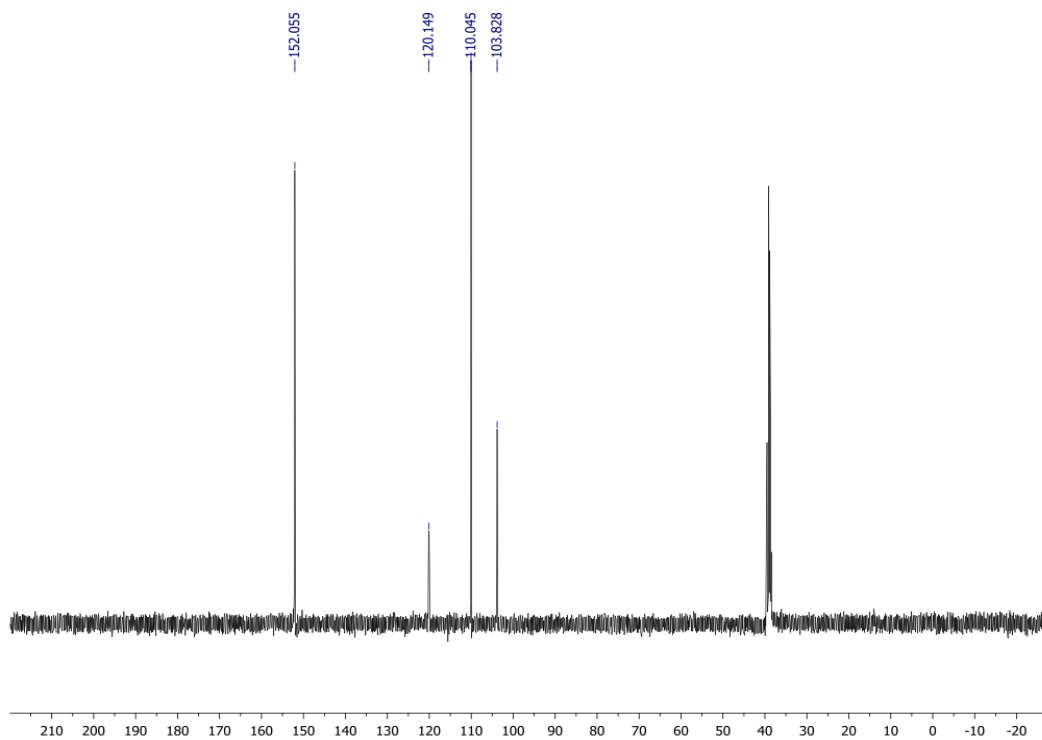
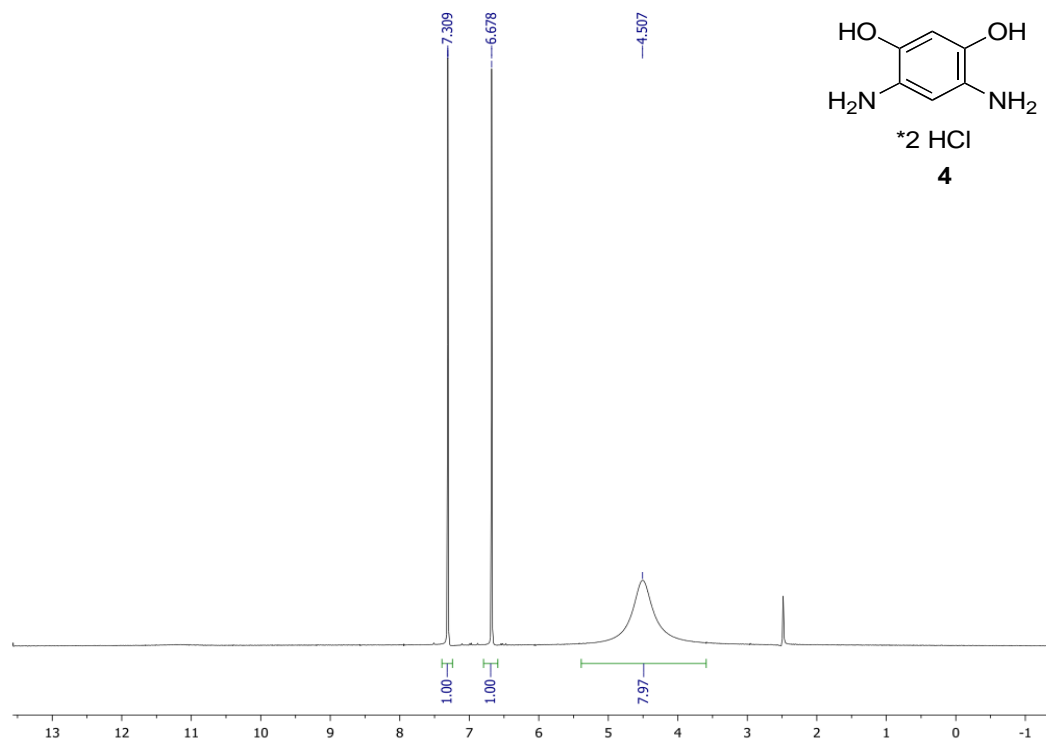
(7) Fries, K.; Beyerlein, F. *Justus Liebig's Annals de Chemie* **1936**, 527, 71-83.

(8) Liao, J.; Wang, Q. *Macromolecules* **2004**, 37(18), 7061-7063.

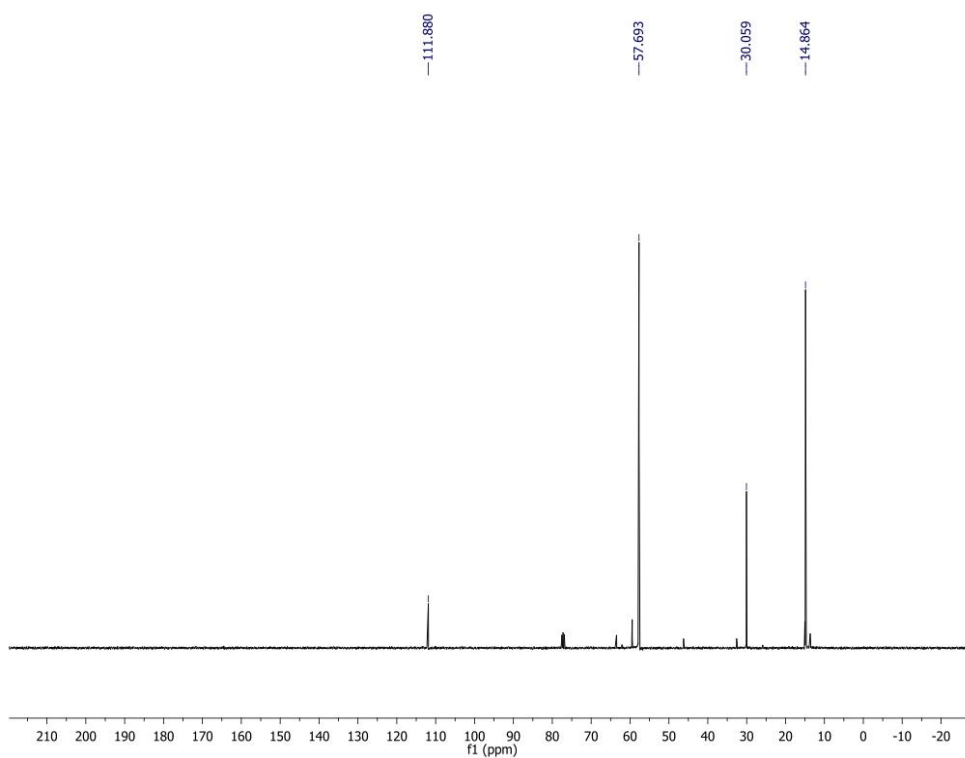
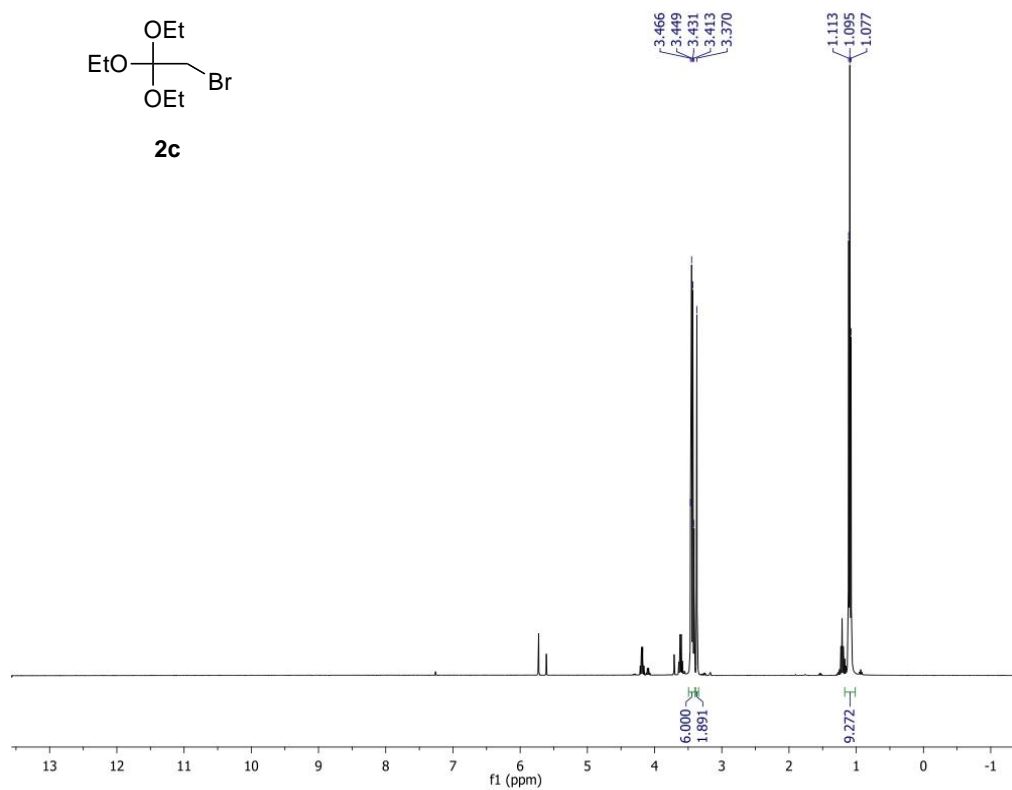
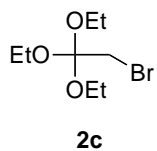
2.7.4 NMR Spectra.



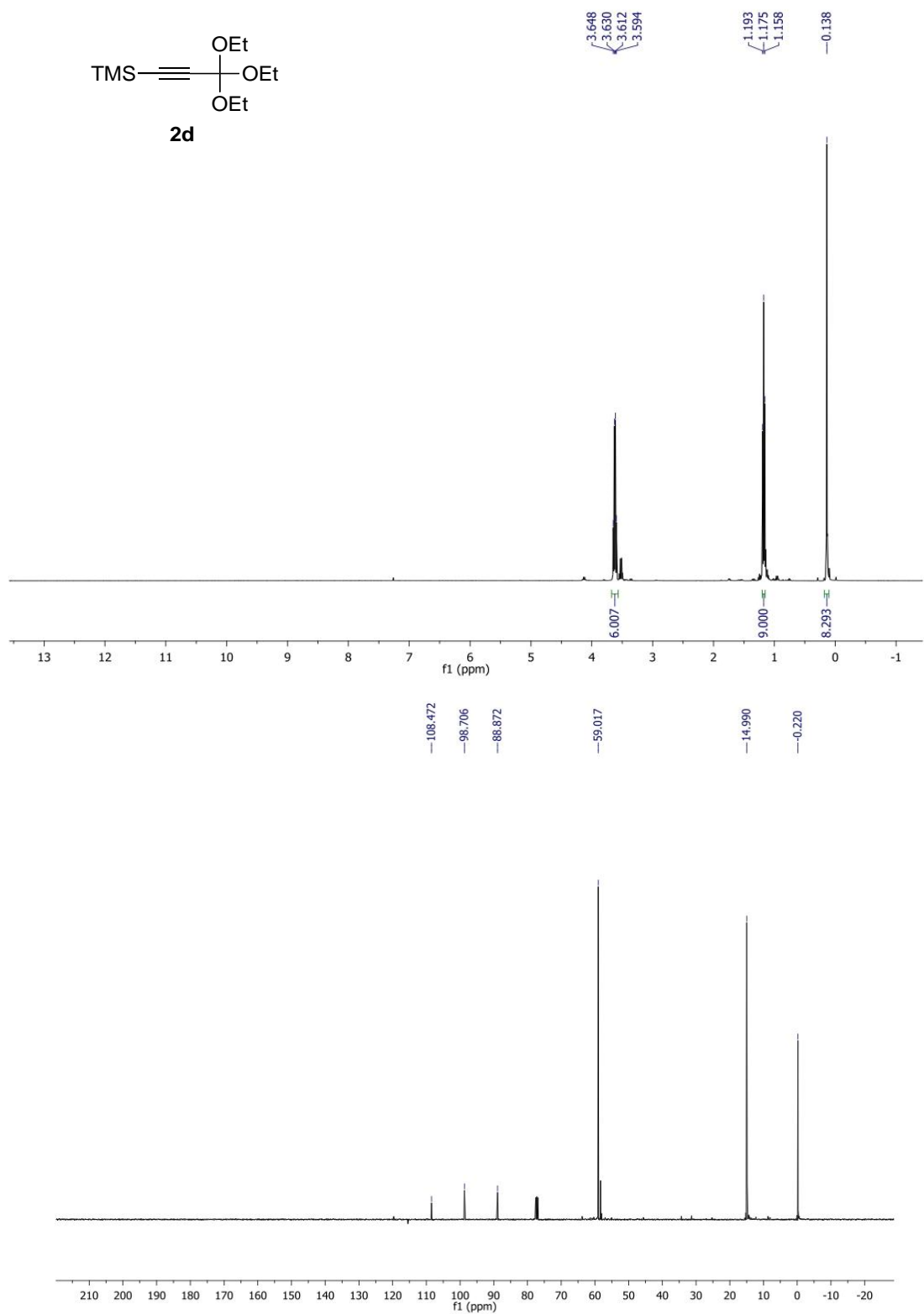
NMR Spectra (cont.)



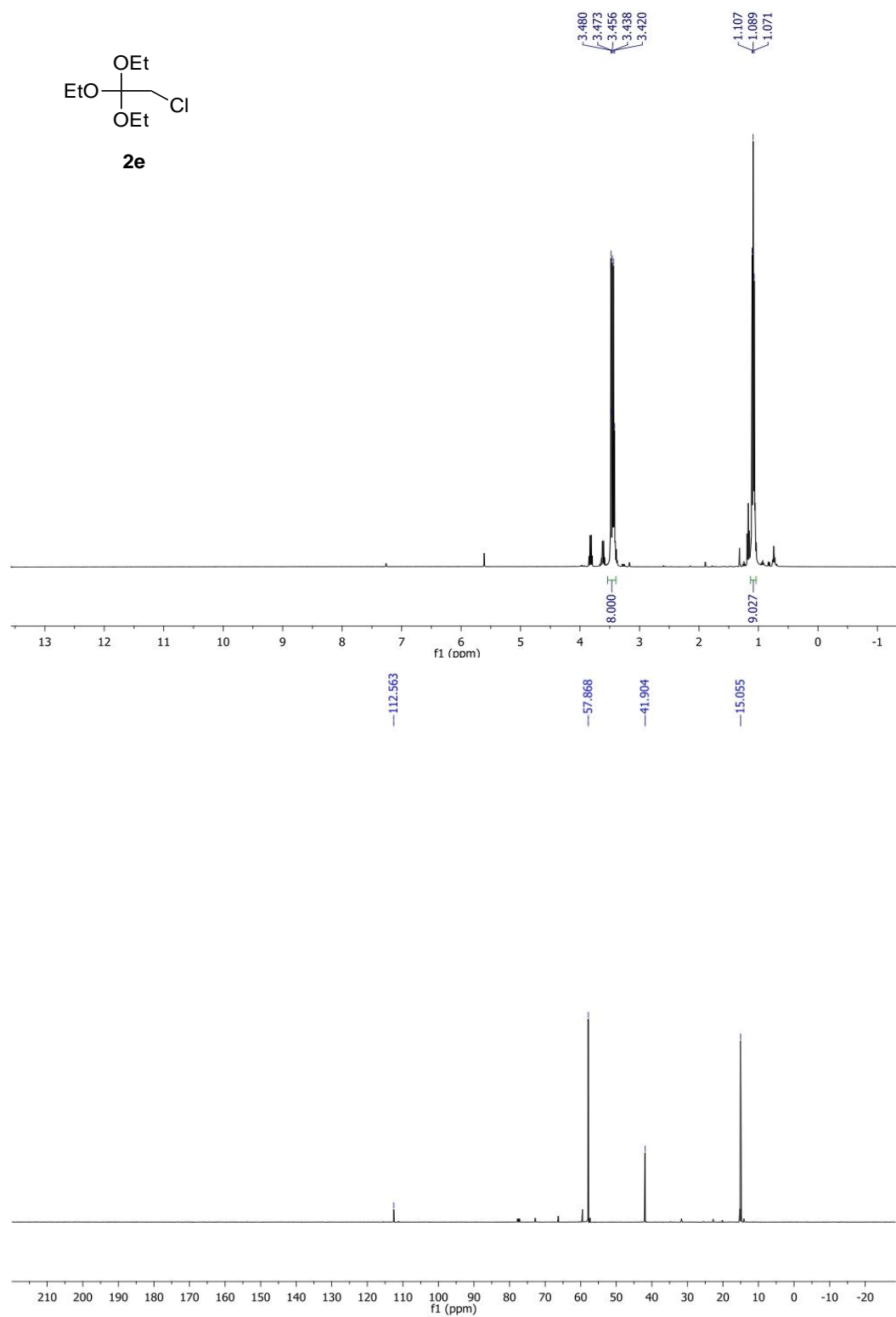
NMR Spectra (cont.)



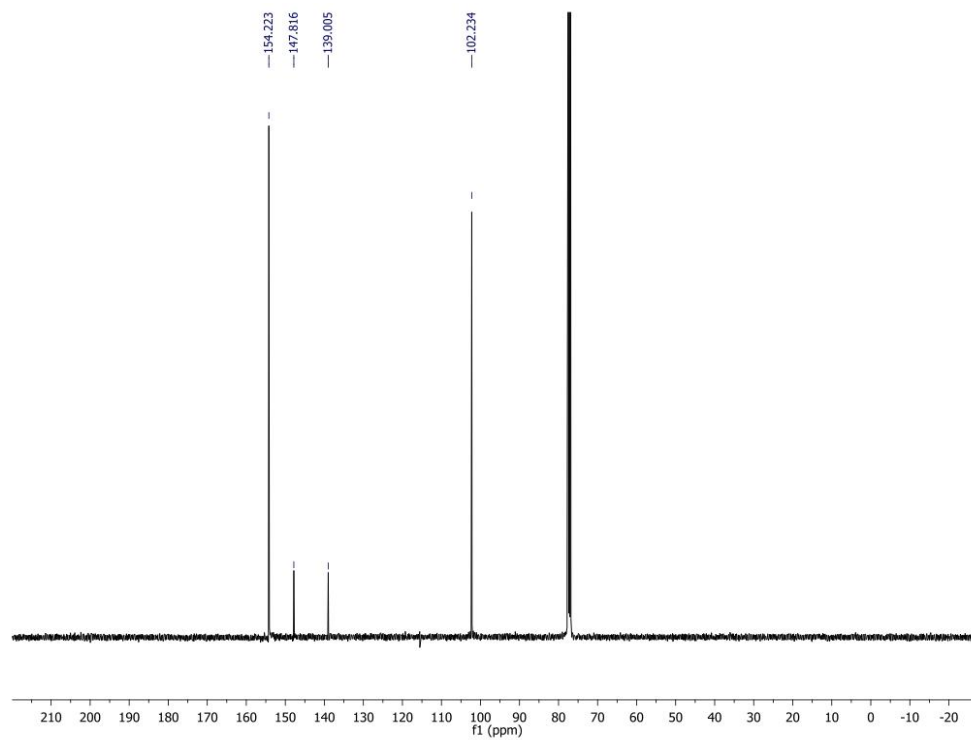
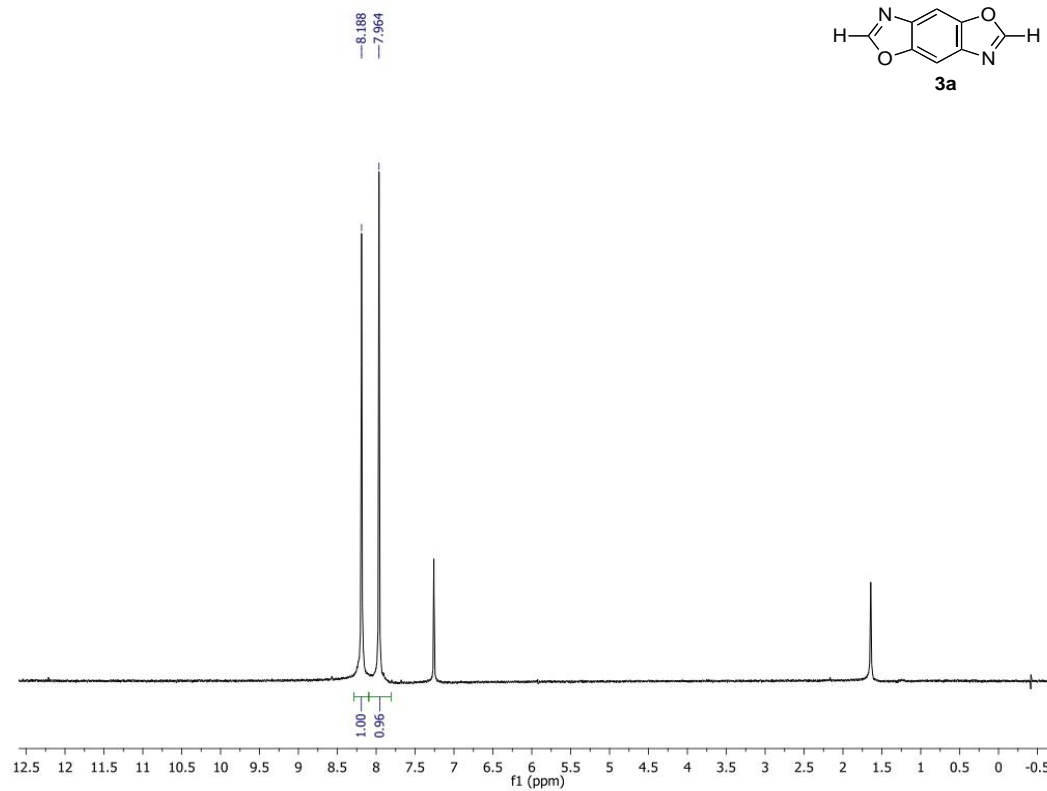
NMR Spectra (cont.)



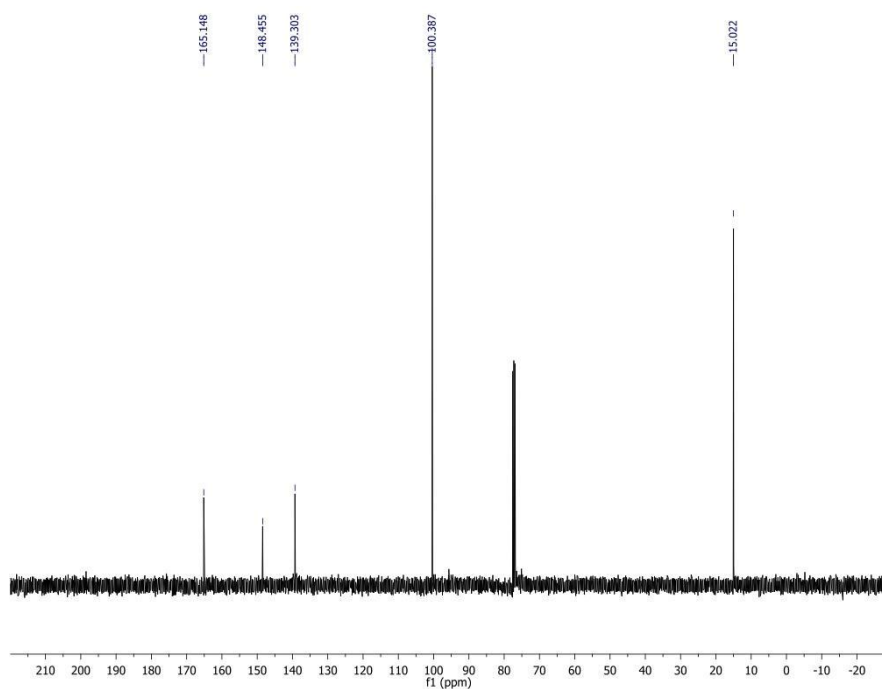
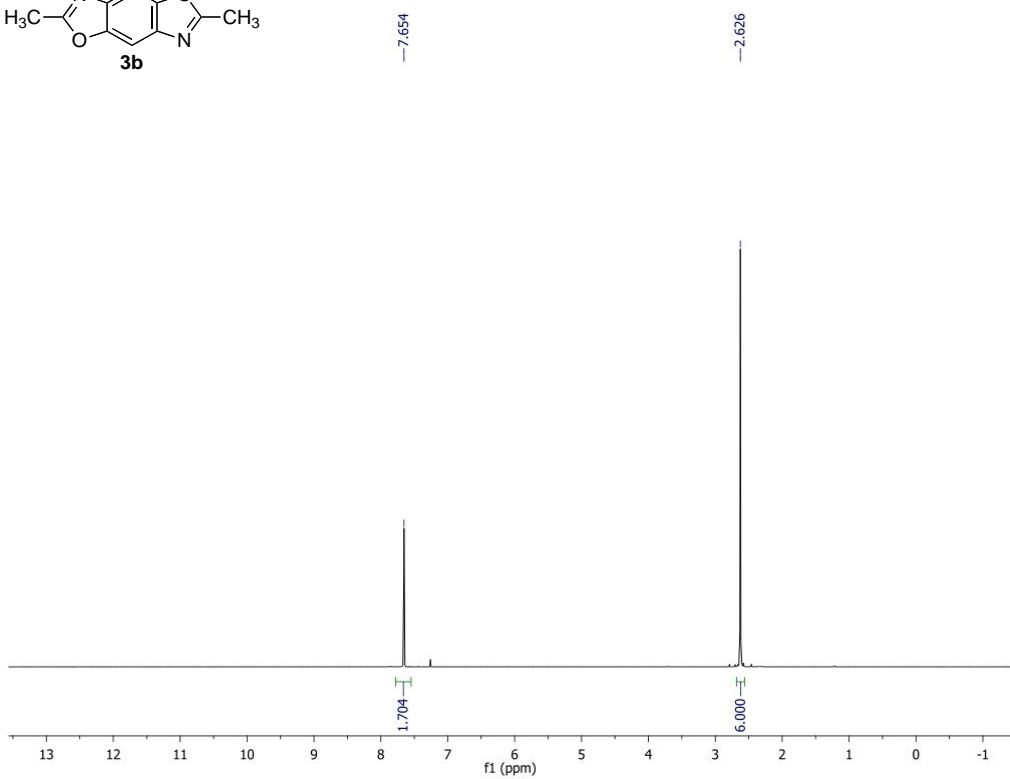
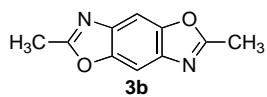
NMR Spectra (cont.)



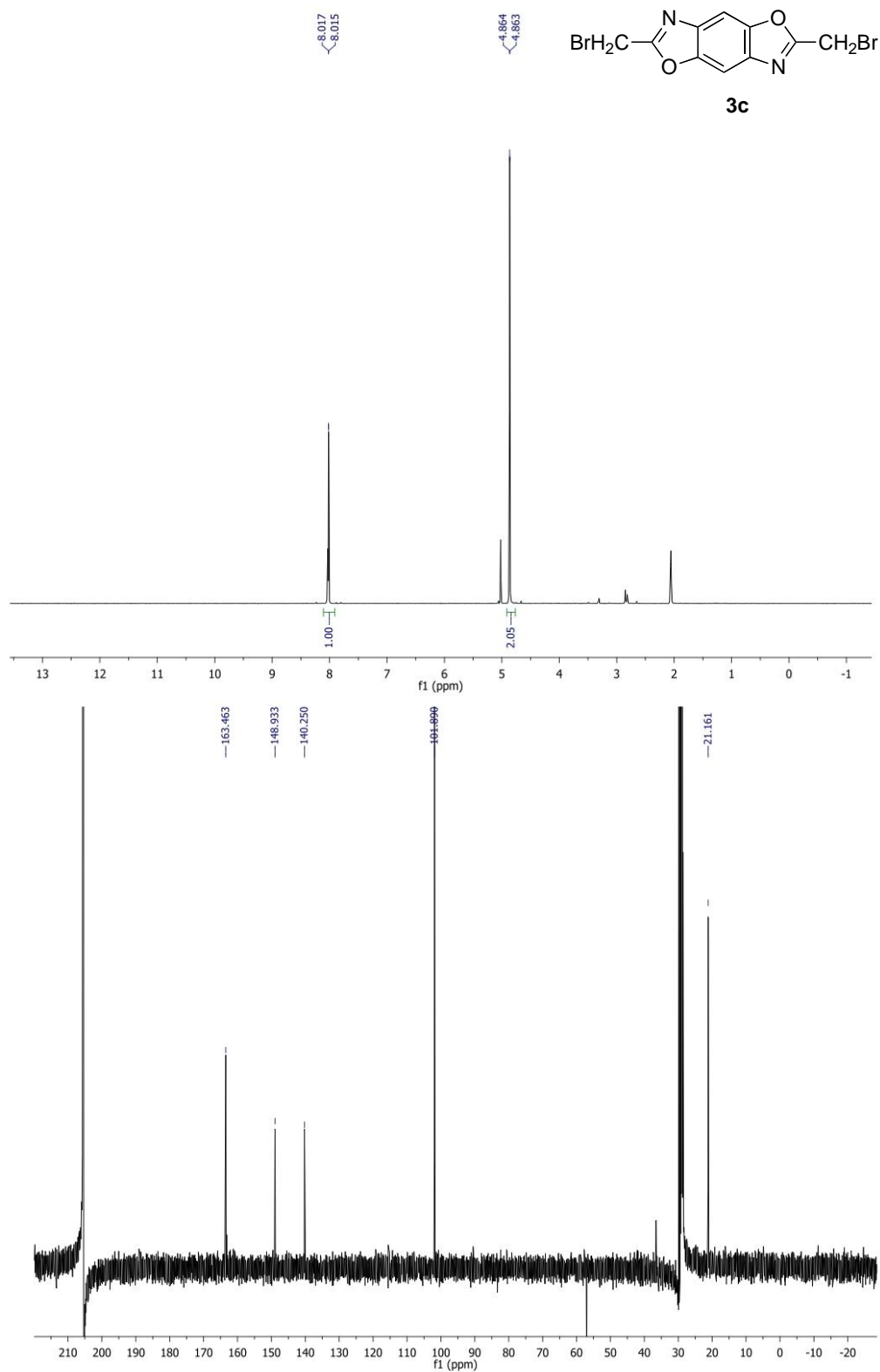
NMR Spectra (cont.)



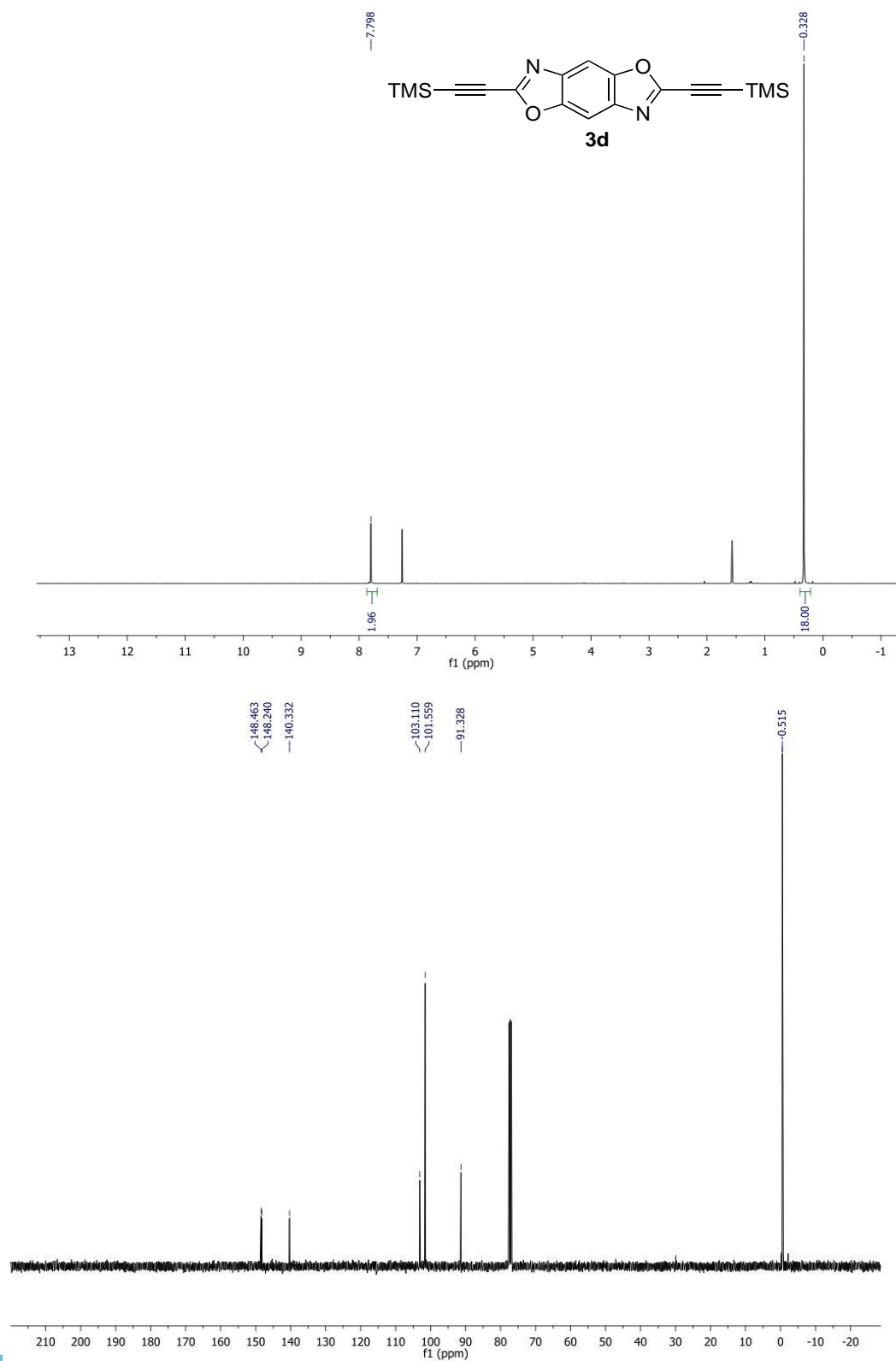
NMR Spectra (cont.)



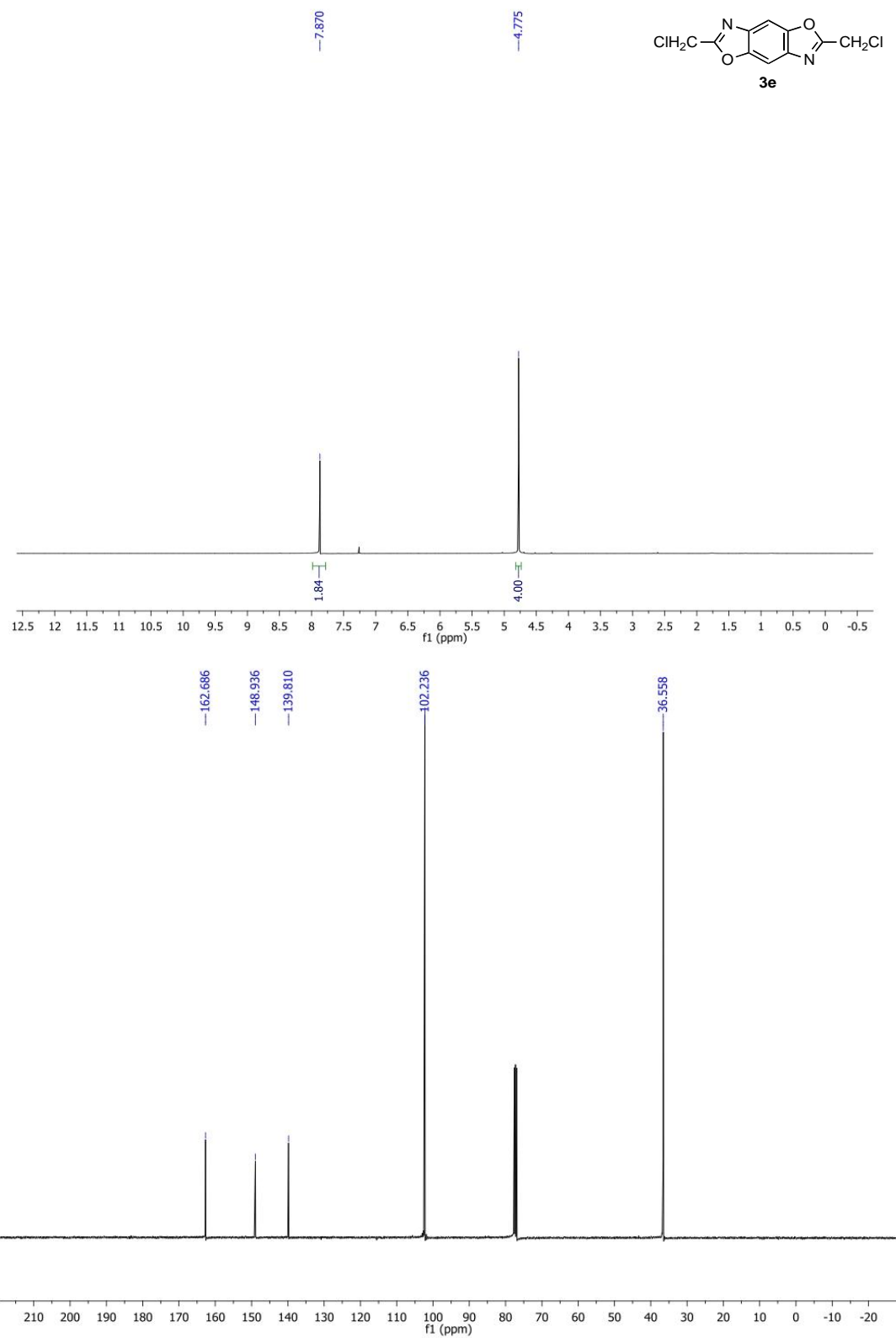
NMR Spectra (cont.)



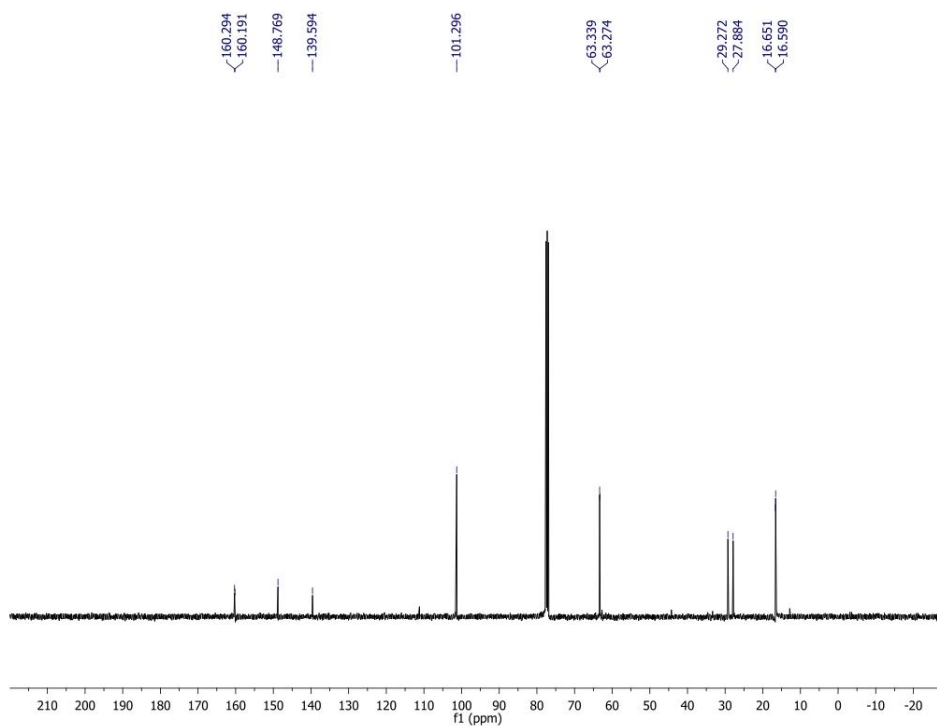
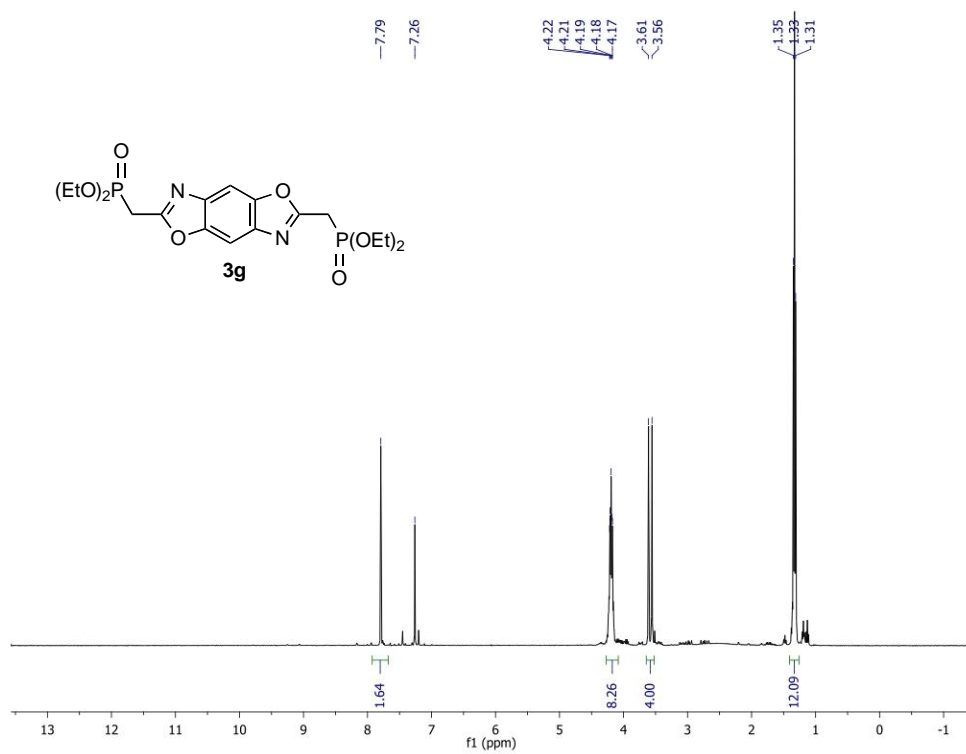
NMR Spectra (cont.)



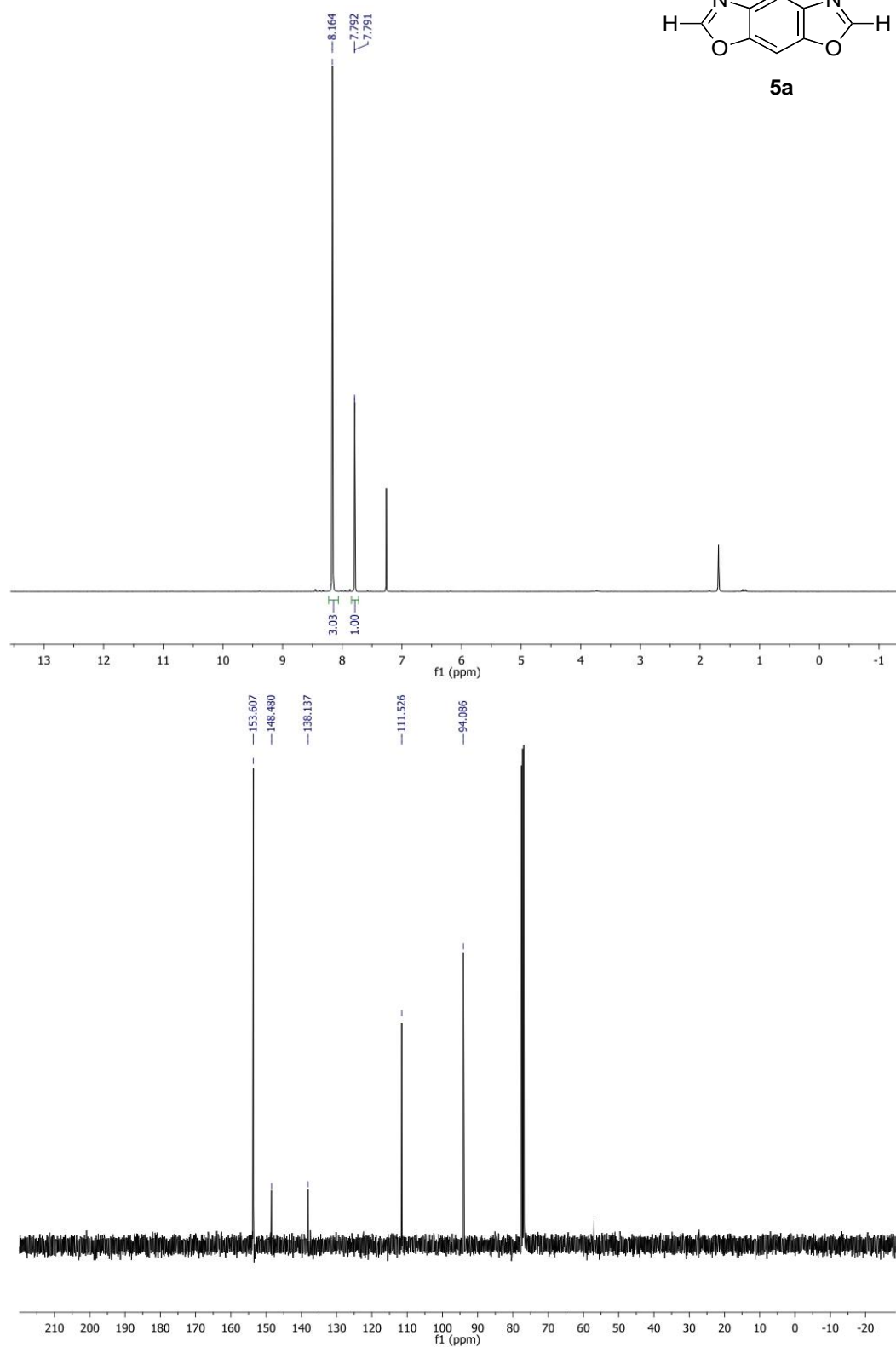
NMR Spectra (cont.)



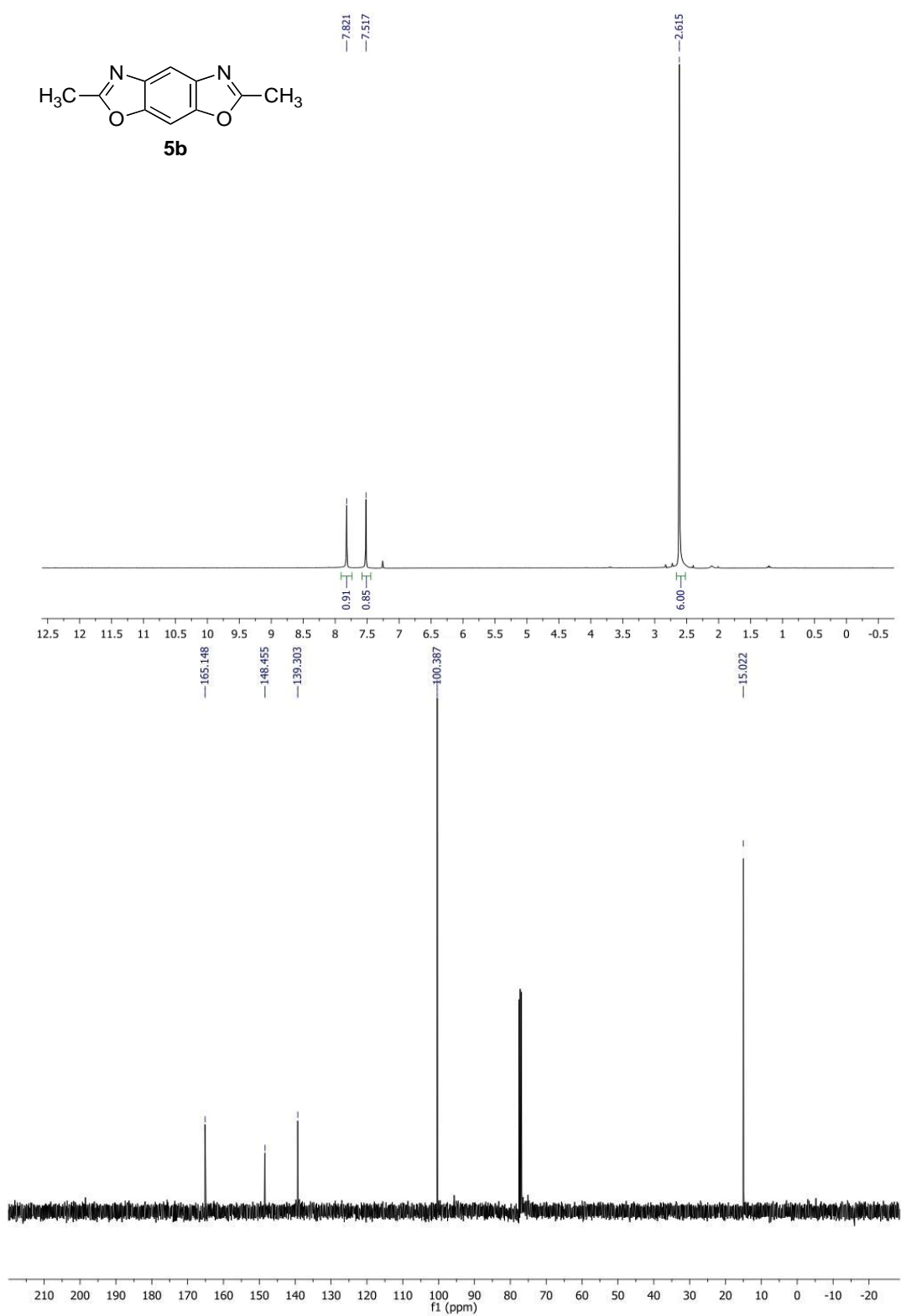
NMR Spectra (cont.)



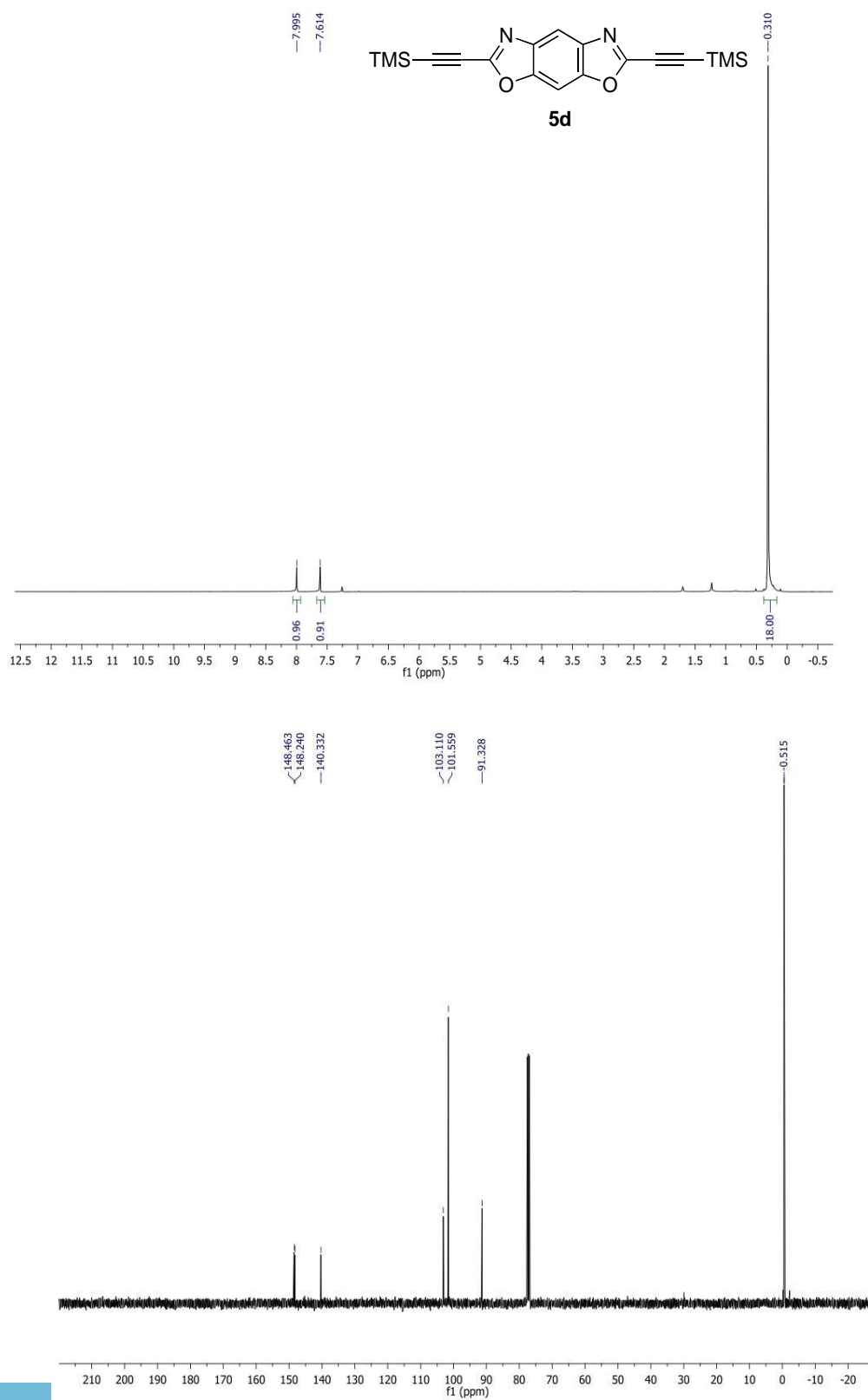
NMR Spectra (cont.)



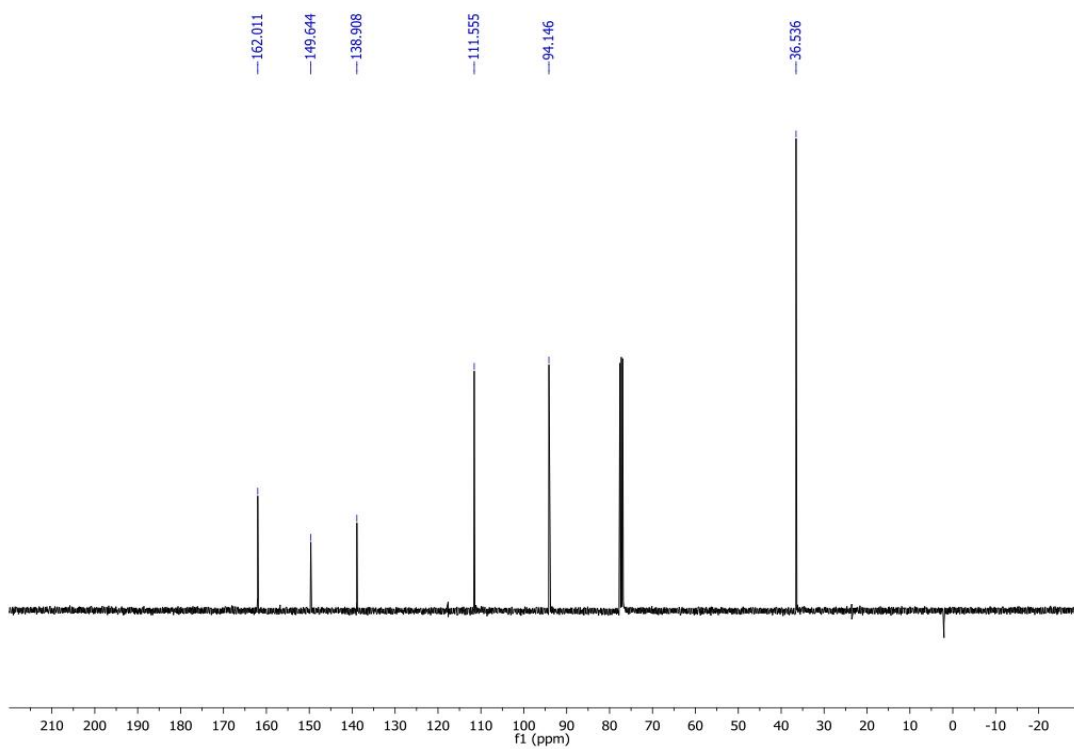
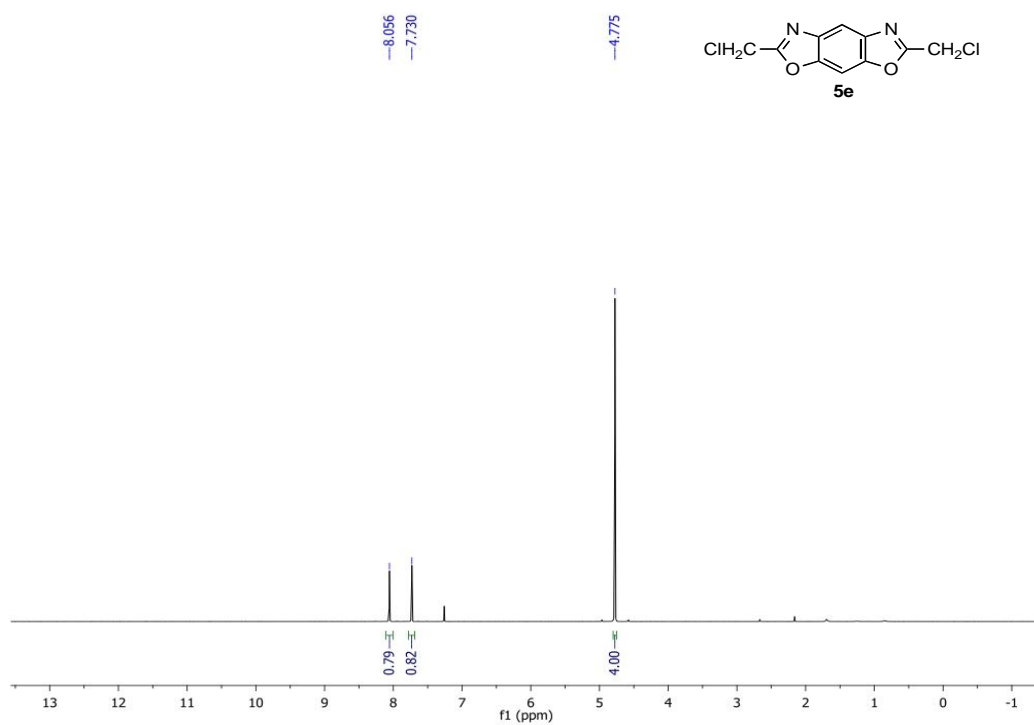
NMR Spectra (cont.)



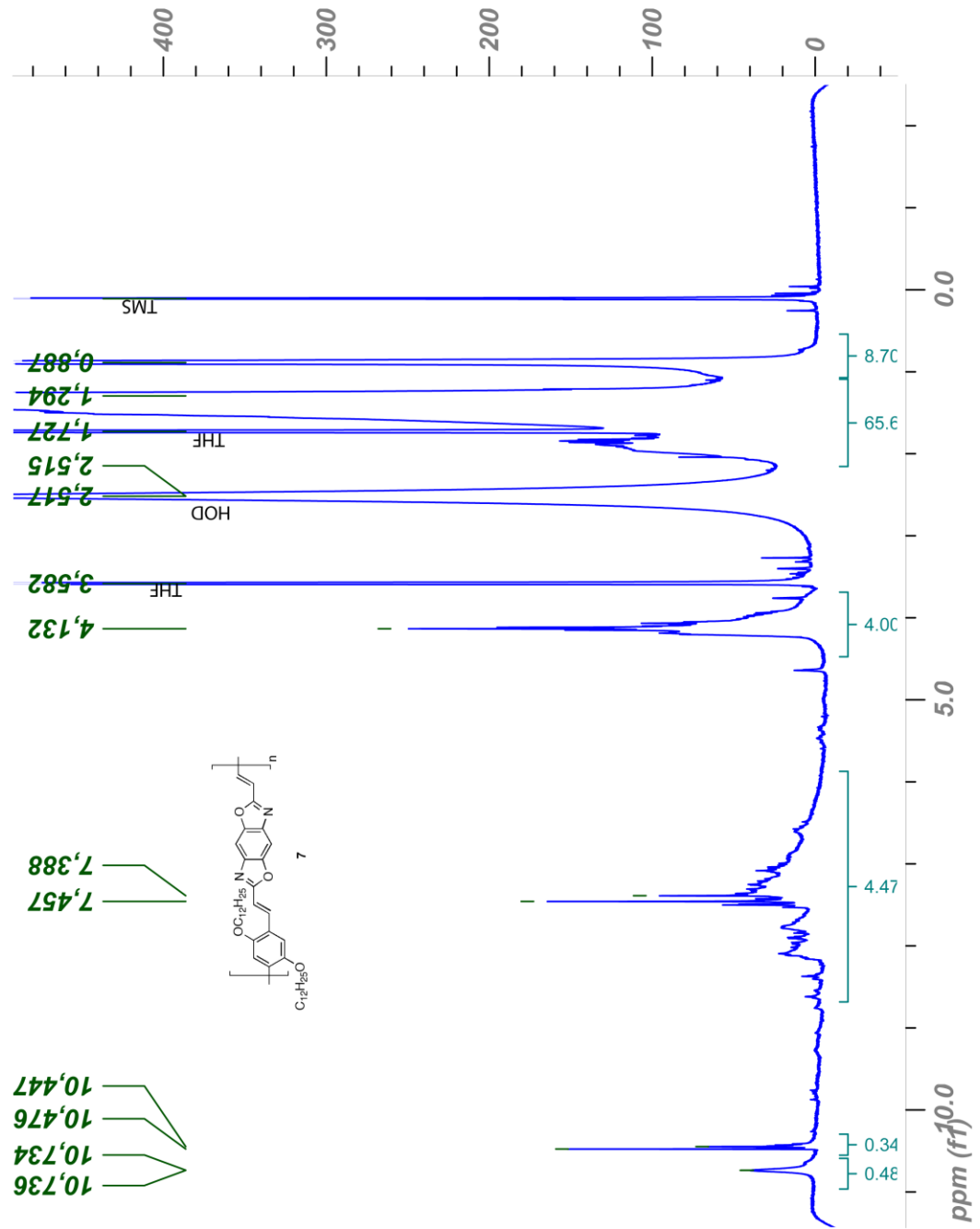
NMR Spectra (cont.)

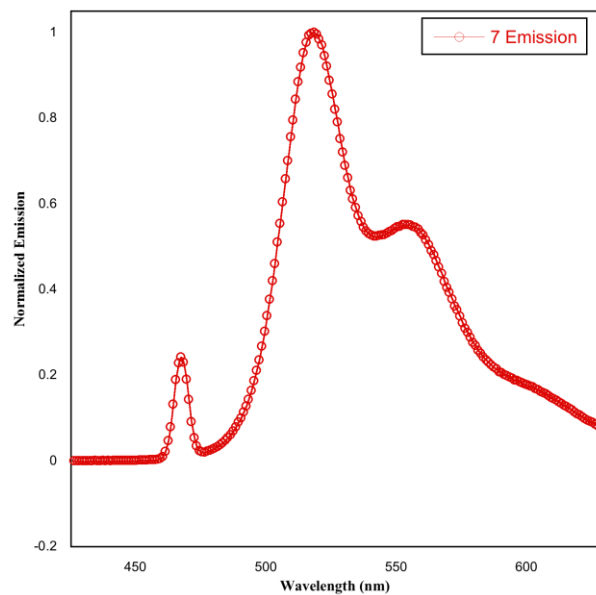
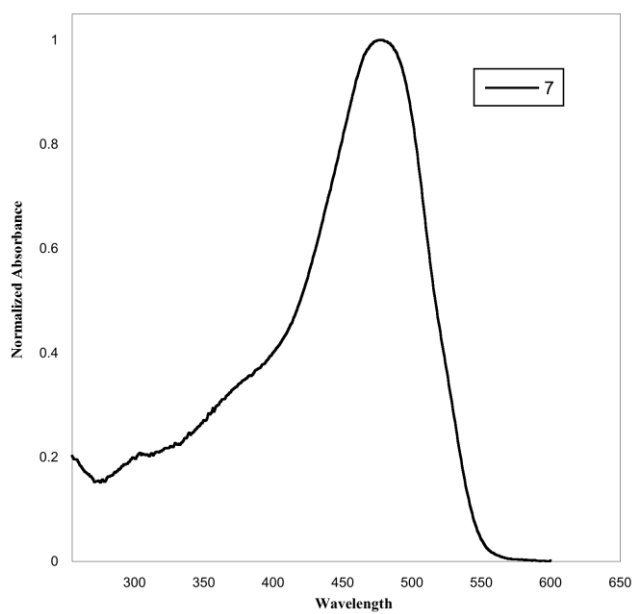
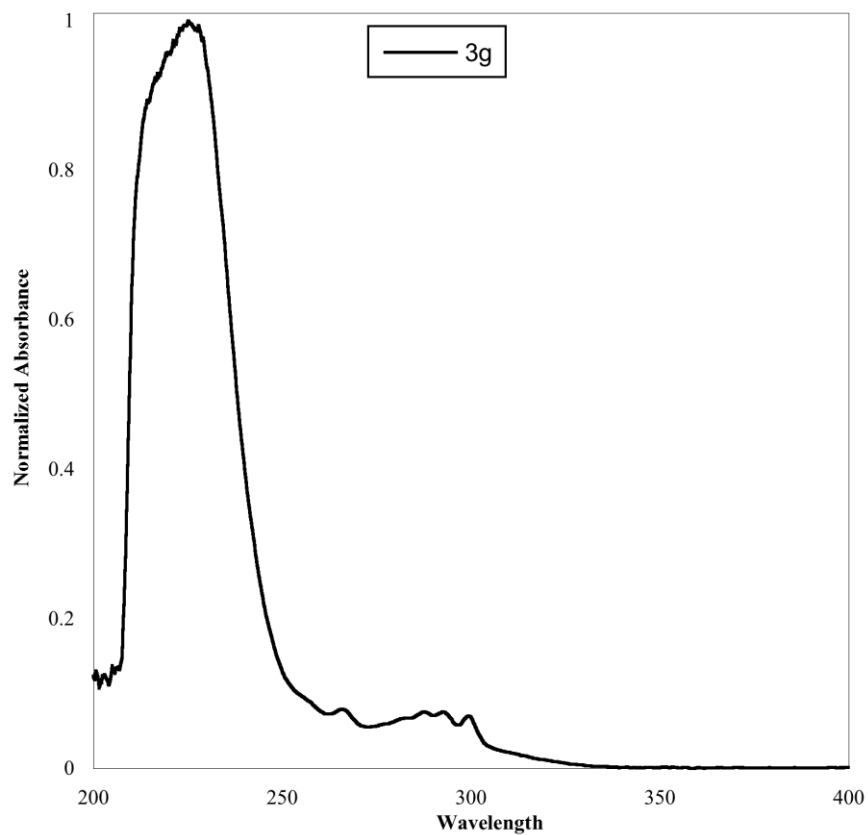


NMR Spectra (cont.)



NMR Spectra (cont.)





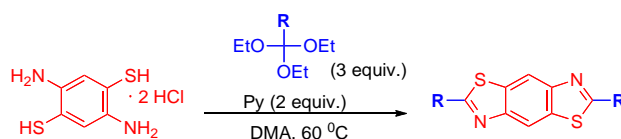
CHAPTER 3

Facile Synthesis of 2,6-Disubstituted Benzobisthiazoles: Functional Monomers for the Design of Organic Semiconductors.

Reproduced from *Journal of Organic Chemistry* **2010**, 75, 495 with permission from American Chemical Society.

Copyright © 2011

Jared F. Mike, Jeremy J. Inteman, Arkady Ellern and Malika Jeffries-EL*
Department of Chemistry, Iowa State University, Ames, IA 50011-3111

3.1 ABSTRACT

The synthesis of several synthetically useful 2,6-disubstituted benzobisthiazoles is described. The method is based on the Lewis Acid catalyzed ring-closing reaction between substituted orthoesters and diamino benzene dithiol. The resulting benzobisthiazoles are obtained cleanly and in good yields. These materials are of interest for the development of new organic semiconductors.

3.2 INTRODUCTION

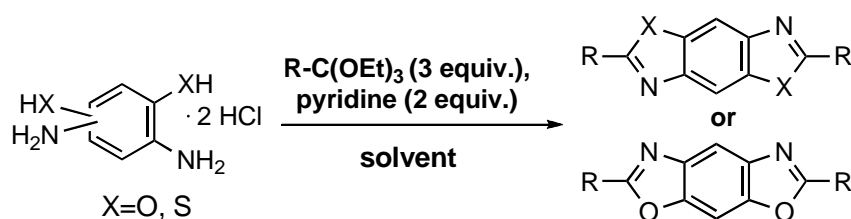
The design and synthesis of new organic semiconducting materials is of current interest due to the important roles these materials play in the development of plastic electronics.¹ Although many π -conjugated materials are known, most of them are electron rich and exhibit electron-donating and hole-transporting (p-type) electronic properties. Thus the synthesis of electron-deficient π -conjugated materials, which can exhibit electron-accepting and electron-transporting properties (n-type), remains an important problem in the field.

The electron-deficient benzo[1,2-*d*;4,5-*d'*]bisthiazole moiety (trans-BBZT) is a

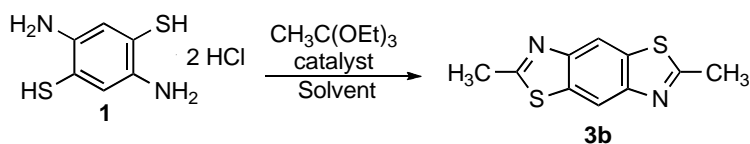
promising building block for the development of new organic semiconductors because materials containing benzobisthiazoles exhibit high fluorescence,² thermal stability,^{3, 4} electron affinity,⁵ and interesting nonlinear optical properties.^{2, 6, 7} Typical synthesis of benzobisthiazoles requires strong acids or oxidants⁸ and high temperatures.⁹ These harsh reaction conditions restrict the types of substituents that can be incorporated onto these moieties, hindering the exploration of materials containing benzobisthiazoles.

Recently we reported the synthesis of 2,6-disubstituted benzobisoxazoles using substituted orthoesters and rare earth metal triflates as catalysts.¹⁰ These reaction conditions facilitated the synthesis of novel benzobisoxazoles bearing a variety of substituents cleanly and in high yield. Inspired by these promising results, we set out to develop a mild, lowtemperature method for the synthesis of the analogous 2,6-disubstituted benzobisthiazoles. Although benzo[1,2-*d*;4,5-*d'*]bisoxazole (*trans*-BBO) and *trans*-BBZT are structurally similar, the sulfur atom is less electronegative than the oxygen atom, and has similar electronegativity to the carbon atom. Thus the electron density is more equally shared between sulfur and carbon in *trans*-BBZT than between oxygen and carbon in *trans*-BBO and the π -orbitals will be more delocalized. Additionally, the empty *d*-orbitals of the sulfur atom can contribute to the molecular π -orbitals decreasing the energy of the π - π^* transition.^{7, 11} These changes can be beneficial for the development of new organic semiconducting materials. Herein, we report the successful synthesis of several new benzobisthiazoles. We also demonstrate that functionality can be increased by a simple reaction following ring formation.

3.3 RESULTS AND DISCUSSION



Scheme 1. Synthesis of 2,6-Disubstituted Benzobisoxazoles



entry	solvent	catalyst	temp (°C)	time (h)	yield ^b (%)
1	DMSO	Y(OTf) ₃	50	n/a	0
2	none	none ^c	90	6	51
3	none	H ₂ SO ₄ ^c	90	3	45
4	DMAc	Eu(OTf) ₃	50	1.5	77
5	DMAc	La(OTf) ₃	50	1.5	72
6	DMAc	Sc(OTf) ₃	50	1.5	75
7	DMAc	Y(OTf) ₃	50	1.5	69
	DMAc	Yb(OTf) ₃	50	1.5	77

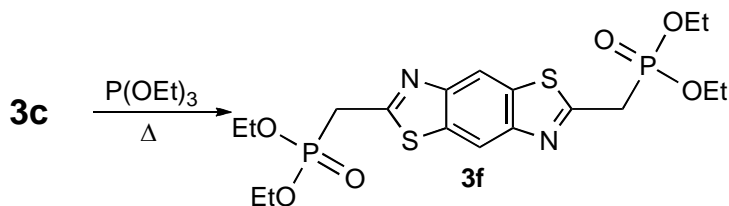
^a Standard reaction conditions: substrate 1 M in solvent, 3 equiv of ortho ester, 5 mol % catalyst, and pyridine 2 equiv. ^b Isolated yields. ^c 10 equiv. of orthoester used without pyridine.

Table 1. Optimization reactions using DABDT **1** and triethyl orthoacetate **2b**.

The general synthetic route for the benzobisazoles is shown in Scheme 1. Previously, we found that best reaction conditions for the synthesis of benzobisoxazoles are DMSO as a solvent, pyridine as a cosolvent, and rare metal triflates as catalysts.¹⁰ The use of the pyridine as a cosolvent is beneficial since it scavenges the hydrochloride salts that coordinate with the diamino diol. Removing the acids prevents the decomposition of the substituted orthoesters, which is catalyzed by protic acids.¹⁰ Using the reaction between 2,5-diamino-1,4-benzenedithiol (DABDT) (**1**) and triethylorthoacetate (**2b**) as a model, we explored these conditions. Unfortunately, when DABDT was mixed with pyridine in DMSO, an insoluble green precipitate was formed. This was most likely caused by the formation of disulfide linkages, although the insolubility of the material prevented its characterization (entry 1). We then attempted to perform the reaction without any additional solvents, using 10 equivalents of the triethylorthoformate and the coordinated hydrochloride salts as an acid catalyst (entry 2). These conditions produced 2,6-dimethylbenzobisthiazole **3b** in a 51% yield. Using the same reaction conditions and

sulfuric acid as a catalyst, similar results were obtained (entry 3). In both cases the resulting products were formed along with some dark impurities, which could be removed after careful recrystallization.

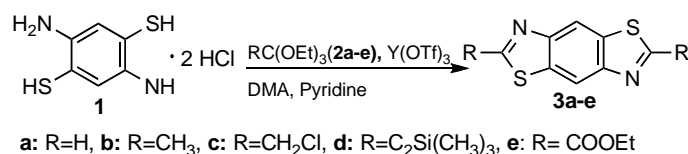
To reduce the amount of orthoester required for these reactions, we performed a solubility test with DABDT to find a cosolvent. We investigated the use of DMA as a solvent, since DABDT dissolves in DMA at room temperature, and this solvent was not prone to the side reactions experienced previously. The reaction of DABDT and triethylorthoformate occurs rapidly, when performed slightly above room temperature. The solid that forms is easily isolated by precipitation into water and filtration. We then explored the use of several different rare earth metal triflates to catalyze the reaction. The results are summarized in Table 1. On the basis of the model reactions, we found that most triflates gave similar results. Since all of these catalysts are commercially available, our bias toward the use of $\text{Eu}(\text{OTf})_3$, $\text{La}(\text{OTf})_3$, or $\text{Y}(\text{OTf})_3$ was due to their lower cost relative to the other rare earth metal triflates.



Scheme 2. Synthesis of monomer **3f**.

Upon determining the optimum reaction conditions, we evaluated the scope of this reaction with respect to the orthoester. To accomplish this we utilized the commercially available triethyl orthoformate (**2a**) in addition to triethyl orthochloroacetate (**2c**), triethyl orthopropiolate (**2d**), and ethyl triethoxyacetate (**2e**), which were prepared in our laboratories. In all cases the orthoesters reacted with DABDT cleanly and in moderate yields. As a follow-up to our previous work, we also explored the use of DMA as a solvent for the synthesis of benzobisoxazoles. Interestingly, significantly lower yields were observed with DMSO as solvent.¹⁰ These lower yields were most likely due to the poor solubility of diaminoquinone and diaminoresorcinol in this solvent. We did

not investigate the synthesis of benzo[1,2-*d*;5,4-*d'*]bisthiazole (*cis*-BBZT) derivatives because of the inability to synthesize 4,6-diamino-1,3-benzene dithiol. Although the synthesis of this compound has been reported previously,¹² we, like those before us, have struggled to obtain pure material due to its instability.⁴



ortho ester	benzobisthiazole	% yield ^a
2a	 3a	68
2c	 3c	59
2d	 3d	38
2e	 3e	53 ^c

^a Standard reaction conditions: substrate 1 M in solvent, 3 equiv of ortho ester, 5 mol % catalyst, and pyridine 2 equiv, 1.5 hours. ^b Isolated Yields. ^c Reaction time was 18 hours.

Table 2. Reaction of **1** with Various Orthoesters **2a**, **2c-e**.

To increase the functionality of these BBZT derivatives, we synthesized the diphosphonate ester **3f** via the Arbuzov reaction of **3c** with triethylphosphite (Scheme 2). This reaction occurred cleanly to produce the **3f** in an 80% yield (Table 2). Monomers of this type have been useful for the synthesis of vinylenes polymers via the Horner-Wadsworth-Emmons reaction.

We were able to obtain X-ray quality crystals of **3a**, **3b**, **3c**, and **3f** suitable for analyses to be performed by recrystallization. Detailed crystallographic data can be found in the Supporting Information, and a representative example is shown in Figure 1. In addition to confirming the identity of these new compounds, the X-ray analyses show that these monomers are all planar with a mean deviation from planarity of 0.0114 Å. The flat

nature of the benzobisthiazoles is beneficial to promoting efficient π -stacking and improving the charge transport of materials derived from them.

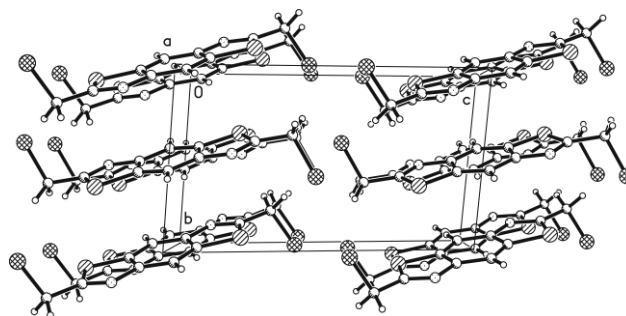


Figure 1. A single crystal X-ray ORTEP structure, (50 % probability) of **3c**.

In summary, we have developed a new method for the synthesis of novel 2,6-disubstituted benzobisthiazoles. The benefits of this approach include the mild reaction conditions and ease of purification without column chromatography. Currently we are developing new organic semiconductors using these compounds.

3.4 EXPERIMENTAL SECTION

Typical Procedure for the Synthesis of Benzobisthiazoles (3a-e). Benzo[1,2-*d*;4,5-*d'*]bisthiazole (**3a**). In a round-bottomed flask 2,5-diamino-1,4-benzene dithiol **1** (1.23 g, 5.0 mmol) and pyridine (791 mg, 10.0 mmol) were dissolved in DMA (10 mL). The resulting solution is added via a syringe to a mixture of triethylorthoformate **2a** (2.22 g, 15.0 mmol) and Y(OTf)₃ (134 mg, 0.255 mmol) in a round-bottomed flask. The reaction is stirred at 55 °C for 1 h and then cooled. The reaction is diluted with water and the crude product collected by filtration. Recrystallization of the crude with dichloromethane/heptanes gave white needles (0.65 g, 68% yield). Melting point >260 °C. ¹HNMR (400 MHz; DMSO-*d*₆) δ 8.92 (2H, s), 9.49 (2H, s); ¹³CNMR (100 MHz; DMSO-*d*₆) δ 116.3, 132.7, 151.2, 157.9. HRMS (EI) 191.98189, C₈H₄N₂S₂ requires 191.98159, deviation 1.6 ppm.

2,6-Dimethylbenzo[1,2-*d*;4,5-*d'*]bisthiazole (3b). Compound **3b** was synthesized following the same protocol as for compound **3a** with **4** and triethylorthoacetate **2b**. The product was obtained after recrystallization from dichloromethane/heptanes as white needles (0.85 g, 77% yield). Melting point 232-233 °C. ¹HNMR (400 MHz; CDCl₃) δ 2.86 (6H, s), 8.34 (2H, s); ¹³CNMR (100 MHz; CDCl₃) δ 20.5, 114.4, 134.5, 151.0, 167.9. HRMS (EI) 220.01289, C₁₀H₈N₂S₂ requires 220.01330, deviation 1.9 ppm.

2,6-Bis(chloromethyl)benzo[1,2-*d*;4,5-*d'*]bisthiazole (3c). Compound **3c** was synthesized following the same protocol as for compound **3a** with **4** and triethyl orthochloroacetate **2c**. The product was obtained after recrystallization from heptanes as pale yellow needles. The reaction was run on 15 mmol scale with a 2.54 g yield (59%). Melting point 219-220 °C. ¹HNMR (400 MHz; DMSO-*d*₆) δ 5.28 (4H, s), 8.82 (2H, s); ¹³CNMR (100 MHz; DMSO-*d*₆) δ 42.1, 116.5, 134.7, 150.5, 168.8. HRMS (EI) 287.93549, C₁₀H₆C₁₂N₂S₂ requires 287.93495, deviation 1.9 ppm.

2,6-Bis(trimethylsilylethynyl)benzo[1,2-*d*;4,5-*d'*]bisthiazole (3d). Compound **3d** was synthesized following the same protocol as for compound **3a** with **4** and triethyl orthopropiolate **2d**. The product was obtained after recrystallization from pentane as pale yellow needles (38% yield). Melting point >260 °C (pentane). ¹HNMR (400 MHz; CDCl₃) δ 0.331 (18H, s), 8.478 (2H, s); ¹³CNMR(100 MHz; CDCl₃) δ -0.4, 96.8, 104.9, 115.9, 135.1, 150.0, 151.7. HRMS (EI) 384.06158, for C₁₈H₂₀N₂S₂Si₂, requires 384.06064, deviation 2.4 ppm.

Benzo[1,2-*d*;4,5-*d'*]bisthiazole Diethyl Ester (3e). Compound **3e** was synthesized following the same protocol as for compound **3a** with **4** and ethyl triethoxyacetate **2e**. The product was obtained after recrystallization from pentane as pale yellow needles (53% yield). Melting point 241-242 °C (chloroform/ethanol). ¹HNMR(400 MHz; CDCl₃) δ 1.52 (6H, t, J=5.4 Hz), 4.59 (4H, q, J=5.4 Hz), 8.83 (2H, s); ¹³CNMR (100 MHz; CDCl₃) δ 14.5, 63.7, 118.9, 136.5, 152.6, 160.4, 161.3. HRMS (EI), found 336.02464, C₁₄H₁₂N₂O₄S₂ requires 336.02385, deviation 2.3 ppm.

2,6-Dimethylbenzo[1,2-*d*;4,5-*d'*]bisthiazole diethylphosphonate Ester (3f). Triethylphosphite (1.12 g, 7.75 mmol) and 2,6-(bischloromethyl) benzo[1,2-*d*;4,5-*d'*]benzobisthiazole 3c (650 mg, 2.25 mmol) were heated to 150 °C for 4 h. The reaction was cooled to yield crude **3f**. Recrystallization from chloroform/heptanes afforded the product as a white solid (885 mg, 80%). Melting point 203-204 °C. ¹H NMR (400 MHz; CDCl₃) δ 1.32 (12H, t, J=6.0 Hz), 3.75 (4H, d, J=15 Hz), 4.18 (8H, m), 8.44 (2H, s). ¹³CNMR(100 MHz; CDCl₃) δ 16.6 (d, J=6.0 Hz), 33.1, 34.5, 63.1 (d, J=6.0 Hz), 115.3, 135.2, 148.8, 151.1, 162.6, 162.7. HRMS (EI) 492.07227, C₁₈H₂₆N₂O₆P₂S₂ requires 492.07075, deviation 3.0 ppm.

3.5 ACKNOWLEDGMENT.

We are grateful to the 3M Foundation and the National Science Foundation (DMR-0846607) for their generous support of this work. We thank Dr. Kamel Harrata and the Mass Spectroscopy Laboratory of Iowa State University (ISU) for analysis of our compounds. We also thank Brian Tlach for help with the synthesis of **2e** and Dr. Jesse Waldo (ISU) for helpful discussions of this research.

3.6 REFERENCES

- (1) Singh, T. B.; Sariciftci, N. S. *Annu. Rev. Mater. Res.* **2006**, *36*, 199. (a) Forrest, S. R. *Nature* **2004**, *428*, 911.
- (2) Osaheni, J. A.; Jenekhe, S. A. *Macromolecules* **1993**, *26*, 4726.
- (3) (a) Evers, R. C.; Dotrong, M. *Mater. Res. Soc. Symp. Proc.* **1989**, *134*, 141. (b) Wolfe, J. F. In *Encyclopedia of Polymer Science and Engineering*; John Wiley and Sons: New York, NY, 1988; Vol. 11, p 601.
- (4) Wolfe, J. F.; Loo, B. H.; Arnold, F. E. *Macromolecules* **1981**, *14*, 915.
- (5) (a) Alam, M. M.; Jenekhe, S. A. *Chem. Mater.* **2002**, *14*, 4775. (b) Babel, A.; Jenekhe, S. A. *J. Phys. Chem. B.* **2002**, *106*, 6129.
- (6) (a) Jenekhe, S. A.; Osaheni, J. A.; Meth, J. S.; Vanherzeele, H. *Chem. Mater.* **1992**, *4*, 683. (b) Lee, S.-H.; Otomo, A.; Nakahama, T.; Yamada, T.; Kamikado, T.; Yokoyama, S.; Mashiko, S. *J. Mater. Chem.* **2002**, *12*, 2187. (c) Jenekhe, S. A.; Osaheni,

J. A. *Chem. Mater.* **1994**, *6*, 1906. (c) Osaheni, J. A.; Jenekhe, S. A. *Chem. Mater.* **1995**, *7*, 672.

(7) Reinhardt, B. A.; Unroe, M. R.; Evers, R. C. *Chem. Mater.* **1991**, *3*, 864.

(8) Pang, H.; Vilela, F.; Skabara, P. J.; McDouall, J. J. W.; Crouch, D. J.; Anthopoulos, T. D.; Bradley, D. D. C.; de Leeuw, D. M.; Horton, P. N.; Hursthouse, M. B. *Adv. Mater.* **2007**, *19*, 4438.

(9) (a) Kricheldorf, H. R.; Domschke, A. *Polymer* **1994**, *35*, 198. (b) Osman, A. M.; Mohamed, S. A. *U.A.R.J. Chem.* **1971**, *14*, 475. (c) Osman, A. M.; Mohamed, S. A. *Indian J. Chem.* **1973**, *11*, 868. (d) Imai, Y.; Itoya, K.; Kakimoto, M.-A. *Macromol. Chem. Phys.* **2000**, *201*, 2251. (e) Imai, Y.; Taoka, I.; Uno, K.; Iwakura, Y. *Makromol. Chem.* **1965**, *83*, 167.

(10) Mike, J. F.; Makowski, A. J.; Jeffries-EL, M. *Org. Lett.* **2008**, *10*, 4915.

(11) Zhao, M.; Samoc, M.; Prasad, P. N.; Reinhardt, B. A.; Unroe, M. R.; Prazak, M.; Evers, R. C.; Kane, J. J.; Jariwala, C.; Sinsky, M. *Chem. Mater.* **2002**, *2*, 670.

(12) Wolf, R.; Okada, M.; Marvel, C. S. *J. Pol. Sc., PC* **1968**, *6*, 1503.

3.7 SUPPORTING INFORMATION

3.7.1 General Experimental Details.

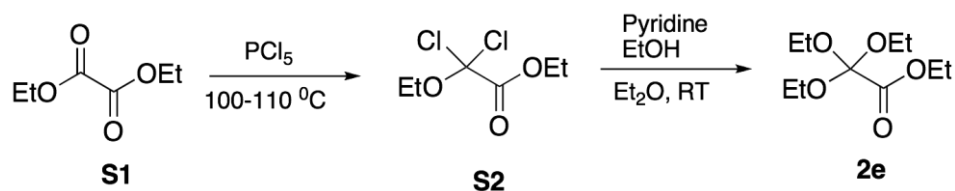
Compounds **1**¹, **2c**,² **2d**,³ were all synthesized according to the literature procedures. All other compounds were purchased from commercial sources and used without further purification. Nuclear magnetic resonance spectra were obtained on a 400 MHz spectrometer (¹H at 400 MHz and ¹³C at 100 MHz). ¹H NMR samples were referenced internally to residual protonated solvent ¹³C NMR are referenced to the middle carbon peak of CDCl₃. In both instances chemical shifts are given in δ relative to solvent. Coupling constants are reported in Hz. High-resolution mass spectra were recorded on a double focusing magnetic sector mass spectrometer using EI at 70 eV. Melting points were obtained using a melting point apparatus, upper temperature limit 260 °C. GC-MS analysis was performed on a GC column was a fused silica capillary column cross-linked with 5% phenylmethylsiloxane and Helium was the carrier gas. X-ray crystal structure data for compounds **3a** (CCDC 747963), **3b** (CCDC 747964), **3c** (CCDC 747962) and **3f**

(CCDC 749471) were deposited with the Cambridge Crystallographic Data Centre, 12 Union Road, Cambridge CB2 1EZ, UK.

3.7.2 References

- (1) Wolfe, J. F.; Loo, B. H.; Arnold, F. E. *Macromolecules* **1981**, 14, 915.
- (2) Mylari, B. L.; Scott, P. J.; Zembrowski, W. *J. Synth. Commun.* **1989**, 19, 2921.
- (3) Yamamoto, K.; Abrecht, S.; Scheffold, R. *Chimia* **1991**, 45, 86.
- (4) Jones, R. G. *J. Am. Chem. Soc.* **1951**, 73, 5168.

3.7.3 Supplemental Experimental



Ethyl dichloroethoxyacetate (S2). This compound was prepared in 54% yield according to the literature procedure.⁴ The product was distilled under reduced pressure to give 3 fractions. The 3rd fraction which was collected between 110°-115°C, contains the purest product (95% pure by GC/MS), with 5% diethyloxalate. ¹H NMR (CDCl₃) δ 1.38 (overlapped-q, 6H), 4.19 (m, 2H), 4.377. (m, 2H).

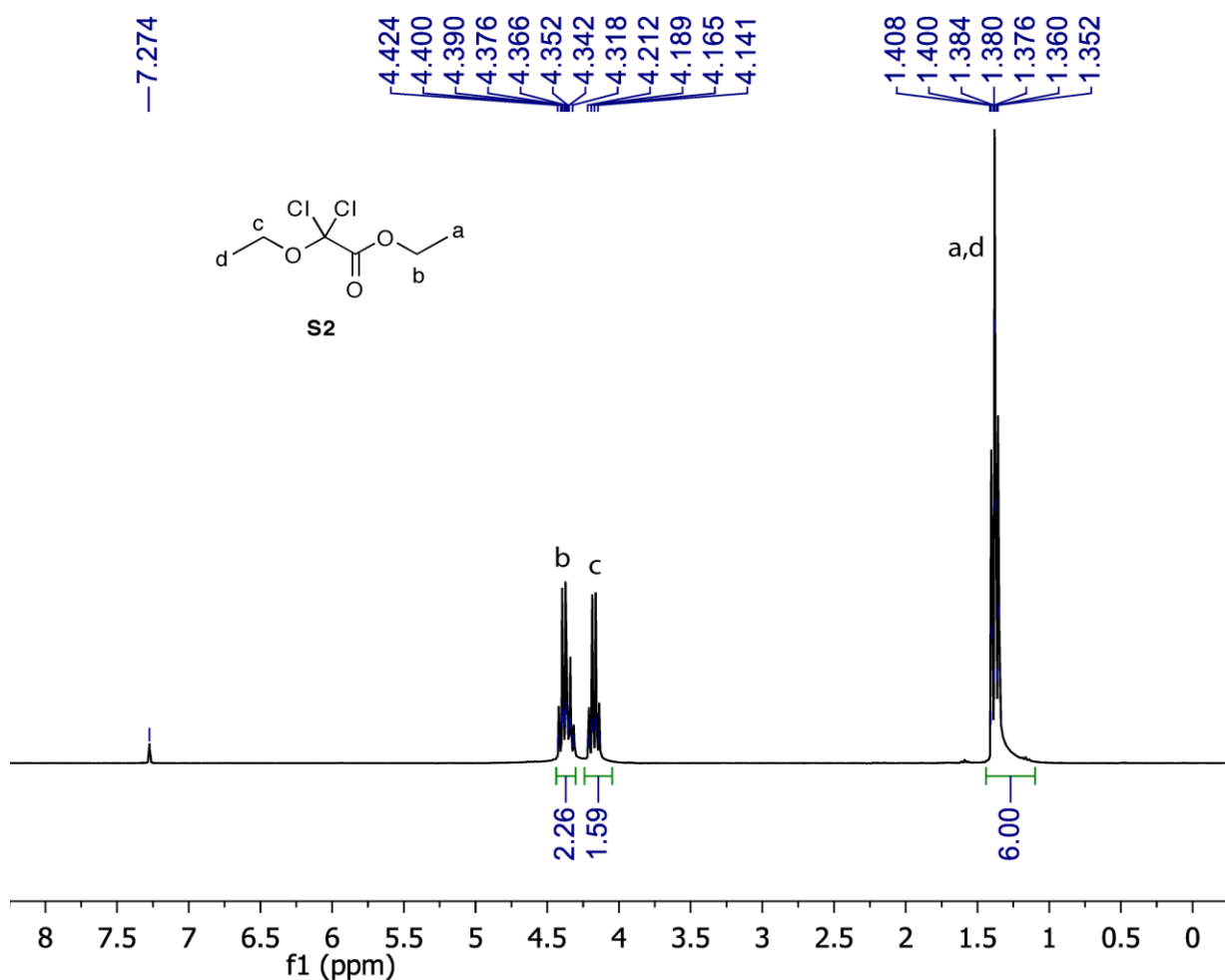


Figure S1. ¹H NMR spectrum of S2

Ethyl triethoxyacetate (2e). This compound was prepared in 45 % yield from according to the literature procedure.⁴ The product was distilled via Kugelhor distillation under reduced pressure. The fraction at 50 °C, contains the purest product (90% pure by GC/MS), diethyl oxalate is the impurity. ¹H NMR (CDCl₃) δ 0.949 (t, 9H, *J*=5.7 Hz), 1.046 (t, 3H, *J*=5.4 Hz), 3.30 (q, 6H, *J*=5.7), 3.99 (q, 2H, *J*=5.4Hz); ¹³C NMR δ 13.5, 14.3, 58.1, 60.9, 109.1, 165.3.

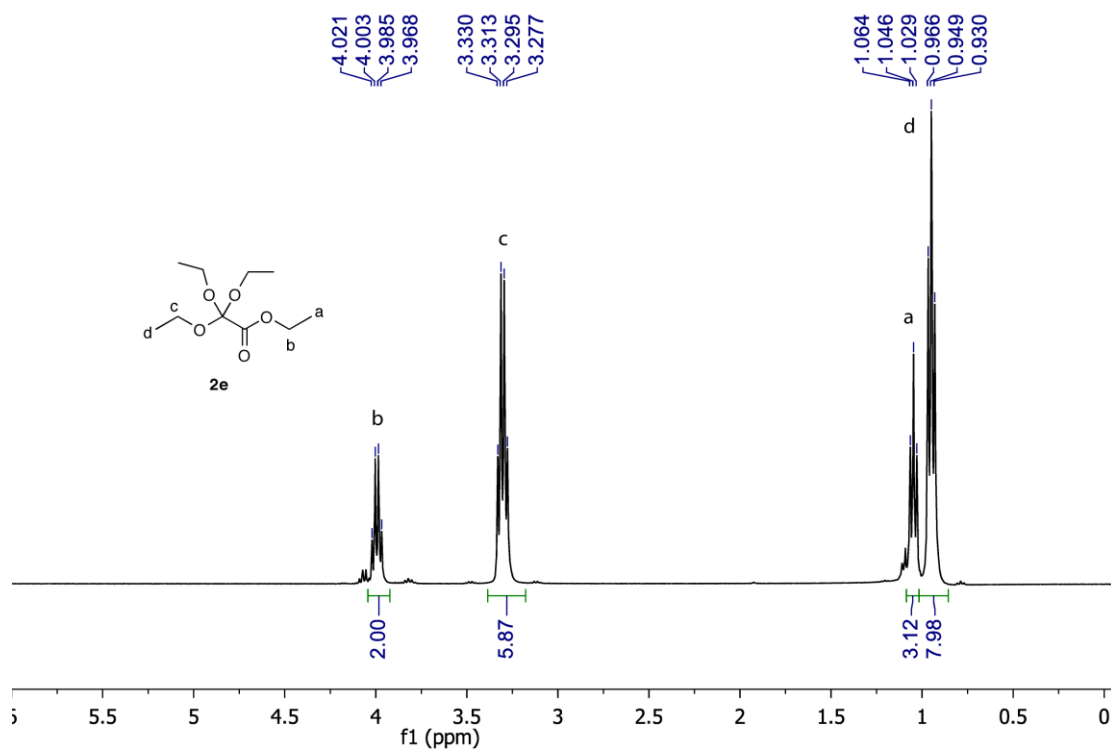


Figure S2. ^1H NMR spectrum of **2e** in CDCl_3

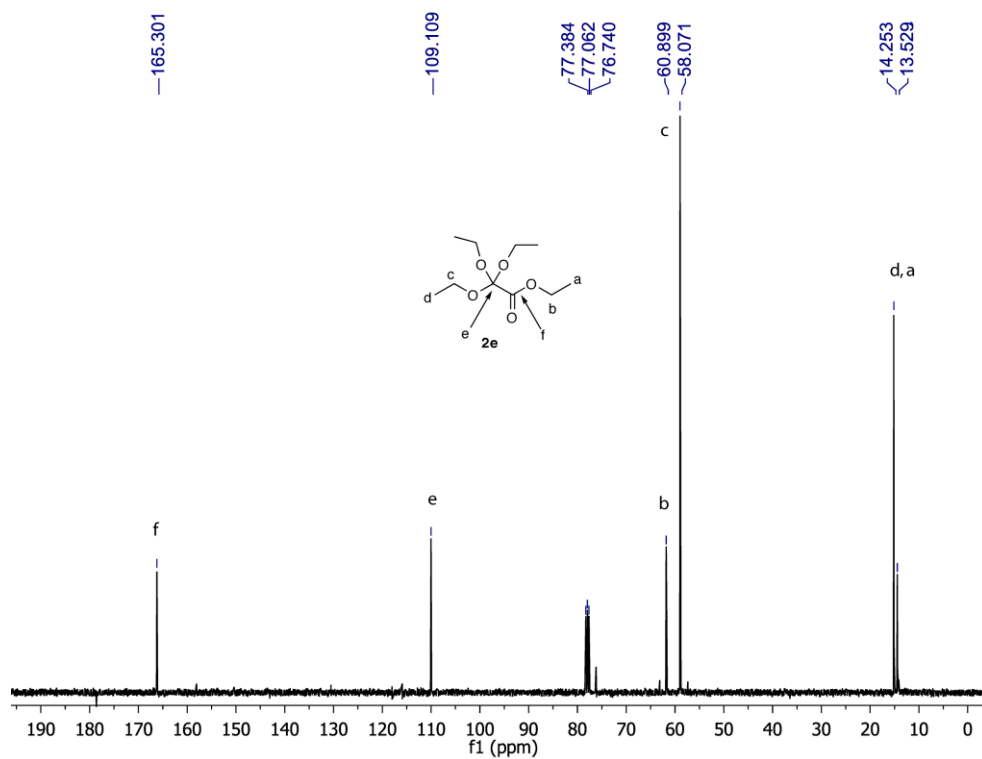


Figure S3. ^{13}C NMR spectrum of **2e**.

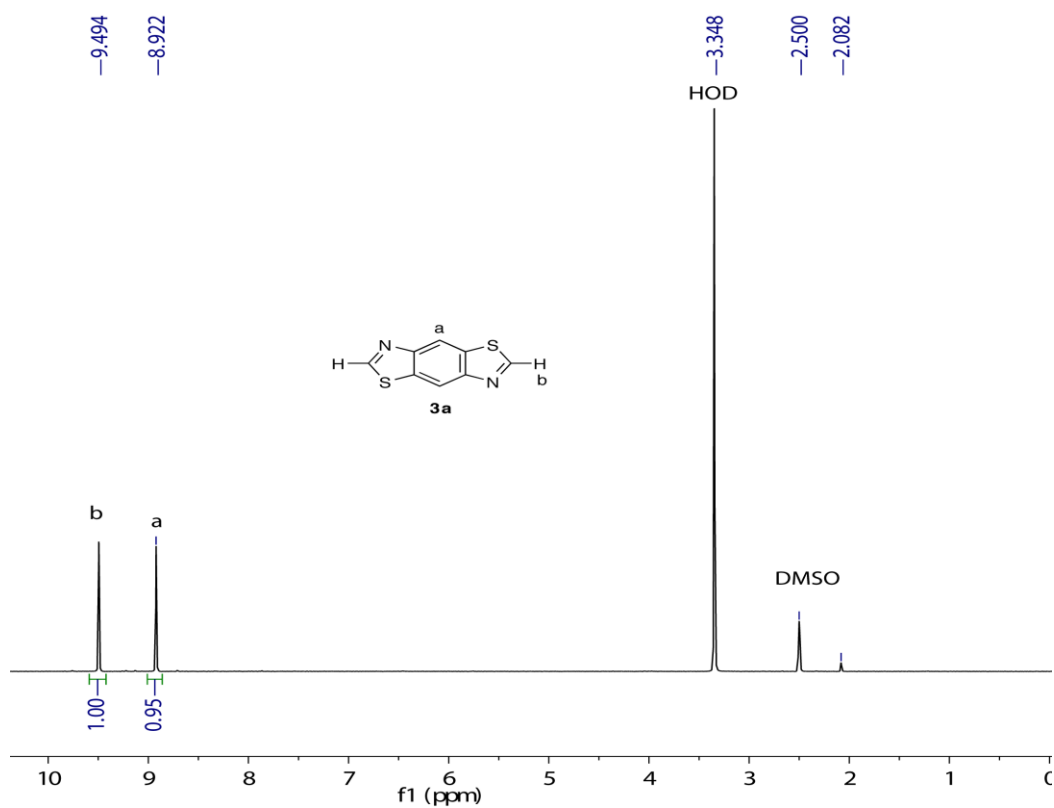


Figure S4. ^1H NMR spectrum of **3a**.

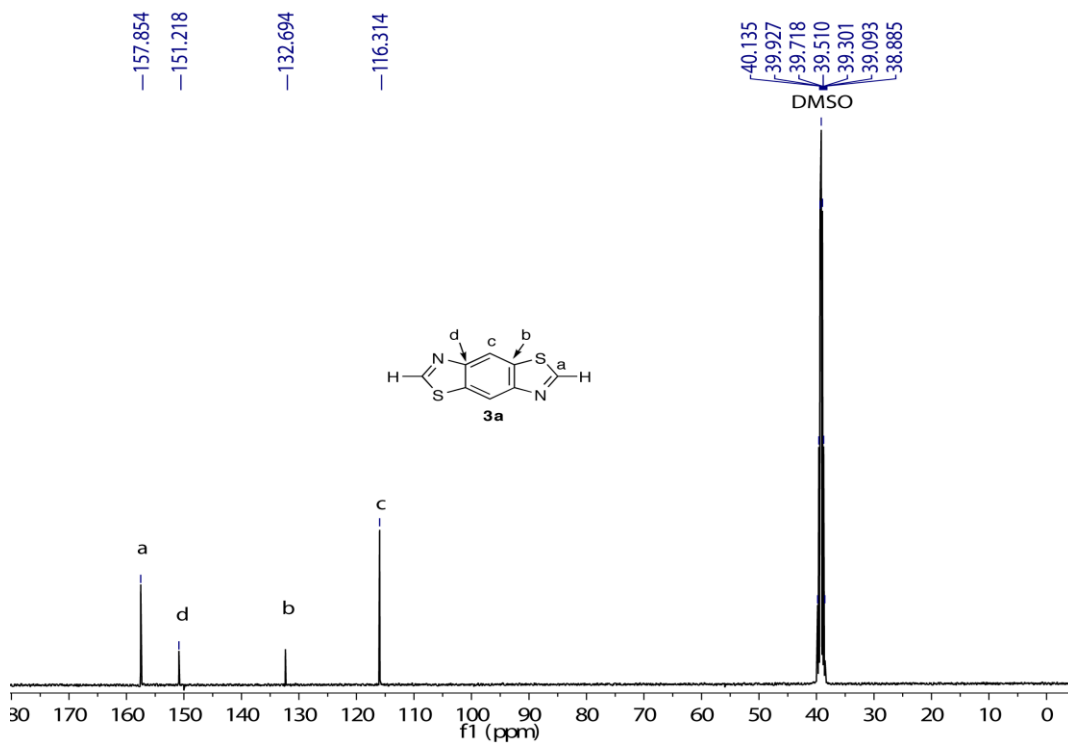


Figure S5. ^{13}C NMR spectrum of **3a**.

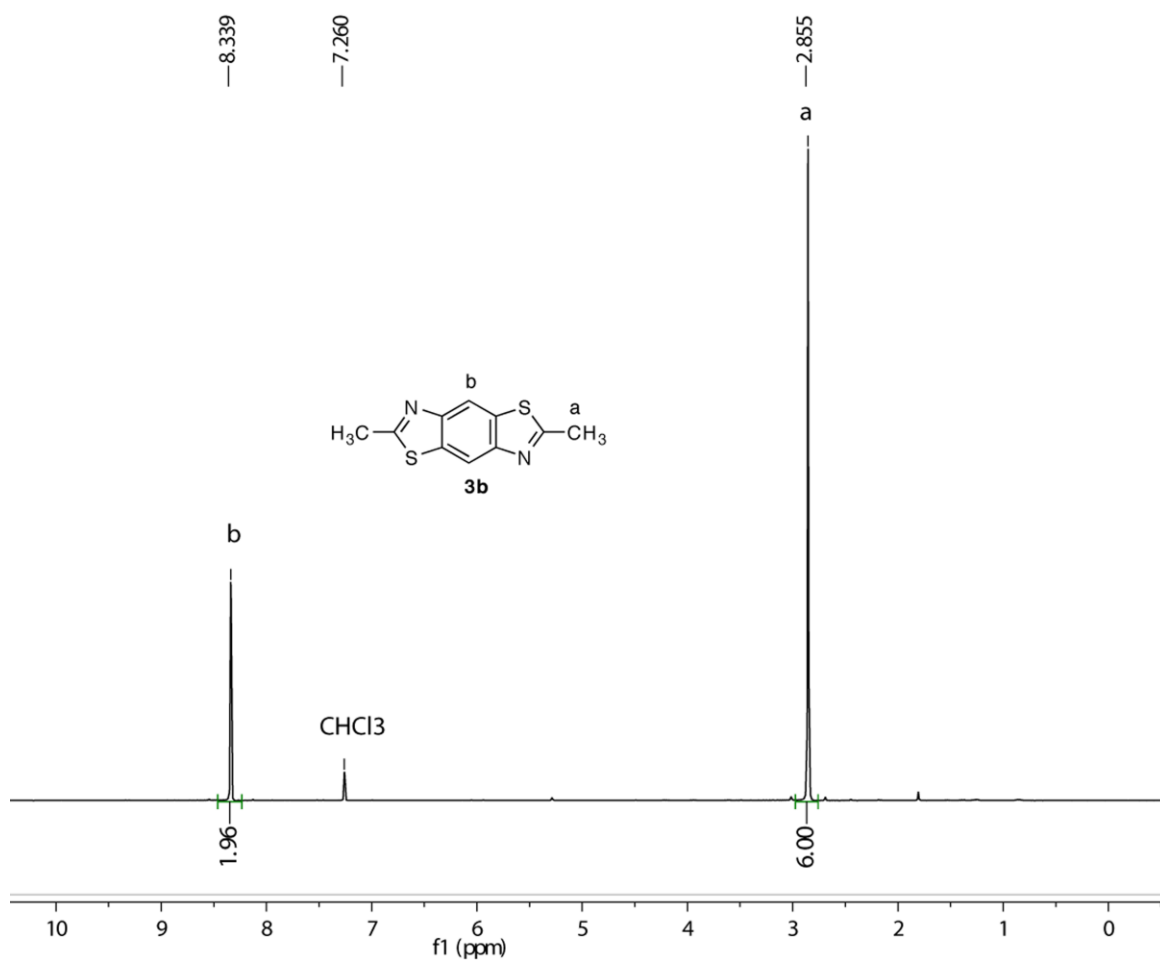


Figure S6. ^1H NMR spectrum of **3b**.

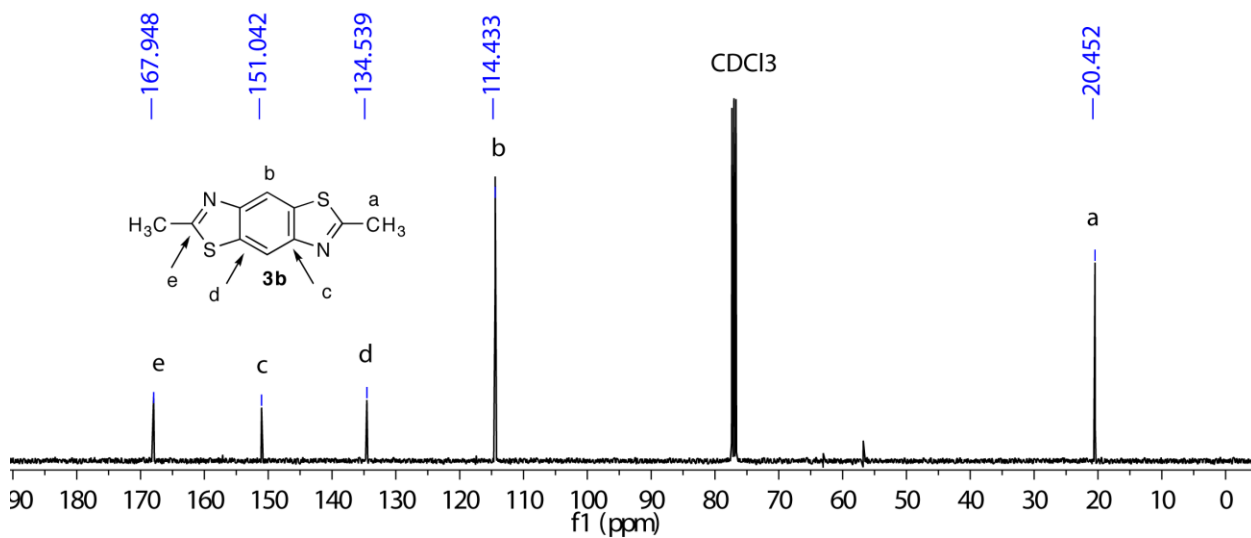


Figure S7. ^{13}C NMR spectrum of **3b**.

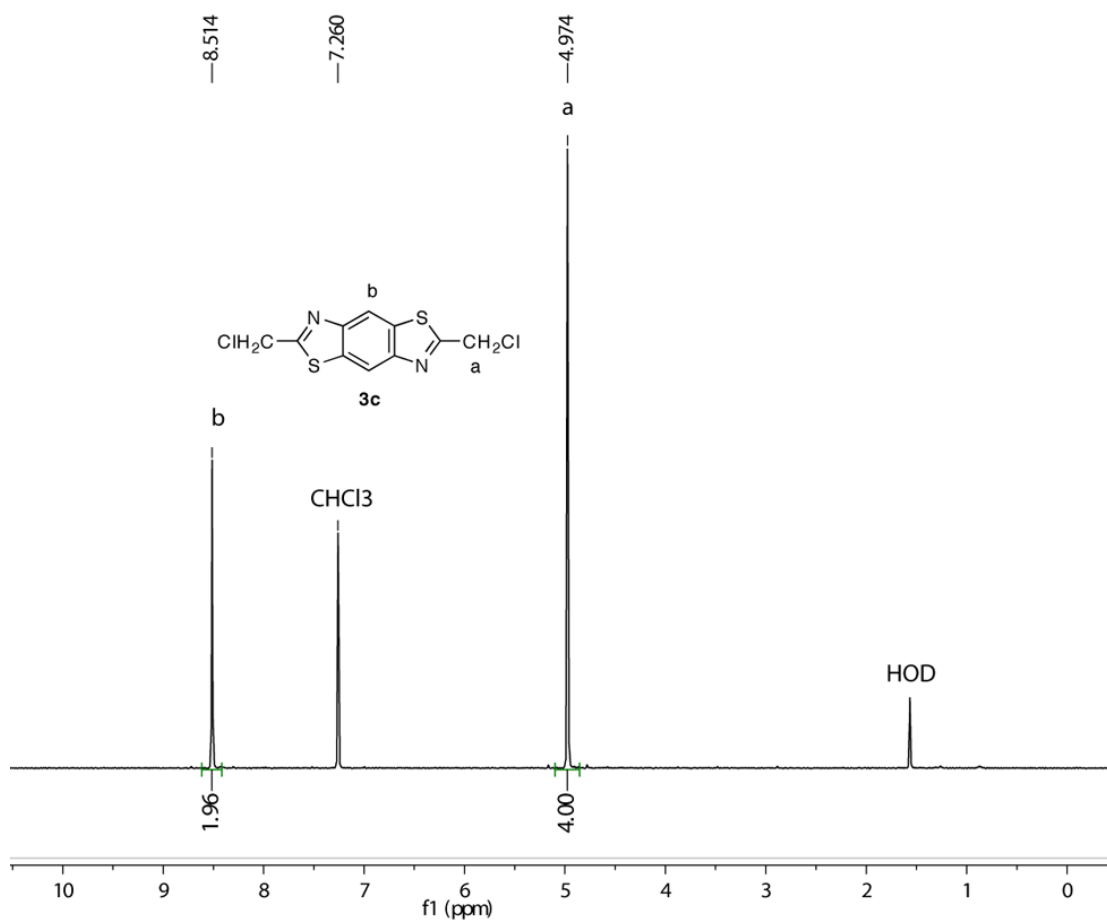


Figure S8. ¹H NMR spectrum of **3c**.

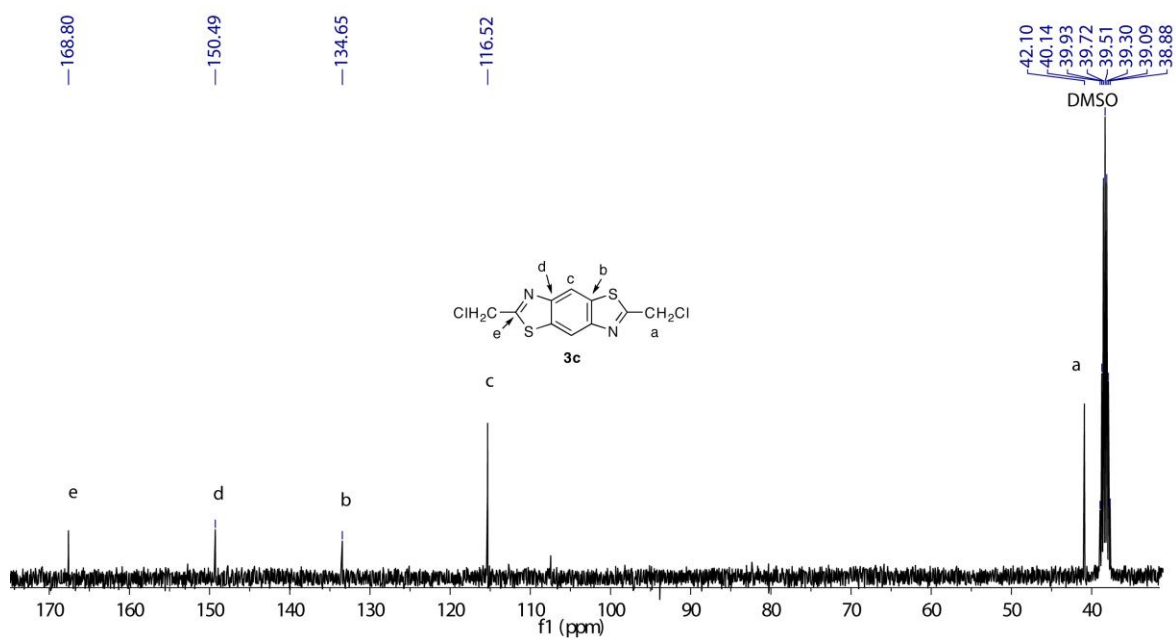


Figure S9. ¹³C NMR spectrum of **3c**.

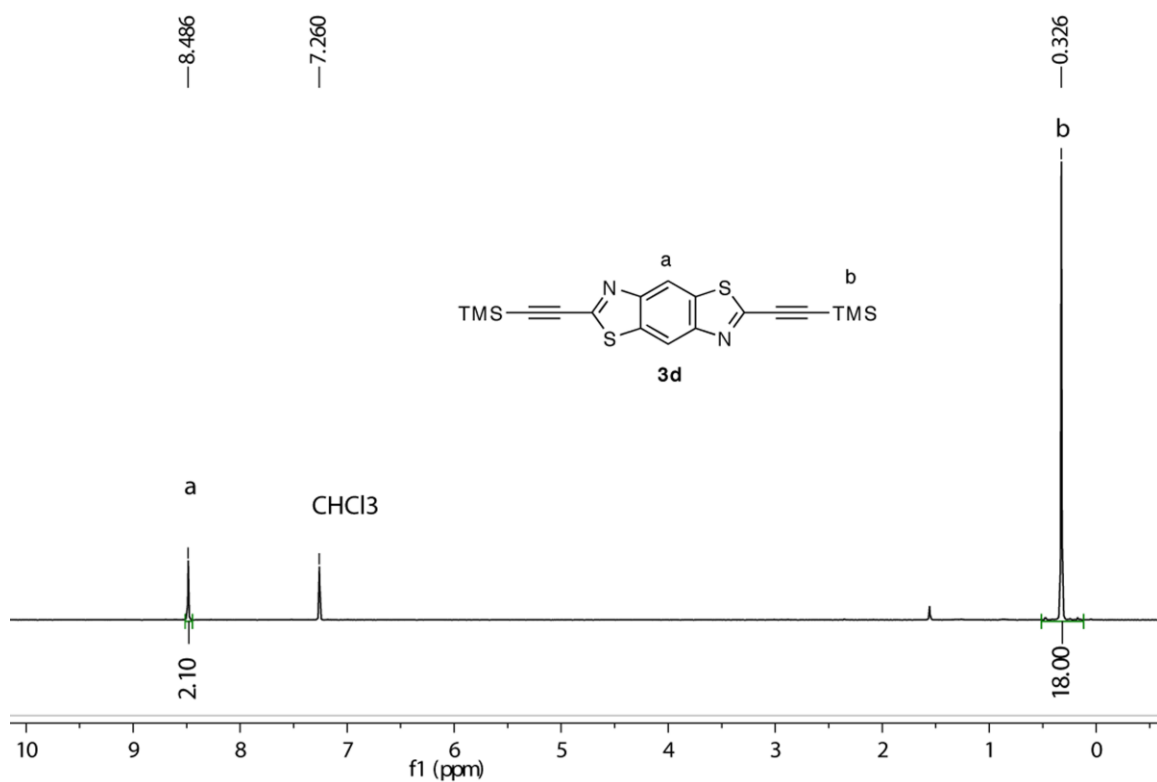


Figure S10. ^1H NMR spectrum of **3d**.

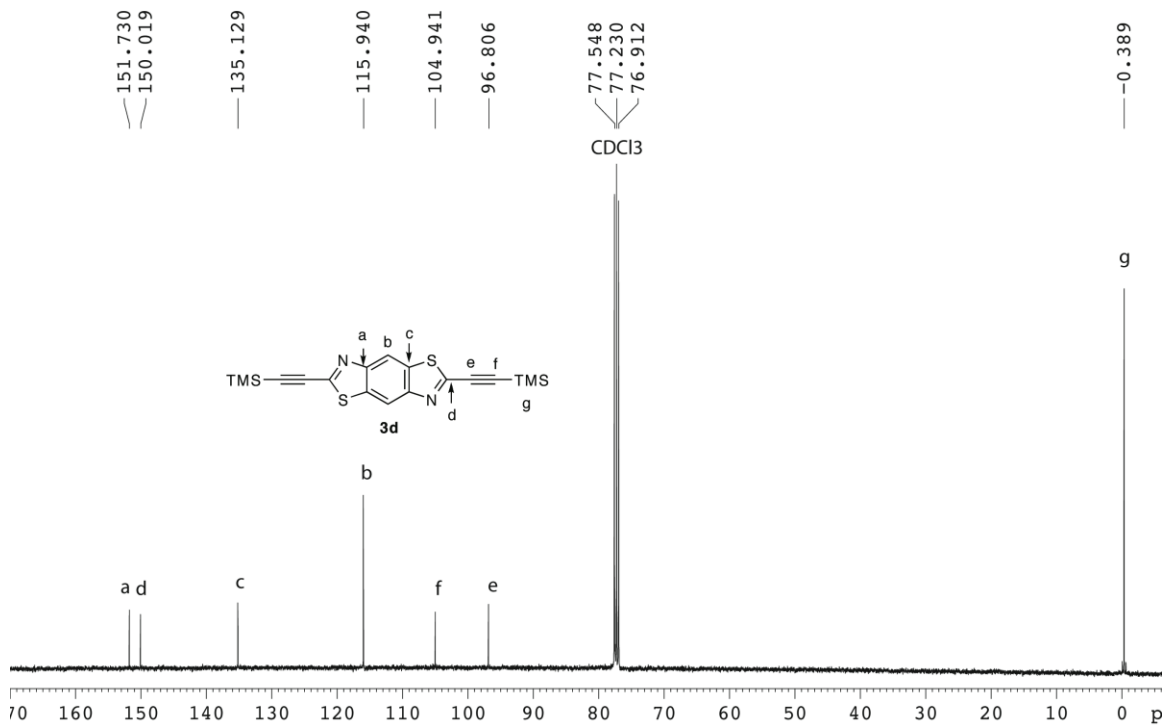


Figure S11. ^{13}C NMR spectrum of **3d**.

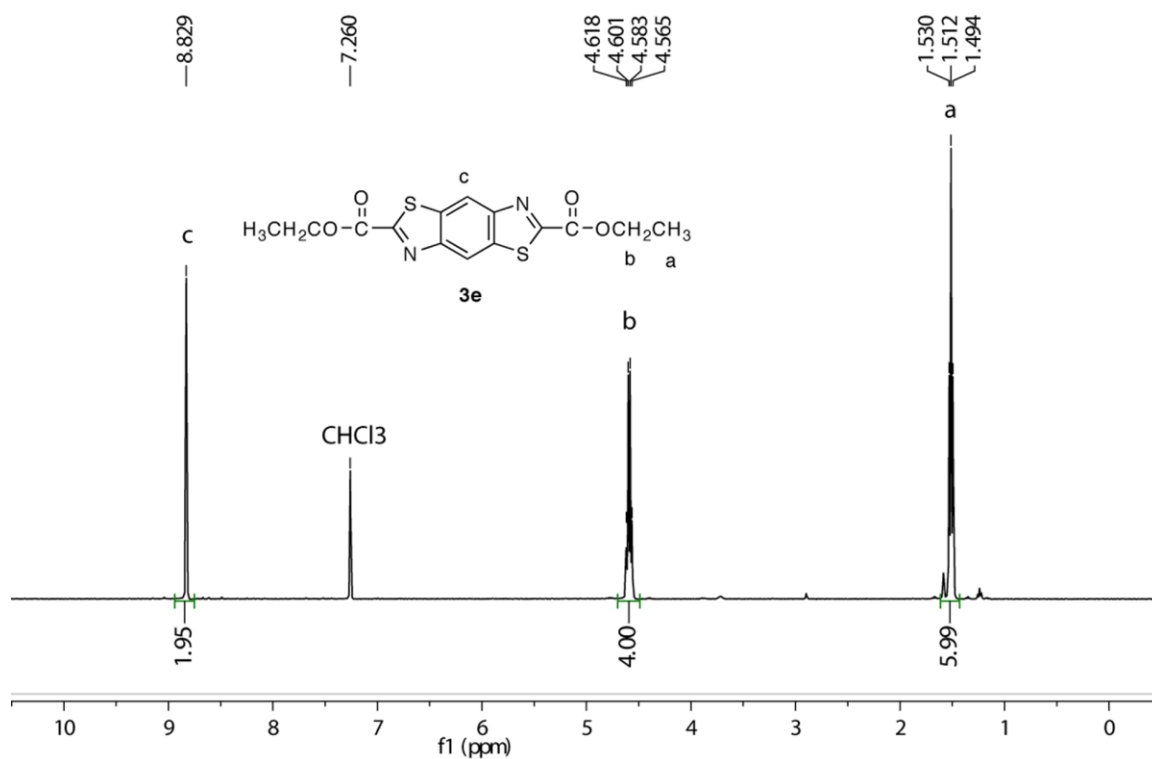


Figure S12. ^1H NMR spectrum of **3e**.

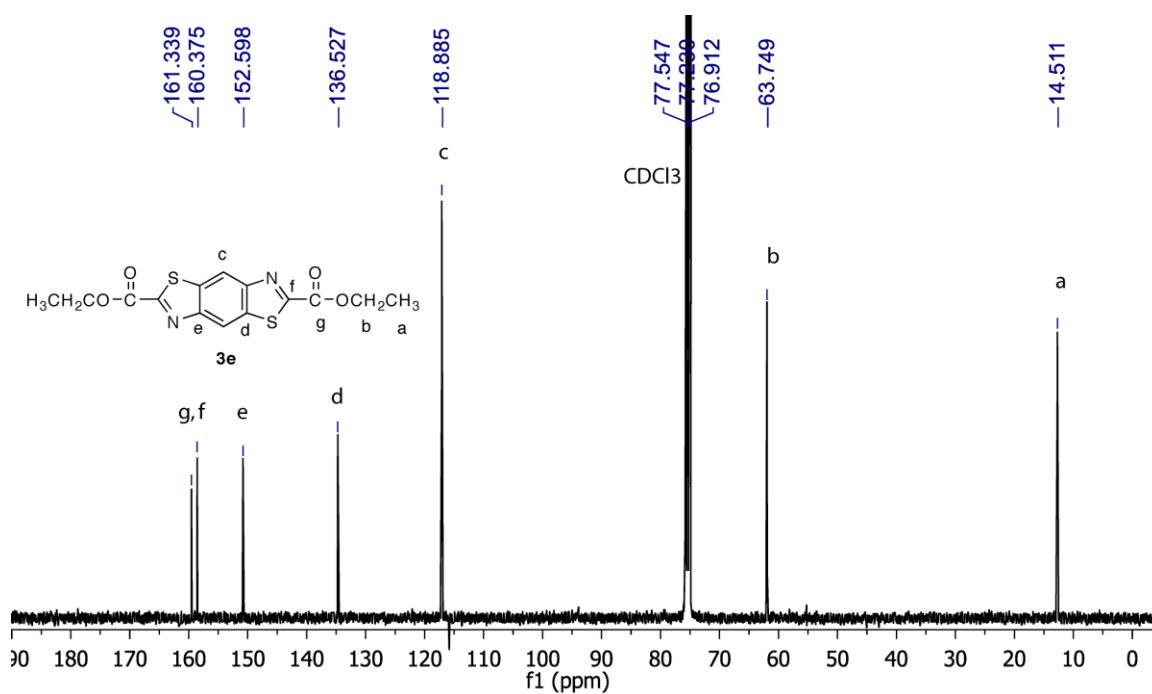


Figure S13. ^{13}C NMR spectrum of **3e**.

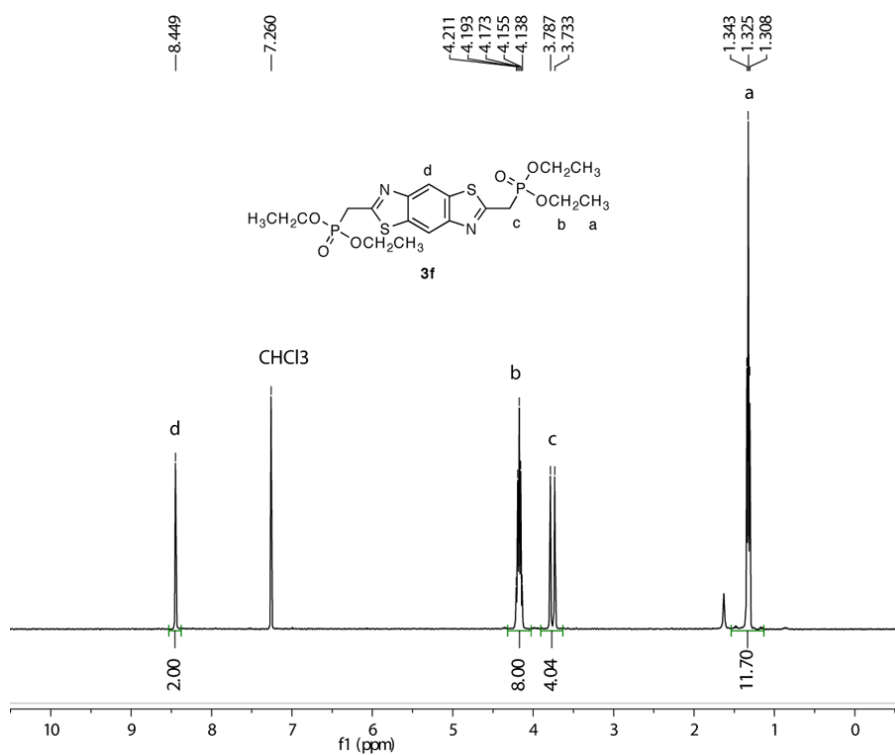


Figure S14. ^1H NMR spectrum of **3f**.

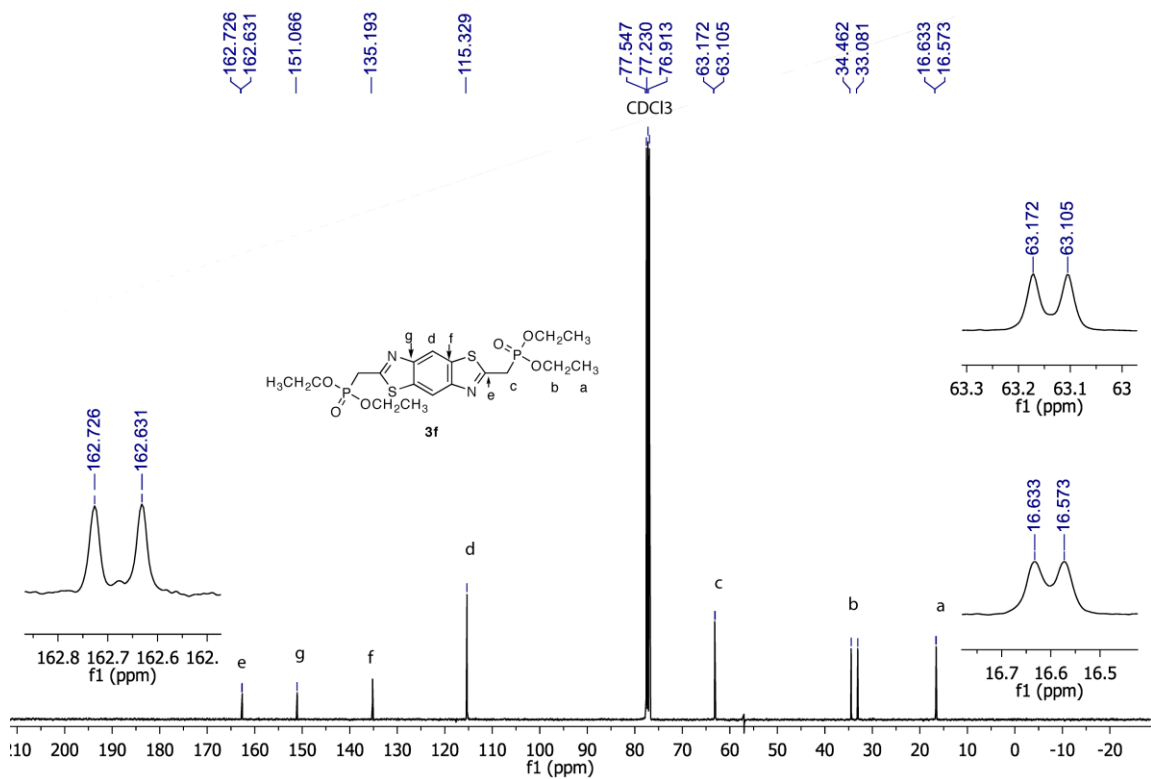


Figure S15. ^{13}C NMR spectrum of **3f**.

Compound reference	3a	3b	3c	3f
Chemical formula	C ₈ H ₄ N ₂ S ₂	C ₁₀ H ₈ N ₂ S ₂	C ₁₀ H ₆ Cl ₂ N ₂ S ₂	C ₁₈ H ₂₄ N ₂ O ₆ P ₂ S ₂
Formula Mass	192.25	220.30	289.19	490.45
Crystal system	Monoclinic	Monoclinic	Triclinic	Triclinic
<i>a</i> /Å	3.8605(15)	8.0071(13)	6.3376(17)	7.9438(6)
<i>b</i> /Å	16.025(6)	6.5112(10)	7.334(2)	8.8059(12)
<i>c</i> /Å	6.053(2)	10.0130(16)	12.454(3)	9.4063(7)
<i>α</i> /°	90	90	93.007(4)	101.6930(10)
<i>β</i> /°	92.310(5)	112.755(2)	100.106(4)	112.5340(10)
<i>γ</i> /°	90	90	99.647(4)	103.4750(10)
Unit cell volume/Å ³	374.2(2)	481.40(13)	559.8(3)	558.93(10)
Temperature/K	153.(2)	153.(2)	153(2)	153(2)
Space group	<i>P</i> 121/ <i>n</i> 1	<i>P</i> 121/ <i>c</i> 1	<i>P</i> 1	<i>P</i> 1
No. of formula units per unit cell, <i>Z</i>	2	2	2	1
No. of reflections measured	4166	5463	4691	6652
No. of independent reflections	1129	1492	2148	3361
<i>R</i> _{int}	0.0380	0.0338	0.0396	0.0150
Final <i>R</i> _{<i>I</i>} values (<i>I</i> > 2σ(<i>I</i>))	0.0409	0.0339	0.0440	0.0375
Final <i>wR</i> (<i>F</i> ²) values (<i>I</i> > 2σ(<i>I</i>))	0.1010	0.0810	0.1063	0.1120
Final <i>R</i> _{<i>I</i>} values (all data)	0.0535	0.0474	0.0707	0.0424
Final <i>wR</i> (<i>F</i> ²) values (all data)	0.1097	0.0882	0.1210	0.1166
CCDC number	747963	747964	747962	749471

Table S1. Crystallographic Data for compounds **3a**, **3b**, **3c** and **3f**.

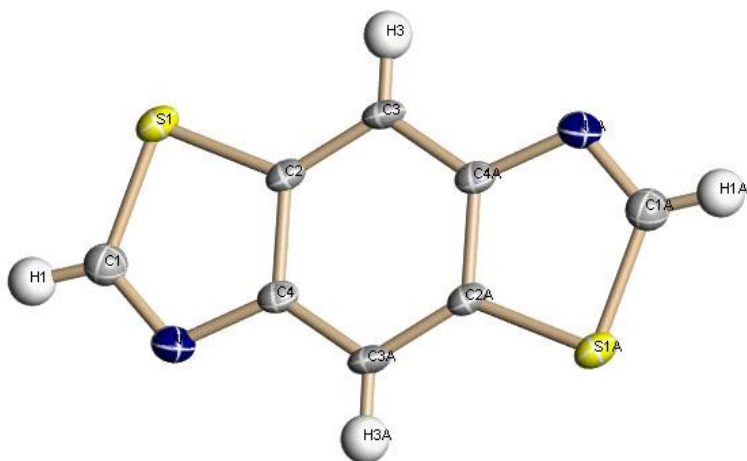


Figure S16. A single crystal X-Ray ORTEP of **3a**.

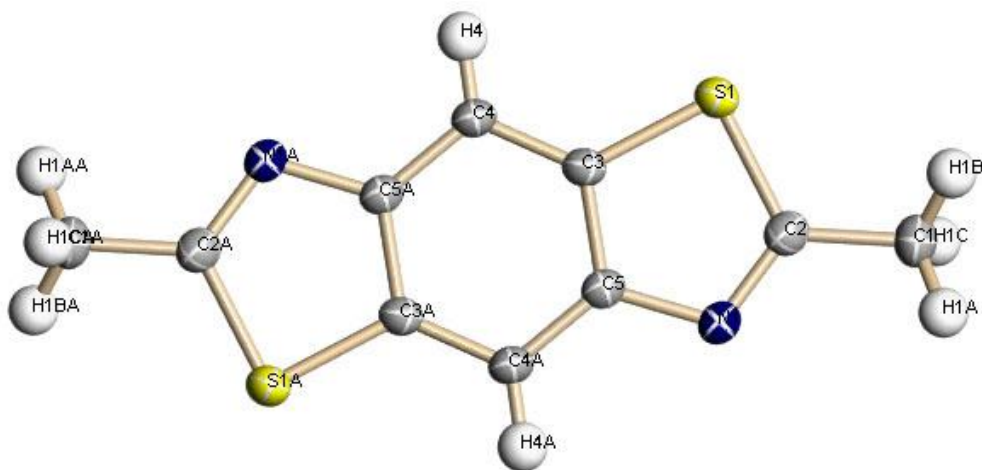


Figure S17. A single crystal X-Ray ORTEP of **3b**.

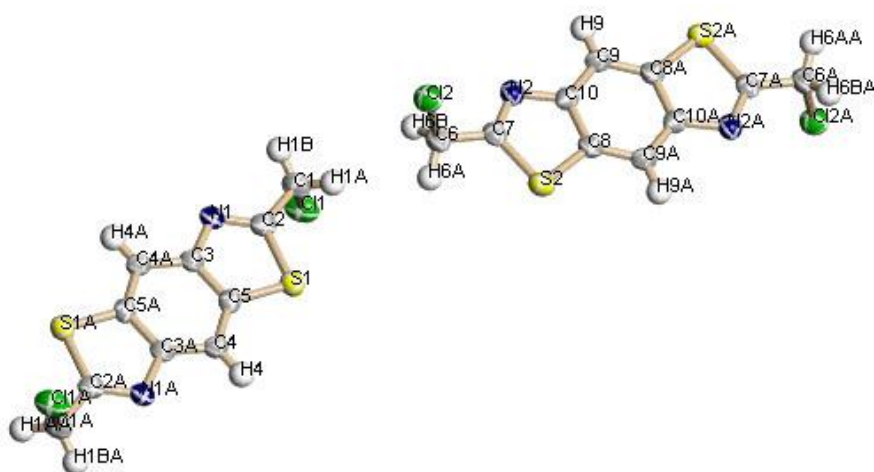


Figure S18. A single crystal X-Ray ORTEP of **3c**.

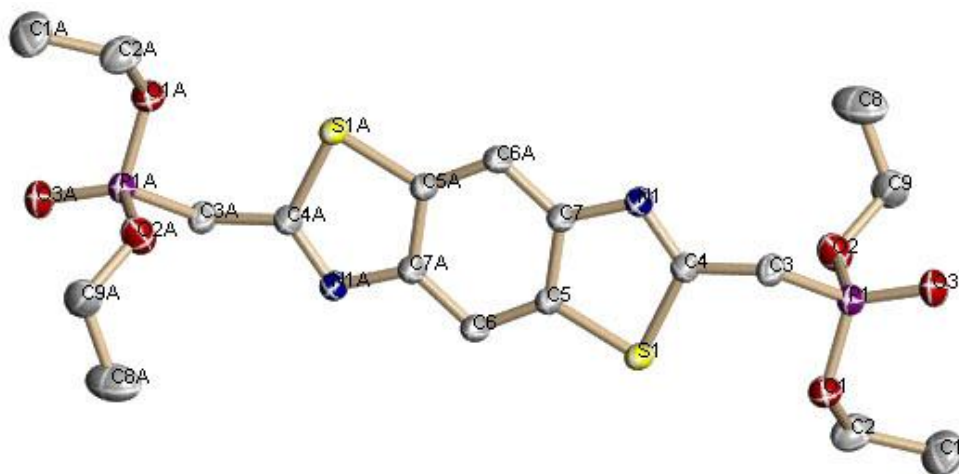


Figure S19. A single crystal X-Ray ORTEP of **3e**.

CHAPTER 4

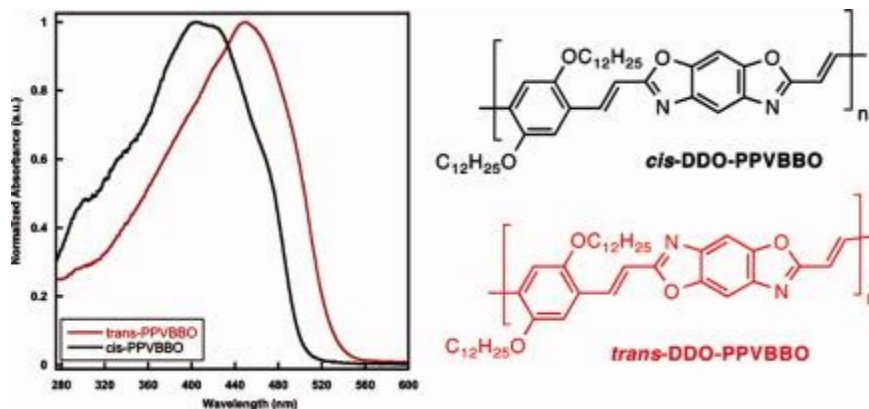
Synthesis and Characterization of Dialkoxy Substituted Poly(phenylenevinylene) Benzobisoxazoles.

Reproduced from *Journal of Polymer Science: Part A: Polymer Chemistry*, **2010**, 48, 1456, with permission from Wiley Interscience.

Copyright © 2011

Jared F. Mike, Andrew J. Makowski, Timothy C. Mauldin, and Malika Jeffries-EL.*
Department of Chemistry, Iowa State University, Ames, IA 50011-3111

4.1 ABSTRACT



A new route for the synthesis of soluble, alkoxy-substituted poly(p-phenylenevinylene) benzobisoxazoles has been developed. The target polymers can be prepared in three steps: the Lewis acid catalyzed condensation of corresponding diamino benzene diols with triethyl orthochloroacetate, the Arbuzov reaction of the resultant benzobisoxazole, and the Horner-Wadsworth-Emmons polymerization of 2,5-didodecyloxyterephthalaldehyde and the resulting 2,6-dimethylbenzobisoxazole-diethylphosphonate esters.

4.2 INTRODUCTION

Conjugated polymers (CPs) are of interest for use in a variety of applications such as

thin film transistors (TFT)s,¹ organic light emitting diodes (OLED)s,² and photovoltaic cells (PVC)s.³ The advantages that CPs possess over inorganic semi-conducting materials include ease of fabrication via solution-based processing techniques and the ability to modify the electronic properties of the material through chemical synthesis.⁴ The latter is beneficial for the optimization of the materials' properties for specific applications. While a large number of CPs are known, the majority of these polymers are electron-donating and hole-transporting in nature (p-type). Soluble CPs with electron-accepting and electron-transporting properties (n-type) are less abundant in the literature but essential for the development of polymer-based electronics.

Among conjugated polymers, polybenzobisoxazoles (PBO)s are promising for use in organic semiconducting applications because they combine efficient electron transport,⁵ photoluminescence,⁶ and third-order nonlinear optical properties⁷ with excellent mechanical strength⁸ and thermal stability.⁹ Unfortunately, fully conjugated PBOs are insoluble in aprotic solvents and must be processed from acidic solvents such as Lewis acid/nitromethane, methane sulfonic acid, trifluoromethanesulfonic acid, or sulfuric acid.^{5a, 10} None of these solvents are ideal for large-scale device fabrication, which limits the use of PBOs in organic semiconducting applications. Generally, the solubility of conjugated polymers can be improved by the attachment of flexible side-chains onto the polymer backbone.¹¹ Such derivations can also serve as a way to modify the polymers' electronic properties. Alas, conventional PBO synthesis requires the high-temperature condensation of bis-*o*-aminophenols and aromatic diacids in the melt or in mixed solvents such as polyphosphoric acid (PPA), phosphorus pentoxide/methanesulfonic acid, or trimethylsilyl polyphosphate (PPSE)/*o*-dichlorobenzene.¹² These harsh reaction conditions limit the types of substituents that can successfully be incorporated onto the polymer backbone.^{12c, 13}

To circumvent these issues, we designed and synthesized new 2,6-functionalized benzobisoxazoles to use as building blocks for new organic semiconductors.¹⁴ As a result, benzobisoxazole polymers with flexible side chains can be synthesized using mild reaction conditions. In this paper, we report the optimization of the Horner-Wadsworth-Emmons reaction (HWE) for the organic soluble poly(phenylenevinylene)-*co*-

benzobisoxazoles (PPVBBO)s. The solubility of these polymers allows for structural characterization using ^1H NMR spectroscopy and gel permeation chromatography. We also evaluated the properties of these polymers using UV-visible and fluorescence spectroscopy, cyclic voltammetry, thermal gravimetric analysis (TGA), and differential scanning calorimetry (DSC).

4.3 EXPERIMENTAL

4.3.1 General Experimental Details

Tetrahydrofuran was dried using an Innovative Technologies solvent purification system. All other compounds were purchased from commercial sources and used without further purification. Nuclear magnetic resonance spectra were obtained on a Varian 400 MHz spectrometer. All samples were referenced internally to the residual protonated solvent, in the case of ^1H spectra and to the center peak of the CDCl_3 triplet for ^{13}C spectra. In both cases the chemical shifts were given in δ , relative to the solvent. Gel permeation chromatography (GPC) measurements were performed on a Viscotek GPC Max 280 separation module equipped with three $5\mu\text{m}$ I-gel columns connected in a series (guard, HMW, MMW and LMW) with a refractive index detector. Analyses were performed at $35\text{ }^\circ\text{C}$ using THF as the eluent with the flow rate at 1.0 mL/min . Calibration was based on polystyrene standards. Fluorescence spectroscopy and UV-Visible spectroscopy were obtained using polymer solutions in THF, and thin films were spun from these solutions. Both polymers were excited at their respective emission maxima. Relative PL quantum yields were obtained using Coumarin 6 in ethanol as a standard for the solution measurements and 10% by weight perylene in PMMA for the solid-state measurements. The polymers solutions were prepared in THF. The quantum yields were corrected for the difference in the refractive index of the solvent using the equation $\Phi_{\text{F}(x)} = (A_{\text{s}}/A_{\text{x}})(F_{\text{x}}/F_{\text{s}})(n_{\text{x}}/n_{\text{s}})^2 \Phi_{\text{F}(s)}$, where Φ_{F} is the fluorescence quantum yield, A is the absorbance at the excitation wavelength, F is the area under the corrected emission curve (expressed in number of photons), and n is the refractive index of the solvents used. Subscripts s and x refer to the standard and to the unknown, respectively.¹⁵ Thermal gravimetric analysis measurements were performed using TA instruments Model Q50,

within the temperature interval of 30 °C - 650 °C, with a heating rate of 20 °C/minute, under ambient atmosphere. Differential scanning calorimetry was performed using a TA instruments Q20 model DSC, with a first scan at a heating rate of 15 °C/min to erase thermal history and a second scan to measure transitions. Transitions were also measured with cooling at 15 °C/min. All runs were performed under nitrogen. Cyclic voltammograms were performed in 0.1M tetrabutylammonium hexafluorophosphate using Ag/AgCl in 3M KCl reference electrode. The potential values obtained versus the Ag/AgCl were converted to the standard calomel electrode (SCE) reference.

4.3.2 Synthesis

2,6-dimethylbenzo[1,2-*d*;5,4-*d'*]bisoxazole-diethylphosphonate ester (2). Triethylphosphite (2.91 g, 17.5 mmol) and 2,6-bis(chloromethyl)benzo[1,2-*d*; 5,4-*d'*]bisoxazole¹⁴ **1** (1.50 g, 5.83 mmol) were heated to 150 °C for 4 h. The reaction was cooled and the crude product solidified. The crude product was purified (recrystallized from heptane), and monomer **2** was obtained as a white solid. Yield: 1.96 g (73%), mp: 104-105 °C. ¹H NMR (300 MHz, CDCl₃, δ, ppm): 1.31 (t, ³*J*_{HH}= 6.0 Hz, 12H), 3.56 (d, ²*J*_{PH}= 24 Hz, 4H), 4.19 (m, ³*J*_{HH}=6.0 Hz, ²*J*_{PH}= 24 Hz, 8H), 7.65 (s, 1H), 7.94 (s, 1H). ¹³C NMR δ (CH₃), 16.57 (d, ⁴*J*_{PC}= 40 Hz), (Ar-CH₂-), 28.49 (d, ¹*J*_{PC}= 138 Hz), (-O-CH₂-), 63.24 (d, ³*J*_{PC}= 60 Hz), (ArC), 93.54, 110.09, 139.06, 149.09, 159.56, 159.67. HRMS (EI) calcd. for C₁₈H₂₆N₂O₈P₂ 460.11643, found 460.11761, deviation 2.6 ppm.

2,6-dimethylbenzo[1,2-*d*;4,5-*d'*]bisoxazole-diethylphosphonate ester (4). The title compound was prepared from 2,6-bis(chloromethyl)benzo[1,2-*d*;4,5-*d'*]bisoxazole¹⁴ **3** as described for **2**. The product was recrystallized from xylenes. Yield 94%, mp: 145-146 °C. ¹H NMR (300 MHz, CDCl₃, δ, ppm) 1.33 (t, *J*= 6.0 Hz, 12H), 3.58 (d, *J*=15 Hz, 4H), 4.19 (m, *J*₁= 6.0 Hz, *J*₂ = 15 Hz, 8H), 7.79 (s, 2H). ¹³C NMR δ (CH₃), 16.62 (d, ⁴*J*_{PC}= 60 Hz), (Ar-CH₂-) 28.58 (d, ¹*J*_{PC}= 138 Hz), (-O-CH₂-), 63.27 (d, ³*J*_{PC}= 70 Hz), (ArC), 101.3, 139.6, 148.8, 160.2, 160.3. HRMS (EI) calcd for C₁₈H₂₆N₂O₈P₂ 460.11643, found 460.11761, deviation 2.6 ppm.

2,5-didodecyloxy-1,4-benzene dicarboxaldehyde (5) was synthesized in 64% yield,

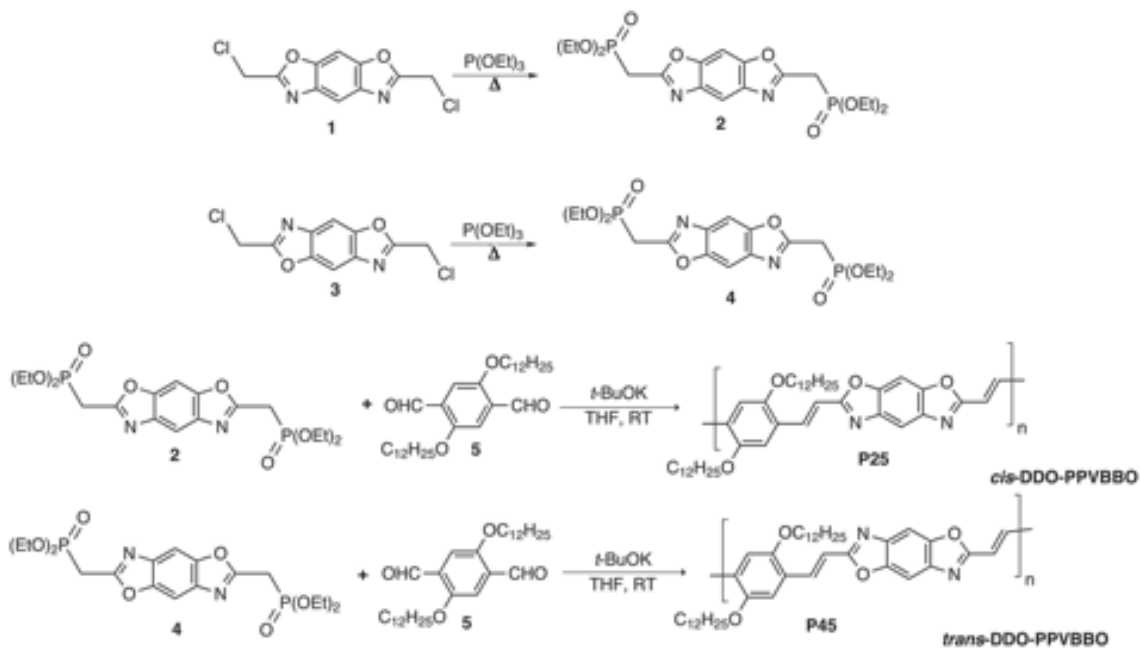
according to the literature procedure.¹⁶ Melting point 72-73 °C. ¹H NMR (300 MHz, CDCl₃): δ 0.877 (t, 6H), 1.26-1.54 (m 40H), 4.08 (t, 4H), 7.43 (s, 2H), 10.52 (s, 2H).

General Method for Polymer Synthesis. Benzobisoxazole monomer (2 or 4) (460 mg, 1.00 mmol) and 2,5-didodecyloxy-1, 4-benzene dicarboxaldehyde 5 (503 mg, 1.00 mmol) were dissolved in THF (15 mL). Then a 1M solution of potassium *tert*-butoxide in THF (2.5 mL, 2.5 mmol) was added to the solution and the mixture and the solution was stirred at room temperature for 48 h to obtain an opaque, dark red solution. Then an additional THF (10 mL) was added and the reaction stirred for an additional 72 hours. The solution was then precipitated by pouring into MeOH and filtered to obtain a red-orange solid. The resultant polymer was purified via Soxhlet extraction (MeOH, hexane and THF). Evaporation of the THF layer yielded the polymer.

***cis*-DDO-PPVBBO (P25) (40% yield).** ¹H-NMR (400 MHz, THF-d₈): δ 0.886 (m, CH₃-), 1.29 (br m, -(CH₂)₁₀-), 4.16 (br m, -OCH₂-), 7.72-8.10 (br m, Ar-H and vinylic peaks), 10.41 terminal aldehyde peak, 10.68 terminal P(=O)(OH)₂. GPC: M_n = 5,885, M_w = 14,424, PDI = 2.45. UV-Vis (THF) λ_{max} = 405 nm. Fluorescence (THF): λ_{em} = 495, 526 nm (λ_{exc} = 405 nm).

***trans*-DDO-PPVBBO (P45) (53% yield).** ¹H-NMR (400 MHz, THF-d₈): δ 0.866 (m, CH₃-), 1.29 (br m, -(CH₂)₁₀-), 4.17 (br m, -OCH₂-), 7.62-8.079 (br m, Ar-H and vinylic peaks). GPC: M_n = 6,843, M_w = 18,082, PDI = 2.64. UV-Vis (THF) λ_{max} = 456 nm. Fluorescence (THF): λ_{em} = 518, 549 nm (λ_{exc} = 450 nm).

4.4 RESULTS AND DISCUSSION



Scheme 1. Synthesis of monomers and polymers.

The synthetic routes for polymers **P25** and **P45** are shown in Scheme 1. The synthesis of monomers **2** and **4** was accomplished by the Arbuzov reaction between triethylphosphite and the corresponding 2,6-bis(chloromethyl)benzobisoxazoles, according to known procedures.¹⁶ Initially, the polymerization was performed at room temperature for 24 hours, and low molecular-weight polymers were obtained. An increase in the reaction temperature to reflux led to an increase in the molecular weight of the polymer; however, this was accompanied by the formation of a substantial amount of insoluble material. Ultimately, we found that performing the reaction at room temperature for a longer time period gave the best results. The optimized conditions for the HWE polymerization were to dissolve both 2,5-didodecyloxyterephthalaldehyde (**5**) and a benzobisoxazole monomer (**2** or **4**) in THF under an inert atmosphere. We then added 2.5 equivalents of potassium tert-butoxide in THF and stirred the reaction at room temperature for 5 days. The resulting polymers were isolated by precipitation into methanol and further purified by Soxhlet extraction. The polymers were obtained in yields of 53% for **P25** and 40% for **P45**. Both polymers were highly soluble in standard

organic solvents, such as THF and chloroform. Thus we were able to confirm the chemical structures of **P25** and **P45** using ^1H NMR, and measure the relative molecular weights of both polymers by gel permeation chromatography (GPC) at 35 °C using THF as an eluent. Polymer **P25** had a molecular weight $M_w=18,100$ and a polydispersity index (PDI) = 2.64. Polymer **P45** had a molecular weight $M_w =14,400$ and a PDI = 2.45. The results are summarized in Table 1.

Polymer	M_w^a	PDI	T_d (°C) ^b	T_g (°C) ^c
P25	14400	2.45	315	118
P45	18100	2.64	304	99

^a Determined by GPC in THF using polystyrene standards. ^b 5% weight loss temperature by TGA under N_2 . ^c Data from second scan reported, heating rate 15 °C/min under N_2 .

Table 1. Physical properties of DDO-PPVBBOs **P25** and **P45**.

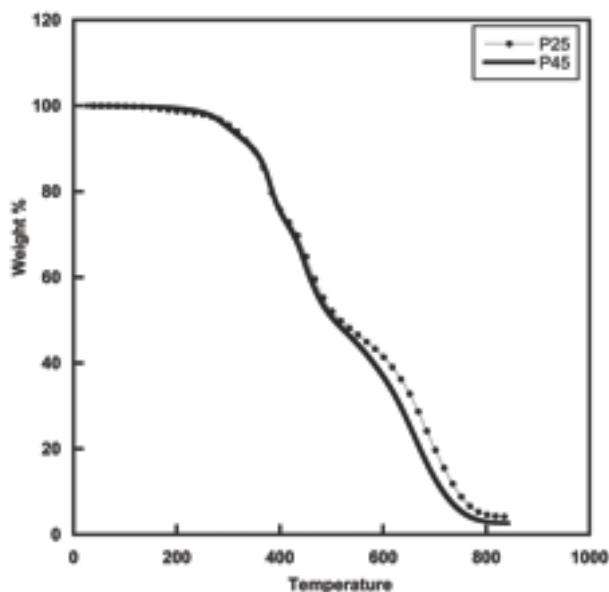


Figure 1. TGA curves of **P25** and **P45**.

To further characterize the properties of **P25** and **P45**, we evaluated their thermal stability using thermogravimetric analysis and differential scanning calorimetry. The TGA curves are shown in Figure 1 and the data summarized in Table 1. We anticipated that using flexible side chains to improve solubility of the polymers would reduce the

thermal stability of the new polymer relative to known unsubstituted PBOs.^{9b} Both polymers were found to be thermally stable with weight loss onsets occurring only above 300 °C under nitrogen. While the T_d is significantly lower than the decomposition temperatures of unsubstituted polybenzobisoxazoles (600 °C),^{9a} it is still high enough for these polymers to be useful in semiconducting applications. Additionally, DSC revealed glass transition temperatures (T_g) of 118°C for **P25** and 99°C for **P45**, whereas unsubstituted polybenzobisoxazoles did not show any observable transitions before their decomposition temperature. The observance of a T_g 's at lower temperatures are due in part to the low molecular weight of the polymers in addition to the presence of the alkoxy side chains.

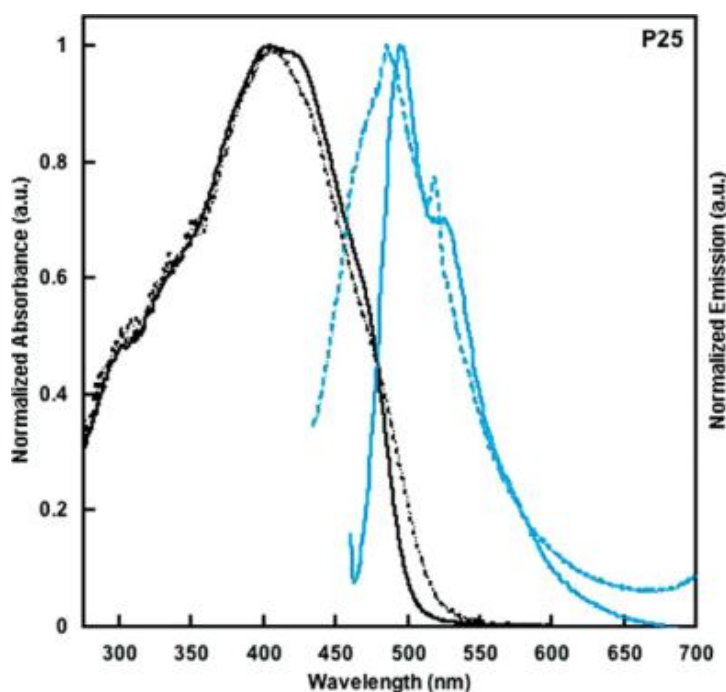


Figure 2. Absorption (black), emission spectra (aqua) of polymers **P25** in solution (THF, solid lines) and of thin films (cast from THF, dashed lines).

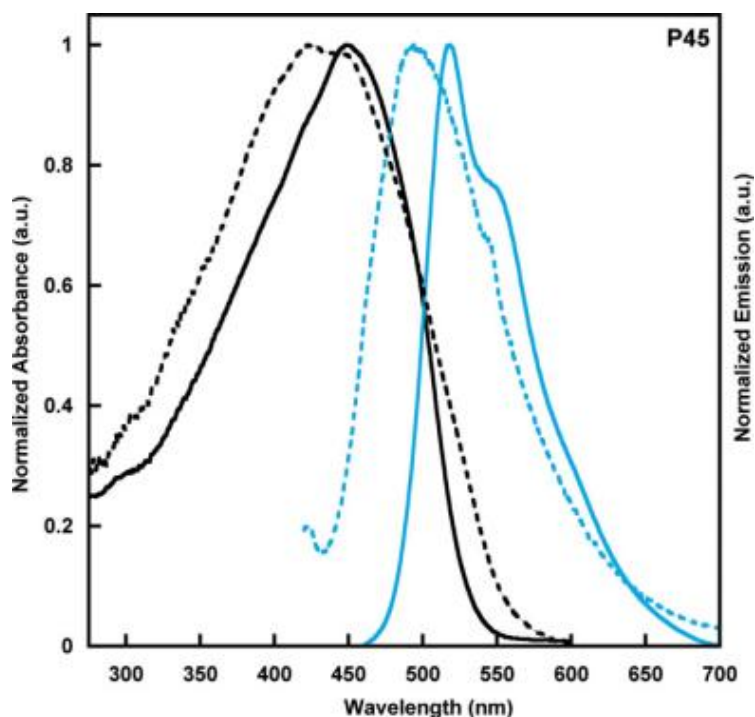


Figure 3. Absorption (black), emission spectra (aqua) of **P45** in solution (THF, solid lines) and of thin films (cast from THF, dashed lines).

To evaluate the optical properties of **P25** and **P45**, we performed UV-Vis and fluorescence and photoluminescence (PL) spectroscopy. The PL quantum yield of **P25** was determined to be 0.40 in solution and 0.01 in the solid state. Similarly, **P45** has a solution PL quantum yield of 0.48 and a solid-state quantum yield of 0.01. These small values are typical of polymers with closely packed chains. The absorption and emission spectra for these polymers were measured both as solutions in THF and as thin films. We observed a $\lambda_{\text{max}}^{\text{ab}}$ at 405 nm for **P25** and $\lambda_{\text{max}}^{\text{ab}}$ at 450 nm for **P45**. Both polymers were highly fluorescent and upon excitation at their respective λ_{max} showed two peaks: **P25** had a $\lambda_{\text{max}}^{\text{em}}$ at 495 nm and shoulder at 526 nm, and **P45** had a $\lambda_{\text{max}}^{\text{em}}$ at 518 nm and a shoulder at 549 nm. The thin film UV-Vis absorption of **P25** showed only a negligible difference compared to the solution spectra with $\lambda_{\text{max}}^{\text{ab}} = 406$ nm, versus the solution $\lambda_{\text{max}}^{\text{ab}} = 405$ nm. Similarly, the thin film fluorescence emission of **P25** showed a slight blue shift compared to the solution spectra with $\lambda_{\text{max}}^{\text{em}} = 490, 520$ nm versus the solution $\lambda_{\text{max}}^{\text{em}} = 495, 518$ nm (Figure 2). In contrast, the thin film UV-Vis absorption of **P45**

showed a considerable blue-shift compared to the solution spectra with $\lambda_{\max}=423$ nm, versus the solution $\lambda_{\max}=450$ nm. Similarly, the thin film fluorescence emission of **P45** showed a blue shift in comparison to the solution spectra with $\lambda_{\max}^{\text{em}}=485$ nm versus the film $\lambda_{\max}^{\text{em}}=518$ nm (Figure 3). Typically, blue shifts suggest a slight decrease of the conjugation length in the solid state, most likely due to inefficient packing. Conversely, red shifts suggest an increase in conjugation length, often due to planarization of the polymer in the solid state. In our case, we are observing a greater blue shift in the *trans*-DDO-PPVBBO **P45**, but not in the *cis*-DDO-PPVBBO **P25**. Thus the origin of the blue shift is most likely due to excited state relaxations. In similar fashion to the well-known planarization of the excited state of biphenyl, where upon the double bond character between rings increases in the excited state and the molecule planarizes.¹⁷

Polymer	Media	λ_{abs} (nm)	λ_{em} (nm)	Φ_{re}	$E_{\text{g}}^{\text{opt}}$ (eV) ^a	E_{red} (V) ^b	EA (eV) ^c	IP (eV) ^d
P25	THF	405	495, 526	0.40 ^e	2.4	-1.34	3.1	5.5
	Film	406	490, 520	0.01 ^f				
P45	THF	450	518, 549	0.48 ^e	2.2	-1.34	3.1	5.3
	Film	423	485	0.01 ^f				

^a Solution fluorescence quantum yield relative to Coumarin 6 in ethanol. ^b Solid-state quantum yield relative to perylene 10 wt% in PMMA. ^c Estimated from the optical absorption edge. ^d Formal reduction potentials (vs SCE). ^eEA= $E_{\text{onset}} + 4.4$ (eV). ^f IP = EA + E_{g} (eV).

Table 2. Electronic and optical properties of DDO-PPVBBOs **P25** and **P45**.

To determine the electronic properties of **P25** and **P45**, we performed cyclic voltammetry of polymer thin films in acetonitrile, using 0.1 M (Bu)₄NPF₆ as the electrolyte. The results are summarized in Table 2. For both polymers we observed quasi-reversible reduction wave, but oxidation waves were not observed. We measured reduction onsets at -1.34 V versus SCE for both **P25** and **P45**. Taking -4.4 eV as the SCE energy level relative to vacuum,¹⁸ we estimated electron affinity (EA) for both polymers to be 3.06 eV. The optical band gaps were 2.4 eV for **P25** and 2.2 eV for **P45**. Using the optical band gaps, and the relation IP = EA + E_{g} (eV) ionization potential (IP) values of 5.5 and 5.3 eV were estimated for **P25** and **P45** respectively. The band gaps measured for these new polymers were smaller than the band gaps for the known PBO derivative

poly(phenylenebenzo[1,2-*d*;5,4-*d'*]bisoazole), ($E_g^{\text{opt}} = 2.76$ and $E_g^{\text{ec}} = 2.93$ eV).^{6a, 6c}

4.5 CONCLUSIONS

In summary, we prepared new organic soluble derivatives of polybenzobisoxazoles using the flexible side chain approach. The resulting polymers were soluble in several organic solvents and still maintained excellent thermal stability. These mild reaction conditions facilitated the synthesis of new polymers that were previously unattainable through conventional synthesis. As a result, we now have the opportunity to modify the thermal, optical, and electronic properties of these polymers in an unprecedented manner, facilitating their optimization for use in organic semiconducting applications.

4.6 ACKNOWLEDGEMENTS

We thank the 3M Foundation, the National Science Foundation (DMR-0846607), Iowa State University and the Institute for Physical Research and Technology (IPRT) for financial support of this work. The authors also thank Kanwar Nalwa and Professor Sumit Chaudhary (ISU) for help with CV measurements and Ms. Trisha Andrew (MIT) for PL spectra and PL quantum yield measurements.

4.7 REFERENCES

- (1) (a) Bao, Z.; Dodabalapur, A.; Lovinger, A. *J. Appl. Phys. Lett.* **1996**, *69*, 4108-4110; (b) Dimitrakopoulos, C. D.; Malenfant, P. R. L. *Adv. Mater.* **2002**, *14*, 99-117; (c) Newman, C. R.; Frisbie, C. D.; daSilva Filho, D. A.; Bredas, J. L.; Ewbank, P. C.; Mann, K. R. *Chem. Mater.* **2004**, *16*, 4436-4451; (d) Zaumseil, J.; Sirringhaus, H. *Chem. Rev.* **2007**, *107*, 1296-1323.
- (2) (a) Friend, R. H.; Gymer, R. W.; Holmes, A. B.; Burroughes, J. H.; Marks, R. N.; Taliani, C.; Bradley, D. D. C.; Dos Santos, D. A.; Bredas, J. L.; Logdlund, M.; Salaneck, W. R. *Nature* **1999**, *397*, 121-128; (b) Kraft, A.; Grimsdale, A. C.; Holmes, A. B. *Angew Chem. Int. Ed. Eng.* **1998**, *37*, 403-428; (c) Tang, C. W.; VanSlyke, S. A. *Appl. Phys. Lett.* **1987**, *51*, 913-915.
- (3) (a) Gunes, S.; Neugebauer, H.; Sariciftci, N. S. *Chem. Rev.* **2007**, *107*, 1324-1338; (b) Scharber, M. C.; Muehlbacher, D.; Koppe, M.; Denk, P.; Waldauf, C.; Heeger,

A. J.; Brabec, C. *J. Adv. Mater.* **2006**, *18*, 789-794; (c) Yu, G.; Gao, J.; Hummelen, J. C.; Wudl, F.; Heeger, A. *J. Science* **1995**, *270*, 1789-1791.

(4) (a) Karastatiris, P.; Mikroyannidis, J. A.; Spiliopoulos, I. K. *Journal of Polymer Science Part A: Polymer Chemistry* **2008**, *46*, 2367-2378; (b) Grisorio, R.; Piliago, C.; Cosma, P.; Fini, P.; Mastroilli, P.; Gigli, G.; Suranna, G. P.; Nobile, C. F. *Journal of Polymer Science Part A: Polymer Chemistry* **2009**, *47*, 2093-2104; (c) Xun, S.; Zhou, Q.; Li, H.; Ma, D.; Wang, L.; Jing, X.; Wang, F. *Journal of Polymer Science Part A: Polymer Chemistry* **2008**, *46*, 1566-1576.

(5) (a) Alam, M. M.; Jenekhe, S. A. *Chem. Mater.* **2002**, *14*, 4775-4780; (b) Jenekhe, S. A.; de Paor, L. R.; Chen, X. L.; Tarkka, R. M. *Chem. Mater.* **1996**, *8*, 2401-2404.

(6) (a) Chen, Y.; Wang, S.; Zhuang, Q.; Li, X.; Wu, P.; Han, Z. *Macromolecules* **2005**, *38*, 9873-9877; (b) Feng, D.; Wang, S.; Zhuang, Q.; Wu, P.; Han, Z. *Polymer* **2004**, *45*, 8871-8879; (c) Jenekhe, S. A.; Osaheni, J. A. *Chem. Mater.* **1994**, *6*, 1906-1909; (d) Osaheni, J. A.; Jenekhe, S. A. *Macromolecules* **1994**, *27*, 739-742; (e) Osaheni, J. A.; Jenekhe, S. A. *Chem. Mater.* **1995**, *7*, 672-682; (f) Osaheni, J. A.; Jenekhe, S. A.; Burns, A.; Du, G.; Joo, J.; Wang, Z.; Epstein, A. J.; Wang, C. S. *Macromolecules* **1992**, *25*, 5828-5835; (g) Zhang, X.; Jenekhe, S. A. *Macromolecules* **2000**, *33*, 2069-2082.

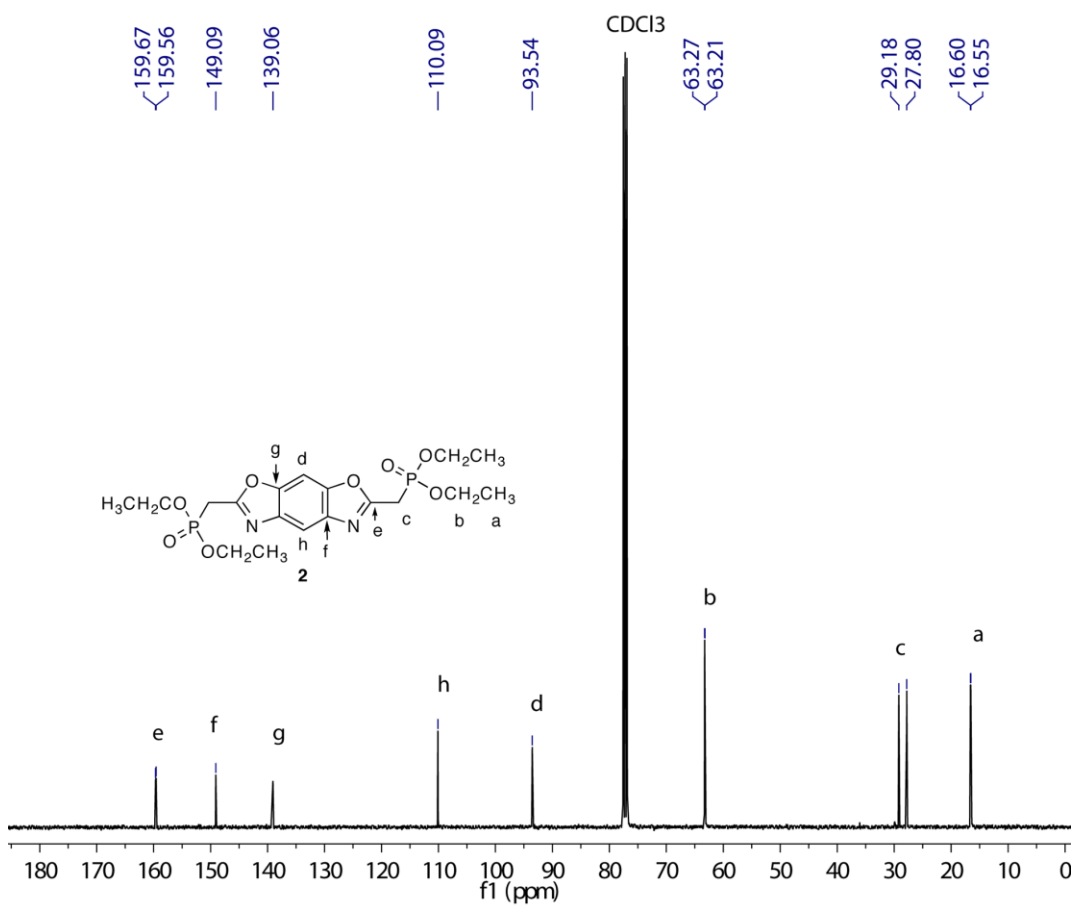
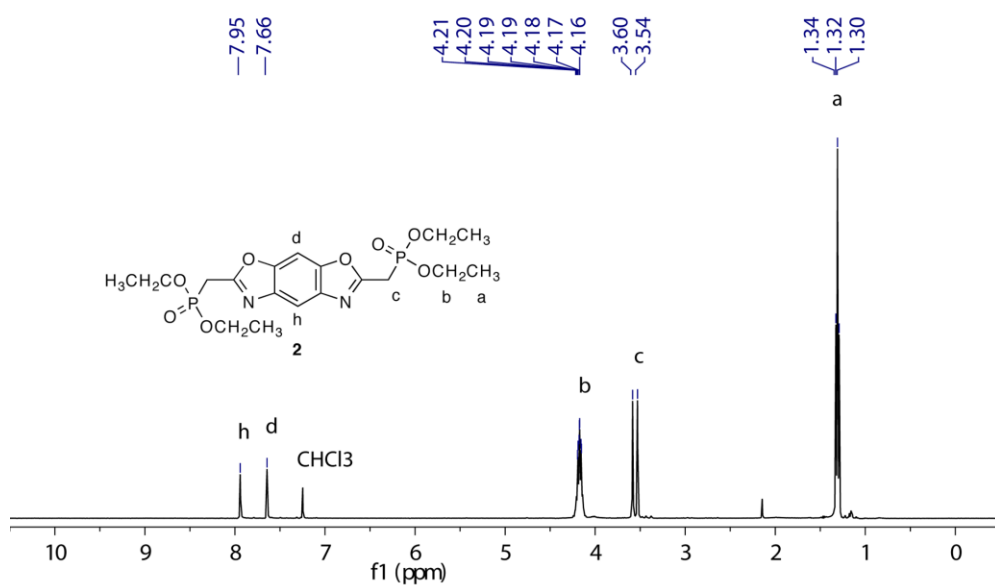
(7) Jenekhe, S. A.; Osaheni, J. A.; Meth, J. S.; Vanherzeele, H. *Chem. Mater.* **1992**, *4*, 683-687.

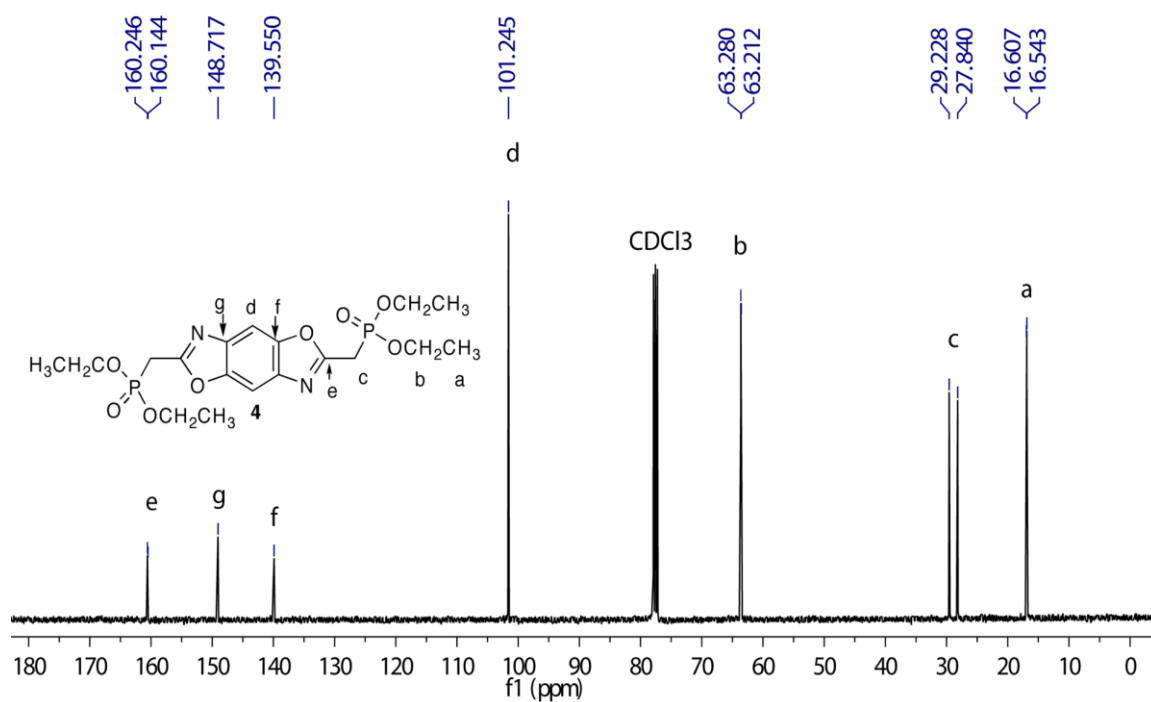
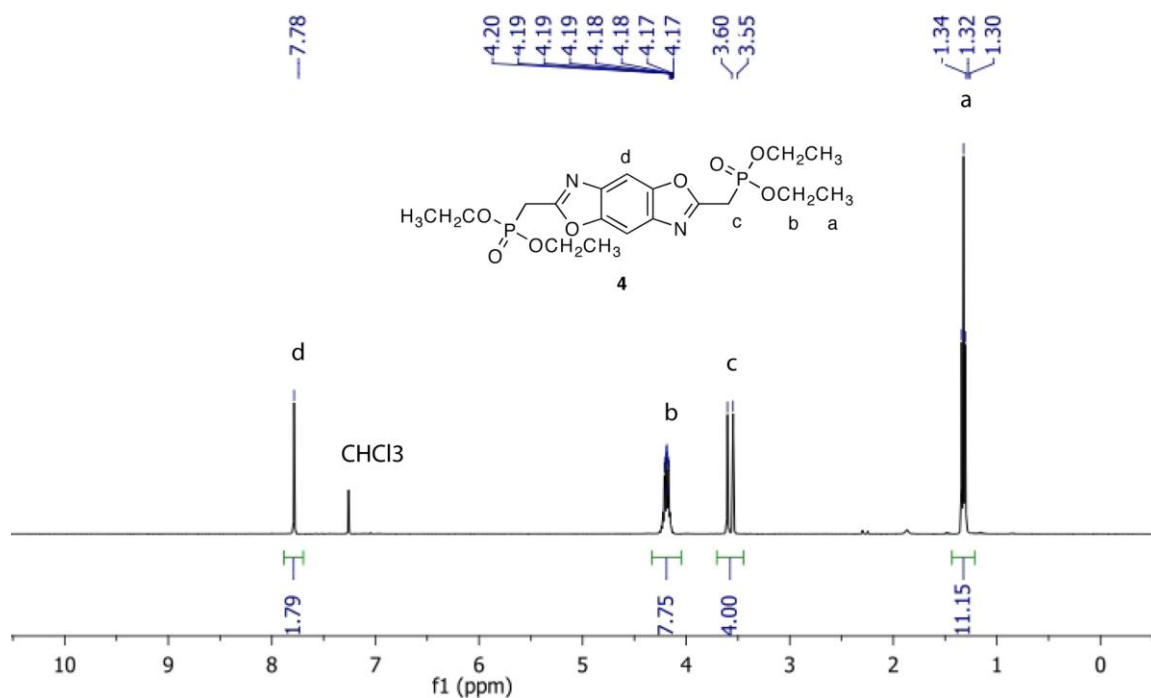
(8) (a) Baek, J. B.; Tan, L. S. *Macromolecules* **2008**, *41*, 1196-1205; (b) Kitagawa, T.; Murase, H.; Yabuki, K. *J. Polym. Sci. Part B: Polym. Phys.* **1998**, *36*, 39-48; (c) So, Y.-H.; Sen, A.; Kim, P.; Jeor, V. S. *J. Polym. Sci. Part A: Polym. Chem.* **1995**, *33*, 2893-2899; (d) Wu, Z. S.; Iwashita, K.; Hayashi, K.; Higuchi, T.; Murakami, S.; Koseki, Y. *J. Reinf. Plast. Compos.* **2003**, *22*, 1269-1286; (e) Xiao-Dong Hu; Jenkins, S. E.; Min, B. G.; Polk, M. B.; Kumar, S. *Macromolecular Materials and Engineering* **2003**, *288*, 823-843.

(9) (a) Wolfe, J. F. In *Encyclopedia of Polymer Science and Engineering*; John Wiley and Sons: New York, NY, **1988**, p. 601-635; (b) Wolfe, J. F.; Arnold, F. E. *Macromolecules* **1981**, *14*, 909-915.

- (10) (a) Choe, E. W.; Kim, S. N. *Macromolecules* **1981**, *14*, 920-924; (b) Jenekhe, S. A.; Johnson, P. O. *Macromolecules* **1990**, *23*, 4419-4429; (c) Roberts, M. F.; Jenekhe, S. A. *Chem. Mater.* **1993**, *5*, 1744-1754.
- (11) (a) Rehahn, M.; Schlueter, A. D.; Wegner, G.; Feast, W. J. *Polymer* **1989**, *30*, 1054-1059; (b) Rehahn, M.; Schluter, A. D.; Wegner, G. *Makromol. Chem.* **1990**, *191*, 1991-2003; (c) Rehahn, M.; Schuler, A.-D. *Makromol. Chem., Rapid Commun.* **1990**, *11*, 375-379; (d) Chen, T. A.; Rieke, R. D. *J. Am. Chem. Soc.* **1992**, *114*, 10087-10088; (e) McCullough, R. D.; Lowe, R. D.; Jayaraman, M.; Anderson, D. L. *J. Org. Chem.* **1993**, *58*, 904-912; (f) Weder, C.; Wrighton, M. S. *Macromolecules* **1996**, *29*, 5157-5165.
- (12) (a) Imai, Y.; Itoya, K.; Kakimoto, M.-A. *Makromol. Chem. Phys.* **2000**, *201*, 2251-2256; (b) Imai, Y.; Taoka, I.; Uno, K.; Iwakura, Y. *Makromol. Chem.* **1965**, *83*, 167-187; (c) Kricheldorf, H. R.; Domschke, A. *Polymer* **1994**, *35*, 198-203; (d) So, Y. H.; Heeschen, J. P. *J. Org. Chem.* **1997**, *62*, 3552-3561.
- (13) Liu, X.; Xu, X.; Zhuang, Q.; Han, Z. *Polym. Bull.* **2008**, *60*, 765-774.
- (14) Mike, J. F.; Makowski, A. J.; Jeffries-EL, M. *Org. Lett.* **2008**, *10*, 4915-4918.
- (15) Fery-Forgues, S.; Lavabre, D. *Journal of Chemical Education* **1999**, *76*, 1260-1264.
- (16) Liao, J.; Wang, Q. *Macromolecules* **2004**, *37*, 7061-7063.
- (17) See pp 7 and 8 in: Lakowicz, J. R. *Principles of Fluorescence Spectroscopy*, Plenum Press: New York, **1986**.
- (18) Agrawal, A. K.; Jenekhe, S. A. *Chem. Mater.* **1996**, *8*, 579-589.

4.8 SUPPORTING INFORMATION





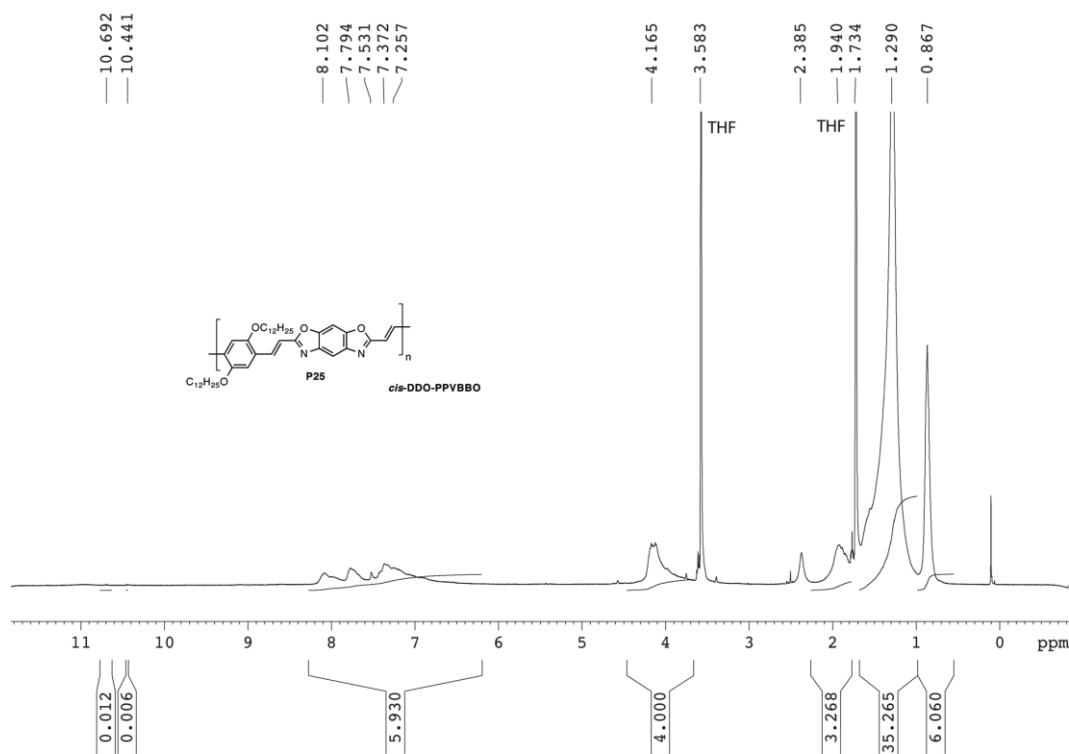


Figure S5. ^1H NMR of **P25** in THF-d_8 .

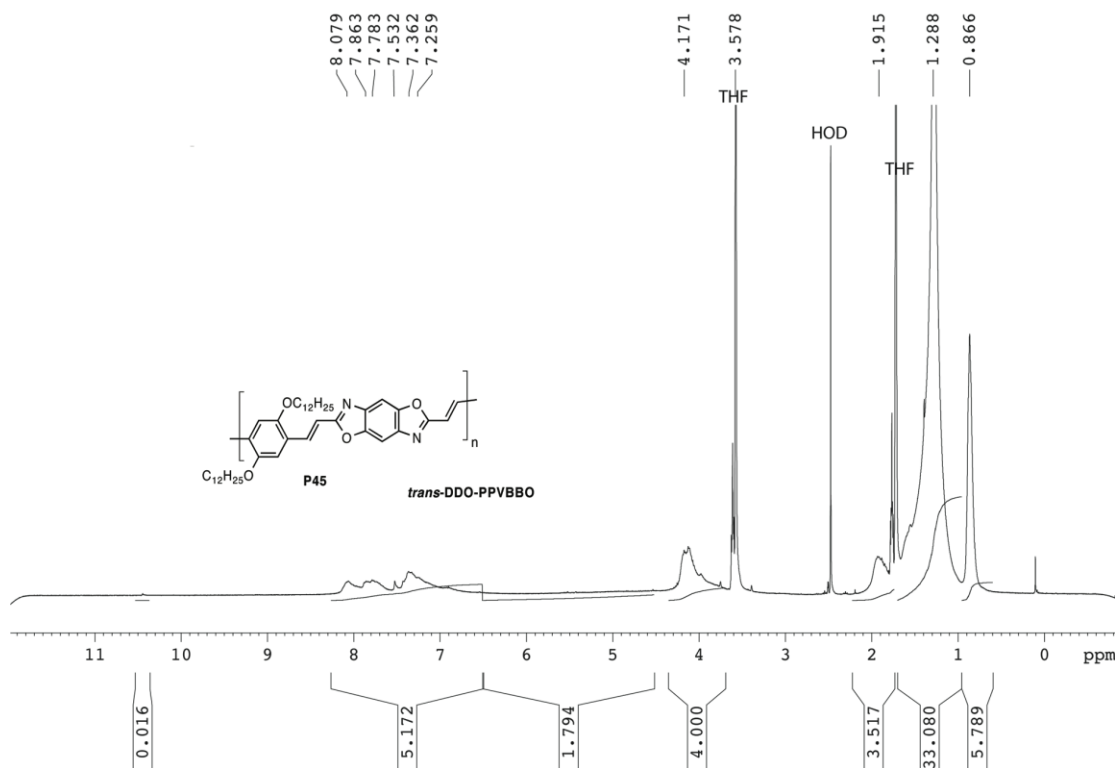


Figure S6. ^1H NMR of **P23** in THF-d_8 .

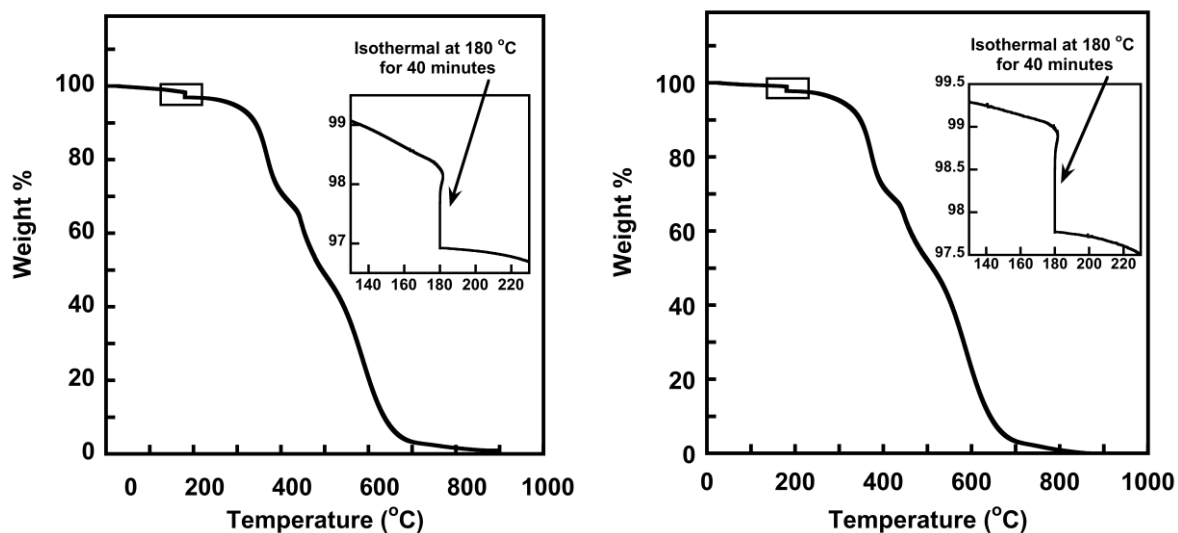


Figure S7. TGA curves of **P25** (left) and **P45** (right).

Scanning rates was performed from RT – 180°C at 20°C/min, then isothermal heating at 180°C for 40 minutes, followed by heating from 180°C – 900°C at 20°C/min in air.

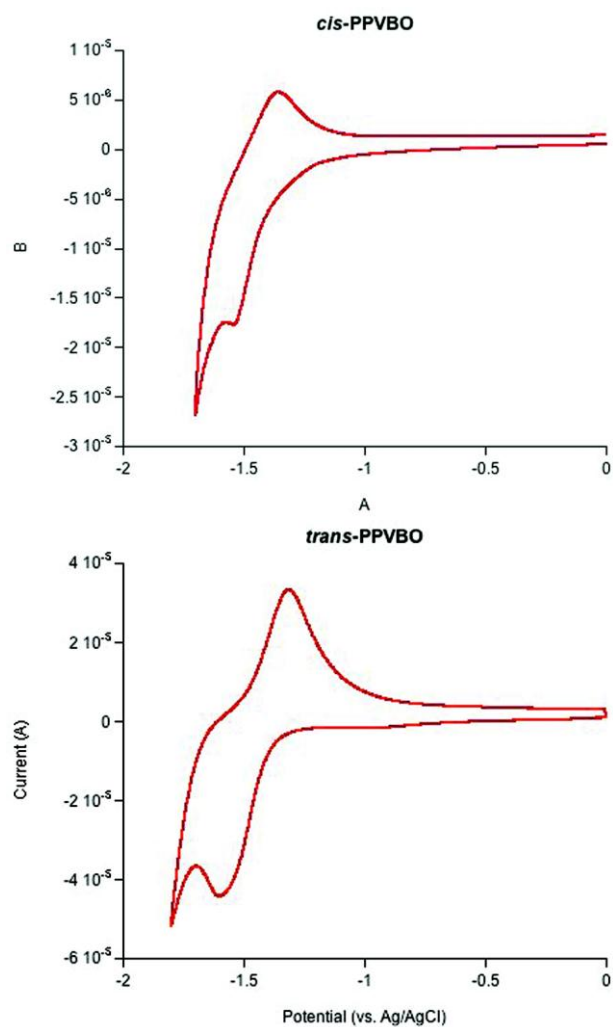


Figure S8. Cyclic voltammogram of **P25** (left) and **P45** (right).

Measurements performed on thin films in 0.1M TBAPF₆ in acetonitrile using Ag/AgCl as reference electrode at a scan rate of 100 mV/s.

CHAPTER 5

Synthesis, Characterization and Photovoltaic Properties of Poly(thiophenevinylene-alt-benzobisoxazole)s.

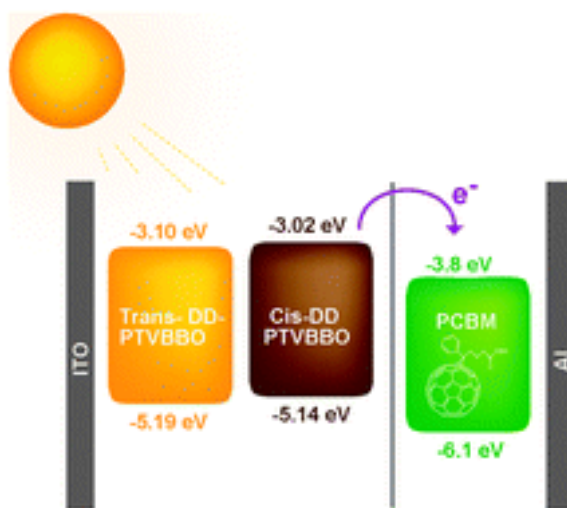
Reproduced from *Physical Chemistry Chemical Physics* **2011**, 13, 1338 with permission from the Owner Societies
Copyright © 2011

Jared F. Mike,^a Kanwar Nalwa,^b Andrew J. Makowski,^a Daniel Putnam,^b Aimée L. Tomlinson,^c Sumit Chaudhary^b and Malika Jeffries-EL^{*a}

^a Department of Chemistry, Iowa State University, 1605 Gilman Hall, Ames, IA 50010

^b Department of Electrical Engineering, Iowa State University, Ames, IA 50011

^c Department of Chemistry, North Georgia College & State University, GA 30597, USA

5.1 ABSTRACT

Herein we report the synthesis of two solution processible, conjugated polymers containing the benzobisoxazole moiety. The polymers were characterized using ¹H NMR, UV-Vis and fluorescence spectroscopy. Thermal gravimetric analysis shows that the polymers do not exhibit significant weight loss until approximately 300 °C under nitrogen. Cyclic voltammetry shows that the polymers have reversible reduction waves with estimated LUMO levels at -3.02 and -3.10 eV relative to vacuum and optical bandgaps of 2.04 - 2.17 eV. Devices based on blends of the copolymers and [6,6]-phenyl

C61 butyric acid methyl ester (PCBM) exhibited modest power conversion efficiencies. Theoretical models reveal that there is poor electron delocalization along the polymer backbone, leading to poor performance. However, the energy levels of these polymers indicate that the incorporation of benzobisoxazoles into the polymer backbone is a promising strategy for the synthesis of new materials.

5.2 INTRODUCTION

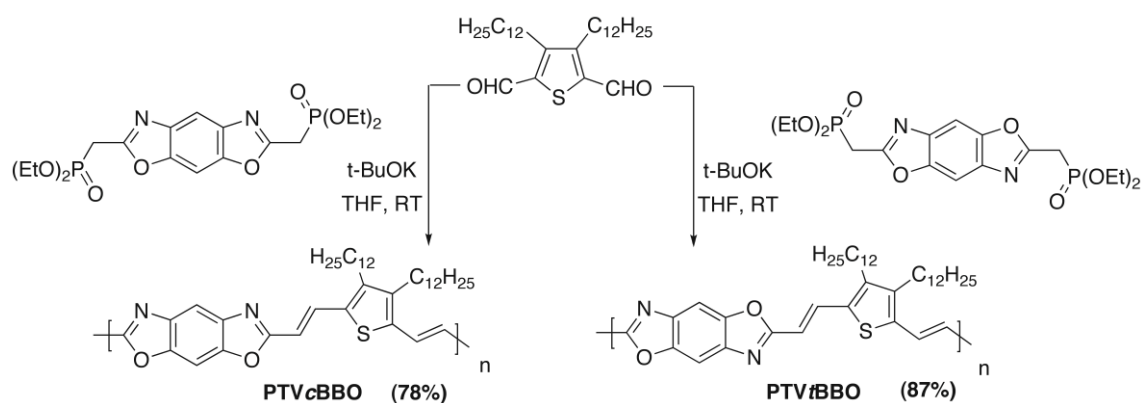
The direct conversion of sunlight into energy using photovoltaic cells (PVC)s has been recognized as an essential component of future global energy production. As a result of their optical and electronic properties, conjugated organic materials are sought after to replace inorganic materials in PVCs. This is due to the many attractive features of organic materials, such as the ability to tune their electron properties for specific applications through chemical synthesis and the simplicity of processing using solution-based techniques.^{1, 2} One current challenge in the field is the development of conjugated polymers with high electron affinity and/or low band gaps for use in bulk heterojunction PVCs.³ High electron affinity can reduce the energy loss during the transfer of electrons from the donor to [6,6]-phenyl C₆₁ butyric acid methyl ester (PCBM), a widely used electron acceptor, increasing the output power of the PVC.⁴⁻⁶ Similarly, low band gap allows for the absorption of photons at longer wavelengths, increasing the percentage of solar energy that can be harvested.^{7, 8} Currently, a popular design strategy for the manipulation of the energy levels of conjugated polymers is the synthesis of so called D-A donating (D) and electron-accepting (A) moieties.⁹ In these polymers the hybridization of the LUMO from the acceptor copolymers, which are comprised of alternating electron- moiety and the HOMO from the donor moiety can be used to reduce the polymers band gap and/or vary its energy levels.⁹⁻¹¹

Poly(3-alkylthiophene)s are widely studied due to their excellent thermal and environmental stability, high hole mobility, and solution processibility.^{12, 13} Accordingly, electron-rich alkylthiophenes have been widely used as donor moieties in D-A polymer architectures.^{11, 14-16} Fully conjugated rigid-rod polybenzobisoxazoles (PBBO)s are multifunctional materials widely known for their excellent tensile strength, thermal

stability,^{17, 18} efficient electron transport,^{19, 20} photoluminescence,²¹⁻²⁷ and high electron affinity.^{21, 28-31} Thus the incorporation of the benzobisoxazole (BBO) moiety into D-A polymer architectures is beneficial due to its high electron affinity.¹⁶ Despite these advantageous properties, the use of PBBO has been limited, largely due to their poor solubility, which requires PBBO to be processed from acidic solutions. Furthermore, the harsh reaction conditions for the synthesis of PBBO prevents their derivatization.^{18, 31-36} To realize the untapped potential of the BBO moiety for the development of novel conjugated polymers, we recently developed an alternative approach toward BBO synthesis using mild conditions.³⁷ As a result, we can now synthesize soluble PBBO by copolymerizing them with aryl monomers bearing flexible side-chains.^{37, 38}

Herein we report the synthesis of two new polymers, namely poly(3,4-didodecylthiophene vinylene)-alt-benzo[1,2-*d*;5,4-*d'*]bisoxazole]-2,6-diyl (PTVcBBO) and poly(3,4-didodecylthiophene vinylene)-alt-benzo[1,2-*d*;4,5-*d'*]bisoxazole]-2,6-diyl (PTVtBBO). The unique combination of the BBO, thiophene, and vinylene moieties greatly enhances the properties of the resultant polymer by: 1) incorporating vinylene linkages to minimize steric interactions between consecutive aromatic rings, reducing the band gap further;³⁹⁻⁴¹ 2) increasing rotational freedom of the polymer backbone, improving the polymer's solubility; and 3) adding alkyl side chains along the polymer backbone to increase solubility significantly.

5.3 RESULTS AND DISCUSSION



Scheme 1. Synthesis of PTVcBBO and PTVtBBO.

5.3.1 Polymer synthesis and physical characterization.

The synthesis of PTVcBBO and PTVtBBO is shown in Scheme 1. The robust BBOs were stable under basic conditions, allowing for their polymerization using the Horner-Wadsworth-Emmons (HWE) reaction. These reaction conditions were selected because the HWE reaction is known to produce polymers with all trans-double bonds. This method also prevents cross-linking, incomplete double bond formation, and other undesirable structural defects. The optimum reaction conditions were to dissolve both 3,4-didodecyl-2,5-thiophenedicarboxaldehyde⁴² and a BBO monomer³⁷ in THF under an inert atmosphere, then add 2.2 equivalents of potassium tert-butoxide, and stir the reaction at room temperature for 3 days. Using these conditions the polymers were obtained in satisfactory yields, after removing low molecular weight material via Soxhlet extraction. Both polymers were highly soluble in standard organic solvents, such as THF, m-cresol and chloroform at room temperature, facilitating characterization using ¹H NMR spectroscopy and gel permeation chromatography (GPC). The ¹H NMR spectra for both polymers were in agreement with the proposed polymer structures. The weight-averaged molecular weights (M_w) of the polymers were good in both cases, with monomodal weight distributions. Thermogravimetric analysis revealed that both polymers were thermally stable with 5% weight loss onsets occurring at approximately 300 °C under air. The results are summarized in Table 1.

	Yield %	M_w^a	M_w/M_n	T_d (°C) ^b
PTVcBBO78		13,400	2.4	303
PTVtBBO 87		10,800	2.7	298

^a Molecular weights and polydispersity indexes determined by GPC versus polystyrene standards using THF as the eluent. ^b Temperature at which 5% weight loss is observed by TGA under N₂ with a heating rate of 10 °C/min.

Table 1. Molecular weights and thermal properties of the PTVBBOs.

5.3.2 Optical properties.

The photophysical characteristics of the polymers were evaluated by UV-vis absorption and fluorescence spectroscopy both as dilute solutions in THF and thin films. The normalized absorbance and emission spectra for the polymers in solutions and thin

films are shown in Figure 1 and the data is summarized in Table 2. In solution, the UV-vis spectra of both polymers have a single broad absorbance bands, whereas the thin film absorbance spectra for both polymers are slightly broader. The absorption maximum for PTVtBBO was red-shifted by 27 nm relative to the absorbance maximum for PTVcBBO. In both cases the UV-vis spectra did not exhibit a second low energy peak typically associated with intramolecular charge-transfer (ICT) transitions within D-A copolymers.^{43, 44}

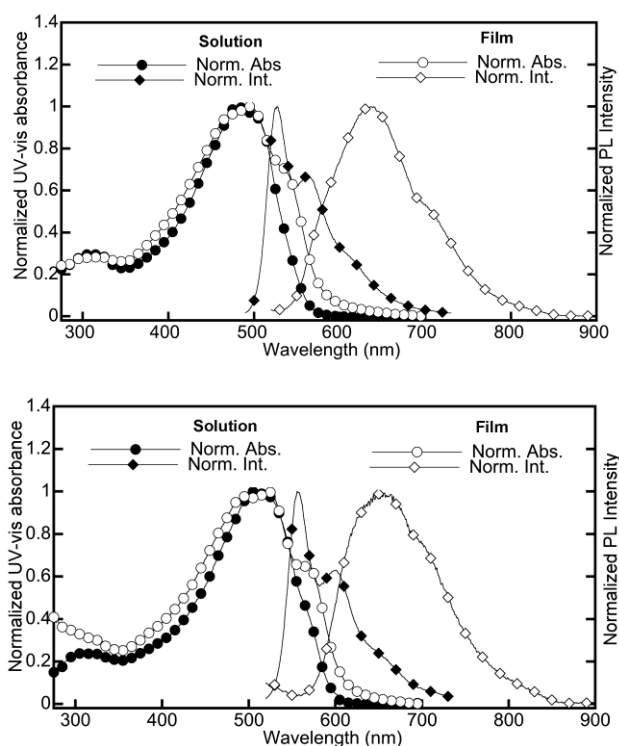


Fig. 1 Uv-vis absorption and PL spectra of a: PTVcBBO (top) and b: PTVtBBO (bottom) in THF and as films spun from THF.

The optical band gaps for the polymers were estimated from absorption onsets and are summarized in Table 2. In solution the photoluminescence spectra of both polymers exhibit vibrational structure in the form of additional low energy bands. As with the UV-vis spectra the emission spectra of the PTVtBBO is red-shifted relative to the PTVcBBO. As films, the emission spectra of the polymer thin films were considerably red-shifted,

relative to corresponding solution spectra. This phenomenon is most likely caused by π -stacking and excimer emission. When the polymers were mixed with PCBM, the fluorescence was quenched, suggesting efficient charge transfer between the two materials.

Polymer	Solution		Film			$E_g^{opt}(eV)^a$	$E_{onset}^{red}{}^b$	LUMO	HOMO
	$\lambda_{abs}(nm)$	λ_{em} (nm)	λ_{abs} (nm)	λ_{em} (nm)	$\lambda_{onset}(nm)$				
PTVcBBO	480	497 (536)	527 (562)	635 (601)	571	2.17	-1.34	-3.02	-5.19
PTVtBBO	507	525 (565)	556 (601)	653 (601)	608	2.04	-1.26	-3.10	-5.14

^aEstimated from the optical absorption edge. ^bOnset reduction potentials (vs Fc). ^cLUMO = + 4.8 (eV). ^dHOMO = LUMO - (eV).

Table 2. Electronic and Optical and Electronic Properties of **PTVcBBO** and **PTVtBBO**.

5.3.3 Electrochemical properties.

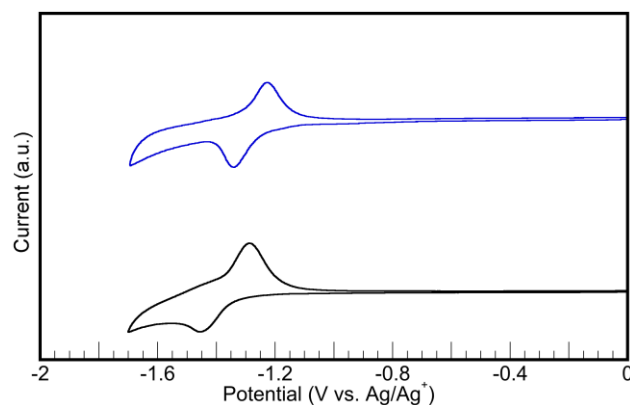


Fig. 2 Cyclic voltammogram of the PTVcBBO (bottom) and PTVtBBO (top) thin films on platinum electrodes with a scan rate of 50 mV s^{-1} .

The electrochemical properties of the polymers were investigated by cyclic voltammetry (CV). The data was obtained from polymer thin films on a platinum

working electrode, in acetonitrile, using 0.1 M Bu_4NPF_6 as the electrolyte and an Ag/Ag^+ reference electrode. The onsets were referenced to Fc/Fc^+ . The CV curves are shown in Figure 2 and the results are summarized in Table 2. Both polymers exhibited fully chemically reversible reduction waves, whereas oxidation waves were not observed for either polymer. Taking -4.8 eV as the ferrocene energy level relative to vacuum,⁴⁴ we estimated the LUMO levels for the polymers (Table 2). Since oxidation onsets could not be measured for the polymers, the highest occupied molecular orbital (HOMO) values were calculated using the optical band gaps and the LUMO levels. Previously, we reported band gaps of 2.2-2.4 eV for poly(2,5-bisdodecyloxyphenylenevinylene-co-benzobisoxazole)s.³⁸ Switching the dialkoxybenzenes for the more electron-rich thiophenes changes the position of the HOMO, resulting in a decrease in the bandgap of the polymer.

5.3.4 Photovoltaic properties.

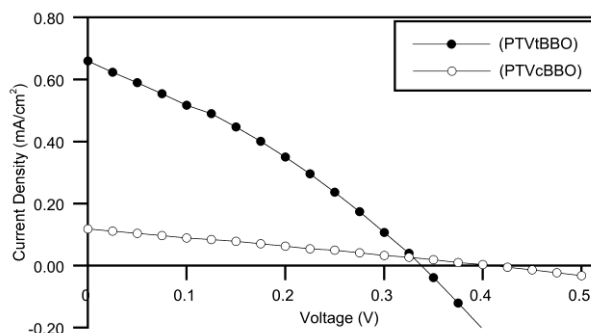


Fig 3. Current-voltage characteristics of PTVBBO:PCBM photovoltaic

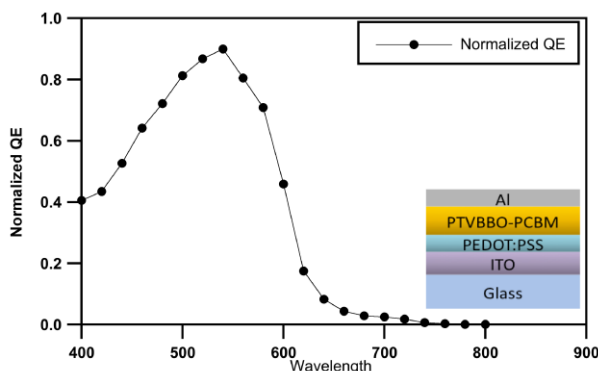


Fig 4. Normalized quantum efficiency vs. wavelength curve of PTVBBO:PCBM cells. Inset shows the device structure.

The chemically reversible reduction waves in the cyclic voltammetry suggested that the PTVBBOs could be used as acceptor materials in PVCs with regioregular poly(3-hexylthiophene) (rr-P3HT) one of the most widely studied conjugated polymers.^{12, 13} However the generally accepted minimum difference between the LUMO levels of the donor and the acceptor is ~ 0.4 eV.^{45, 46} Since rr-P3HT has a LUMO of approximately -3.0 eV,^{4, 47-49} the LUMO values of -3.02 and -3.10 eV for PTVcBBO and PTVtBBO respectively were insufficient to facilitate efficient electron transfer. However, the energy levels of these polymers suggest that they would be suitable candidates for use in bulk heterojunction PVCs with PCBM. We fabricated such PVCs from (1:1) PTVBBO:PCBM blends, using both PTVcBBO and PTVtBBO. We selected *ortho*-dichlorobenzene (*o*-DCB) as the solvent due to its high boiling point, which previously has resulted in better self-organization of conjugated polymers, enhancing the performance of PVCs.⁵⁰⁻⁵² Figure 3 shows the current-voltage (*I-V*) characteristics of our devices under illumination of 100 mW/cm^2 . For both polymers the open circuit voltages were comparable, 0.35 V and 0.40 V for PTVcBBO and PTVtBBO respectively. Overall, PTVtBBO-based PVCs had much better performance than PTVcBBO-based PVCs with a short-circuit current of 0.66 mA/cm^2 and a fill factor of 31%. In comparison, PTVcBBO-based PVCs had a short-circuit current of 0.12 mA/cm^2 and fill factor of 26%. These results are summarized in Table 3. The superior performance of PVCs based on PTVtBBO in comparison to PTVcBBO can be attributed to higher electron affinity and smaller band gap of PTVtBBO.

Polymer	$V_{oc}(\text{V})$	$J_{sc}(\text{mA/cm}^2)$	FF	PCE (%)
PTVcBBO	0.35	0.12	26%	0.01
PTVtBBO	0.40	0.66	31%	0.08

Polymers films were prepared from solutions in *o*-DCB 10 mg/mL

Table 3. Photovoltaic Performance of PTVBBOs with PCBM.

While the performance of the PTVtBBO devices is lower than other state-of-the-art

conjugated polymers, we note that these PVCs are the first to be fabricated from copolymers containing BBOs and thiophene. As a result, many processing parameters such as choice of solvent (or solvent mixtures), annealing, annealing temperatures, and polymer/PCBM ratios are not yet optimized. All of these parameters are critical, and their optimization alone has led to drastic improvements in the power conversion efficiencies of PVCs, based on other conjugated polymers such as rr-P3HT and poly[N-9'-heptadecanyl-2,7-carbazole-alt-5,5-(4',7'-di-2-thienyl-2',1',3'-benzothiadiazole)] (PCDTBT). In part, the poor performance of the PVCs fabricated in this report can be ascribed to a non-optimal phase separation, as shown in the atomic force microscopy AFM phase image (Supporting Information). Aggregates of size 50-100 nm are observed, which are much larger than typical exciton diffusion lengths of conjugated polymers (~10 nm). Further evidence of the phase separation can be seen by Raman spectroscopy. When PTVtBBO film are more crystalline, the thiophene rings are, on average, more closely stacked. This should lead to narrowing of the peaks.^{53, 54} The spectra of the neat PTVtBBO film shows peaks at 1560-1570, 1180 and 1230 cm^{-1} . In comparison, PTVtBBO:PCBM blend films exhibited broadening of these peaks which indicates a decrease in the crystallinity of PTVtBBO film. This loss of crystallinity can be attributed to very fine intermixing of PTVtBBO and PCBM domains, limiting the PTVtBBO crystallites to nanometer scale. Such poor separation or nanoscale fine mixing of phases prevents the formation continuous pathways for carrier transport to the electrodes, reducing the device efficiency. Although we could dissolve PTVtBBO in DCB, this solution does not pass through 0.2 micron filter as readily as solutions of rr-P3HT in DCB. This suggests that there are large aggregates of polymer in the solution. Thus improving the processibility of BBO polymers is expected to improve performance. Due to the superior performance of PVCs based on PTVtBBO in comparison to PTVcBBO, we evaluated the impact of solvent choice on the mobility of PTVtBBO. We first prepared thin films by dissolving PTVtBBO in four different solvents (*o*-dichlorobenzene, chlorobenzene, chloroform, and toluene), and the spun thin films from these solutions. We measured current-density-voltage (*I-V*) characteristics of hole-only diodes of these films and then extracted hole mobilities using the space-charge limited

current (SCLC) model (Supporting Information). Not accounting for the electric field dependence of the SCLC model,⁵⁵⁻⁵⁷ we found zero-field hole mobilities to be $1.76 \times 10^{-5} \text{ cm}^2\text{V}^{-1}\text{s}^{-1}$ in chlorobenzene, $3.8 \times 10^{-5} \text{ cm}^2\text{V}^{-1}\text{s}^{-1}$ in o-dichlorobenzene, $5.09 \times 10^{-5} \text{ cm}^2\text{V}^{-1}\text{s}^{-1}$ in toluene, and $3.33 \times 10^{-5} \text{ cm}^2\text{V}^{-1}\text{s}^{-1}$ in chloroform. These values are of the same order of magnitude as those reported in literature for rr-P3HT using a similar hole-only diode architecture.^{58, 59} These results indicate that PTVtBBO is promising for use as an efficient hole transporter in PVCs.⁵⁰⁻⁵² Given its poor performance in PVCs, we did not evaluate the mobility of PTVcBBO.

5.3.5 Theoretical Electronic Structure Calculations

To understand the difference in the performance between PTVcBBO and PTVtBBO we performed theoretical calculations using density functional theory. While the superior performance of PVCs based on PTVtBBO in comparison to PTVcBBO can be attributed to higher electron affinity and smaller band gap of PTVtBBO, the small difference between the two suggests that other factors are involved. The geometries of model oligomers (n=1, 2, 3, and 4) for PTVcBBO and PTVtBBO were optimized at the density functional theory B3LYP/6-31G* level in which the didodecyl substituents were replaced with hydrogen atoms to reduce computational costs. The optimized geometries indicate that the model oligomers are planar, which should optimize conjugation and facilitate delocalization of electrons. The geometries of the model dimers indicated that the PTVcBBO structure had a much larger dipole moment (6.7 D) than that of the PTVtBBO (3.1 D). This phenomenon can be explained by the differences in the symmetry of the two BBOs. The trans-BBO moiety in the PTVtBBO molecule has three mirror planes and a center of inversion (C_{2h} point group) whereas the cis-BBO moiety in the PTVcBBO structure only possesses two mirror planes (C_{2v} point group). These symmetry differences could impact the electronic properties of the two polymers.

The HOMO, LUMO, band gap, and lowest lying singlet excited states (S1) were computed at the TDDFT B3LYP/6-31G* and ZINDO/S60 levels, respectively. Polymeric results were generated by fitting the aforementioned set of oligomers (n = 1, 2, 3, and 4) with the Kuhn expression^{61, 62}

$$E = E_0 \sqrt{1 + 2 \frac{k'}{k_0} \cos \frac{\pi}{N+1}} \quad (1)$$

where E_0 is the transition energy of a formal double bond, N is the number of double bonds in the oligomer (thought to be identical oscillators), and k'/k_0 is an adjustable parameter (indicative of the strength of coupling between the oscillators). These fits were performed on both sets of data and are shown in Figure 5. The results of these fits are summarized in Table 4.

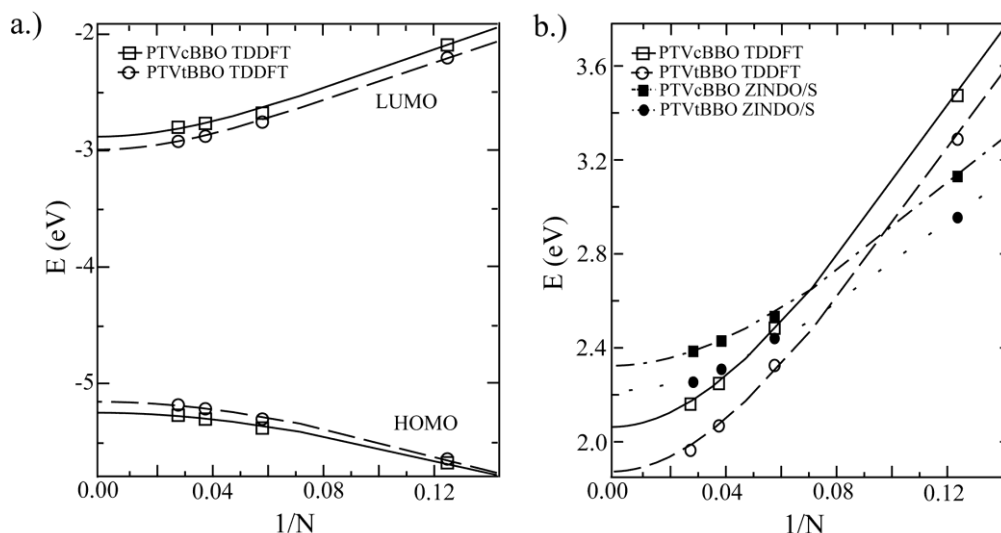


Fig 5. Kuhn fits for a.) HOMOs, LUMOs, (TDDFT level) and b.) bandgaps, E_g , (TDDFT level) and first excited states, S_1 , (ZINDO/S level) for PTV c BBO and PTV t BBO.

	HOMO ^a	LUMO ^a	E_g ^a	S_1 ^b
PTV c BBO	-5.25 (1.2%)	-2.88 (4.6%)	2.06 (5.1%)	2.32 (6.9%)
PTV t BBO	-5.16 (0.4%)	-2.99 (3.5%)	1.87 (9.1%)	2.22 (8.8%)

^aComputed from TDDFT B3LYP/6-31G* level. ^bComputed from the ZINDO/S level.

Table 4. HOMO and LUMO orbital energies, band gaps, and energies of the lowest lying singlet excited states in eV derived from the Kuhn fits of the two data sets with percent error relative to experiment in parentheses.

The computational results for the HOMO and LUMO show relatively good agreement with experimental values. The bandgaps obtained at the DFT level are significantly underestimated which is a consequence of the overestimation of the chain-length dependence of the transition energies.⁶¹ However, they are comparable in deviation from experiment as the ZINDO results whose level of theory was parametrized to reproduce the band gaps for a large number of compounds in apolar solvents.⁶⁰ In either case, these results confirm that the electronic properties of PTVcBBO and PTVtBBO are different as suggested by their point groups. While PTVtBBO has a higher HOMO, a lower LUMO and thus a smaller band gap than PTVcBBO, neither polymer has a high enough LUMO for use as an acceptor polymer with rr-P3HT as the donor in PVCs.

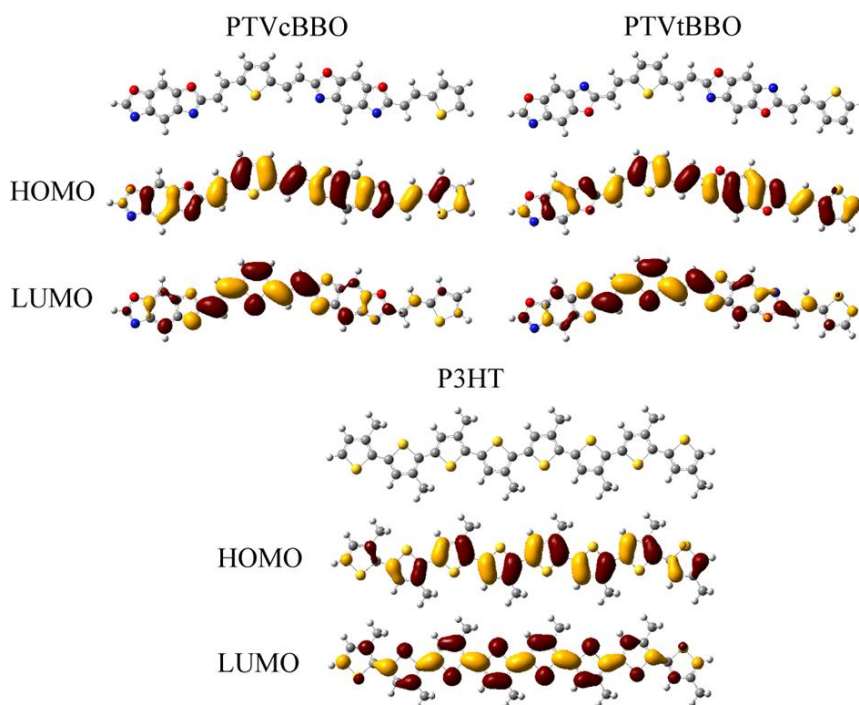


Fig 6. HOMO and LUMO frontier orbitals of the PTVcBBO, and PTVtBBO dimers and P3HT oligomer, obtained at the DFT B3LYP/6-31G* level.

The HOMO and LUMO wavefunctions for model dimers ($n=2$) of PTVcBBO and

PTVtBBO are shown in Fig. 6 along with the wavefunction for an oligomer ($n=8$) of rr-P3HT whose hexyl groups have been replaced with methyl groups to reduce computational cost. In all cases the HOMO wavefunction is delocalized along the entire dimer. In contrast, the LUMO wavefunctions for PTVcBBO and PTVtBBO illustrate that the electron density of these materials is centered on the thiophene moieties, instead of being localized on the electron-accepting BBO subunits. This is the opposite of what is commonly seen in polymers which possess alternating donor and acceptor subunits.^{43, 63, 64} In these polymers the electron density of the LUMO is localized on the electron-accepting group. The fact that the LUMO wavefunction for PTVcBBO and PTVtBBO is localized on the thiophene moieties justifies the PVC results in that 1) the frontier orbitals demonstrate a similar localization as is found in P3HT, leading to electron donating rather than electron accepting behavior in this system;⁶⁵ 2) the LUMO wavefunction of PTVtBBO is more delocalized than that of PTVcBBO, in that more density is located on the acceptor moiety, elucidating the origin of better performance in the PVCs; 3) the lesser extent of delocalization in the LUMO wavefunction of PTVtBBO in comparison to that of rr-P3HT explains why the performance of PTVtBBO was not as good as rr-P3HT despite the higher LUMO level. Thus the development of new polymers that exhibit a higher degree of delocalization from the donor moieties to the BBO moiety in the LUMO could result in improved performance in PVCs.

5.4 CONCLUSIONS

In conclusion two new organic-soluble, thiophene-BBO copolymers have been synthesized. Both polymers were shown to exhibit reversible reduction, while PTVtBBO behaved as a donor in bulk heterojunction PVCs with PCBM. DFT calculations reveal that both polymers have high electron affinities, but poor delocalization in the LUMO wavefunction. Thus, while the polymers were designed to be a D-A system, the thiophene rings do not donate electron density to the BBO moieties. The narrow-band gap, low lying LUMO and reversible electrochemistry of these polymers suggests that BBOs are useful building blocks for the synthesis of conjugated polymers. Future research will focus on increasing the extent of delocalization in these polymers.

5.5 EXPERIMENTAL SECTION

The monomers 2,6-dimethylbenzo[1,2-d;5,4-d']bisoxazole-diethylphosphonate ester,³⁷ 2,6-dimethylbenzo[1,2-d;4,5-d']bisoxazole-diethylphosphonate ester³⁸ and 3,4-didodecylthiophene-2,5-dicarboxaldehyde,⁴² were all synthesized according to the previously reported methods. Tetrahydrofuran was dried using an Innovative Technologies solvent purification system. All other compounds were purchased from commercial sources and used without further purification. Nuclear magnetic resonance spectra were obtained on a Varian 400 MHz spectrometer. All samples were referenced internally to the residual protonated solvent and the chemical shifts are given in δ , relative to the solvent. Gel permeation chromatography (GPC) measurements were performed on a Viscotek GPC Max 280 separation module equipped with three 5 μ m I-gel columns connected in a series (guard, HMW, MMW and LMW) with a refractive index detector. Analyses were performed at 35 °C using THF as the eluent with the flow rate at 1.0 mL/min. Calibration was based on polystyrene standards. Fluorescence spectroscopy and UV-Visible spectroscopy were obtained using polymer solutions in THF, and thin films were spun from these solutions. Both polymers were excited at their respective emission maxima. Thermal gravimetric analysis measurements were performed using TA instruments Model Q50, within the temperature interval of 30 °C - 650 °C, with a heating rate of 20 °C/minute, under ambient atmosphere. Cyclic voltammograms were performed in 0.1 M tetrabutylammonium hexafluorophosphate using 0.01 M AgNO₃ in acetonitrile reference electrode. The potential values obtained versus the Ag⁺ were converted to the ferrocene (Fc) reference.

5.5.1 General Methods for Polymer Synthesis.

We dissolved the BBO monomer (460 mg, 1.00 mmol) and 3,4-didodecylthiophene (503 mg, 1.00 mmol) in 15 mL of THF. Then we added a 1 M solution of potassium tert-butoxide in THF (2.5 mL, 2.5 mmol) to the solution and the mixture, and we stirred the solution at room temperature for 48 h to obtain an opaque, dark red solution. Then we added an additional 10 mL of THF and stirred the reaction for an additional 72 hours. We then precipitated the solution by pouring it into MeOH and collected the resulting red-

orange solid by filtration. We purified the polymer via Soxhlet extraction washing first with MeOH for 8 hours, followed by hexane for 8 hours and lastly THF for 8 hours. The polymer was obtained upon evaporation of the THF solution.

PTVcBBO (78% yield). $^1\text{H-NMR}$ (400 MHz, THF-d8): δ 0.89 (m, CH₃-), 1.30(br m, -(CH₂)₄-), 2.39-2.77 (br m, -Ar-CH₂-), 6.19, 7.75 (br s, vinylic peaks), 7.85 and 7.95 (br, s., Ar-H).

PTVtBBO (87% yield). $^1\text{H-NMR}$ (400 MHz, THF-d8): δ 0.89 (m, CH₃-), 1.30 (br m, -(CH₂)₄-), 2.79-2.95 (br m, -Ar-CH₂-), 6.91, 7.79 (bs, vinylic peaks), 7.98 (br m, Ar-H).

5.5.2 Fabrication and Characterization of Polymer Solar Cells.

Photovoltaic cells were fabricated from quartz slides coated with indium tin oxide (ITO) (Delta Technologies Inc.). The slides were then cleaned by sonication in acetone, isopropanol, detergent, and de-ionized water. The slides were then dried under nitrogen and exposed to air plasma for one minute. Poly(3,4-ethylenedioxythiophene) (PEDOT:PSS) (Clevios PTM) was filtered through a 0.45 μm and spin-coated (600 rpm for 60 s) onto the slides to serve as a hole transport layer. The slides were then dried on a hot plate at 120 °C for 10 minutes. After cooling, the slides were transferred to a glove box with and Ar atmosphere. PTVtBBO and PTVcBBO were mixed with PCBM (Sigma Aldrich) in 1:1 weight ratio. Total solute concentration in all solutions was 20 mg/ml. o-DCB was the solvent used for PVCs and hole-mobility measurements. Additionally, chloroform, toluene and chlorobenzene were also used to mobility measurements. All active-layer solutions were passed through 0.22 μm PTFE syringe filters (Whatman) and spin coated on the PEDOT:PSS layer at 600 rpm for 60 s. The samples were then dried under a petri dish. Finally, aluminum electrode (100 nm) was thermally evaporated for PVCs, and gold electrode (100 nm) was evaporated in an E-beam evaporator for hole-mobility measurements. The area of metal electrode for both types of devices was 4 mm².

The current density–voltage (I–V) characteristics of the PVCs and hole-only diodes were measured using a Keithley 276 source-measurement unit and HP 4156A semiconductor parameter analyzer, respectively. The PVCs were illuminated through the ITO side using a GE ELH bulb, the intensity of which was adjusted to 100 mW/cm²

using a crystalline silicon reference cell.

For optical measurements, solutions were spin-coated onto quartz slides to form active layers. The optical absorption spectra of these films were recorded using a UV-VIS spectrophotometer (Cary 50 Bio). The steady state PL spectra were measured using Spex Fluorolog Tau-3 fluorescence spectrophotometer.

5.5.3 Theoretical Calculations.

All of the calculations on these oligomers were studied using the Gaussian 03W66 program package with the GaussView 4 GUI interface program package. The electronic ground states were optimized using density functional theory (DFT), B3LYP/6-31G*. Excited states were generated through time dependent density functional theory (TD-DFT) applied to the optimized ground state for each oligomer. The HOMO, LUMO, band gap, first ten excited states, frontier orbitals and UV-Vis simulations were generated from these excited computations. Finally, electrostatic potential maps were created using a coarse setting and an isovalue of 0.03.

5.6 ACKNOWLEDGEMENTS

This work was funded by the National Science Foundation (DMR-0846607), the 3M foundation, and the Iowa Office of Energy Independence through the Iowa Power Fund. The device fabrication and characterization was performed at the Iowa State University Microelectronics Research Center. We thank Mr. Robert Roggers (ISU) for X-ray analysis and Ms. Kimberly Topp (ISU) for help with the abstract graphic.

5.7 NOTES AND REFERENCES

The band diagram that is shown in the graphical abstract uses HOMO and LUMO values for PCBM and rr-P3HT from reference 4.

- (1) K. M. Coakley and M. D. McGehee, *Chem. Mater.*, **2004**, *16*, 4533-4542.
- (2) B. C. Thompson and J. M. J. Frechet, *Angew, Chem. Int. Ed.*, **2008**, *47*, 58-77.
- (3) B. C. Thompson, Y.-G. Kim and J. R. Reynolds, *Macromolecules*, **2005**, *38*,

5359-5362.

(4) L. J. A. Koster, V. D. Mihailetschi and P. W. M. Blom, *Appl. Phys. Lett.*, **2006**, *88*, 093511- 093513.

(5) L. J. A. Koster, V. D. Mihailetschi, R. Ramaker and P. W. M. Blom, *Appl. Phys. Lett.*, **2005**, *86*, 123509-123512.

(6) C. J. Brabec, A. Cravino, D. Meissne, N. S. Sariciftci, T. Fromherz, M. T. Rispens, L. Sanchez and J. C. Hummelen, *Adv. Fun. Mater.*, **2001**, *11*, 374-380.

(7) E. Bundgaard and F. C. Krebs, *Sol. Energy Mater. Sol. Cells*, **2007**, *91*, 954-985.

(8) C. Winder and N. S. Sariciftci, *J. Mater. Chem.*, **2004**, *14*, 1077-1086.

(9) H. A. M. van Mullekom, J. A. J. M. Vekemans, E. E. Havinga and E. W. Meijer, *Mater. Sci. Eng., R*, **2001**, *32*, 1-40.

(10) S. A. Jenekhe, L. Lu and M. M. Alam, *Macromolecules*, **2001**, *34*, 7315-7324.

(11) J. Mei, N. C. Heston, S. V. Vasilyeva and J. R. Reynolds, *Macromolecules* **2009**, *42*, 1482-1487.

(12) M. Jeffries-El and R. D. McCullough, in *Handbook of Conducting Polymers*, ed. T. A. Skotheim, Reynolds, John R., London, Boca Raton, Fla, 3rd edn./edited by Terje A. Skotheim and John Reynolds., **2007**, pp. 331-380.

(13) R. D. McCullough, in *Handbook of Conducting Polymers*, ed. T. A. Skotheim, Elsenbaumer, Ronald L., Reynolds, John R., Marcell Dekker, New York, 2nd edn., **1998**, pp. 225-258.

(14) J. Liu, R. Zhang, G. Sauve, T. Kowalewski and R. D. McCullough, *J. Am. Chem. Soc.*, **2008**, *130*, 13167-13176.

(15) Y. Li, L. Xue, H. Li, Z. Li, B. Xu, S. Wen and W. Tian, *Macromolecules*, **2009**, *42*, 4491-4499.

(16) E. Ahmed, F. S. Kim, H. Xin and S. A. Jenekhe, *Macromolecules*, **2009**, *42*, 8615-8618.

(17) J. F. Wolfe, in *Encyclopedia of Polymer Science and Engineering*, John Wiley and Sons, New York, NY, **1988**, vol. 11, pp. 601-635.

- (18) J. F. Wolfe and F. E. Arnold, *Macromolecules*, **1981**, *14*, 909-915.
- (19) M. M. Alam and S. A. Jenekhe, *Chem. Mater.*, **2002**, *14*, 4775-4780.
- (20) S. A. Jenekhe, L. R. de Paor, X. L. Chen and R. M. Tarkka, *Chem. Mater.*, **1996**, *8*, 2401-2404.
- (21) Y. Chen, S. Wang, Q. Zhuang, X. Li, P. Wu and Z. Han, *Macromolecules*, **2005**, *38*, 9873-9877.
- (22) D. Feng, S. Wang, Q. Zhuang, P. Wu and Z. Han, *Polymer*, **2004**, *45*, 8871-8879.
- (23) S. A. Jenekhe and J. A. Osaheni, *Chem. Mater.*, **1994**, *6*, 1906-1909.
- (24) J. A. Osaheni and S. A. Jenekhe, *Macromolecules*, **1994**, *27*, 739-742.
- (25) J. A. Osaheni and S. A. Jenekhe, *Chem. Mater.*, **1995**, *7*, 672-682.
- (26) J. A. Osaheni, S. A. Jenekhe, A. Burns, G. Du, J. Joo, Z. Wang, A. J. Epstein and C. S. Wang, *Macromolecules*, **1992**, *25*, 5828-5835.
- (27) X. Zhang and S. A. Jenekhe, *Macromolecules*, **2000**, *33*, 2069-2082.
- (28) L.-S. Tan, J. L. Burkett, S. R. Simko and M. D. Alexander, Jr., *Macromol. Rapid Comm.*, **1999**, *20*, 16-20.
- (29) S. Wang, Y. Chen, Q. Zhuang, X. Li, P. Wu and Z. Han, *Macromol. Chem. Phys.*, **2006**, *207*, 2336-2342.
- (30) S. Wang, P. Guo, P. Wu and Z. Han, *Macromolecules*, **2004**, *37*, 3815-3822.
- (31) S. Wang, H. Lei, P. Guo, P. Wu and Z. Han, *Eur. Polym. J.*, **2004**, *40*, 1163-1167.
- (32) P. Guo, S. Wang, P. Wu and Z. Han, *Polymer*, **2004**, *45*, 1885-1893.
- (33) H. R. Kricheldorf and A. Domschke, *Polymer*, **1994**, *35*, 198-203.
- (34) X. Liu, X. Xu, Q. Zhuang and Z. Han, *Polym. Bull.*, **2008**, *60*, 765-774.
- (35) Y. Imai, K. Itoya and M.-A. Kakimoto, *Macromol. Chem. Phys.*, **2000**, *201*, 2251-2256.
- (36) Y. So, J. P. Heeschen, B. Bell, P. Bonk, M. Briggs and R. DeCaire, *Macromolecules*, **1998**, *31*, 5229-5239.
- (37) J. F. Mike, A. J. Makowski and M. Jeffries-EL, *Org. Lett.*, **2008**, *10*, 4915-4918.

- (38) J. F. Mike, A. J. Makowski, T. C. Mauldin and M. Jeffries-El, *J. Poly. Sci. A*, **2010**, *48*, 1456-1460.
- (39) P. M. Beaujuge, S. V. Vasilyeva, S. Ellinger, T. D. McCarley and J. R. Reynolds, *Macromolecules*, **2009**, *42*, 3694-3706.
- (40) J. Roncali, *Chem. Rev.*, **1997**, *97*, 173-205.
- (41) D. A. M. Egbe, C. P. Roll, E. Birckner, U.-W. Grummt, R. Stockmann and E. Klemm, *Macromolecules*, **2002**, *35*, 3825-3837.
- (42) S. Destri, M. Pasini, C. Pelizzi, W. Porzio, G. Predieri and C. Vignali, *Macromolecules*, **1999**, *32*, 353-360.
- (43) E. Zhou, M. Nakamura, T. Nishizawa, Y. Zhang, Q. Wei, K. Tajima, C. Yang and K. Hashimoto, *Macromolecules*, **2008**, *41*, 8302-8305.
- (44) E. Zhou, K. Tajima, C. Yang and K. Hashimoto, *J. Mater. Chem.*, **2010**, *20*, 2362-2368.
- (45) J. J. M. Halls, J. Cornil, D. A. dos Santos, R. Silbey, D. H. Hwang, A. B. Holmes, J. L. Brédas and R. H. Friend, *Physical Review B*, **1999**, *60*, 5721.
- (46) S. Barth and H. Bassler, *Physical Review Letters*, **1997**, *79*, 4445.
- (47) B. Friedel, C. R. McNeill and N. C. Greenham, *Chem. Mater.*, **2010**, *22*, 3389-3398.
- (48) M. Scharber, D. Mühlbacher, M. Koppe, P. Denk, C. Waldauf, A. Heeger and C. Brabec, *Adv. Mater.*, **2006**, *18*, 789-794.
- (49) J. Y. Kim, K. Lee, N. E. Coates, D. Moses, T.-Q. Nguyen, M. Dante and A. J. Heeger, *Science*, **2007**, *317*, 222-225.
- (50) G. Li, V. Shrotriya, J. Huang, Y. Yao, T. Moriarty, K. Emery and Y. Yang, *Nat. Mater.*, **2005**, *4*, 864-868.
- (51) J. Y. Kim, S. H. Kim, H.-H. Lee, K. Lee, W. Ma, X. Gong and A. J. Heeger, *Adv. Mater.*, **2006**, *18*, 572-576.
- (52) S. H. Park, A. Roy, S. Beaupre, S. Cho, N. Coates, J. S. Moon, D. Moses, M. Leclerc, K. Lee and A. J. Heeger, *Nat. Photon.*, **2009**, *3*, 297-302.
- (53) J. Casado, R. G. Hicks, V. Hernandez, D. J. T. Myles, M. C. Ruiz Delgado and J. T. Lopez Navarrete, *Journal of Chemical Physics*, **2003**, *118*, 1912-1920.

- (54) E. Klimov, W. Li, X. Yang, G. G. Hoffmann and J. Loos, *Macromolecules*, **2006**, *39*, 4493-4496.
- (55) C. Tanase, P. W. M. Blom and D. M. De Leeuw, *Phys. Rev. B Condens. Matter Mater. Phys.*, **2004**, *70*, 193202/193201-193202/193204.
- (56) P. N. Murgatroyd, *J. Phys. D*, **1970**, *3*, 151-157.
- (57) M. A. Lampert, A. Many and P. Mark, *Physical Review*, **1964**, *135*, A1444-A1453.
- (58) O. G. Reid, K. Munechika and D. S. Ginger, *Nano Lett.*, **2008**, *8*, 1602-1609.
- (59) C. Goh, R. J. Kline, M. D. McGehee, E. N. Kadnikova and J. M. J. Frechet, *Appl. Phys. Lett.*, **2005**, *86*, 122110-122113.
- (60) A. Hartman and M. C. Zerner, *Theor. Chim. Acta*, **1975**, *37*, 47-65.
- (61) J. Gierschner, J. Cornil and H.-J. Egelhaaf, *Advanced Materials*, **2007**, *19*, 173-191.
- (62) B. Milian Medina, A. VanVooren, P. Brocorens, J. Gierschner, M. Shkunov, M. Heeney, I. McCulloch, R. Lazzaroni and J. Cornil, *Chem. Mater.*, **2007**, *19*, 4949-4956.
- (63) X. Zhang, T. T. Steckler, R. R. Dasari, S. Ohira, W. J. Potscavage Jr, S. P. Tiwari, S. Coppee, S. Ellinger, S. Barlow, J.-L. Bredas, B. Kippelen, J. R. Reynolds and S. R. Marder, *J. Mater. Chem.*, **2010**, *20*, 123-134.
- (64) B. P. Karsten, L. Viani, J. Gierschner, J. Cornil and R. A. J. Janssen, *J. Phys. Chem. A*, **2008**, *112*, 10764-10773.
- (65) M. Chen, X. Crispin, E. Perzon, M. R. Andersson, T. Pullerits, M. Andersson, O. Inganas and M. Berggren, *Appl. Phys. Lett.*, **2005**, *87*, 252105-252103.
- (66) M. J. T. Frisch, G. W.; Schlegel, H. B.; Scuseria, G. E.; Robb, M. A.; Cheeseman, J. R.; Montgomery, J. A., Jr.; Vreven, T.; Kudin, K. N.; Burant, J. C.; Millam, J. M.; Iyengar, S. S.; Tomasi, J.; Barone, V.; Mennucci, B.; Cossi, M.; Scalmani, G.; Rega, N.; Petersson, G. A.; Nakatsuji, H.; Hada, M.; Ehara, M.; Toyota, K.; Fukuda, R.; Hasegawa, J.; Ishida, M.; Nakajima, T.; Honda, Y.; Kitao, O.; Nakai, H.; Klene, M.; Li, X.; Knox, J. E.; Hratchian, H. P.; Cross, J. B.; Bakken, V.; Adamo, C.; Jaramillo, J.; Gomperts, R.; Stratmann, R. E.; Yazyev, O.; Austin, A. J.; Cammi, R.; Pomelli, C.;

Ochterski, J. W.; Ayala, P. Y.; Morokuma, K.; Voth, G. A.; Salvador, P.; Dannenberg, J. J.; Zakrzewski, V. G.; Dapprich, S.; Daniels, A. D.; Strain, M. C.; Farkas, O.; Malick, D. K.; Rabuck, A. D.; Raghavachari, K.; Foresman, J. B.; Ortiz, J. V.; Cui, Q.; Baboul, A. G.; Clifford, S.; Cioslowski, J.; Stefanov, B. B.; Liu, G.; Liashenko, A.; Piskorz, P.; Komaromi, I.; Martin, R. L.; Fox, D. J.; Keith, T.; Al-Laham, M. A.; Peng, C. Y.; Nanayakkara, A.; Challacombe, M.; Gill, P. M. W.; Johnson, B.; Chen, W.; Wong, M. W.; Gonzalez, C.; Pople, J. A. , *Gaussian 03, revision C.02*; , (2004) Gaussian, Inc.: , Wallingford, CT, .

5.8 SUPPORTING INFORMATION

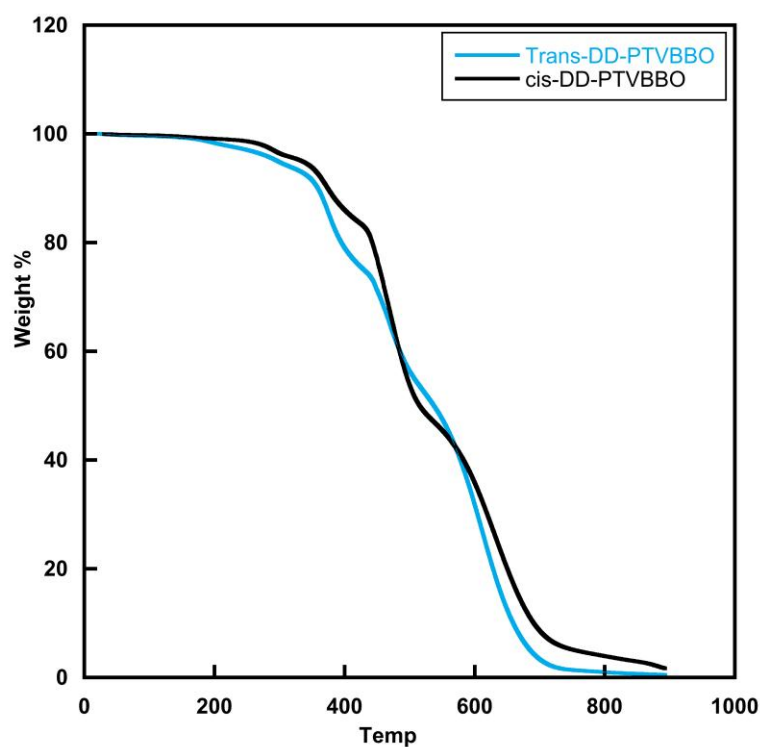


Figure S1. TGA curves of PTV_cBBO and PTV_tBBO.

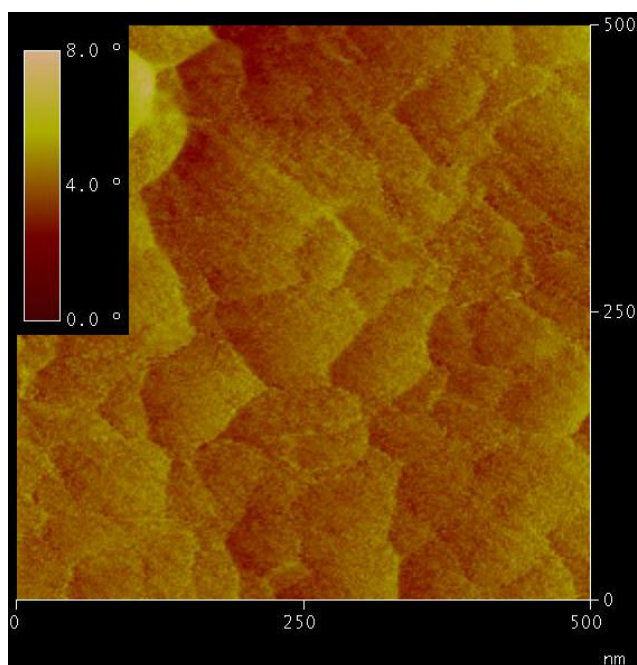


Fig S2. AFM phase image of PTVtBBO thin film. phase images. Scan Size: 500 nm square.

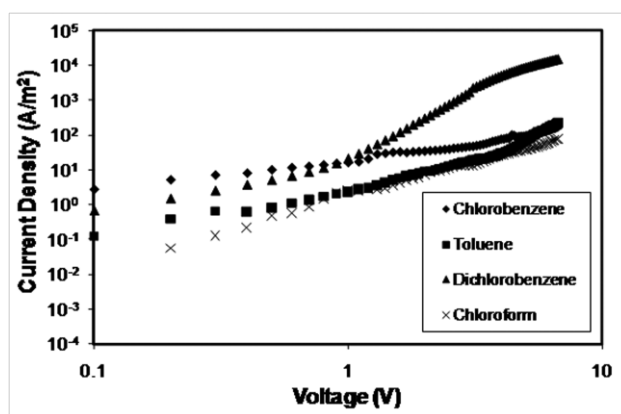


Fig S3. Current-voltage characteristics of PTVtBBO hole only device sandwiched between ITO/PEDOT: PSS and gold electrodes. Thicknesses of the films were 140 nm (chlorobenzene), 137 nm (DCB), 176 nm (toluene), and 179 nm (chloroform), as measured by AFM.

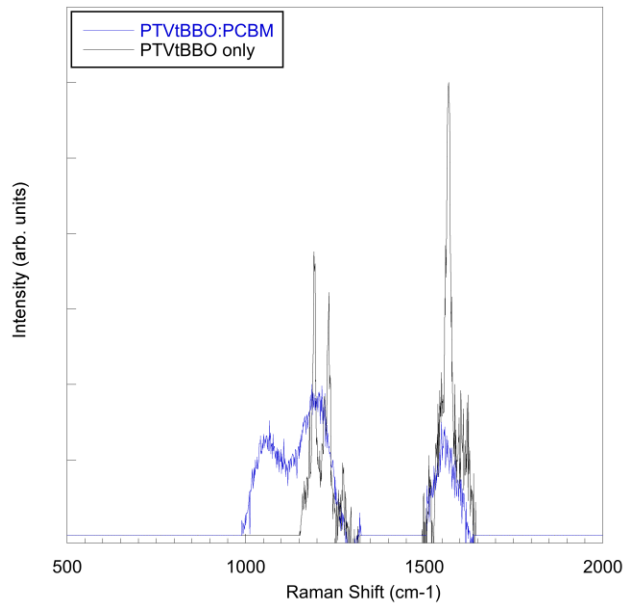


Figure S4. Raman spectra for PTVtBBO only and PTVtBBO:PCBM blend films.

CHAPTER 6

Efficient Synthesis of Benzobisazole Terpolymers Containing Thiophene and Fluorene.

Reproduced from *Polymer Chemistry* Accepted Jun 23, 2011 with permission from The Royal Society of Chemistry.
Copyright © 2011

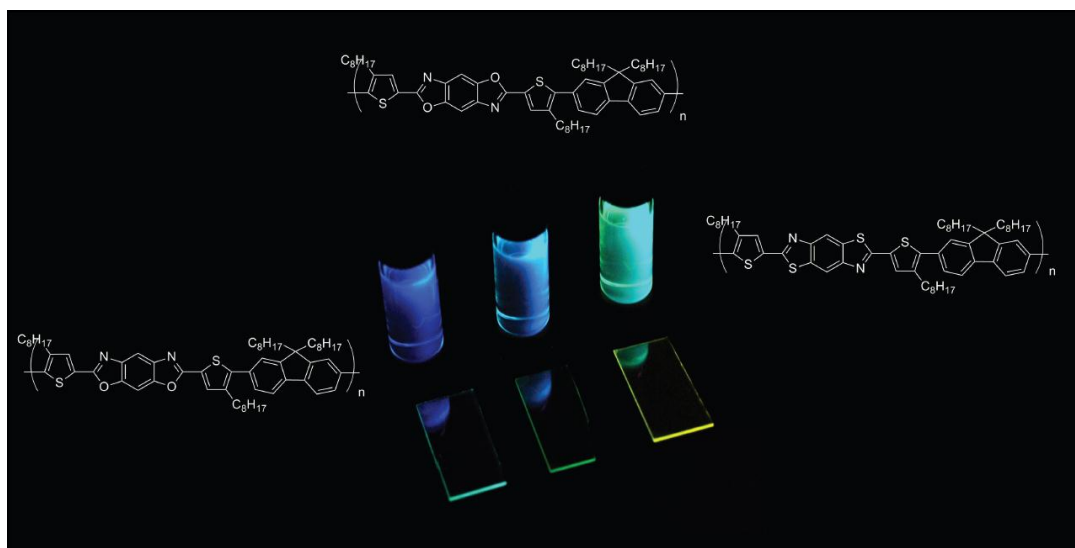
Jared F. Mike^a, Jeremy J. Intemann^a, Min Cai^b, Teng Xiao^b, Ruth Shinar^c, Joseph Shinar^b and Malika Jeffries-EL^{*a}

^aDepartment of Chemistry, Iowa State University, Ames, IA 50011

^bAmes Laboratory-USDOE and Department of Physics, Iowa State University, Ames, IA 50011.

^cMicroelectronics Research Center and Department of Electrical Engineering, Iowa State University, Ames, IA 50011.

6.1 ABSTRACT



We report the synthesis and luminescence properties of three novel polymers composed of 9,9-dioctylfluorene and a donor-acceptor-donor (D-A-D) triad of a benzobisazole moiety sandwiched between two octylthiophenes. The requisite monomers, 2,6-bis(5-bromo-3-octylthiophen-2-yl)-benzobisazoles were obtained efficiently via the Lewis acid catalyzed cyclization of 2-bromo-3-octyl-5-(triethoxymethyl)thiophene and

the corresponding diamino diols or dithiols. The polymers were synthesized in excellent yield by the Suzuki coupling reaction between the D-A-D benzobisazole monomers and 9,9-dioctylfluorene bisboronic acid. Alkyl side chains provided the polymers with solubility in common organic solvents, enabling characterization using gel permeation chromatography, ^1H NMR, UV-Vis and fluorescence spectroscopy. The polymers have optical bandgaps of 2.43 - 2.63 eV and HOMO levels at -5.54 to -5.65 eV relative to vacuum as determined by UV visible and photoelectron spectroscopy respectively. Light-emitting diodes using blends of the copolymers in a poly(N-vinyl carbazole) matrix yielded blue-green emission with luminous efficiencies of 0.86 Cd/A at ~505 nm. This efficient and high-yielding route is a promising approach for the synthesis of polymers containing benzobisazole moieties.

6.2 INTRODUCTION

As a result of their optical and electronic properties, conjugated polymers are finding widespread use in semiconducting applications such as field-effect transistors, light-emitting diodes and photovoltaic cells.¹ The benefits of conjugated polymers include the ability to tune their optical and electronic properties through chemical synthesis and the ability to fabricate devices from them using solution based techniques. Among conjugated polymers, polyfluorenes are widely investigated for use in polymer light-emitting diodes due to their excellent solubility, high solid state photoluminescence quantum yield and good charge carrier mobility. However, poly(9,9-dioctylfluorene) is a blue light emitting polymer with a large band gap (3.1 eV), a low electron affinity (EA = 2.5 eV), and a high ionization potential (IP = 5.6 eV), which makes it difficult to inject both holes and electrons into the polymer.²

One way to change the positions of the frontier orbitals is to copolymerize fluorene with electron-deficient comonomers.³ In this regard benzobisazoles, such as benzobisoxazole and benzobisthiazole are promising building blocks for the synthesis of novel materials. These electron-deficient heterocycles are known for improving the charge transport, photoluminescence, and third-order nonlinear optical properties of materials containing them.^{4,5,6} Recently, new materials based on a donor-acceptor-donor

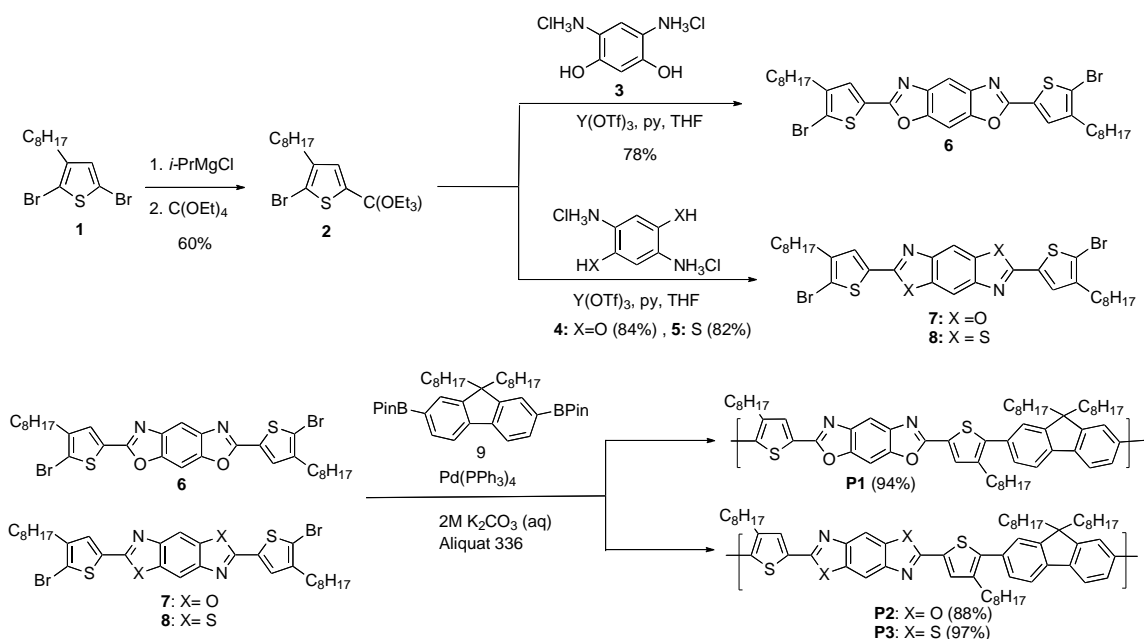
(D-A-D) triad composed of a benzobisthiazole ring sandwiched between two alkylthiophenes have been reported.⁷⁻¹⁰ Organic field effect transistors using small molecules based on this D-A-D triad exhibited excellent hole mobility as a result of the materials' high crystallinity.^{8, 10} Copolymers composed of this triad and alkylthiophenes also have excellent hole mobility when used in field-effect transistors⁹ and good performance in photovoltaic cells as a result of the polymers high ionization potential.⁷

Historically the synthesis of polybenzobisazoles requires strong acids or oxidants and high temperatures, limiting the types of substituents that can be incorporated into the polymer.^{11, 12} Thus, from a synthetic standpoint, a functional triad already containing the benzobisazole moiety is a useful building block as it enables the synthesis of conjugated polymers using transition metal catalyzed cross coupling reactions, instead of condensation polymerization. Unfortunately, the reported methods for the formation of this triad: the Stille coupling of 2,6-dibromo-benzo[1,2-*d*;4,5-*d'*]bisthiazole with 2-trimethylstannyl-4-hexylthiophene⁸ or the acid-catalyzed condensation of 3-octylthiophene-2-carboxylaldehyde with 2,5-diamino-1,4-benzenedithiol dihydrochloride both occur in low yields, minimizing its usefulness.⁷ Previously, we reported an efficient method for the synthesis of 2,6-disubstituted benzobisazoles using Lewis acid catalyzed cyclization of substituted orthoesters and corresponding diaminediols or dithiols.¹³ These new building blocks have been used for the synthesis of novel poly(arylenevinylene)-alt-benzobisazoles.^{6, 14} Based on our earlier success, we set out to develop an efficient approach for the synthesis of new monomers that would enable the synthesis of the polymers containing benzobisazole-arene single bonds.

6.3 RESULTS AND DISCUSSION

6.3.1 Synthesis and Physical Characterization

The synthetic approach for the D-A-D benzobisazole monomers is shown in Scheme 1. 2,5-Dibromo-3-octylthiophene (**1**) was synthesized in two steps from 3-bromothiophene according to a literature procedure.¹⁵ The Grignard metathesis reaction of **1** affords the intermediate 5-bromomagnesio-2-bromo-3-octylthiophene as the major product.¹⁶ Using the method described by Tschitschibabin,¹⁷ this intermediate is



Scheme 1. Synthesis of Benzobisazole Monomers and Polymers

directly converted to 2-bromo-3-octyl-5-(triethoxymethyl)thiophene **2** without isolation. The orthoester **2** is a stable compound that is readily purified by vacuum distillation. The reaction conditions used for the synthesis of **2** enable the incorporation of a bromine at the 2-position of the thiophene ring at the start of the reaction sequence, reducing the total number of synthetic steps. The Lewis acid catalyzed cyclization of the orthoester **2** with 4,6-diaminoresorcinol **3**,¹¹ 2,5-diaminohydroquinone **4**¹⁸ or 2,5-diaminobenzene-1,4-dithiol **5**¹² in THF yielded the corresponding monomers 2,6-bis(4-octylthiophen-2-yl)-benzo[1,2-*d*; 5,4-*d'*]bisoxazole **6**, 2,6-bis(4-octylthiophen-2-yl)-benzo[1,2-*d*; 4,5-*d'*]bisoxazole **7**, and 2,6-bis(4-octylthiophen-2-yl)-benzo[1,2-*d*; 4,5-*d'*]bisthiazole **8**. All of these monomers were solids that were readily purified by recrystallization, with isolated yields ranging from 82 to 86 %.

The synthesis of the fluorene-bisthienylbenzobisazole copolymers is also shown in Scheme 1. The polymerization of monomers **6**, **7** or **8** with 2,7-bis(4,4,5,5-tetramethyl-1,3,2-dioxaborolan-2-yl)-9,9-dioctylfluorene **9**¹⁹ via the Suzuki cross-coupling reaction afforded the polymers **P1**, **P2** and **P3**. All polymers were obtained in excellent yields after purification by Soxhlet extraction with methanol followed by hexanes, to remove

residual catalyst and low molecular weight material. The higher molecular weight material was soluble in standard organic solvents, such as THF, *m*-cresol and chloroform at room temperature, facilitating characterization using ^1H NMR spectroscopy and gel permeation chromatography (GPC). The ^1H NMR spectra for both polymers were in agreement with the proposed polymer structures (Figures S10 - S15 ESI). The number averaged degree of polymerization (DP_n) ranged from 22 – 86 and all of the polymers showed excellent film forming ability. Thermogravimetric analysis revealed that both polymers were thermally stable with 5% weight loss onsets occurring above 290 °C under air (Figure S1). The results are summarized in Table 1.

	Yield %	M_w^a	M_w/M_n	T_d (°C) ^b	T_g/ T_m (°C)
P1	94	80,900	3.2	295	110.3/ 230.1
P2	88	74,200	2.5	292	108.1/ NA
P3	97	21,500	1.8	341	108.4/ 257.6

^a Molecular weights and polydispersity indexes determined by GPC versus polystyrene standards using THF as the eluent. ^b Temperature at which 5% weight loss is observed by TGA under N_2 with a heating rate of 20 °C/min.

Table 1 Molecular weights and thermal properties of the PTVBBOs.

6.3.2 Electrochemical properties.

The electrochemical properties of the polymers were investigated by cyclic voltammetry (CV) and differential pulse voltammetry. The data were obtained from polymer thin films on a platinum working electrode in acetonitrile, using 0.1 M Bu_4NPF_6 as the electrolyte and an Ag/Ag^+ reference electrode. The onsets were referenced to Fc/Fc^+ . All of the polymers exhibit measureable and reproducible oxidation and reduction processes. The HOMO levels were also determined using ultraviolet photoelectron spectroscopy (UPS). This technique determines the highest occupied molecular orbital (HOMO) level in organic thin films by bombarding the sample with ultraviolet photons and measuring the kinetic energies of the ejected valence electrons.²⁰ Thus the HOMO values obtained using this method are very accurate. The results are summarized in Table 2. The values obtained for the HOMO levels from the CV waves are in good agreement with the values obtained using UPS. The electrochemical bandgaps are somewhat larger

than the optical bandgaps, but are within reasonable limits.

It was anticipated that structural differences of the benzobisazoles would result in different optical properties. The isomeric benzoxazole polymers **P1** and **P2** have different arrangements of oxygen atoms around the central benzene ring. This modification impacts the symmetry of the monomers, their dipole moments and ultimately impacts the optoelectronic properties of the resulting polymers. Similarly, the benzobisthiazole polymer **P3**, is structurally analogous to **P2** with sulfur atoms replacing the oxygen atoms. Since, sulfur has a lower electronegativity than oxygen and a similar electronegativity to the carbon atom the electron density is more equally shared between sulfur and carbon. Thus the π -orbitals will be more delocalized. Additionally the empty d -orbitals of the sulfur atom can contribute to the molecular π -orbitals decreasing the energy of the π - π^* transition.^{5, 21} Based on the UPS data it appears that changing the position of the oxygen atoms destabilizes the HOMO level, while slightly stabilizing the LUMO level. Whereas exchanging the oxygen atoms for sulfur stabilizes both the HOMO and LUMO levels.

Overall, the LUMO values of **P1**, **P2**, and **P3** (-2.71 to -2.85 eV), are also higher than those reported previously for the related PFO3, a copolymer of 9,9-dioctylfluorene and 4,7-dithien-5-yl-2,1,3-benzodithiazole (-3.53 eV),²² since benzobisazoles are weaker acceptors than benzothiadiazoles. The HOMO values for **P1**, **P2**, and **P3** of -5.54 to -5.63 eV are more negative than those reported previously for the related poly(9,9-dioctylfluorenevinylene-co-benzobisoxazole)s,⁶ which had HOMO values of -5.29 to -5.36 eV. We attribute this to exchanging the vinylene linkage between the benzobisazole and fluorene moieties for a thiophene ring.

6.3.3 Optical and electronic properties.

The photophysical characteristics of the polymers, both as dilute solutions in chloroform and thin films, were evaluated by UV-vis absorption and fluorescence spectroscopy. The normalized absorbance and emission spectra for the polymers as solutions and as thin films are shown in Figure 1; the data are summarized in Table 2. In solution, the spectra for all the polymers exhibit a single broad absorbance band. **P2** has a λ_{\max} at approximately 418 nm; relative to **P2** the λ_{\max} for **P1** was blue-shifted 8 nm to 410

nm and the λ_{\max} of **P3** was red-shifted 16 nm to 434 nm. The thin film absorbance spectra for all of the polymers were broader than their solution counterparts, and show some weak vibronic coupling. The onsets of absorption for the polymers were obtained from the UV-vis spectra of polymer films and ranged from 471 to 511 nm, resulting in optical band gaps of 2.43 - 2.64 eV. None of the UV-vis spectra exhibited a second low energy peak typically associated with intramolecular charge-transfer transitions within D-A copolymers.²³

Polymer	Solution		Film			E_g^{opt} (eV) ^a	E_{onset}^{ox} (eV) ^b	E_{onset}^{red} (eV) ^b	HOMO (eV) ^c	LUMO (eV) ^d
	λ_{\max}^{abs} (nm)	λ_{\max}^{em} (nm)	λ_{\max}^{abs} (nm)	λ_{\max}^{em} (nm)	λ_{\max}^{em} (nm)					
P1	410	461	410	482	2.64	0.79	-1.95	-5.59 ^c / -5.63 ^d	-2.85 ^e / -2.99 ^f	
P2	418	471	439	524	2.52	0.82	-2.09	-5.62 ^c / -5.54 ^d	-2.71 ^e / -3.02 ^f	
P3	434	487	456	538	2.43	0.67	-1.87	-5.47 ^c / -5.59 ^d	-2.93 ^e / -3.16 ^f	

^a Estimated from the intersection of absorption and fluorescence in the solid state. ^b Onset of potentials (vs Fc). ^c HOMO = $-(E_{onset}^{ox} + 4.8)$ (eV). ^d From UPS. ^e LUMO = $-(E_{onset}^{red} + 4.8)$ (eV). ^f LUMO = HOMO (UPS) + E_g^{opt} (eV).

Table 2. Electronic and Optical Properties of poly(arylenebenzobisazoles).

In solution the fluorescence spectra of the polymers is characterized by one strong emission peak with a shoulder. The emission spectra of the polymer thin films were considerably red-shifted, relative to the corresponding solution spectra. This phenomenon is most likely caused by geometrical changes between the polymer in solution and in film.

In solution the λ_{\max}^{abs} of the benzobisoxazole polymer **P1** is blue-shifted relative to the related poly(fluorene-co-benzobisoxazole)s (458 nm), although the later was measured as a solution in methane sulfonic acid, which protonates the polymer.²⁴ Whereas the λ_{\max}^{em} of 468 nm is the same as the reported value of 468 nm. In contrast, the λ_{\max}^{abs} of the benzobisthiazole polymer **P3** is red-shifted relative to the related the poly(fluorene-co-benzobisthiazole) (409 nm).²⁵ The emission spectra for this polymer

was not reported. The $\lambda_{\text{max}}^{\text{abs}}$ of the benzobisoxazole polymers **P1** and **P2** are blue-shifted relative to those reported previously for the related poly(fluorenevinylene-co-benzobisoxazole)s (450 - 470 nm),⁶ whereas the $\lambda_{\text{max}}^{\text{em}}$ of 461 - 471 nm are similar to the reported values, indicating that the thiophene π -bridges have little impact on the emission spectra.

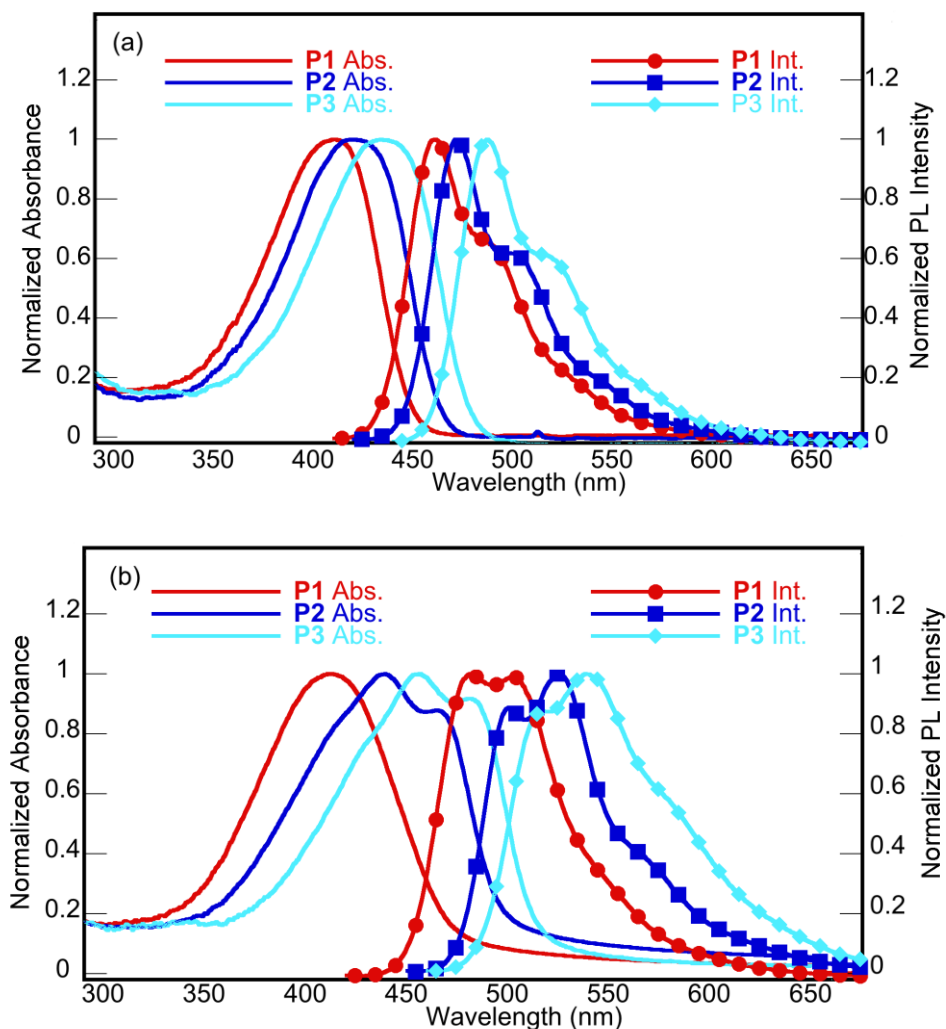


Fig. 1 UV-vis absorption and PL spectra of the polymers in: a) solution (top) and b) thin film (bottom).

6.3.4 Solid-state morphology

The thin films were analyzed by X-ray diffraction. The diffraction patterns for the polymers are shown in (Figure S3, ESI) The pattern for **P1** does not exhibit any peaks, indicating a lack of regular spacing in the film. X-ray analyses of small molecules containing *cis*-benzobisoxazole indicates that it has a slight bend along the 2,6 axis.¹³ The reason for a lack of order in **P1** may be due to this bent structure. **P3**, however, and **P2**, albeit to a lesser extent, have peaks corresponding to a regular spacing of 15.5 Å. This number is slightly larger than the length of one octyl chain. This suggests a spatial arrangement where octyl chains on neighboring polymers intercalate to some degree. This type of spacing can be seen in other 9,9-dioctylfluorene copolymers.²⁶

6.3.5 Electroluminescent Devices.

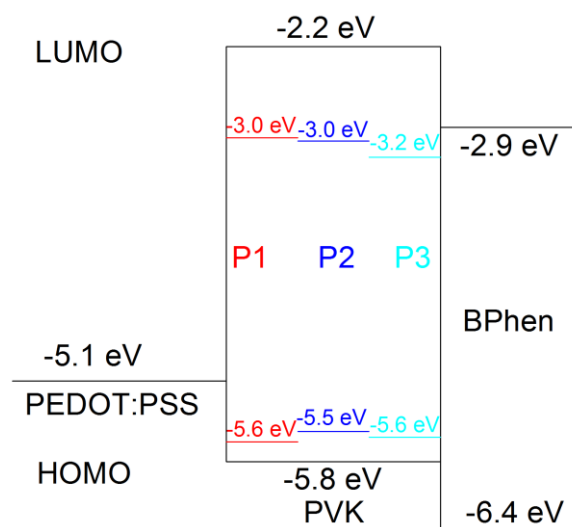


Fig. 2. Energy level diagram for the devices.

We first examined the use of the polymers as neat emitting layers in polymer light emitting diodes (PLEDs) with the structure ITO/PEDOT:PSS (60 nm)/**P1-P3**/BPhen (40 nm)/LiF(1 nm)/Al(100 nm), where ITO is indium tin oxide, PEDOT:PSS is poly(3,4-ethylenedioxy thiophene):poly(4-styrenesulfonate), and BPhen is 4,7-diphenyl-1,10-phenanthroline. All of the polymers are efficient fluorophores in solution, with quantum yields of 0.80, 0.82 and 0.85 for **P1**, **P2**, and **P3**, respectively.

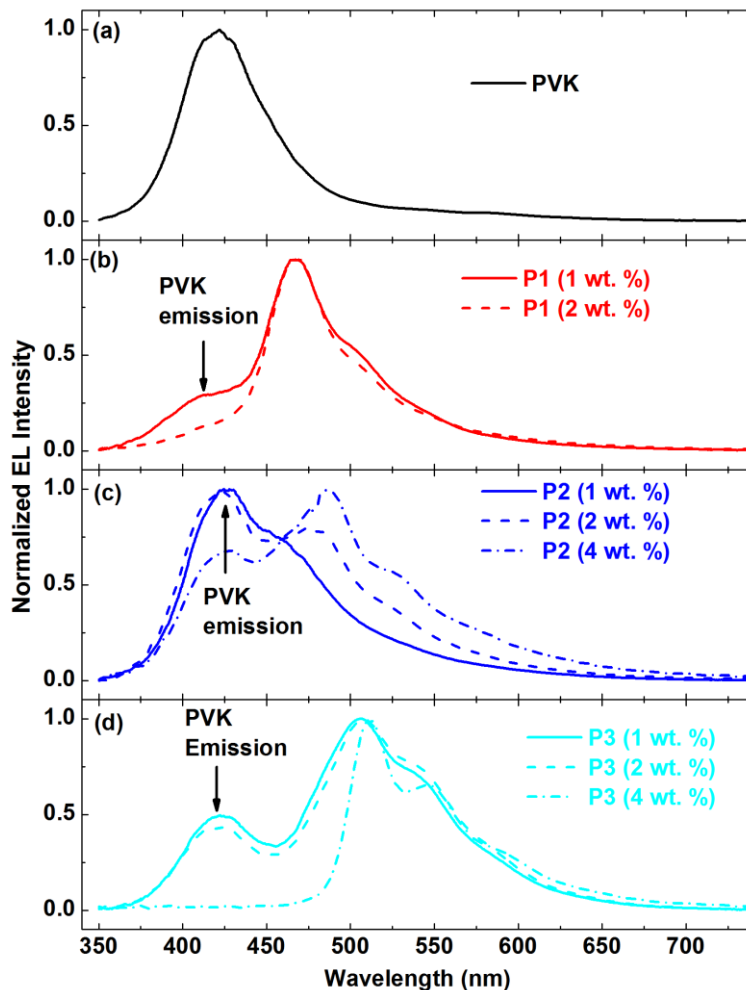


Fig. 3. Normalized EL spectra of the OLEDs driven at 57 mA/cm^2 .

Unfortunately, this fluorescence was quenched in the solid state. Thus no electroluminescence (EL) was observed from devices with these polymers as neat emitting films. However, since all these polymers have high fluorescence quantum yield in solution and good solubility in organic solvents, they were suitable candidates for use in guest-host PLEDs.²⁷ We therefore evaluated them as low level dopants in poly(*N*-vinyl carbazole) (PVK)-based PLEDs using low molecular weight PVK as the host material (average molecular weight: $\sim 50,000\text{--}100,000 \text{ g/mol}$). The electroluminescent properties of the PLEDs are summarized in Table 3. The structure of the PLEDs was ITO/PEDOT:PSS(60 nm)/ PVK:**P1-P3**/BPhen(40 nm)/LiF(1 nm)/Al(100 nm) (Fig.2). In these devices, the benzobisazole terpolymers were blended with PVK at different weight

ratios. When the concentration of the conjugated polymers in the blend was increased, the overall performance of the devices decreased. This is especially prominent for polymer **P1**. The highest brightness of the 2 wt. % **P1**:PVK device was only $\sim 60 \text{ Cd/m}^2$ and the 4 wt. % **P1**:PVK device did not light up. Among all the polymers, **P3** showed the best performance with 1860 Cd/m^2 at 2 wt.%. The normalized EL spectra of the PLEDs are shown in Figure 3. As seen, the intensity of the PVK emission, which peaks at $\sim 420 \text{ nm}$, decreased relative to that of the benzobisazole terpolymers emission when the concentration of the latter increased. This is particularly notable for the 4 wt % **P3**:PVK PLEDs, where the PVK emission totally vanishes and the **P3** emission becomes the only emission. This behavior indicates energy transfer from PVK to the benzobisazole terpolymers or direct carrier injection to the benzobisazole terpolymers. This reduced performance of the polymer is suspected to result from quenching due to aggregation. As a result the fluorescence quantum yield is diminished.²⁸

Dopant	Device ^a wt. %	V _{on} ^b [V]	Drive Voltage [V]	Current Density [J, mA/cm ²]	Brightness [Cd/m ²]	Efficiency [Cd/A, (%EQE) ^c]	$\lambda_{\text{max}}^{\text{EL}}$ [nm] polymer, PVK	r _{max}	CIE 1931 [x,y]
PVK	0.0	4.4	9.2	303	296	0.44, 0.76	422	0	(0.17, 0.07)
P1	1.0	6.0	10.0	205	363	0.52, 0.37	466, 422	4.56	(0.16, 0.19)
	2.0	5.4	8.2	53	68	0.14, 0.09	469		(0.17, 0.20)
P2	1.0	4.0	8.6	313	377	0.35, 0.37	461, 421	0.74	(0.17, 0.12)
	2.0	4.6	8.8	454	550	0.29, 0.26	478, 418	0.81	(0.18, 0.17)
	4.0	4.6	8.4	271	362	0.14, 0.10	483, 421	1.46	(0.20, 0.25)
P3	1.0	3.8	8.2	220	788	0.76, 0.31	504, 419	2.57	(0.23, 0.40)
	2.0	4.3	8.8	458	1862	0.86, 0.35	504, 418	2.24	(0.23, 0.41)
	4.0	3.7	8.8	864	1077	0.17, 0.06	511		(0.31, 0.58)

Device type structure: ITO/PEDOT:PSS/PVK: poly(arylenebenzobisazole)s/BPhen/LiF/Al ^b Turn-on voltage (at which EL is 1 Cd/m^2). ^c EQE = external quantum efficiency.

Table 3. Device characteristics of PLEDs based poly(arylenebenzobisazoles).

6.4 CONCLUSIONS

In conclusion, three new benzobisazole terpolymers containing thiophene and fluorene have been synthesized in two steps and in high yields via the Suzuki coupling reaction of fluorene with three new thiophene-benzobisazole-thiophene monomers. The flexible side chains on the thiophene and fluorene ring resulted in polymer which possessed good solubility, while maintaining good thermal stability. Preliminary electroluminescence studies showed that these polymers exhibit moderate brightness in

guest-host PLEDs. Although these polymers have comparable electron affinity to previously synthesized benzobisazole/fluorene copolymers, the incorporation of the alkyl thiophene rings into the polymer backbone proved to be detrimental to the polymers' performance in OLEDs. However, the facile synthetic approach described herein will enable the development of new benzobisazole terpolymers with improved properties. The synthesis of such materials is currently ongoing in our laboratories.

6.5 EXPERIMENTAL SECTION

The starting materials 2,5-dibromo-3-octylthiophene **1**,¹⁵ 4,6-diamino resorcinol **3**,¹¹ diaminohydroquinone **4**,¹⁸ diaminobenzene dithiol **5**,¹² and 2,7-bis(4,4,5,5-tetramethyl-1,3,2-dioxaborolan-2-yl)-9,9-dioctylfluorene **9**¹⁹ were all synthesized according to previously reported methods. Tetrahydrofuran was dried using an Innovative Technologies solvent purification system. All other compounds were purchased from commercial sources and used without further purification. Nuclear magnetic resonance spectra were obtained on a 400 MHz spectrometer. All samples were referenced internally to the residual protonated solvent. Gel permeation chromatography (GPC) measurements were performed on a GPC separation module equipped with four columns connected in a series (guard, 10,000 Å, 1,000 Å and 100 Å from American Polymer Service Corporation), a refractive index detector and a UV-Vis detector. Analyses were performed at 35 °C using chloroform as the eluent with the flow rate at 1.0 mL/min. Calibration was based on polystyrene standards. Fluorescence spectroscopy and UV-Visible spectroscopy were performed using polymer solutions in chloroform, and thin films were spun from these solutions. All of the polymers were excited at their respective emission maxima. Quantum yield measurements were taken using Rhodamine B ($\phi = 0.65$) in 1-hexanol as a standard (excitation at 410 nm; emission was taken from 420-700 nm).²⁹ All values were corrected for the differences in the refractive index of the solvent. Thermal gravimetric analysis measurements were performed within the temperature interval of 30 °C - 750 °C, using a heating rate of 20 °C/minute under ambient atmosphere. Differential scanning calorimetry was performed with a first scan at a heating rate of 15 °C/min to erase thermal history and a second scan to measure

transitions from 0 °C to 275 °C under nitrogen. Transitions were also measured with cooling at 15 °C/min. Cyclic voltammograms were performed in 0.1 M tetrabutylammonium hexafluorophosphate using 0.01 M AgNO₃ in acetonitrile as the reference electrode. The potential values obtained versus the Ag⁺ were converted to the ferrocene (Fc) reference using it as an internal standard. Ultraviolet Photoelectron Spectroscopy measurements were performed using a RKI Instruments Model AC-2 instrument. The measurements were performed on polymer films.

2-bromo-3-dodecyl-5-(triethoxymethyl)thiophene (S1). A dry, round bottom flask was equipped with a reflux condenser and addition funnel then placed under argon. The flask was charged with 60 mL of dry diethyl ether and 2,5-dibromo-3-octylthiophene (21.27 g, 60.06 mmol). Isopropyl magnesium chloride (30.1 mL, 60.2 mmol, 2.0 M) was then added dropwise to the flask via the addition funnel and the mixture was brought to reflux. After an hour, metathesis was completed (monitored by GC/MS), and the reaction was cooled to room temperature. Once cool, tetraethyl orthocarbonate (13.86 g, 72.07 mmol) was added dropwise. The mixture was then heated to reflux and stirred overnight. The crude mixture was poured into 200 mL of saturated aqueous ammonium chloride and extracted with 3 x 150 mL diethyl ether. The combined organic layers were washed with brine and dried over sodium sulfate. The solution was filtered and the filtrate concentrated *in vacuo*. The crude product was purified by Kugel-rohr distillation to yield 5-bromo-2-triethoxymethyl-3-octylthiophene (17.80 g, 42.24 mmol, 70% yield). ¹H-NMR (400 MHz, CDCl₃): δ 6.85 (s, 1H), 3.43 (q, 6H), 2.50 (t, 2H) 1.57 (m, 2H), 1.57 (m, 10H), 1.18 (t, 9H), 0.86 (t, 3H). ¹³C-NMR (100 MHz, CDCl₃): δ 141.7, 141.3, 127.6, 112.8, 109.8, 58.2, 32.0, 29.7, 29.5, 29.4, 29.3, 22.9, 15.0, 14.3. GC/MS (QP, M⁺ for C₁₉H₃₃BrO₃S): calcd, 420.13; found, 420.35.

2,6-bis(2-bromo-3-octyl-thiophene-5-yl) benzobis[1,2-*d*:5,4-*d*]bisoxazole 6. 4,6-Diamino-1,3-dihydroxybenzene bishydrochloride **3** (0.91 g, 4.3 mmol) was placed under argon in a dry round bottom flask. To it was added 4 mL anhydrous DMSO and pyridine (0.67 g, 8.3 mmol); the mixture was stirred until the solids had all dissolved. Meanwhile,

a solution of Yttrium(III) triflate (0.11g, 0.21 mmol) in 4 mL dry THF was prepared and heated to 60 °C. The DMSO solution was then transferred dropwise into the THF solution. The reaction was stirred at 60 °C overnight. After stirring, the mixture was cooled and an excess amount of methanol was added to precipitate any dissolved product. The solids were filtered and recrystallized from chloroform and methanol to yield **6** (89%). Mp. 105 - 106 °C. ¹H-NMR (400 MHz, CDCl₃): δ 7.80 (s, 2H), 7.62 (s, 2H), 2.62 (t, 4H) 1.65 (t, 4H), 1.28 (m, 20H), 0.88 (t, 3H). ¹³C-NMR (100 MHz, CDCl₃): δ 159.5, 148.4, 144.1, 140.4, 130.9, 128.8, 115.6, 100.8, 32.1, 29.8, 29.7, 29.6, 29.5, 29.4, 22.9, 14.3. HRMS (ESI, [M+H]⁺ for C₃₂H₃₈Br₂N₂O₂S₂): calcd, 705.815; found, 705.814.

2,6-bis(2-bromo-3-dodecyl-thiophene-5-yl)benzo[1,2-*d*;4,5-*d'*]bisoxazole 7. 2,5-Diamino-1,4-hydroquinone bishydrochloride **4** (0.91 g, 4.3 mmol) was placed under Argon in a dry round bottom flask. To it was added 4 mL anhydrous DMSO and pyridine (0.67 g, 8.3 mmol) and the mixture was stirred until the solids had all dissolved. Meanwhile, a solution of Lanthanum(III) triflate (0.12g, 0.21 mmol) in 4 mL dry THF was prepared and heated to 60 °C. The DMSO solution was then transferred dropwise into the THF solution. The reaction was stirred at 60 °C overnight. After stirring, the mixture was cooled and an excess amount of methanol was added to precipitate any dissolved product. The solids were filtered and recrystallized from chloroform and methanol to yield **7** (78%). Mp. 148 - 150 °C. ¹H-NMR (400 MHz, CDCl₃): δ 7.94 (s, 1H), 7.61 (s, 1H), 2.60 (t, 4H) 1.62 (t, 4H), 1.28 (m, 20H), 0.88 (t, 3H). ¹³C-NMR (100 MHz, CDCl₃): δ 159.0, 148.5, 144.0, 130.8, 128.7, 115.4, 109.6, 93.3, 32.1, 29.8, 29.7, 29.6, 29.5, 29.4, 22.9, 14.4. HRMS (ESI, [M+H]⁺ for C₃₂H₃₈Br₂N₂O₂S₂): calcd, 705.815; found, 705.814.

2,6-bis(2-bromo-3-dodecyl-thiophene-5-yl)benzo[1,2-*d*;4,5-*d'*]bisthiazole 8. 2,5-Diamino-1,4-benzenedithiol bishydrochloride **5** (0.91 g, 4.3 mmol) was placed under Argon in a dry round bottom flask. To it was added 4 mL anhydrous dimethyl acetamide and pyridine (0.67 g, 8.3 mmol) and the mixture was stirred until the solids had all dissolved. Meanwhile, a solution of Ytterbium(III) triflate (0.13g, 0.21 mmol) in 4 mL

dry THF was prepared and heated to 60°C. The DMSO solution was then transferred dropwise into the THF solution. The reaction was stirred at 60 °C overnight. After stirring, the mixture was cooled and an excess amount of methanol was added to precipitate any dissolved product. The solids were filtered and recrystallized from chloroform and methanol to yield **8** (84%). Mp. 223 - 224 °C. ¹H-NMR (400 MHz, CDCl₃): δ 8.36 (s, 2H), 7.34 (s, 2H), 2.60 (t, 4H) 1.63 (t, 4H), 1.30 (m, 20H), 0.90 (t, 3H). ¹³C-NMR (100 MHz, CDCl₃): δ 161.5, 152.0, 143.8, 136.8, 134.4, 129.7, 115.2, 114.9, 32.1, 29.9, 29.8, 29.6, 29.5, 29.4, 22.9, 14.3. HRMS (ESI, [M+H]⁺ for C₃₂H₃₈Br₂N₂S₄): calcd, 737.0358; found, 737.0357.

6.5.1 General Methods for Polymer Synthesis.

A solution of 70 mg Aliquat 336, one of the monomers [**6** (353.3 mg, 0.500 mmol), **7** (353.3 mg, 0.500 mmol), or **8** (369.4 mg, 0.500 mmol)] and 2,7-bis(pinacolatoboro)-9,9-dioctylfluorene (321.3 mg, .500 mmol) in 10 mL of toluene was prepared. To this solution was added 10 mL of 2M aqueous sodium carbonate. The biphasic system was degassed with Argon for 30 mins before adding Pd(PPh₃)₄ (11.6 mg, 0.010 mmol, dissolved in 5 mL degassed toluene). The mixture was heated to reflux and stirred for 4 days. After 4 days, the organic layer was separated and precipitated in MeOH. The polymers were then purified by soxhlet extraction first rinsing with MeOH and hexanes before extraction by chloroform. The chloroform was evaporated to yield polymer.

P1 (439 mg, 94% yield). ¹H-NMR (400 MHz, CDCl₃): δ 8.04 (s, 1H), 7.8 (m, 5H), 7.50 (m, 5H), 2.78 (b, 4H), 2.11 (b, 4H), 1.73 (b, 4H), 1.28-1.11 (bm, 40H), 0.88-0.80 (bm, 16H) ¹³C-NMR (100 MHz, CDCl₃): δ160.0, 151.8, 148.7, 144.4, 140.8, 140.4, 140.3, 132.7, 128.5, 126.7, 123.9, 120.5, 109.3, 93.2, 55.6, 40.7, 32.1, 32.0, 31.1, 30.4, 29.8, 29.7, 29.6, 29.5, 29.4, 29.3, 24.3, 22.9, 22.8, 14.4, 14.3

P2 (410 mg, 88% yield). ¹H-NMR (400 MHz, CDCl₃): δ 7.86 (m, 5H), 7.52 (m, 5H), 2.79 (b, 4H), 2.11 (b, 4H), 1.73 (b, 4H), 1.30-1.12 (bm, 40H), 0.89-0.83 (bm, 16H) ¹³C-NMR (100 MHz, CDCl₃): δ160.5, 151.9, 148.7, 144.7, 140.9, 140.7, 140.5, 133.0, 132.9, 128.5, 126.9, 123.9, 120.4, 100.6, 55.7, 40.7, 32.1, 32.0, 31.1, 30.4, 29.8, 29.7, 29.6, 29.5, 29.4, 29.3, 24.3, 22.9, 22.8, 14.3, 14.2

P3 (469 mg, 97% yield). ¹H-NMR (400 MHz, CDCl₃): δ 8.46 (s, 2H), 7.80 (d, 2H),

7.61-7.52 (m, 6H), 2.78 (b, 4H), 2.05 (b, 4H), 1.73 (b, 4H), 1.30-1.12 (bm, 40H), 0.90-0.82 (bm, 16H) ^{13}C -NMR (100 MHz, CDCl_3): δ 162.3, 152.2, 151.9, 143.8, 140.9, 140.4, 134.9, 134.7, 133.2, 131.8, 128.4, 124.0, 120.4, 115.0, 55.7, 40.7, 32.1, 32.0, 31.1, 30.4, 29.8, 29.7, 29.6, 29.5, 29.4, 29.3, 24.3, 22.9, 22.8, 14.3, 14.2

6.5.2 Fabrication and Characterization of PLEDs.

PLEDs were fabricated on nominally 20 Ω /square, 140 nm-thick ITO-coated glass substrates (Colorado Concept Coatings). The substrates were first cleaned with a detergent and organic solvents; they were then treated in a UV/ozone oven to increase the work function of the ITO and hence facilitate hole injection, as described elsewhere.³⁰ A 60 nm PEDOT:PSS layer was spin-coated on the ITO and then baked in air at 160 °C for 1 hour. Blends of PVK and the poly(arylenebenzobisoxazole) copolymers in chlorobenzene solutions were spin-coated on top of the PEDOT:PSS layer in an Ar-filled glovebox; the thickness of the poly(arylenebenzobisoxazole) copolymers layers was 30 nm. The combined concentration of the PVK and polymer dopants was kept constant at 9 mg/mL; the poly(arylenebenzobisoxazole)s concentration was varied in the range 0.09 to 0.36 mg/mL. The solution was spin coated at 4000 rpm for 60 s. The fabricated structure was then annealed at 60 °C for 30 min. Following this annealing step, the samples were transferred into a thermal evaporator within the glovebox and the BPhen, LiF, and Al layers were deposited sequentially by thermal evaporation at a base pressure of $\sim 2 \times 10^{-6}$ Torr. The PLEDs were characterized by monitoring their electroluminescence (EL) spectra, brightness as a function of the applied voltage, and luminous efficiency.

6.6 ACKNOWLEDGEMENTS

We thank Mr. Robert Roggers (ISU) for X-ray analysis. We thank Ms. Dana Drochner and Mr. Timothy Mauldin for thermal analysis. We thank Ms. Atta Gueye, Dr. Elena Sheina and Dr. Christopher Brown of Plextronics for providing UPS measurements. This work was funded by the National Science Foundation (DMR-0846607), and the 3M foundation. MC and TX were supported by the US Department of Energy, Basic Energy Sciences, Materials Sciences and Engineering Division, under Contract No. DE-AC 02-07CH11358.

6.7 NOTES AND REFERENCES

(1) X. Zhan and D. Zhu, *Polym. Chem.*, **2010**, *1*, 409-419; T. A. Skotheim and J. R. Reynolds, *Handbook of conducting polymers*, 3rd ed / edited by Terje A. Skotheim and John Reynolds. edn., London, Boca Raton, Fla., **2007**; A. C. Grimsdale, K. Leok Chan, R. E. Martin, P. G. Jokisz and A. B. Holmes, *Chem. Rev.*, **2009**, *109*, 897-1091; B. C. Thompson and J. M. J. Frechet, *Angew, Chem. Int. Ed.*, **2008**, *47*, 58-77; A. Facchetti, *Chem. Mater.*, **2010**, *23*, 733-758.

(2) A. P. Kulkarni, X. Kong and S. A. Jenekhe, *Macromolecules*, **2006**, *39*, 8699-8711; A. P. Kulkarni, Y. Zhu and S. A. Jenekhe, *Macromolecules*, **2005**, *38*, 1553-1563; M. Leclerc, *J. Poly. Sci. A.*, **2001**, *39*, 2867-2873.

(3) M. Al-Hashimi, J. G. Labram, S. Watkins, M. Motevalli, T. D. Anthopoulos and M. Heeney, *Org. Lett.*, **2010**, *12*, 5478-5481; X. Zhang, T. T. Steckler, R. R. Dasari, S. Ohira, W. J. Potscavage Jr, S. P. Tiwari, S. Coppee, S. Ellinger, S. Barlow, J.-L. Bredas, B. Kippelen, J. R. Reynolds and S. R. Marder, *J. Mater. Chem.*, **2010**, *20*, 123-134; L. Zhang, C. He, J. Chen, P. Yuan, L. Huang, C. Zhang, W. Cai, Z. Liu and Y. Cao, *Macromolecules*, **2010**, *43*, 9771-9778; Z. Li, J. Ding, N. Song, J. Lu and Y. Tao, *J. Am. Chem. Soc.*, **2010**, *132*, 13160-13161; M. Zhang, H. Fan, X. Guo, Y. He, Z.-G. Zhang, J. Min, J. Zhang, G. Zhao, X. Zhan and Y. Li, *Macromolecules*, **2010**, *43*, 8714-8717; X. Guo, H. Xin, F. S. Kim, A. D. T. Liyanage, S. A. Jenekhe and M. D. Watson, *Macromolecules*, **2010**, *44*, 269-277; P. Herguth, X. Jiang, M. S. Liu and A. K. Y. Jen, *Macromolecules*, **2002**, *35*, 6094-6100.

(4) M. M. Alam and S. A. Jenekhe, *Chem. Mater.*, **2002**, *14*, 4775-4780; S. A. Jenekhe, J. A. Osaheni, J. S. Meth and H. Vanherzeele, *Chem. Mater.*, **1992**, *4*, 683-687.

(5) B. A. Reinhardt, M. R. Unroe and R. C. Evers, *Chem. Mater.*, **1991**, *3*, 864-871.

(6) J. J. Intemann, J. F. Mike, M. Cai, S. Bose, T. Xiao, T. C. Mauldin, R. A. Rogers, J. Shinar, R. Shinar and M. Jeffries-El, *Macromolecules*, **2011**, *44*, 248-255.

(7) E. Ahmed, F. S. Kim, H. Xin and S. A. Jenekhe, *Macromolecules*, **2009**, *42*, 8615-8618.

(8) H. Pang, F. Vilela, P. J. Skabara, J. J. W. McDouall, D. J. Crouch, T. D.

Anthopoulos, D. D. C. Bradley, D. M. de Leeuw, P. N. Horton and M. B. Hursthouse, *Adv. Mater.*, **2007**, *19*, 4438-4442.

(9) I. Osaka, K. Takimiya and R. D. McCullough, *Adv. Mater.*, **2010**, *22*, 4993-4997.

(10) M. Mamada, J.-i. Nishida, S. Tokito and Y. Yamashita, *Chem. Lett.*, **2008**, *37*, 766-767; G. J. McEntee, F. Vilela, P. J. Skabara, T. D. Anthopoulos, J. G. Labram, S. Tierney, R. W. Harrington and W. Clegg, *J. Mater. Chem.*, **2011**, *21*, 2091-2097.

(11) J. F. Wolfe and F. E. Arnold, *Macromolecules*, **1981**, *14*, 909-915.

(12) J. F. Wolfe, B. H. Loo and F. E. Arnold, *Macromolecules*, **1981**, *14*, 915-920.

(13) J. F. Mike, J. J. Inteman, A. Ellern and M. Jeffries-El, *J. Org. Chem.*, **2010**, *75*, 495-497; J. F. Mike, A. J. Makowski and M. Jeffries-EL, *Org. Lett.*, **2008**, *10*, 4915-4918.

(14) J. F. Mike, A. J. Makowski, T. C. Mauldin and M. Jeffries-El, *J. Poly. Sci. A.*, **2010**, *48*, 1456-1460; J. F. Mike, K. Nalwa, A. J. Makowski, D. Putnam, A. L. Tomlinson, S. Chaudhary and M. Jeffries-El, *Phys. Chem. Chem. Phys.*, **2011**, *13*, 1338-1344; A. V. Patil, H. Park, E. W. Lee and S.-H. Lee, *Synth. Met.*, **2010**, *160*, 2128-2134.

(15) T. A. Chen, X. Wu and R. D. Rieke, *J. Am. Chem. Soc.*, **1995**, *117*, 233.

(16) R. S. Loewe, P. C. Ewbank, J. Liu, L. Zhai and R. D. McCullough, *Macromolecules*, **2001**, *34*, 4324-4333; R. S. Loewe, S. M. Khersonsky and R. D. McCullough, *Adv. Mater.*, **1999**, *11*, 250-258.

(17) A. E. Tschitschibabin, *Ber.*, **1905**, *38*, 561-566.

(18) M. Inbasekaran and R. Strom, *OPPI Briefs*, **1994**, *23*, 447-450.

(19) A. P. Zoombelt, S. G. J. Mathijssen, M. G. R. Turbiez, M. M. Wienk and R. A. J. Janssen, *J. Mater. Chem.*, **2010**, *20*, 2240-2246.

(20) T. Miyamae, D. Yoshimura, H. Ishii, Y. Ouchi, T. Miyazaki, T. Koike, T. Yamamoto, Y. Muramatsu, H. Etori, T. Maruyama and K. Seki, *Synth. Met.*, **1997**, *84*, 939-940.

(21) M. Zhao, M. Samoc, P. N. Prasad, B. A. Reinhardt, M. R. Unroe, M. Prazak, R. C. Evers, J. J. Kane, C. Jariwala and M. Sinsky, *Chem. Mater.*, **1990**, *2*, 670-678.

(22) S. Admassie, O. Ingaas, W. Mammo, E. Perzon and M. R. Andersson, *Synth.*

Met., **2006**, *156*, 614-623.

(23) E. Zhou, M. Nakamura, T. Nishizawa, Y. Zhang, Q. Wei, K. Tajima, C. Yang and K. Hashimoto, *Macromolecules*, **2008**, *41*, 8302-8305; E. Zhou, K. Tajima, C. Yang and K. Hashimoto, *J. Mater. Chem.*, **2010**, *20*, 2362-2368; P. M. Beaujuge, C. M. Amb and J. R. Reynolds, *Acc. Chem. Res.*, **2010**, *43*, 1396-1407.

(24) X. Liu, X. Xu, Q. Zhuang and Z. Han, *Polym. Bull.*, **2008**, *60*, 765-774.

(25) K. D. Belfield, S. Yao, A. R. Morales, J. M. Hales, D. J. Hagan, E. W. Van Stryland, V. M. Chapela and J. Percino, *Polym. Adv. Technol.*, **2005**, *16*, 150-155.

(26) Y. M. Kim, E. Lim, I.-N. Kang, B.-J. Jung, J. Lee, B. W. Koo, L.-M. Do and H.-K. Shim, *Macromolecules*, **2006**, *39*, 4081-4085; E. Lim, B.-J. Jung, J. Lee, H.-K. Shim, J.-I. Lee, Y. S. Yang and L.-M. Do, *Macromolecules*, **2005**, *38*, 4531-4535; M. Grell, D. D. C. Bradley, G. Ungar, J. Hill and K. S. Whitehead, *Macromolecules*, **1999**, *32*, 5810-5817; S. Kawana, M. Durrell, J. Lu, J. E. Macdonald, M. Grell, D. D. C. Bradley, P. C. Jukes, R. A. L. Jones and S. L. Bennett, *Polymer*, **2002**, *43*, 1907-1913.

(27) I. Gontia, S. V. Frolov, M. Liess, E. Ehrenfreund, Z. V. Vardeny, K. Tada, H. Kajii, R. Hidayat, A. Fujii, K. Yoshino, M. Teraguchi and T. Masuda, *Phys. Rev. B*, **1999**, *82*, 4058; R. Hidayat, S. Tatsuhara, D. W. Kim, M. Ozaki, K. Yoshino, M. Teraguchi and T. Masuda, *Phys. Rev. B*, **2000**, *61*, 10167.

(28) B. Liu, W.-L. Yu, Y.-H. Lai and W. Huang, *Macromolecules*, **2000**, *33*, 8945-8952; M. R. Andersson, O. Thomas, W. Mammo, M. Svensson, M. Theander and O. Inganäs, *J. Mater. Chem.*, **1999**, *9*, 1933-1940.

(29) R. F. Kubin and A. N. Fletcher, *J. Lumin.*, **1982**, *27*, 455-462.

(30) Z. Zhou, R. Shinar, A. J. Allison and J. Shinar, *Adv. Fun. Mater.*, **2007**, *17*, 3530-3537.

6.8 SUPPORTING INFORMATION

Figure S1. TGA curves of poly(arylenebenzobisazoles). TGA's were obtained under N₂ at a heating rate of 15°C/min.

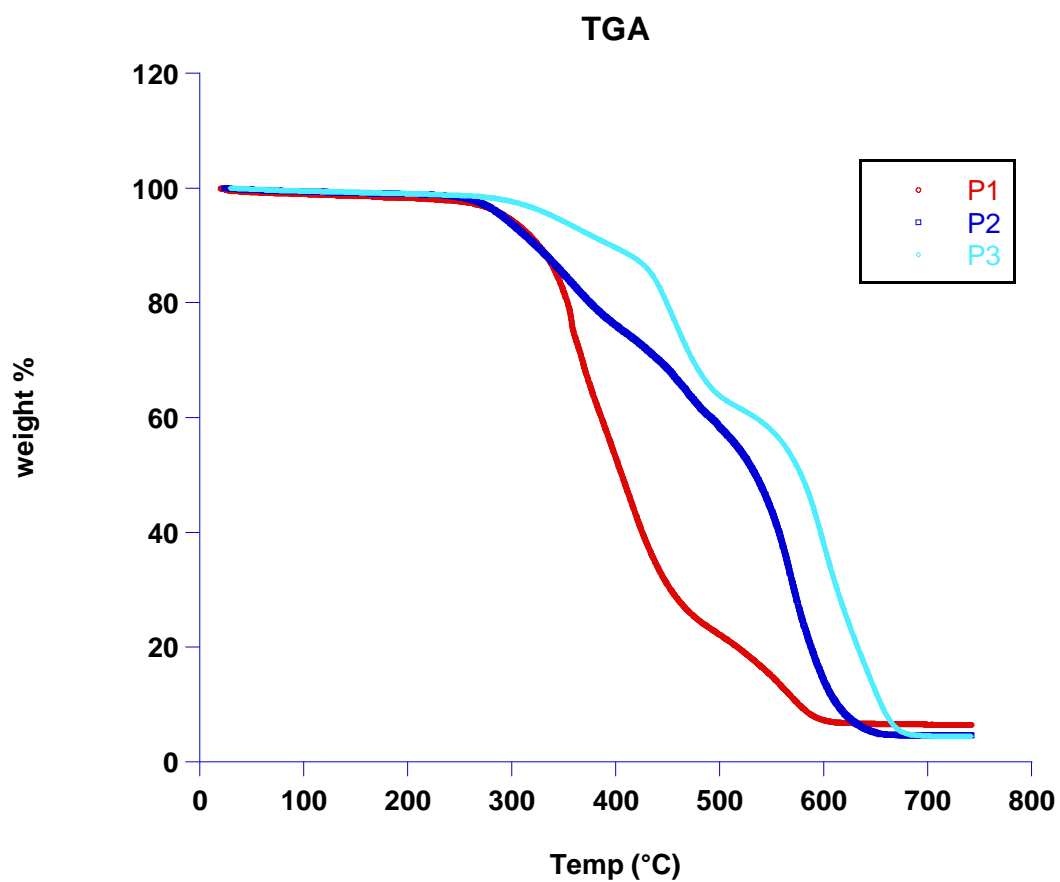


Figure S2. DSC curves.

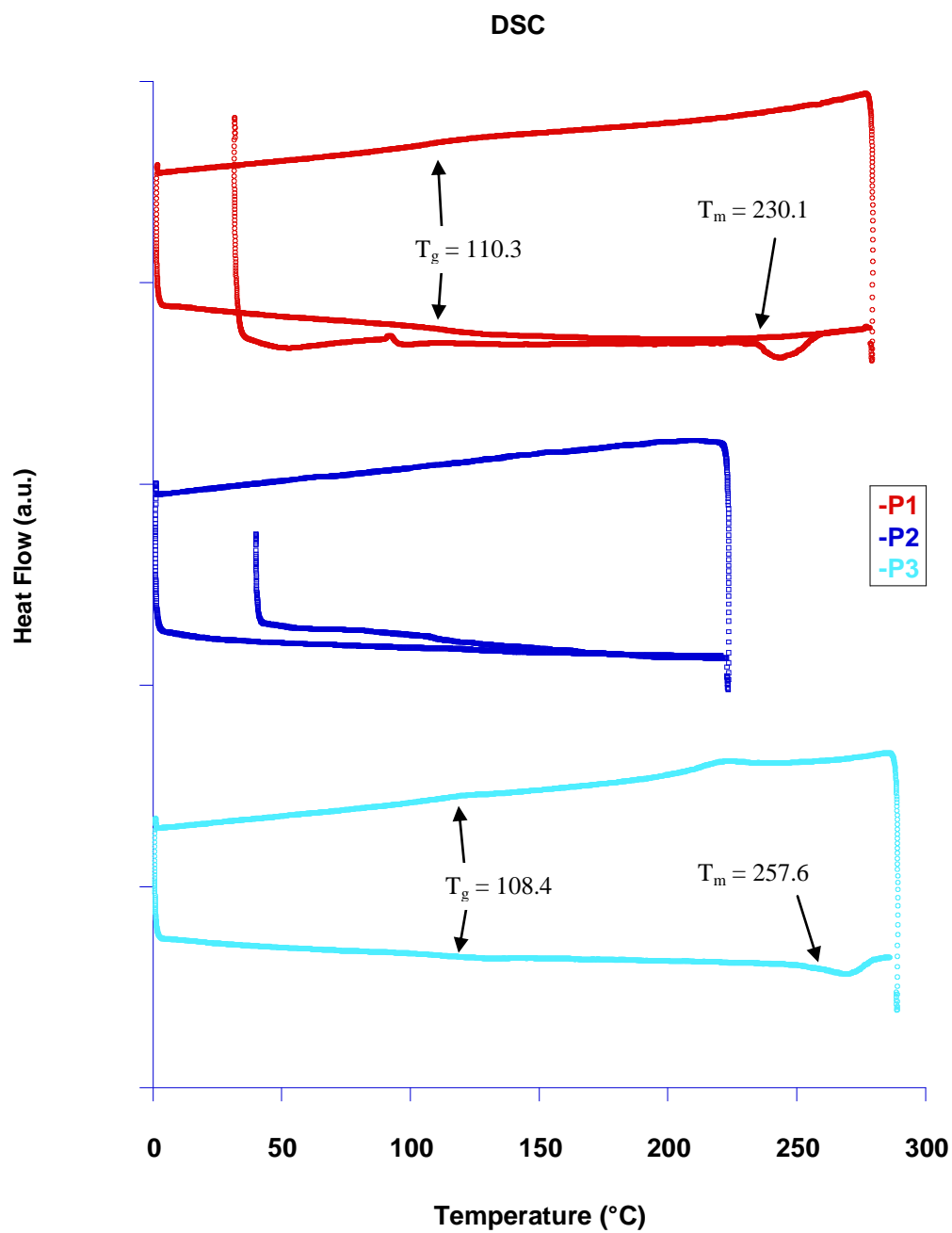
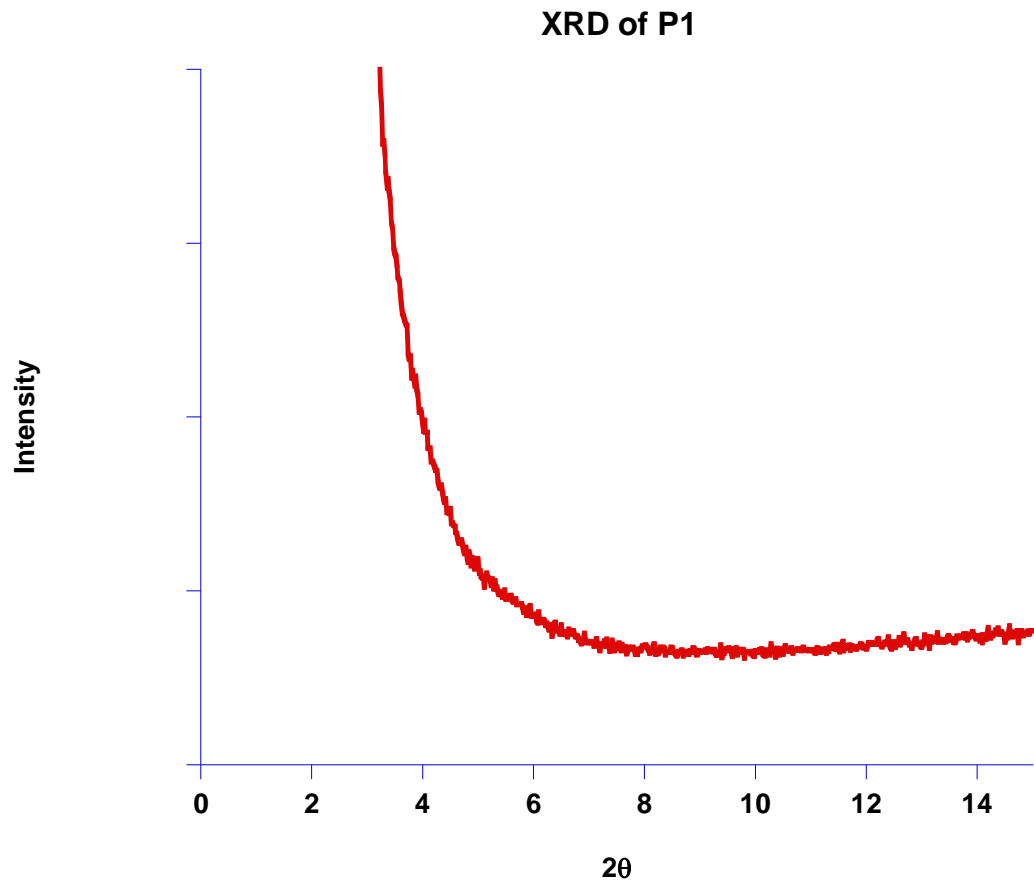
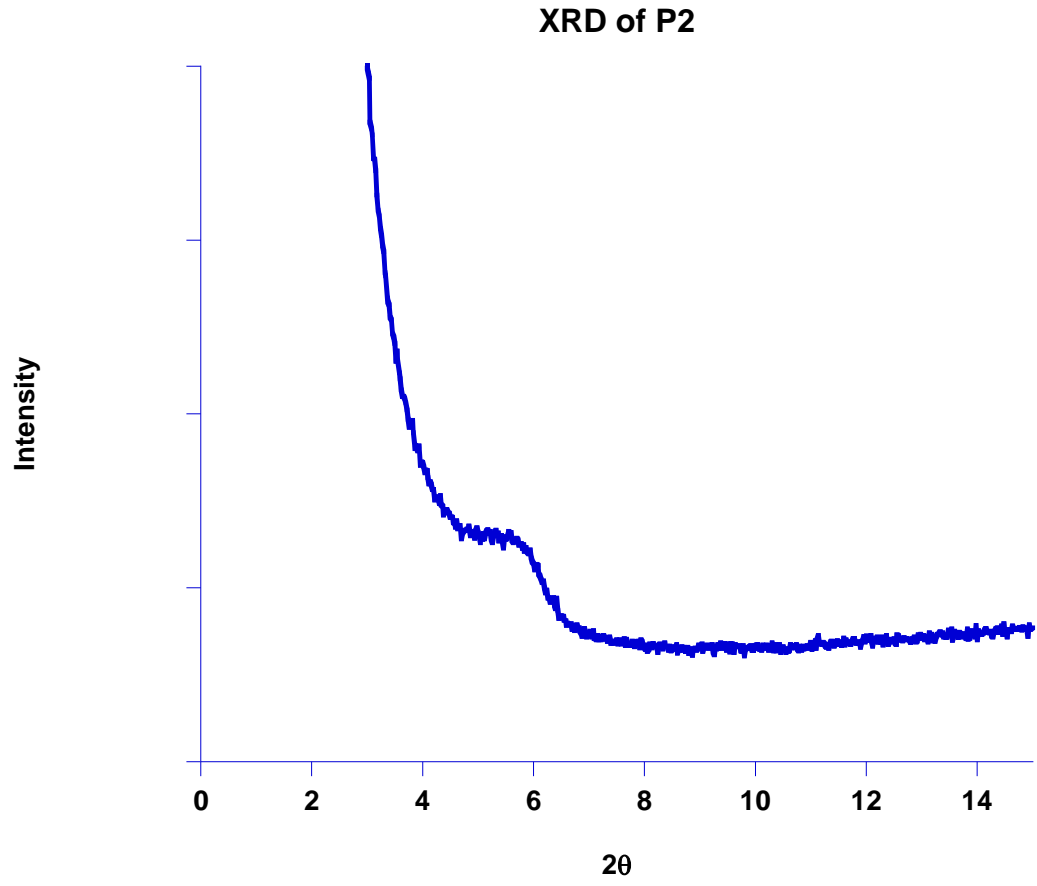


Fig S3. XRD.



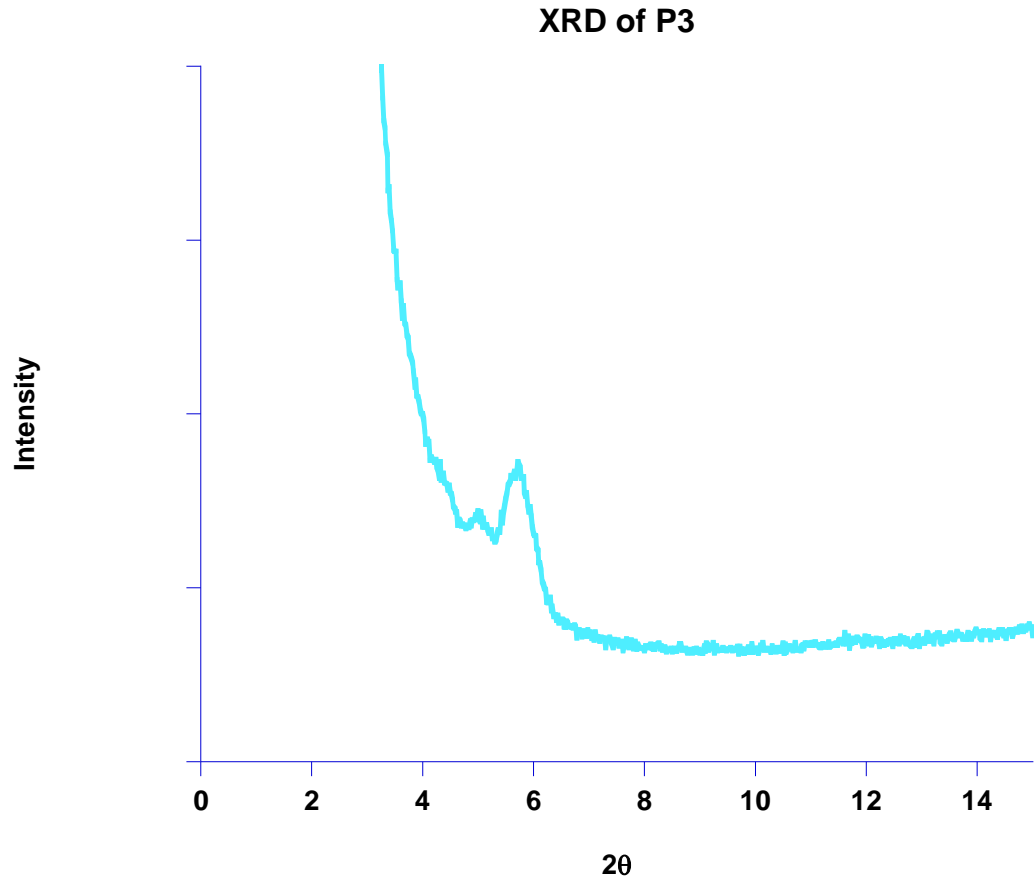


Figure S4. Cyclic voltammetry was performed on thin films of polymers that were drop-casted onto the ends of 1mm platinum button electrodes using a platinum wire as counter-electrode and a Ag/Ag^+ reference electrode. Ferrocene was used as an internal standard. Measurements were recorded at a scan rate of 100 mV/s.

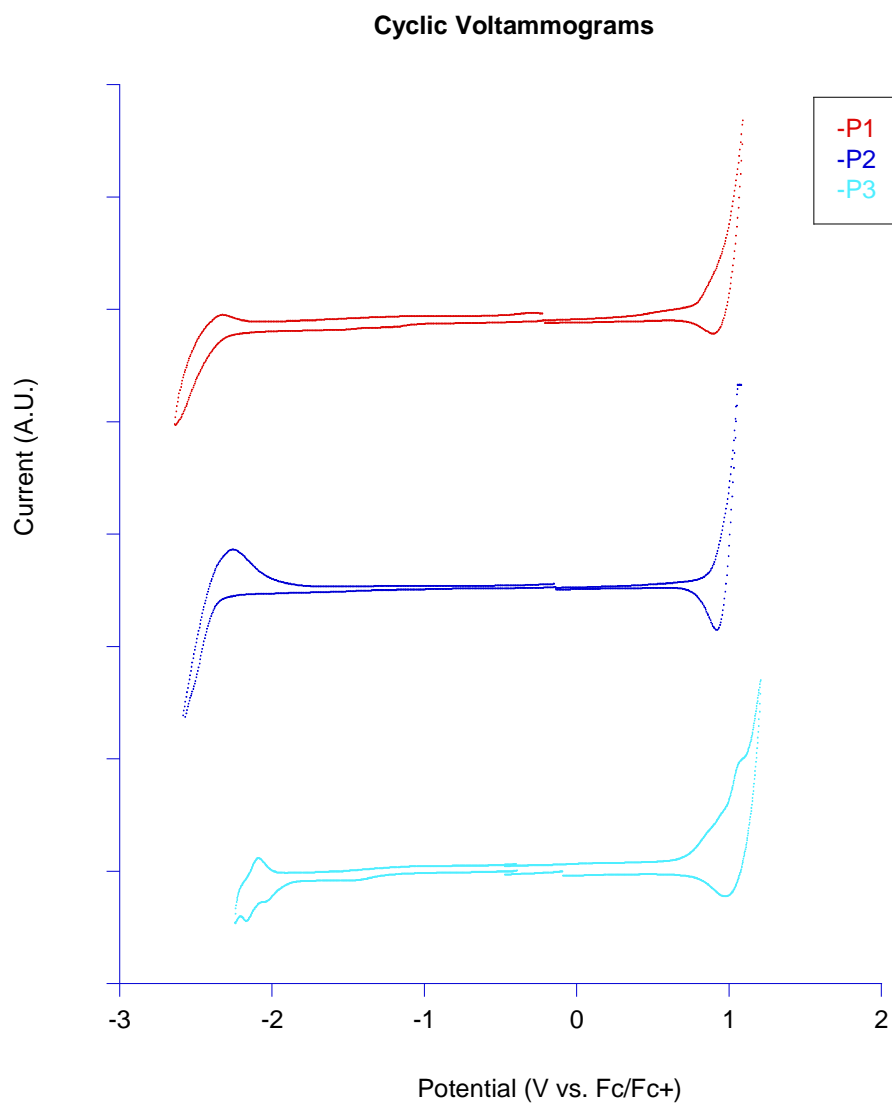


Figure S5. Differential pulse voltammetry was performed on thin films of polymers that were drop-casted onto the ends of 1mm platinum button electrodes using a platinum wire as counter-electrode and a Ag/Ag⁺ reference electrode. Ferrocene was used as an internal standard. Measurements were recorded at a scan rate of 100 mV/s with a pulse height of 100 mV, step width of 50 ms, and pulse time of 25 ms.

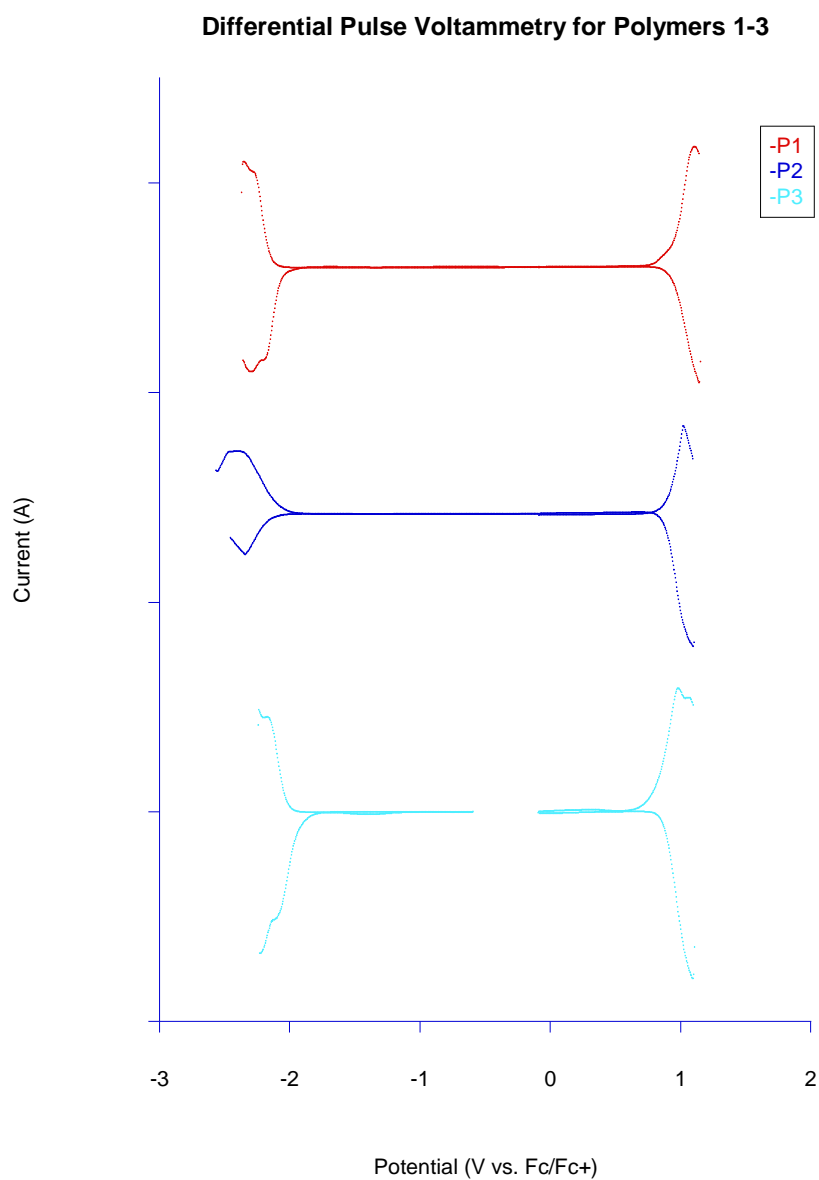


Figure S6. NMR Spectra.

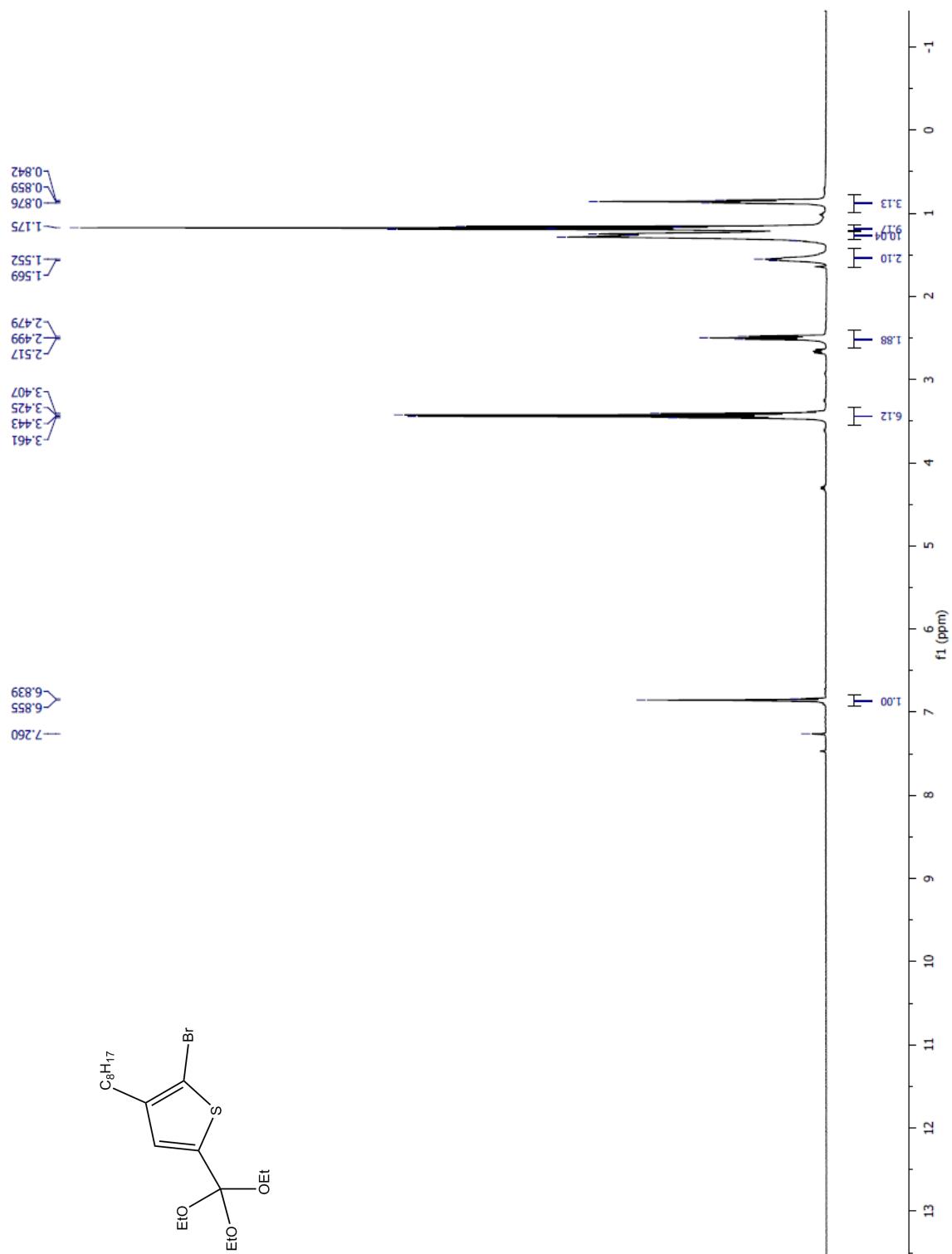


Figure S6 (cont.).

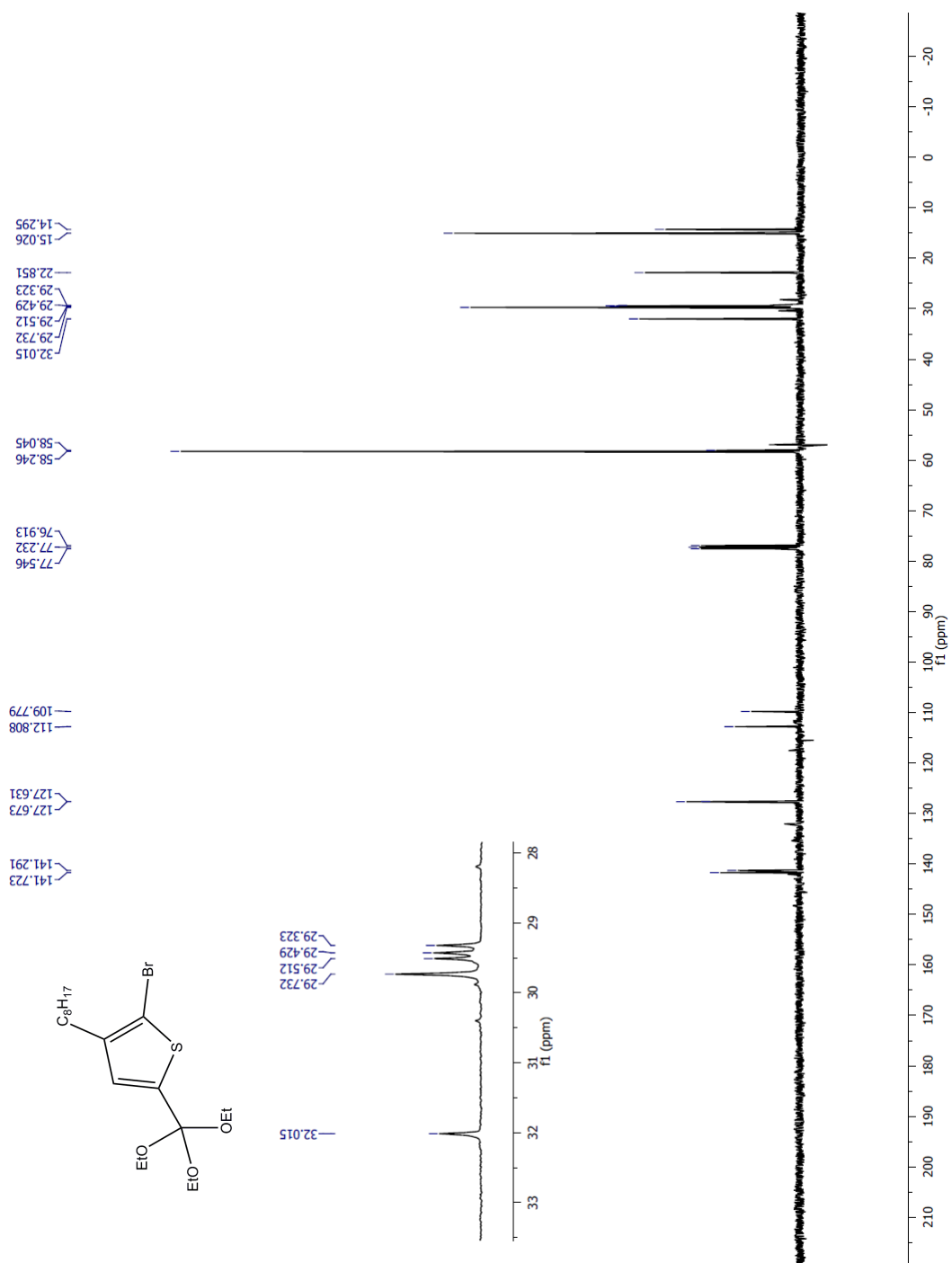


Figure S6 (cont.).

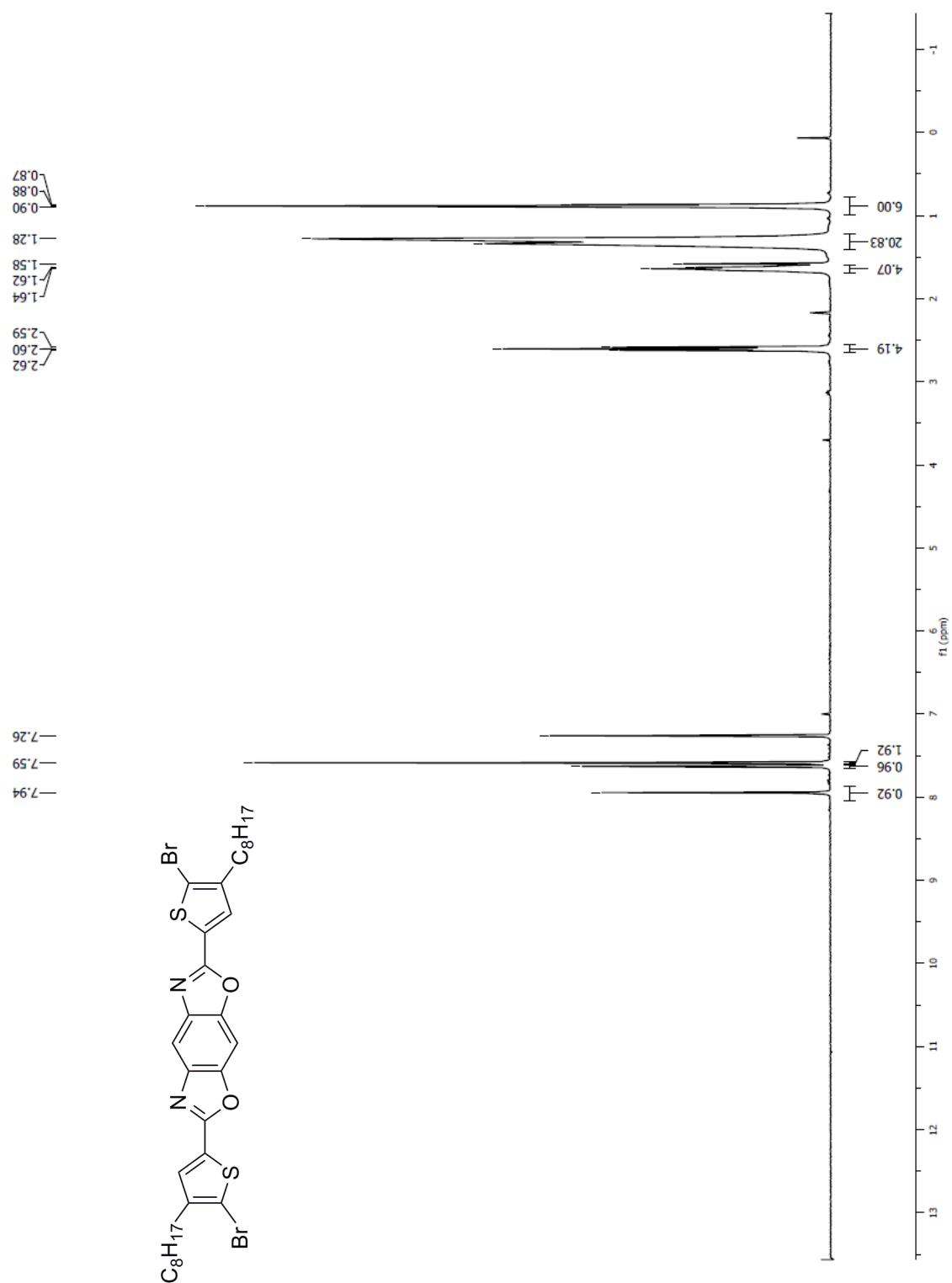


Figure S6 (cont.).

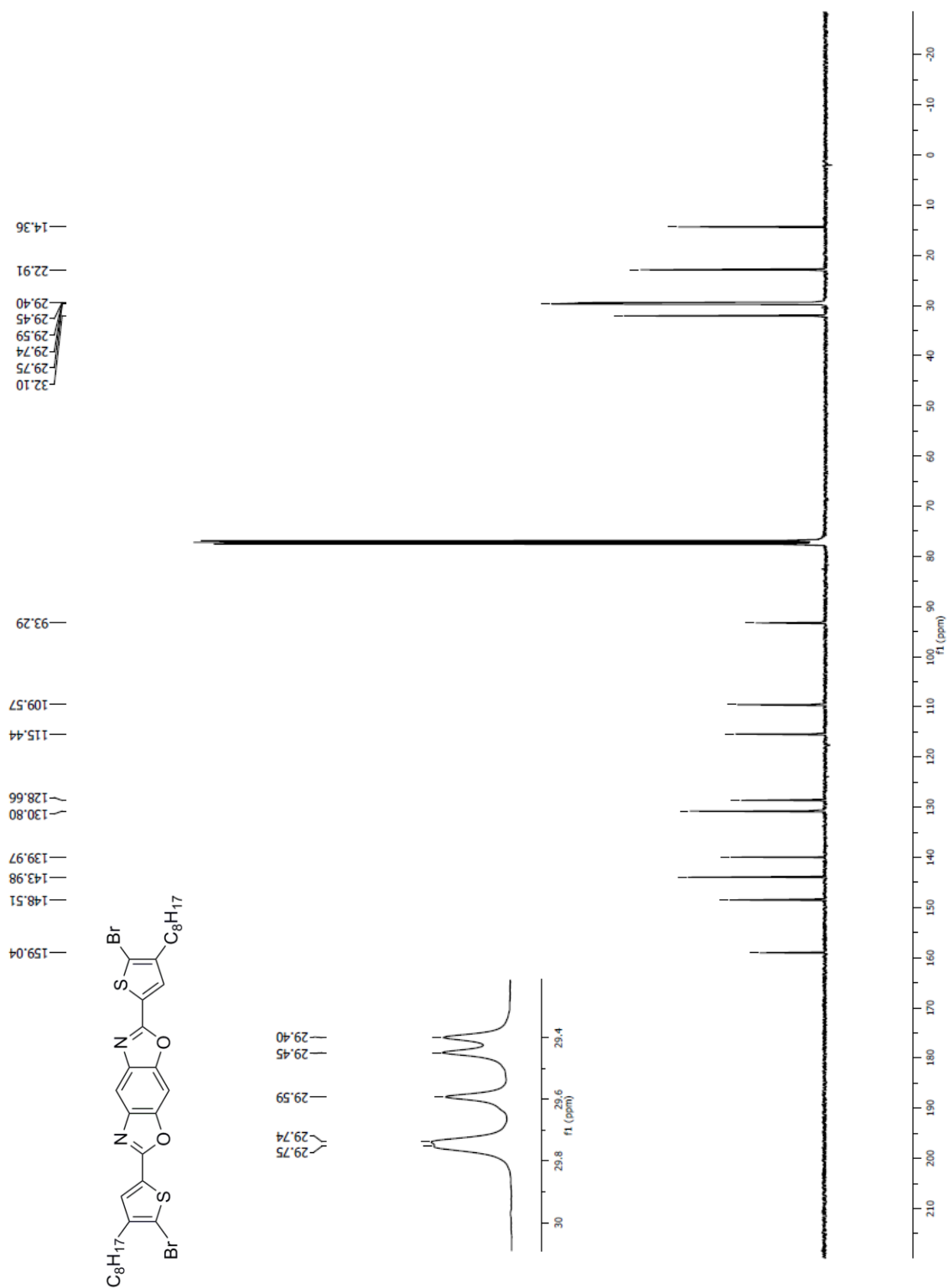


Figure S6 (cont.).

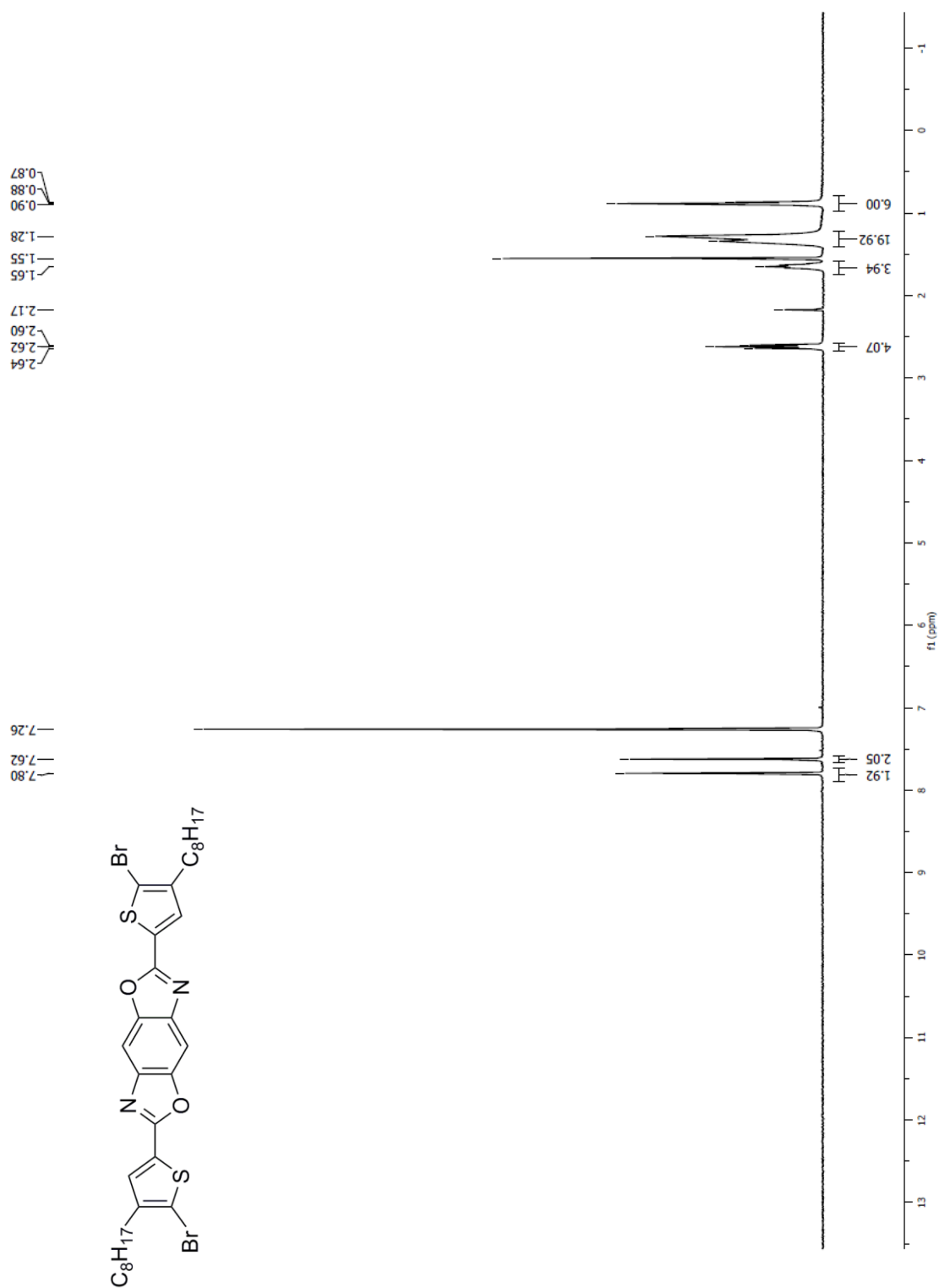


Figure S6 (cont.).

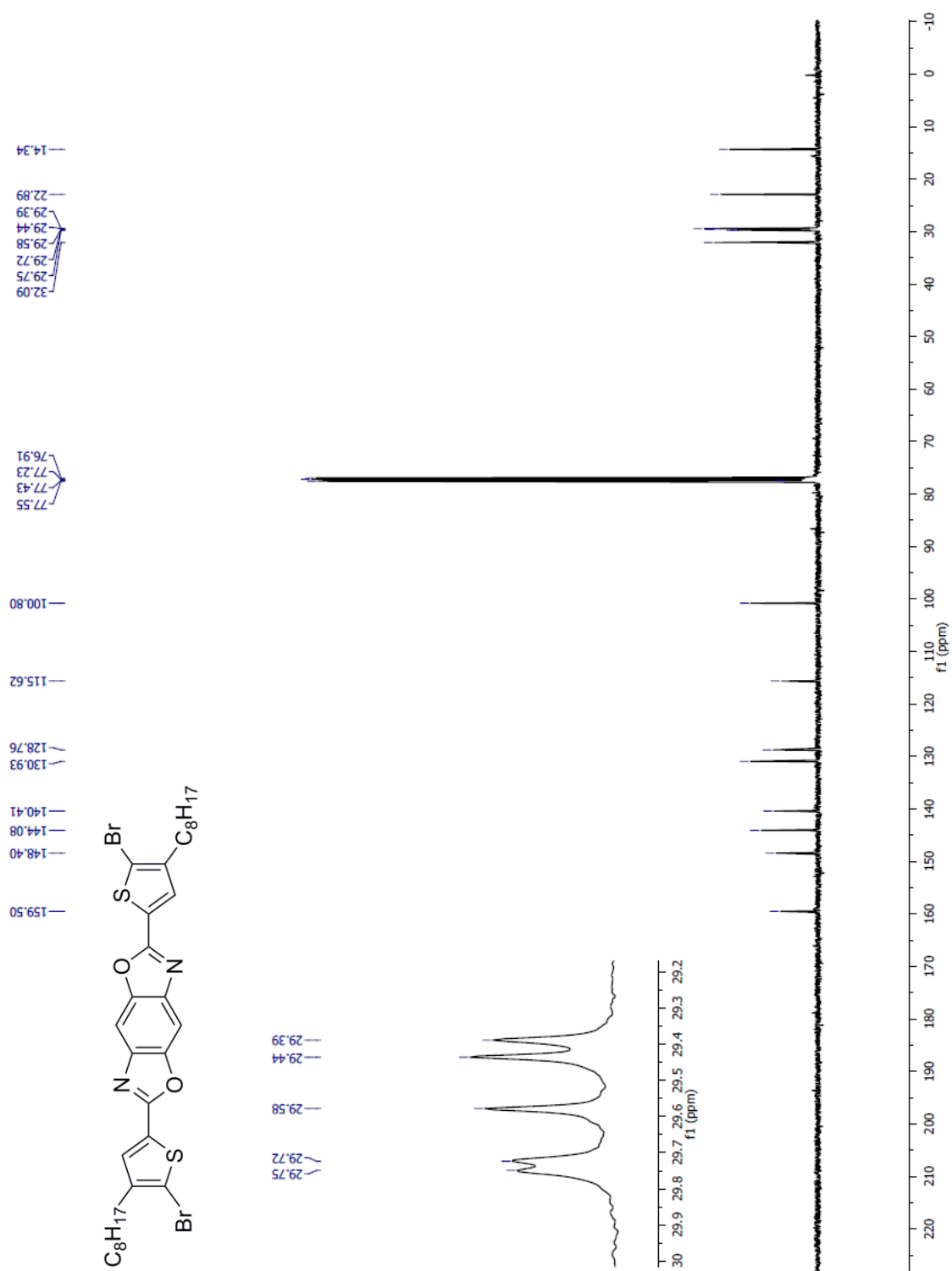


Figure S6 (cont.).

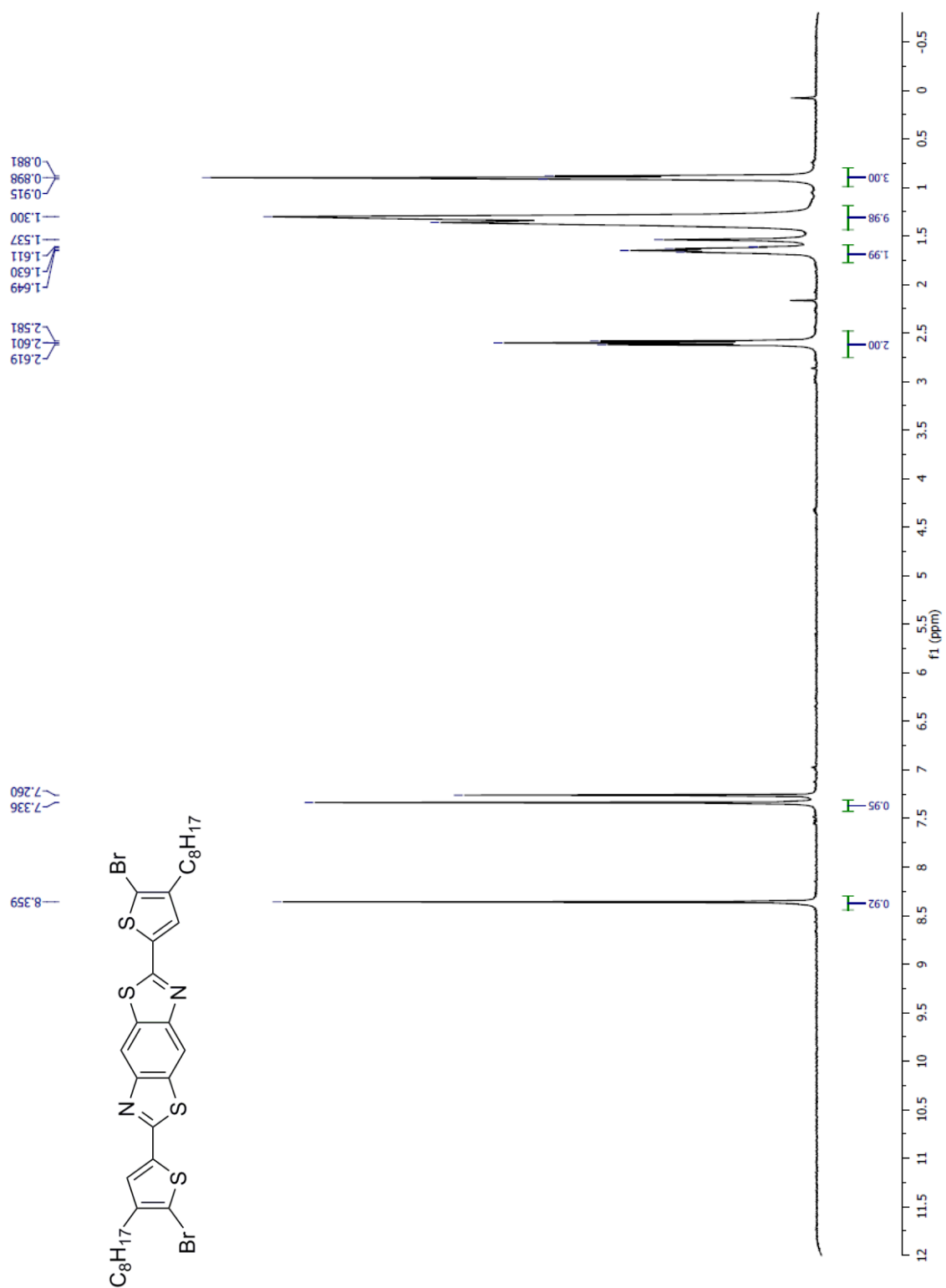


Figure S6 (cont.).

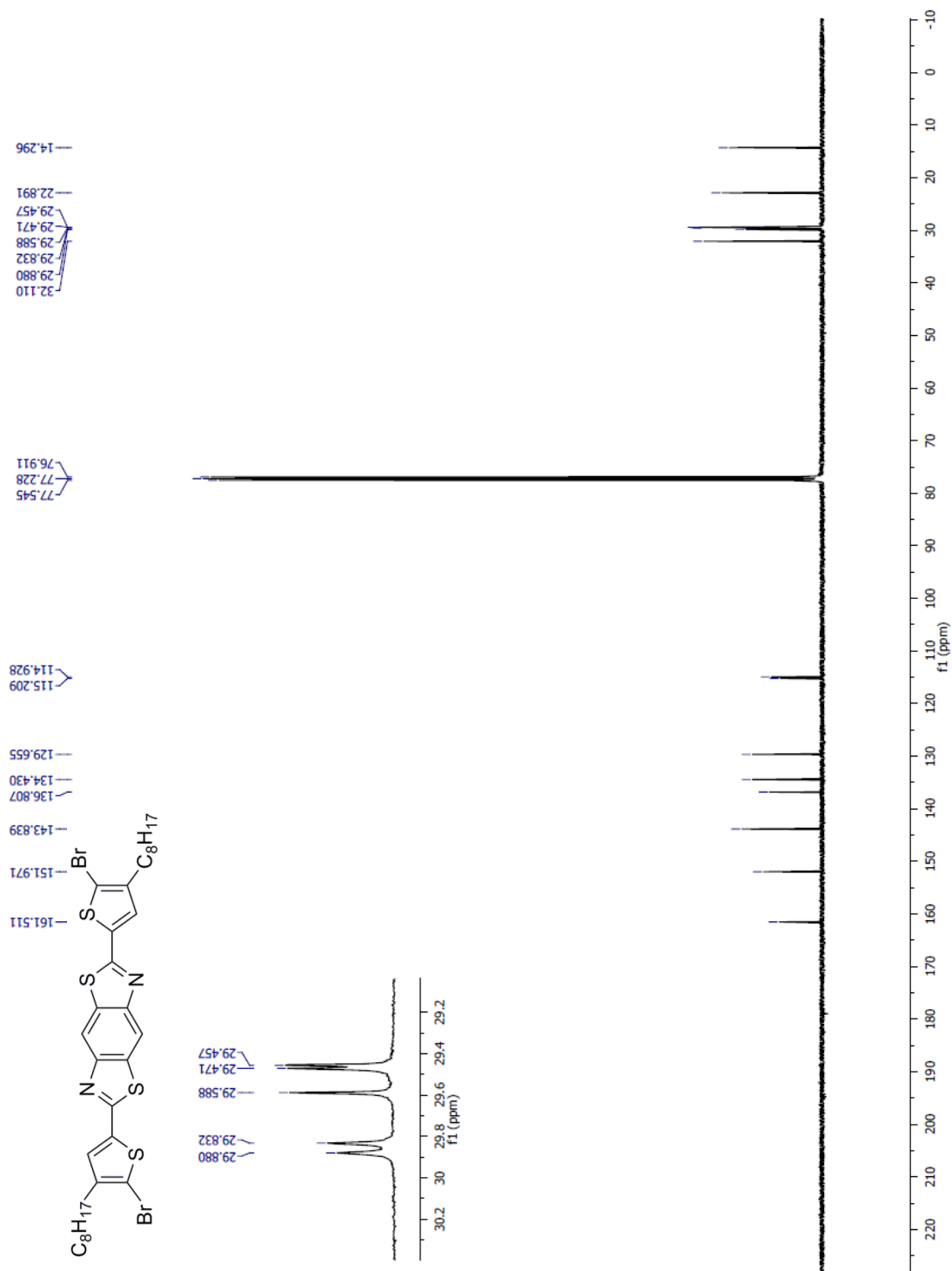


Figure S6 (cont.).

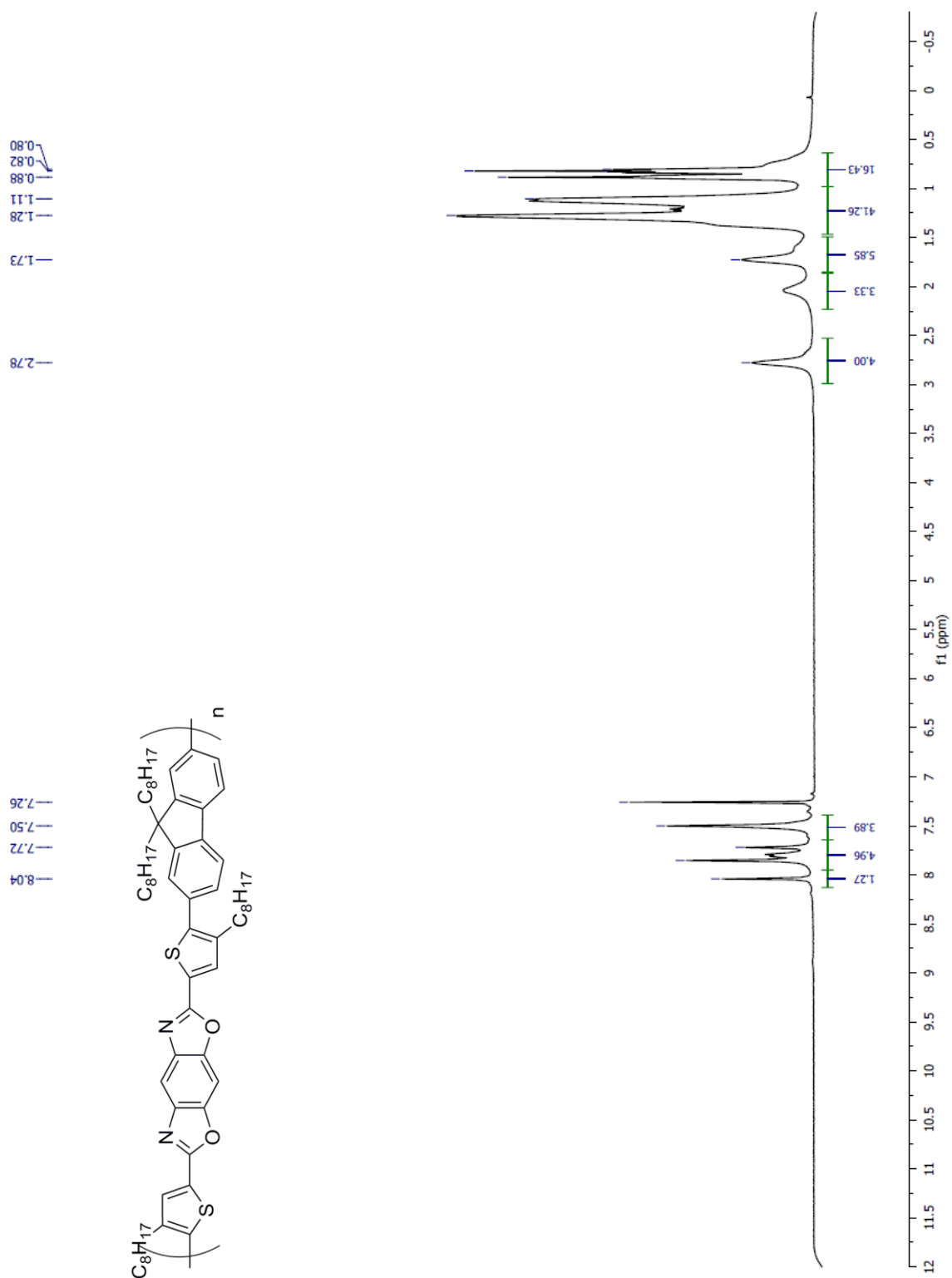


Figure S6 (cont.).

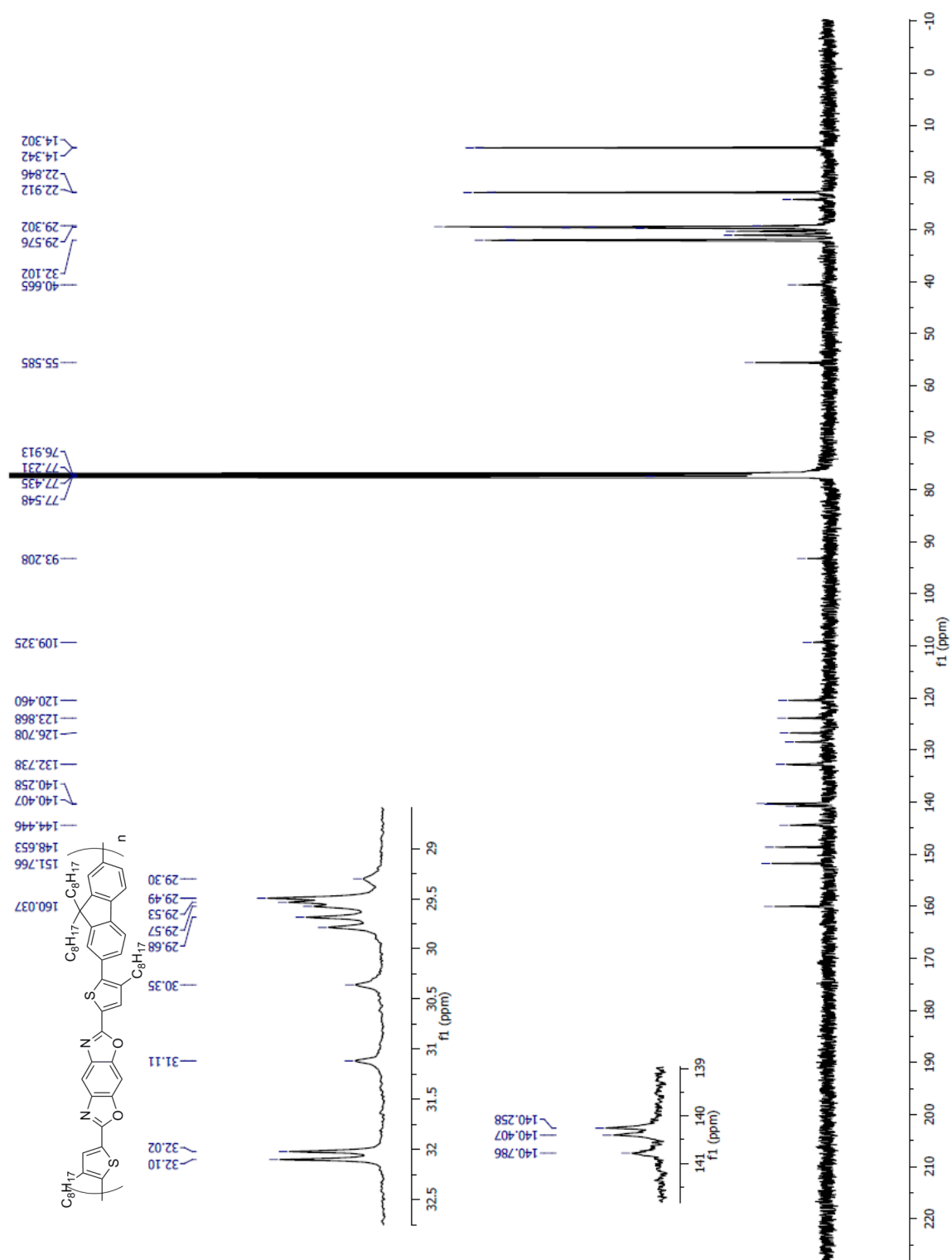


Figure S6 (cont.).

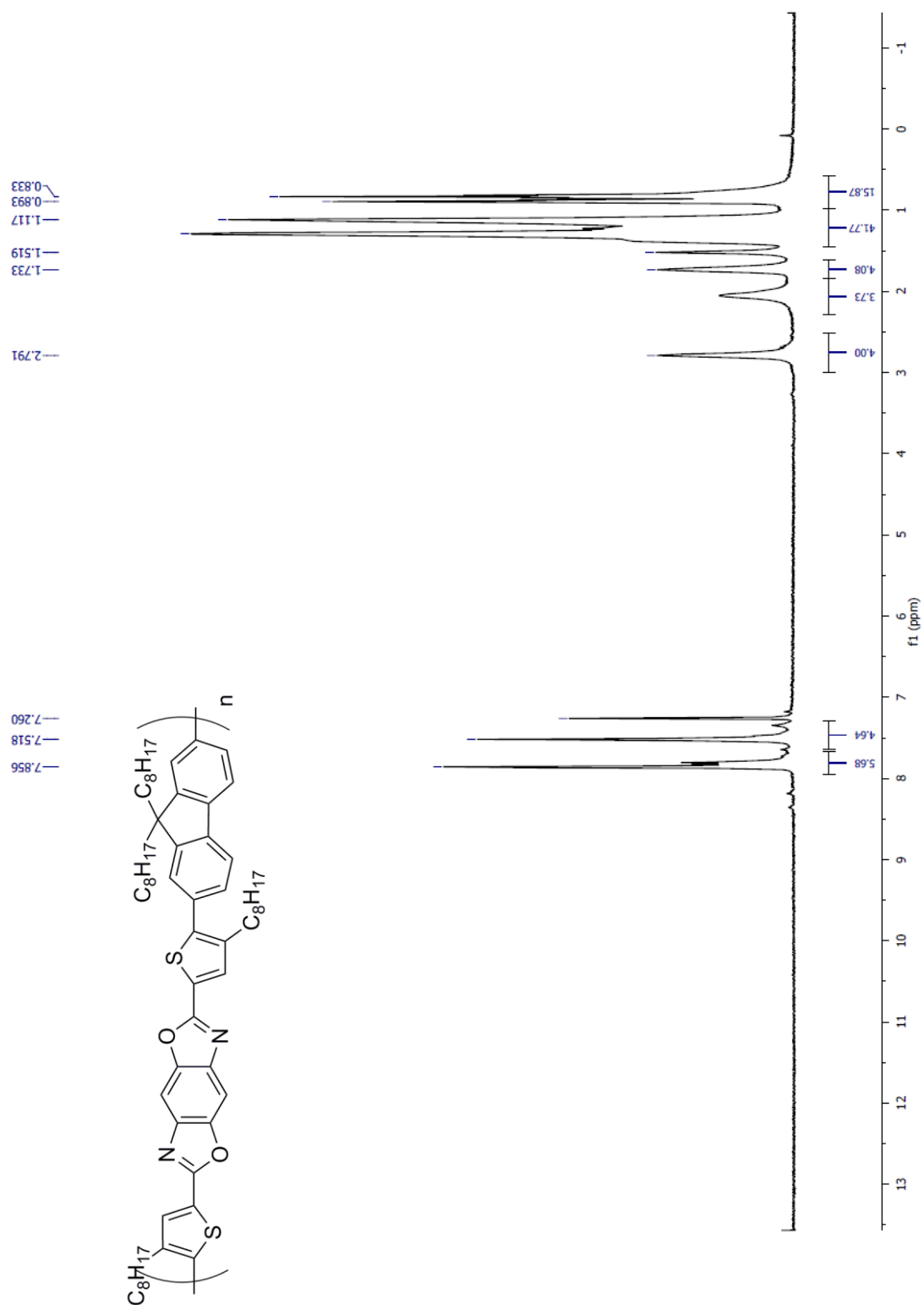


Figure S6 (cont.).

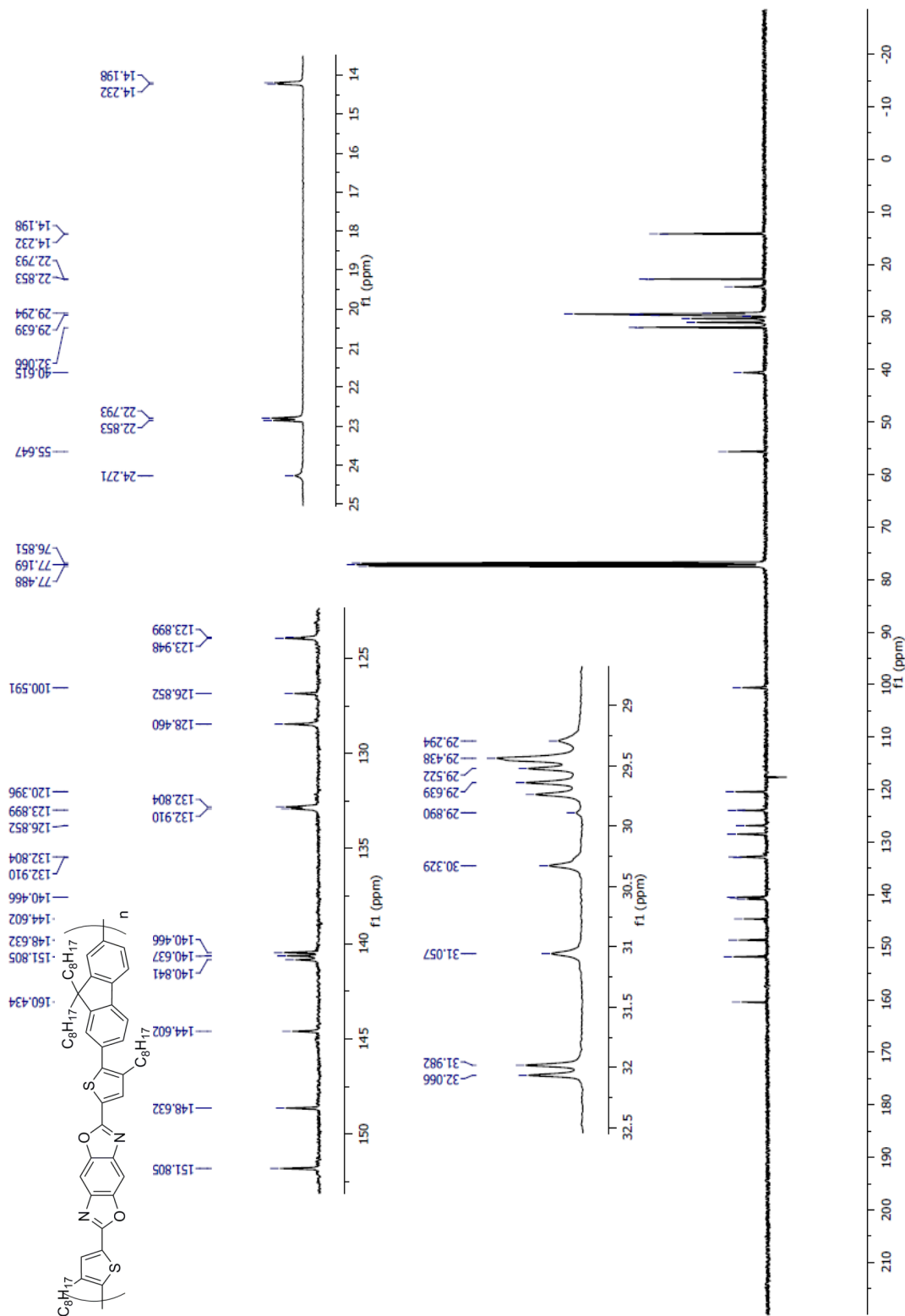


Figure S6 (cont.).

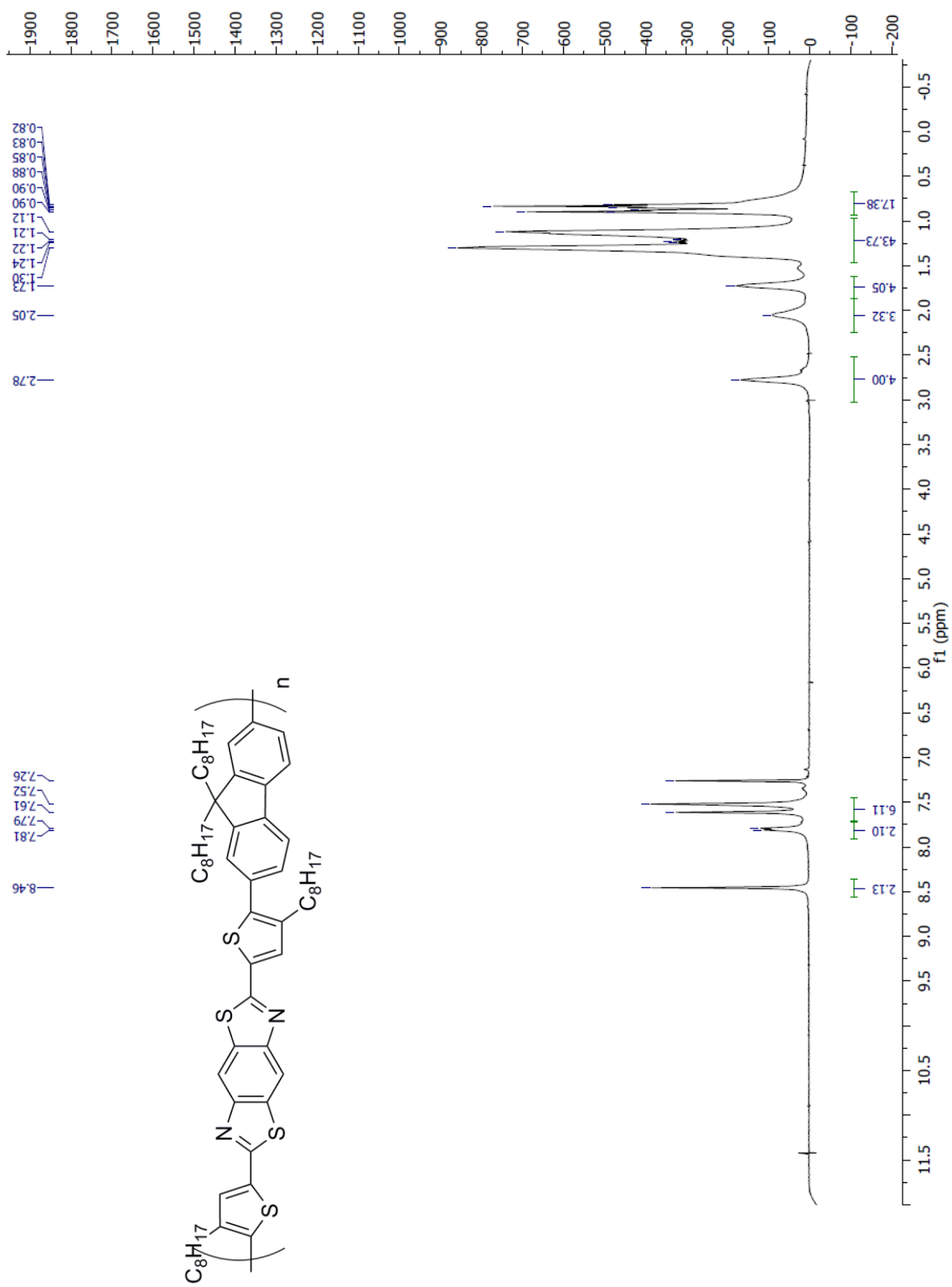
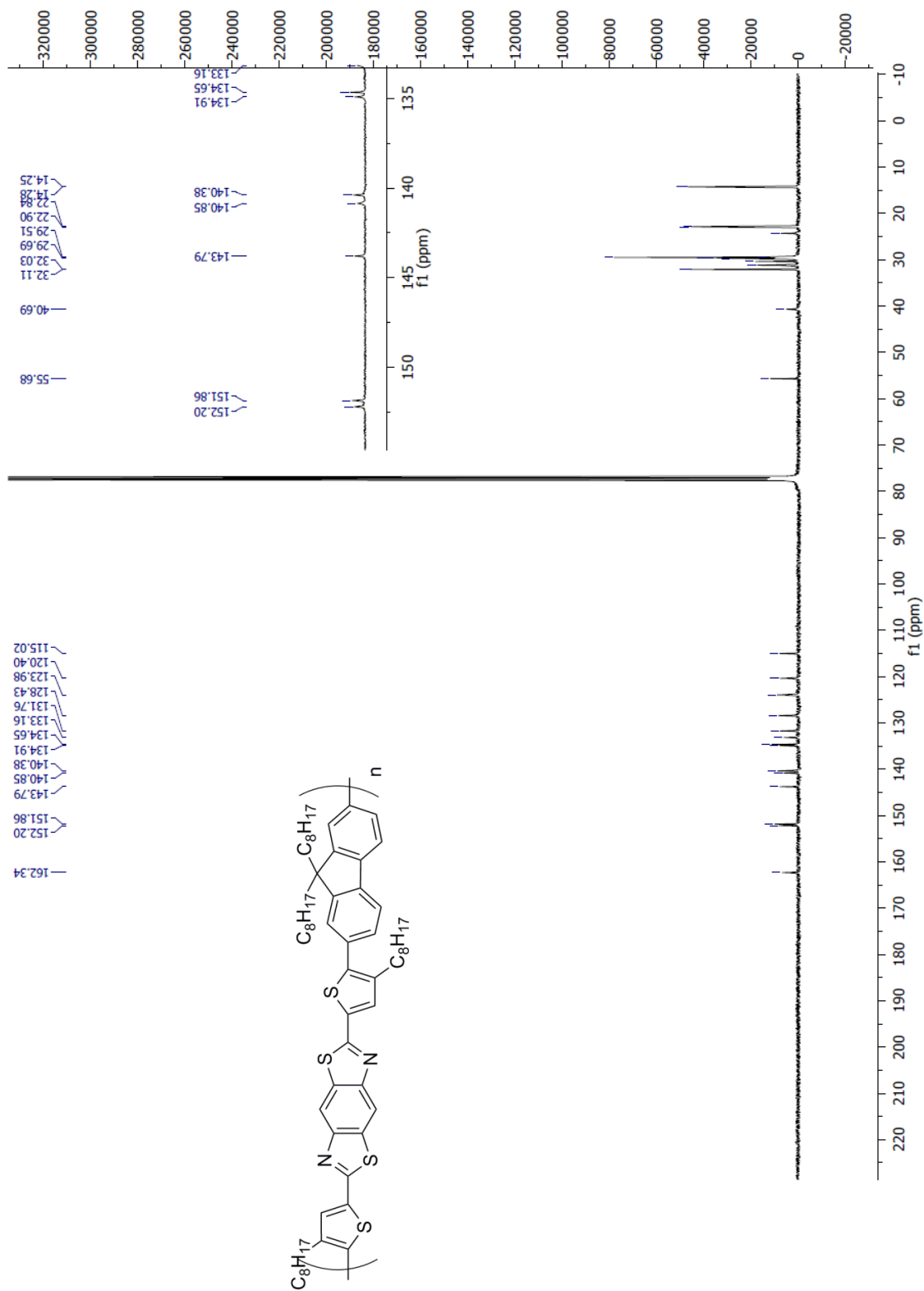


Figure S6 (cont.).



solar cells.^{9, 10} The active layer typically consists of a blend containing an electron-donating conjugated polymer and an electron accepting material, usually a soluble fullerene derivative such as PC₆₀BM or PC₇₀BM. By casting the two components together in a single layer, the distance an exciton must travel to reach a donor/acceptor junction is reduced considerably while still maintaining a thick absorbing layer.^{11, 12} Currently, one of the most effective strategies to produce useful donor polymers is the incorporation of alternating donor and acceptor moieties, resulting in a narrower bandgap and better harvest of the solar spectrum.¹³⁻¹⁵ These so-called donor acceptor (D-A) copolymers have led to vast improvements in device efficiencies over the past ten years.

Our group has been exploring benzo[1,2-*d*;5,4-*d'*] bisoxazole (*cis*-BBO), benzo[1,2-*d*;4,5-*d'*] bisoxazole (*trans*-BBO), and benzo[1,2-*d*;4,5-*d'*] bithiazole (*trans*-BBZT) units as part of polymers.¹⁶⁻¹⁸ Inspired by the work of Jenekhe,¹⁹ our group seeks to incorporate these units as the acceptor portion of D-A copolymers for OPVs. Electron deficient poly(benzobisazoles) (PBAs) are attractive options for use in organic electronics. Benzobisoxazole and benzobisthiazole polymers have excellent thermal stability, high electron affinity, and efficient electron transport.²⁰⁻²⁶ They are liquid crystalline in concentrated solution, and stack efficiently in the solid-state.²⁷⁻³¹ Unfortunately, PBAs are processed under harsh reaction conditions using strong acids and high temperatures. These conditions limit the functionality that can be included along the backbone of the polymer. Additionally, residual acid from casting can serve to unintentionally dope the resultant polymer.^{25, 28, 29, 32-38}

To circumvent this, we developed synthesis conditions for *cis*-BBO, *trans*-BBO, and *trans*-BBZT that use orthoesters in mild condensation reactions.^{39, 40} This has allowed us to fabricate functional building blocks for conjugated polymers in high yields. The inclusion of alkyl chains as part of these polymers allows for solubility in common laboratory solvents like THF, chloroform, or 1,2-dichlorobenzene. We have recently reported the synthesis of PBAs for use in OPVs and OLEDs.^{16, 17, 41} These, along with Jenekhe's report, represent the first examples of efficient devices constructed from organic soluble PBAs. Herein we report the synthesis of six new D-A copolymers incorporating *cis*BBO, *trans*BBO and BBZT acceptors as part of their main chain. We

seek an understanding of the differences among the three isomers as well as how changing the comonomer affects the optoelectronic and morphological characteristics of these materials.

We chose two heterocyclic bithiophenes as comonomers – dithienosilole (DTS) and dithienopyrrole (DTP). These monomers were chosen for several reasons, among them their fused-ring bithiophene structure (increasing conjugation), good performance records in devices, and solubilizing side chains.⁴²

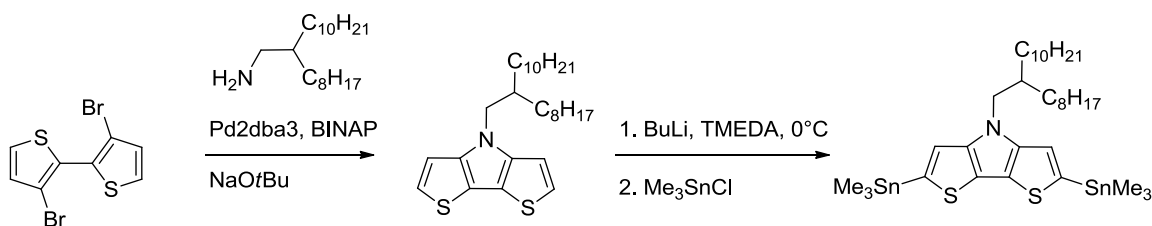
DTP is a particularly electron rich heterocycle^{43, 44} Therefore, its incorporation into conjugated polymers leads to high-lying HOMOs,⁴⁵⁻⁴⁷ which can reduce the open-circuit voltage (V_{oc}),⁴⁸⁻⁵¹ though this is not always the case.^{50, 52-54} However, DTP-containing polymers are known for their narrow bandgaps and high mobilities.^{45, 46, 55} McCullough et al. synthesized what they referred to as “transistor paint.”⁵⁶ They reported mobilities as high as $0.14 \text{ cm}^2 \text{ V}^{-1} \text{ s}^{-1}$. In addition to this, the polymers were air-stable, with device performance after 60 days being nearly indistinguishable from initial device performance. DTP has seen success in D-A copolymers as part of solar cells, as well, and we wish to add to the research into this heterocycle.^{48-50, 53, 54}

DTS is a versatile heterocyclic bithiophene that has exhibited desirable electronic properties in its polymers, including ambipolar transport capabilities and oxidative stability.⁵⁷⁻⁶⁰ Although the silicon is σ -bonded to the bithiophene, its σ^* -orbital is able to interact with the π^* -orbital of the bithiophene, giving a conjugated, planar system.⁶¹⁻⁶³ DTS has a lower-lying LUMO and HOMO in respect to other heterocyclic bithiophenes, along with a decreased bandgap.^{64, 65} This makes it an ideal donor unit in D-A copolymers. The low-lying energy levels and decreased bandgap are able to produce polymers with high V_{oc} 's and excellent solar spectrum overlap.^{53, 66-71} Of particular note is the 7.3% power conversion efficiency reported by Chu et al. for an OPV based on a DTS/thienopyrrole-4,6-dione copolymer.⁶⁶ Part of the reason for the excellent performance of DTS solar cells has been attributed to the long C-Si bonds, which move the alkyl chains away from the ring system, and allowing for ordered stacking.^{67, 72} Reynolds et al. successfully expanded upon this idea to create dithienogermole units for OPVs.⁶⁷

7.3 RESULTS AND DISCUSSION

7.3.1 Synthesis and Physical Properties

The DTP comonomer was synthesized according to Scheme 1, using the procedure developed by Samyn and co-workers, starting from 3,3'-dibromo-2,2'-bithiophene.⁷³ Making the Stille reagent by deprotonating unsubstituted DTP using *t*BuLi at -78°C proved to be particularly difficult, giving widely varying yields and producing impure product. This is attributed to the instability and insolubility of the dianion, especially at cold temperatures.⁴⁴ However, Rasmussen et al. recently reported a new synthesis of a DTP bisstannane using a mixture of TMEDA and *n*BuLi at 0°C .⁷⁴ It is thought that the warmer temperatures aid in the deprotonation, while the TMEDA helps to keep the dianion solubilized through favorable interactions with the lithiated DTP. This procedure consistently produced the DTP Stille reagent in high yields.



Scheme 1. Synthesis of DTP comonomer.

The DTS Stille reagent can also be synthesized starting from 3,3'-dibromo-2,2'-bithiophene.^{60, 75, 76} However, Yang's group reported inconsistencies in the yields using this procedure.⁷¹ Trusting his results, the synthesis of DTS was accomplished according to the method of Ohshita, whereby 3,3'-dibromo-5,5'-trimethylsilyl-2,2'-bithiophene is used as the starting material.^{63, 76} The full synthesis for this compound was adapted from literature and can be found elsewhere.^{71, 77, 78}

material, suggesting that given proper conditions, they may be able to reach higher molecular weights. It should be noted that synthesis conditions for **PS1-3** took only 16 hrs to produce polymer as compared to 4 days for the **PN1-3**. However, when **PN1** was synthesized according to the same conditions as **PS1-3**, it yielded the same results as the original conditions. No further exploration of synthesis was conducted for these polymers.

Thermal stability and phase transitions were measured with thermal gravimetric analysis (TGA) and differential scanning calorimetry (DSC), respectively. The polymers all exhibit thermal stability up to 300°C and above. However, not all of the polymers possessed observable glass transition and/or melting temperatures. The polymers dissolved readily in 1,2-dichlorobenzene (DCB), chloroform, and THF. NMRs of the polymers matched well with the structures and can be found in the supporting information.

Polymer	M_w^a	M_w/M_n	T_d (°C) ^b	T_g/ T_m (°C)
PN1	8319	1.34	333	217
PN2	7969	1.44	331	N/A
PN3	7216	1.21	299	N/A
PS1	23997	2.23		211
PS2	36146	2.95	326	103
PS3	24605	2.74	309	112

^a Molecular weights and polydispersity indexes determined by GPC versus polystyrene standards using THF as the eluent. ^b Temperature at which 5% weight loss is observed by TGA under N₂ with a heating rate of 20 °C/min.

Table 1. Molecular weights and thermal properties of PP1-3 and PS-1.

7.3.2 Optical Properties

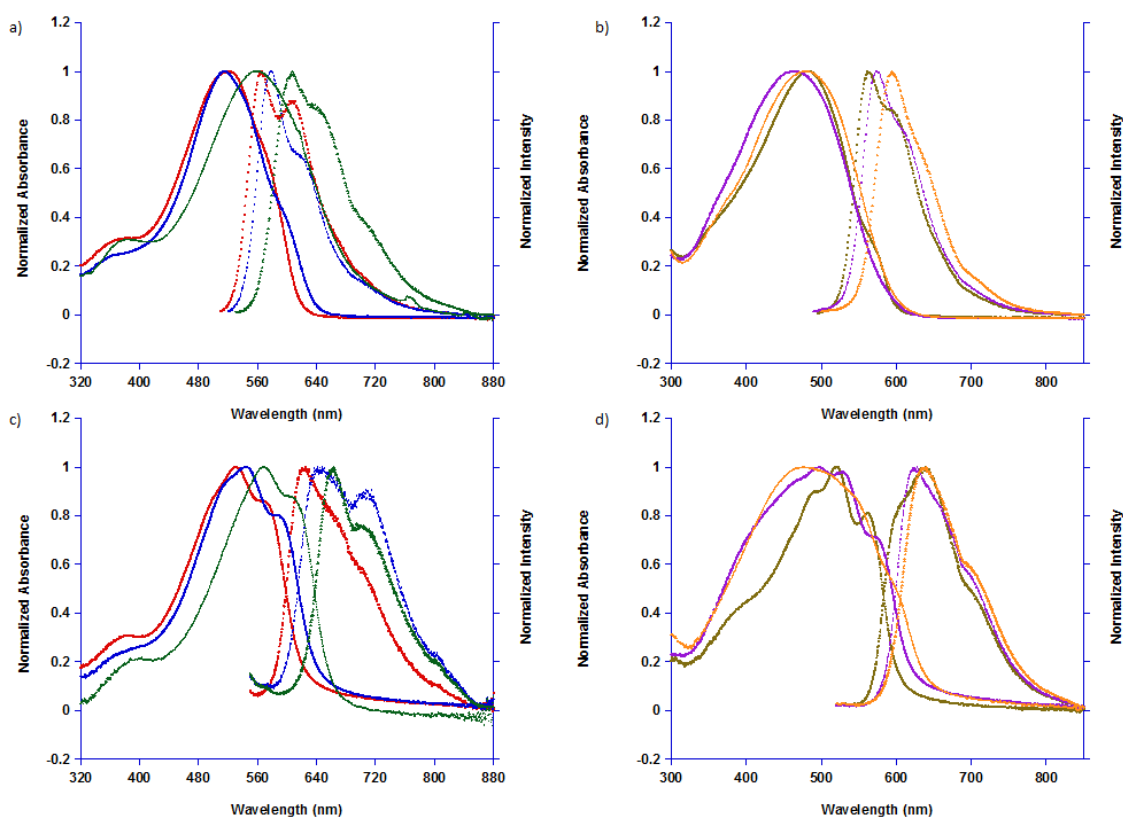


Figure 1. UV/Vis (solid lines) and Fluorescence (dotted lines) data for **PN1**, **PN2**, **PN3**, **PS1**, **PS2** and **PS3** in solution (a and b) and as thin films (c and d)

The optical properties of the polymers were measured using UV/Vis absorbance spectroscopy and fluorescence spectroscopy in both solution and solid state (Figure 1). The relevant data is reported in Table 2. In general, the DTP polymers were more redshifted in both absorbance and fluorescence than the corresponding DTS polymers. This is due to the stronger donor ability and lower ionization potential that DTP contributes to the polymer systems. Consequently, **PN1-3** also have lower bandgaps than **PS1-3**.

In order to calculate the bandgaps of these materials, the intersection of the UV-Vis with the fluorescence spectrum in the solid state was used in lieu of the absorption onset. We feel that the lack of a standard method for obtaining the so-called onset can produce misleading results. The intersection makes a good standard as it represents the 0-0 transition from the lowest vibronic ground state to the first excited state and is an energy

transition shared by both the fluorescence and absorbance for any molecule or polymer.⁸⁰ The optical bandgaps become smaller as one goes from *cis*-BBO to *trans*-BBO to *trans*-BBZT for each DTX comonomer. This is a trend that we have noticed in all of our previous work.^{16-18, 39, 40} However, the $\lambda_{\max}^{\text{abs}}$ for PN1 and PS1 (*cis*-BBO) does not follow this trend as it has in our previous work. This value should intuitively be the bluest, and indeed, the $\lambda_{\max}^{\text{em}}$ for the polymers follow this trend. The solutions for absorbance measurements were dilute solutions that were sonicated and filtered to prevent aggregation. Therefore, the reason for the red-shift in the bulk of the absorbance of the *cis* isomers most likely has something to do with the symmetry of *cis*-BBO and/or the presence of strong donor groups. More research is needed to determine the precise cause.

Polymer	Solution		Film		E_g^{opt} (eV) ^a	$E_{\text{onset}}^{\text{ox}}$ (eV) ^b	$E_{\text{onset}}^{\text{red}}$ (eV) ^b	HOMO (eV) ^c	LUMO (eV) ^d	E_g^{elec} (eV) ^e
	$\lambda_{\max}^{\text{abs}}$ (nm)	$\lambda_{\max}^{\text{em}}$ (nm)	$\lambda_{\max}^{\text{abs}}$ (nm)	$\lambda_{\max}^{\text{em}}$ (nm)						
PN1	521	566	531	625	2.07	0.2	-1.9	-5.0	-2.9	2.1
PN2	514	579	545	645	2.02	0.1	-1.9	-4.9	-2.9	2.0
PN3	544	607	567	663	1.94	0.1	-1.8	-4.9	-3.0	1.9
PS1	483	562	521	640	2.12	0.4	-1.9	-5.2	-2.9	2.3
PS2	463	575	497	628	2.07	0.3	-1.8	-5.1	-3.0	2.1
PS3	479	594	476	640	2.05	0.4	-1.7	-5.2	-3.1	2.1

^a Estimated from the optical absorption edge. ^b Onset of potentials (vs Fc). ^c HOMO = $-(E_{\text{onset}}^{\text{ox}} + 4.8)$ (eV). ^d LUMO = $-(E_{\text{onset}}^{\text{red}} + 4.8)$ (eV). ^e $E_g^{\text{elec}} = \text{LUMO-HOMO}$

Table 2. Electronic and Optical Properties of DA poly(arylenebenzobisazoles).

In the solid state, both the absorbance and fluorescence spectra are redshifted and slightly broadened relative to the solution phase. The appearance of a shoulder on the red side of the absorbance spectrum is noticeable for **PN1-3**. For **PS2** and **PS3**, the absorbance spectra are significantly broadened. **PS1**, however, develops more defined peak shapes. The fluorescence spectra of the polymers are characterized by a main peak and a shoulder in both solution and film with broadening similar to what is seen with the absorbance. This is most likely caused by increased interchain interactions and π -stacking in the solid state.⁸¹

PN1-3 showed significantly weaker fluorescence than **PS1-3**. This suggests that

interchain interactions are stronger in the DTP polymers relative to the DTS polymers. One reason for this could be because the alkyl chains on DTS are orthogonal to the plane of the polymer, similar to what is found in poly(fluorene).^{72, 82, 83} Another interesting feature is the large red shift in the film fluorescence versus the solution fluorescence associated with **PS1** (80 nm vs. 45-60nm for the other polymers). The extra features found in **PS1**'s absorbance and fluorescence spectra in the film warrant further investigation by solid state characterization methods such as X-ray, TEM, or AFM.

7.3.3 Electronic Properties

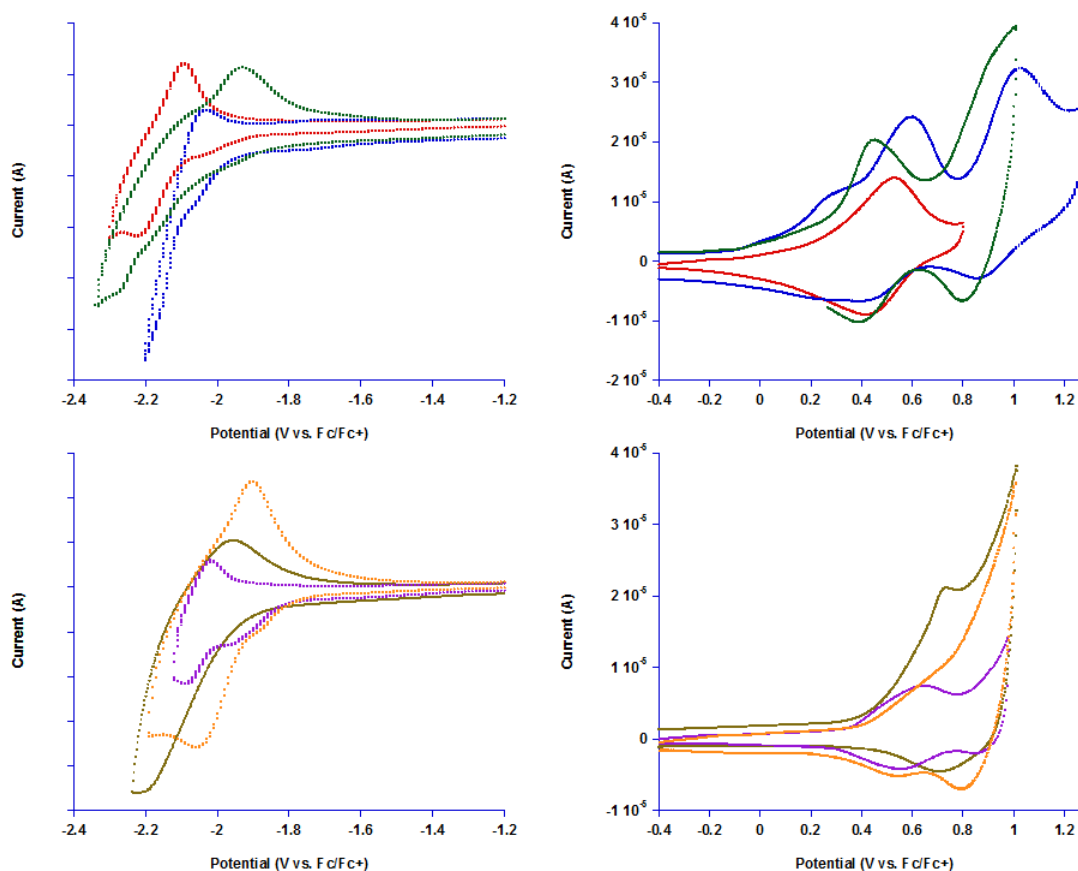


Figure 2. Reduction (left) and oxidation (right) cyclic voltammograms for **PN1**, **PN2**, **PN3**, **PS1**, **PS2** and **PS3**.

The electronic energy levels of the polymer were estimated using cyclic voltammetry (CV) with ferrocene as an internal standard (Figure 2). All of the waves show some level

of reversibility, though none appear to be fully reversible. The HOMO and LUMO levels were calculated using the onsets obtained from the oxidation and reduction waves, respectively (Table 2). The electrochemical bandgaps calculated from these waves match well with the optical bandgaps.

Recent reports on the accuracy of HOMO and LUMO values obtained from CV suggest the ferrocene couple is approximately -5.1 eV relative to vacuum.^{67, 84} However, the value of -4.8 eV is commonly used. In an earlier study, we compared values obtained by ultraviolet photoelectron spectroscopy (UPS), an absolute measurement, with those obtained by CV.⁴¹ Judging from the results, it appears that -4.8 eV was a more accurate determining value than -5.1 eV for unknown reasons. Since we obtained better results using -4.8 eV, the values reported herein are calculated using that value.

From the electronic measurements obtained from CVs, one can see that the values of the LUMO decrease in going from *cis*-BBO to *trans*-BBO to *trans*-BBZT. The LUMO levels for all the polymers are approximately -3 eV relative to vacuum with the LUMOs from **PS1-3** being slightly lower than **PN1-3**. This is consistent with DTS being a better acceptor than DTP.^{57, 61} The LUMO values are determined by the benzobisazole unit and these values are consistent with those obtained in our other published work. The HOMO level, however, is then determined by the donor DTS or DTP, with DTP polymers having higher HOMO levels, in general. The reason for the reduced bandgaps in **PN1-3** is therefore due primarily to higher HOMO levels.

From these results, and from previous reports, benzobisazoles appear to only have weak acceptor properties. The bandgaps and LUMO levels (even when adjusted for differences in CV calibration methods) attained in other D-A conjugated polymers are much lower than those we have obtained.^{41, 49, 53, 59, 68} Unfortunately, this moves the LUMO away from the common OPV acceptor fullerenes (PC₆₀BM or PC₇₀BM). However, with high LUMO levels and good donor properties, there is promise for the use of these polymers in conjunction with narrow bandgap, low LUMO D-A polymers in all polymer solar cells.⁵⁴

7.3.4 Organic Photovoltaic Devices

We evaluated our polymers as absorbers and donor materials in OPV devices under

illumination of 100 mW/cm². The results are summarized in Table 3. PC₇₀BM has recently become a popular acceptor owing to its ability to increase charge photogeneration by absorbing a portion of the blue part of the spectrum.⁸⁵ This effect does not, however, serve to improve the performance of the polymer in a solar cell. Since the polymers reported herein, specifically **PS1-3**, absorb in the blue region of the spectrum, unlike many donor materials (*e.g.* P3HT), PC₆₀BM was used in the blends.

Polymer	J _{sc} (mA/cm ²)	V _{oc} (V)	FF%	PCE%
PN1	1.54	0.54	20	0.17
PN2	1.81	0.52	25	0.24
PS1	3.01	0.66	31	0.63
PS2	1.73	0.73	26	0.33
PS3	0.21	0.65	24	0.03

Table 3. Photovoltaic data for the polymers.

The polymers exhibited mediocre performances with **PS1** giving the best PCE. However, these efficiencies are improved relative to our work using poly(thiophenevinylene-alt-benzobisoxazoles). This may, in part, be due to the delocalization of both HOMO and LUMO levels (see Figure S6), a feature that was not present in the polymers from earlier research.¹⁶ Interestingly, the worst performers were the *trans*-BBZT polymers, with **PN3** producing no observable photocurrent. When a -1.0 V bias voltage was applied to operating devices, the external quantum efficiency was improved considerably, especially in the devices made with DTP containing polymers (see Figure S3). This suggests that excitons are becoming trapped and not dissociating at the D-A interface.

We theorize that insufficient blending of the donor and acceptor phases is partly responsible for the poor performances of these polymers. The placement of side chains on the thiophene units that face outwards towards the donor (Scheme 2) as opposed to inwards toward the benzobisazole¹⁹ may be having a negative impact on nanoscale morphology and electronics, especially blended systems.⁸⁶⁻⁸⁸ Benzobisazole units are

very efficient at stacking with each other,^{17, 81, 89} and the high electron-poor nitrogen content may make interaction with the acceptor phase unfavorable. Facing side chains inwards toward the benzobisazole may help to alleviate these problems.

7.4 CONCLUSIONS

In conclusion, six new, organic soluble polymers based on benzobisoxazole and benzobisthiazole have been synthesized and tested as donor materials in OPV devices. Even though the polymers exhibited only modest performance in solar cells, the positioning and branching of side chains may be modified to potentially improve the photovoltaic device performance of these polymers. The high LUMO levels, while still maintaining good electrochemical reversibility, indicate benzobisazole polymers may be suitable for all polymer solar cells. In addition, solvent additives or device structure may be altered to improve performance. These polymers prove that benzobisazole polymers are promising for OPVs, but that more research needs to be done in both synthesis and device construction.

7.5 ACKNOWLEDGEMENT

We thank Ms. Dana Drochner and Ms. Achala Bhuwalka for aiding with thermal analysis. We thank Aimée L. Tomlinson from North Georgia College and State University for theoretical calculations. The device fabrication and characterization was performed at the Iowa State University Microelectronics Research Center. This work was funded by the National Science Foundation (DMR-0846607), and the 3M foundation.

7.6 EXPERIMENTAL

2,6-bis(2-bromo-3-octyl-thiophene-5-yl) benzobis[1,2-*d*:5,4-*d'*]bisoxazole, 2,6-bis(2-bromo-3-dodecyl-thiophene-5-yl)benzo[1,2-*d*:4,5-*d'*]bisoxazole and 2,6-bis(2-bromo-3-dodecyl-thiophene-5-yl)benzo[1,2-*d*:4,5-*d'*]bisthiazole were synthesized according to previously published results. 3,3'-dibromo-5,5'-trimethylsilyl-2,2'-bithiophene,⁷¹ and 3,3'-dibromo-2,2'-bithiophene⁹⁰ were synthesized according to literature procedures, starting from commercially available 2-bromothiophene. The synthesis of 2,6-dibromo-4,4'-dioctyl-4H-silolo[3,2-*b*:4,5-*b'*]dithiophene was adapted from Yang et al.,^{71, 78} while

the synthesis of 4,4-dioctyl-2,6-bis(trimethylstannyl)-4H-silolo[3,2-*b*:4,5-*b'*]dithiophene was synthesized from the previous compound according to Beaujuge et al.⁵⁹ Tetrahydrofuran and toluene were dried using an Innovative Technologies solvent purification system. All other compounds were purchased from commercial sources and used without further purification. Nuclear magnetic resonance spectra were obtained on a 400 MHz spectrometer. All samples were referenced internally to the residual protonated solvent. Gel permeation chromatography (GPC) measurements were performed on a Viscotek GPC Max 280 separation module equipped with four 5 μ m I-gel columns connected in series (guard, 10,000 Å, 1,000 Å and 100 Å), a refractive index detector and a UV-Vis detector. Analyses were performed at 35 °C using THF as the eluent with the flow rate at 1.0 mL/min. Calibration was based on polystyrene standards. Fluorescence spectroscopy and UV-Visible spectroscopy were performed using dilute polymer solutions in chloroform, and thin films were spun from DCB after being filtered through Whatman GTX 0.2 μ m filters. All of the polymers were excited at their respective emission maxima. Thermal gravimetric analysis measurements were performed within the temperature interval of 30 °C - 850 °C, using a heating rate of 20 °C/minute under ambient atmosphere. Differential scanning calorimetry was performed with a first scan at a heating rate of 15 °C/min to erase thermal history and a second scan to measure transitions from 0 °C to 275 °C under nitrogen. Transitions were also measured with cooling at 15 °C/min. Cyclic voltammograms were performed in 0.1 M tetrabutylammonium hexafluorophosphate using 0.01 M AgNO₃ in acetonitrile as the reference electrode with a platinum wire counter electrode. The potential values obtained versus the Ag⁺ were converted to the ferrocene (Fc) reference using an internal standard. The measurements were performed on polymer films drop cast onto 1 mm platinum button electrodes.

N-(2-octyldodecyl)-phthalimide. Triphenylphosphine (7.87 g, 30.0 mmol), phthalimide (4.41 g, 30.0 mmol), and 2-octyldodecanol (8.84 g, 30.0 mmol) were dissolved in 30 mL dry diethyl ether and cooled in an ice bath. Diisopropylazodicarboxylate (6.07 g (95%), 30.0 mmol, dissolved in 15 mL dry diethyl

ether) was then added dropwise. After the addition was complete, the ice bath was removed and the reaction was stirred at room temperature overnight. The precipitates were filtered, the solvent was removed by rotary evaporation, and the product was purified by column chromatography using 4:1 hexanes to diethyl ether as eluent to yield pure product (10.11 g, 80%). ^1H NMR (400 MHz, CDCl_3) δ 7.82 (m, 2H), 7.69 (m, 2H), 3.56 (d, $J=7.2$ Hz, 2H), 1.86 (b, 1H), 1.25 (b, 32H), 0.86 (m, 6H). ^{13}C NMR (100 MHz, CDCl_3) δ 168.86, 133.96, 132.32, 123.31, 42.49, 37.20, 32.11, 32.08, 31.67, 30.15, 29.82, 29.79, 29.74, 29.53, 29.48, 26.48, 22.88, 22.86, 14.31, 14.30.

2-octyldodecylamine. N-(2-octyldodecyl)-phthalimide (10.11 g, 23.6 mmol) was dissolved in 50 mL of absolute ethanol. To this was added hydrazine (55% in water, 4.0 mL, 71 mmol) and the mixture was heated to reflux overnight. Hydrochloric acid was then added (6M, 70 mL), followed by 20 mL ethanol, and the reaction was refluxed for an additional 2 hours. The reaction was cooled, the precipitates were filtered, and the solvent was removed under vacuum to yield pure 2-octyldodecylamine (6.06 g, 86%). ^1H NMR (400 MHz, CDCl_3) δ 2.56 (d, 2H), 1.36 (b, 1H), 1.23 (b, 33H), 0.85 (m, 6H). ^{13}C NMR (100 MHz, CDCl_3) δ 45.33, 40.96, 32.10, 32.09, 31.70, 30.28, 29.86, 29.82, 29.53, 26.95, 22.86, 14.27.

N-(2-octyldodecyl)dithieno[3,2-b:2',3'-d]pyrrole. 3,3'-dibromo-2,2'-bithiophene (1.62 g, 5.00 mmol) was dissolved in 10 mL toluene and purged with argon for 20 minutes. To this solution was added bis(palladium) tris(benzylidene)acetone (0.13g, .15 mmol), BINAP (0.31 g, .50 mmol) and sodium t-butoxide (1.15 g, 12.0 mmol). The solution was further purged with argon for another 10 minutes and heated to 35°C before adding 2-octyldodecylamine (1.49 g, 5.00 mmol) in one portion. The reaction mix was refluxed for 16 hours (monitored by TLC for disappearance of the bithiophene). The reaction was cooled, water (~15mL) was added, and the mixture extracted with 2x100 mL diethyl ether. The ether layers are combined and washed with brine and dried over anhydrous sodium sulfate. Solvent is removed under vacuum and the crude product is purified by column chromatography using 9:1 hexane: methylene chloride to yield 1.97 g

(2.35 mmol) of N-(2-decyltetradecyl)dithieno[3,2-b:2',3'-d]pyrrole (86%). ^1H NMR (400 MHz, CDCl_3) δ 7.12 (d, $J=5.2$ Hz, 2H), 6.98 (d, $J=5.3$ Hz, 2H), 4.05 (d, 2H), 2.01 (b, 1H), 1.27 (b, 32H), 0.90 (m, 6H). ^{13}C NMR (100 MHz, CDCl_3) δ 145.49, 122.85, 114.73, 111.28, 51.92, 39.26, 32.14, 32.09, 31.80, 30.09, 29.83, 29.82, 29.77, 29.72, 29.56, 29.48, 26.64, 22.92, 22.89, 14.36, 14.35.

N-(2-octyldodecyl)-2,6-bis(trimethylstannyl)dithieno[3,2-b:2',3'-d]pyrrole. In a typical procedure, N-(2-octyldodecyl)dithieno[3,2-b:2',3'-d]pyrrole (0.63 g, 0.75 mmol) was dissolved in 40 mL dry hexane. The solution was cooled to 0°C in an ice bath and to it was added TMEDA (0.261g, .225 mmol). After 5 mins of stirring, *n*BuLi (2.5 M in hexane, 0.90 mL, 2.25 mmol) was added dropwise and stirred for 2 hours before adding trimethyltin chloride (1.0 M in THF, 2.25 mL, 2.25 mmol) in one portion. The solution was stirred overnight before washing with water and brine and extracting with additional hexanes. The hexane layer was dried over sodium sulfate before evaporating the solvent to yield light brown syrupy liquid as the product (0.52 g, 88%). ^1H NMR (400 MHz, CDCl_3) δ 6.96 (s, 2H), 4.04 (d, 2H), 2.01 (b, 1H), 1.24 (b, 32H), 0.88 (m, 6H), 0.40 (s, 18H). ^{13}C NMR (100 MHz, CDCl_3) δ 148.49, 135.68, 120.32, 118.26, 51.74, 39.15, 32.14, 31.65, 30.20, 29.92, 29.89, 29.83, 29.58, 26.53, 22.92, 22.90, 14.35, -7.91.

PN1. N-(2-octyldodecyl)-2,6-bis(trimethylstannyl)dithieno[3,2-b:2',3'-d]pyrrole (0.52 g, 0.66 mmol) and **1** (0.47 mg, 0.66 mmol), bispalladium trisbenzylideneacetone (12 mg, .013 mmol, 2% catalyst) and tri(*o*-tolyl)phosphine (16 mg, .051 mmol, 8% ligand) were dissolved in 12 mL dry, deoxygenated toluene. The solution was purged with argon gas for 10 more minutes before heating to 95°C . After 4 days, the reaction was cooled to room temperature and poured into methanol with 5% conc. HCl. The resultant precipitate was purified by Soxhlet extraction using methanol, acetone and hexanes. Finally, chloroform was used to extract the highest molecular weight material. The solvent was removed to yield PN1 as a black, lustrous solid (0.58 g, 87%). ^1H -NMR (400 MHz, CDCl_3): δ 7.65-6.68 (b, 6H), 3.93 (b, 2H), 2.76 (b, 4H), 1.25 (bm, 69H).

PN2. This was prepared in the same manner as **PN1**, using 0.64 mmol of starting

material to yield a plastic-like solid (0.43 g, 67%). $^1\text{H-NMR}$ (400 MHz, CDCl_3): δ 7.70-6.67 (b, 6H), 3.98 (b, 2H), 2.74 (b, 4H), 1.25 (bm, 69H).

PN3. This was prepared in the same manner as **PN1**, using 0.40 mmol of starting material to yield lustrous solid (0.20 g, 49%). $^1\text{H-NMR}$ (400 MHz, CDCl_3): δ

PS1. 4,4-dioctyl-2,6-bis(trimethylstannyl)-4H-silolo[3,2-*b*:4,5-*b'*]dithiophene (0.52 g, 0.70 mmol) and **1** (0.47g, 0.67 mmol) were dissolved in 12 mL dry, deoxygenated toluene. The solution was purged for 20 minutes with argon before adding palladium tetrakis(triphenyl)phosphine (19 mg, .016 mmol). After the addition, the solution was purged for an additional 20 minutes with argon then heated to reflux and stirred overnight (16 hours). The reaction was cooled and precipitated into methanol. The solid was subjected to Soxhlet extraction using methanol, acetone and hexane. Finally, the highest soluble molecular weight fraction was removed by chloroform. The chloroform was removed to yield a red, plastic solid (0.21 g, 33%). $^1\text{H-NMR}$ (400 MHz, CDCl_3): δ 7.92-7.19 (b, 6H), 2.81 (b, 4H), 1.30 (b, 64H).

PS2. Prepared in the same manner as PS1 to yield a red solid (0.26 g, 40%) $^1\text{H-NMR}$ (400 MHz, CDCl_3): δ 7.77-7.20 (b, 6H), 2.86 (b, 4H), 1.27 (bm, 64H).

PS3. Prepared in the same manner as PS1 to yield a black-red solid (0.24 g, 38%). $^1\text{H-NMR}$ (400 MHz, CDCl_3): δ 8.36 (b, 2H), 7.48-7.21(b, 4H), 2.79 (b, 4H), 1.32 (bm, 64H).

7.7 REFERENCES

- (1) Liang, Y.; Xu, Z.; Xia, J.; Tsai, S.-T.; Wu, Y.; Li, G.; Ray, C.; Yu, L. *Advanced Materials*, **2010**, 22(20), E135-E138.
- (2) Shaheen, S.E.; Ginley, D.S.; Jabbour, G.E. *MRS Bulletin*, **2005**, 30(1), 10-19.
- (3) Facchetti, A. *Chemistry of Materials*, **2010**, 23(3), 733-758.
- (4) Hains, A.W.; Liang, Z.; Woodhouse, M.A.; Gregg, B.A. *Chemical Reviews*, **2010**, 110(11), 6689-6735.
- (5) Cheng, Y.-J.; Yang, S.-H.; Hsu, C.-S. *Chemical Reviews*, **2009**, 109(11), 5868-5923.

- (6) Günes, S.; Neugebauer, H.; Sariciftci, N.S. *Chemical Reviews*, **2007**, *107*(4), 1324-1338.
- (7) Krebs, F.C. *Sol. Energ. Mat. Sol. Cells*, **2009**, *93*(4), 394-412.
- (8) Pron, A.; Rannou, P. *Progress in Polymer Science*, **2001**, *27*(1), 135-190.
- (9) Roncali, J. *Chemical Society Reviews*, **2005**, *34*(6), 483-495.
- (10) Thompson, B.C.; Frechet, J.M.J. *Angewandte Chemie International Edition*, **2008**, *47*(1), 58-77.
- (11) Yang, X.; Loos, J.; Veenstra, S.C.; Verhees, W.J.H.; Wienk, M.M.; Kroon, J.M.; Michels, M.A.J.; Janssen, R.A.J. *Nano Letters*, **2005**, *5*(4), 579-583.
- (12) Hoppe, H.; Niggemann, M.; Winder, C.; Kraut, J.; Hiesgen, R.; Hinsch, A.; Meissner, D.; Sariciftci, N.S. *Advanced Functional Materials*, **2004**, *14*(10), 1005-1011.
- (13) Colladet, K.; Fourier, S.; Cleij, T.J.; Lutsen, L.; Gelan, J.; Vanderzande, D.; Huong Nguyen, L.; Neugebauer, H.; Sariciftci, S.; Aguirre, A.; Janssen, G.; Goovaerts, E. *Macromolecules*, **2006**, *40*(1), 65-72.
- (14) Guo, X.; Xin, H.; Kim, F.S.; Liyanage, A.D.T.; Jenekhe, S.A.; Watson, M.D. *Macromolecules*, **2010**, *44*(2), 269-277.
- (15) Chen, J.; Cao, Y. *Accounts of Chemical Research*, **2009**, *42*(11), 1709-1718.
- (16) Mike, J.F.; Nalwa, K.; Makowski, A.J.; Putnam, D.; Tomlinson, A.L.; Chaudhary, S.; Jeffries-El, M. *Physical Chemistry Chemical Physics*, **2011**, *13*(4), 1338-1344.
- (17) Intemann, J.J.; Mike, J.F.; Cai, M.; Bose, S.; Xiao, T.; Mauldin, T.C.; Rogers, R.A.; Shinar, J.; Shinar, R.; Jeffries-El, M. *Macromolecules*, **2010**, *44*(2), 248-255.
- (18) Mike, J.F.; Makowski, A.J.; Mauldin, T.C.; Jeffries-El, M. *Journal of Polymer Science Part A: Polymer Chemistry*, **2010**, *48*(6), 1456-1460.
- (19) Ahmed, E.; Kim, F.S.; Xin, H.; Jenekhe, S.A. *Macromolecules*, **2009**, *42*(22), 8615-8618.
- (20) Wolfe, J.F. *Polybenzothiazoles and Polybenzoxazoles*, in *Encyclopedia of Polymer Science and Engineering*; John Wiley and Sons: **1988**, New York, NY. p. 601-635.

- (21) Wolfe, J.F.; Arnold, F.E. *Macromolecules*, **1981**, *14*, 909-915.
- (22) Alam, M.M.; Jenekhe, S.A. *Chemistry of Materials*, **2002**, *14*(11), 4775-4780.
- (23) Jenekhe, S.A.; de Paor, L.R.; Chen, X.L.; Tarkka, R.M. *Chemistry of Materials*, **1996**, *8*(10), 2401-2404.
- (24) Wang, S.; Chen, Y.; Zhuang, Q.; Li, X.; Wu, P.; Han, Z. *Macromolecular Chemistry and Physics*, **2006**, *207*(24), 2336-2342.
- (25) Wang, S.; Lei, H.; Guo, P.; Wu, P.; Han, Z. *European Polymer Journal*, **2004**, *40*(6), 1163-1167.
- (26) Wang, S.; Guo, P.; Wu, P.; Han, Z. *Macromolecules*, **2004**, *37*(10), 3815-3822.
- (27) Wang, S.; Wu, P.; Han, Z. *Macromolecules*, **2003**, *36*(12), 4567-4576.
- (28) Hu, X.-D.; Jenkins, S.E.; Min, B.G.; Polk, M.B.; Kumar, S. *Macromolecular Materials and Engineering*, **2003**, *288*(11), 823-843.
- (29) Roitman, D.B.; Wessling, R.A.; McAlister, J. *Macromolecules*, **1993**, *26*, 5174-5184.
- (30) Dobrolyubova, E.I.; Drushlyak, A.G.; Ivashchenko, A.V. *Mol. Cryst. Liq. Cryst.*, **1990**, *191*, 219-21.
- (31) Krause, S.J.; Haddock, T.B.; Vezie, D.L.; Lenhert, P.G.; Hwang, W.F.; Price, G.E.; Helminiak, T.E.; O'Brien, J.F.; Adams, W.W. *Polymer*, **1988**, *29*(8), 1354-64.
- (32) Choe, E.W.; Kim, S.N. *Macromolecules*, **1981**, *14*, 920-924.
- (33) Wolfe, J.F. *Polymeric Materials Science and Engineering*, **1986**, *54*, 99-101.
- (34) Hunsaker, M.E.; Price, G.E.; Bai, S.J. *Polymer*, **1992**, *33*(10), 2128-35.
- (35) Promislow, J.H.; Preston, J.; Samulski, E.T. *Macromolecules*, **1993**, *26*(7), 1793-5.
- (36) Kricheldorf, H.R.; Domschke, A. *Polymer*, **1994**, *35*(1), 198-203.
- (37) Tan, L.-S.; Burkett, J.L.; Simko, S.R.; Alexander, M.D., Jr. *Macromolecular Rapid Communications*, **1999**, *20*(1), 16-20.
- (38) Liu, X.; Xu, X.; Zhuang, Q.; Han, Z. *Polymer Bulletin* **2008**, *60*(6), 765-774.
- (39) Mike, J.F.; Inteman, J.J.; Ellern, A.; Jeffries-El, M. *Journal of Organic*

Chemistry, **2010**, 75(2), 495-497.

(40) Mike, J.F.; Makowski, A.J.; Jeffries-EL, M. *Organic Letters*, **2008**, 10(21), 4915-4918.

(41) Mike, J.F.; Intemann, J.J.; Cai, M.; Xiao, T.; Shinar, R.; Shinar, J.; Jeffries-EL, M. *Polym. Chem.*, **2011**, DOI:10.1039/C1PY00218J.

(42) Liu, Y.; Liu, Y.; Zhan, X. *Macromolecular Chemistry and Physics*, **2011**, 212(5), 428-443.

(43) Kwon, O.; Barlow, S.; Odom, S.A.; Beverina, L.; Thompson, N.J.; Zojer, E.; Brédas, J.-L.; Marder, S.R. *The Journal of Physical Chemistry A*, **2005**, 109(41), 9346-9352.

(44) Radke, K.R.; Ogawa, K.; Rasmussen, S.C. *Organic Letters*, **2005**, 7(23), 5253-5256.

(45) Liu, J.; Zhang, R.; Sauve, G.; Kowalewski, T.; McCullough, R.D. *Journal of the American Chemical Society*, **2008**, 130(39), 13167-13176.

(46) Steckler, T.T.; Zhang, X.; Hwang, J.; Honeyager, R.; Ohira, S.; Zhang, X.-H.; Grant, A.; Ellinger, S.; Odom, S.A.; Sweat, D.; Tanner, D.B.; Rinzler, A.G.; Barlow, S.; Bredas, J.-L.; Kippelen, B.; Marder, S.R.; Reynolds, J.R. *Journal of the American Chemical Society*, **2009**, 131(8), 2824-2826.

(47) Zhang, W.; Li, J.; Zhang, B.; Qin, J. *Macromolecular Rapid Communications*, **2008**, 29(19), 1603-1608.

(48) Zhou, E.; Nakamura, M.; Nishizawa, T.; Zhang, Y.; Wei, Q.; Tajima, K.; Yang, C.; Hashimoto, K. *Macromolecules*, **2008**, 41(22), 8302-8305.

(49) Yue, W.; Zhao, Y.; Shao, S.; Tian, H.; Xie, Z.; Geng, Y.; Wang, F. *Journal of Materials Chemistry*, **2009**, 19(15), 2199-2206.

(50) Zhang, X.; Shim, J.W.; Tiwari, S.P.; Zhang, Q.; Norton, J.E.; Wu, P.-T.; Barlow, S.; Jenekhe, S.A.; Kippelen, B.; Bredas, J.-L.; Marder, S.R. *Journal of Materials Chemistry*, **2011**, 21(13), 4971-4982.

(51) Zhou, E.; Yamakawa, S.; Tajima, K.; Yang, C.; Hashimoto, K. *Chemistry of Materials*, **2009**, 21(17), 4055-4061.

(52) Mishra, S.P.; Palai, A.K.; Srivastava, R.; Kamalasanan, M.N.; Patri, M.

Journal of Polymer Science Part A: Polymer Chemistry, **2009**, 47(23), 6514-6525.

(53) Zhang, Y.; Zou, J.; Yip, H.-L.; Sun, Y.; Davies, J.A.; Chen, K.-S.; Acton, O.; Jen, A.K.Y. *Journal of Materials Chemistry*, **2011**, 21(11), 3895-3902.

(54) Zhan, X.; Tan, Z.a.; Zhou, E.; Li, Y.; Misra, R.; Grant, A.; Domercq, B.; Zhang, X.-H.; An, Z.; Zhang, X.; Barlow, S.; Kippelen, B.; Marder, S.R. *Journal of Materials Chemistry*, **2009**, 19(32), 5794-5803.

(55) Ogawa, K.; Rasmussen, S.C. *Macromolecules*, **2006**, 39(5), 1771-1778.

(56) Liu, J.; Zhang, R.; Osaka, I.; Mishra, S.; Javier, A.E.; Smilgies, D.-M.; Kowalewski, T.; McCullough, R.D. *Advanced Functional Materials*, **2009**, 19(21), 3427-3434.

(57) Ohshita, J.; Kai, H.; Sumida, T.; Kunai, A.; Adachi, A.; Sakamaki, K.; Okita, K. *Journal of Organometallic Chemistry*, **2002**, 642(1-2), 137-142.

(58) Ohshita, J.; Sumida, T.; Kunai, A.; Adachi, A.; Sakamaki, K.; Okita, K. *Macromolecules*, **2000**, 33(23), 8890-8893.

(59) Beaujuge, P.M.; Pisula, W.; Tsao, H.N.; Ellinger, S.; Müllen, K.; Reynolds, J.R. *Journal of the American Chemical Society*, **2009**, 131(22), 7514-7515.

(60) Lu, G.; Usta, H.; Risko, C.; Wang, L.; Facchetti, A.; Ratner, M.A.; Marks, T.J. *Journal of the American Chemical Society*, **2008**, 130(24), 7670-7685.

(61) Tamao, K.; Uchida, M.; Izumizawa, T.; Furukawa, K.; Yamaguchi, S. *Journal of the American Chemical Society*, **1996**, 118(47), 11974-11975.

(62) Chen, J.; Cao, Y. *Macromolecular Rapid Communications*, **2007**, 28(17), 1714-1742.

(63) Ohshita, J.; Nodono, M.; Kai, H.; Watanabe, T.; Kunai, A.; Komaguchi, K.; Shiotani, M.; Adachi, A.; Okita, K.; Harima, Y.; Yamashita, K.; Ishikawa, M. *Organometallics*, **1999**, 18(8), 1453-1459.

(64) Ohshita, J. *Macromolecular Chemistry and Physics*, **2009**, 210(17), 1360-1370.

(65) Chen, J.; Cao, Y. *Silole-Containing Conjugated Polymers*, in *Design and Synthesis of Conjugated Polymers*; Wiley-VCH Verlag GmbH & Co. KGaA: **2010**. p. 247-285.

- (66) Chu, T.-Y.; Lu, J.; Beaupré, S.; Zhang, Y.; Pouliot, J.-R.m.; Wakim, S.; Zhou, J.; Leclerc, M.; Li, Z.; Ding, J.; Tao, Y. *Journal of the American Chemical Society*, **2011**, *133*(12), 4250-4253.
- (67) Amb, C.M.; Chen, S.; Graham, K.R.; Subbiah, J.; Small, C.E.; So, F.; Reynolds, J.R. *Journal of the American Chemical Society*, **2011**, *133*(26), 10062-10065.
- (68) Huo, L.; Hou, J.; Chen, H.-Y.; Zhang, S.; Jiang, Y.; Chen, T.L.; Yang, Y. *Macromolecules*, **2009**, *42*(17), 6564-6571.
- (69) Hong, Y.-R.; Wong, H.-K.; Moh, L.C.H.; Tan, H.-S.; Chen, Z.-K. *Chemical Communications*, **2011**, *47*(17), 4920-4922.
- (70) Coffin, R.C.; Peet, J.; Rogers, J.; Bazan, G.C. *Nat Chem*, **2009**, *1*(8), 657-661.
- (71) Hou, J.; Chen, H.-Y.; Zhang, S.; Li, G.; Yang, Y. *Journal of the American Chemical Society*, **2008**, *130*(48), 16144-16145.
- (72) Chen, H.-Y.; Hou, J.; Hayden, A.E.; Yang, H.; Houk, K.N.; Yang, Y. *Advanced Materials*, **2010**, *22*(3), 371-375.
- (73) Koeckelberghs, G.; De Cremer, L.; Vanormelingen, W.; Dehaen, W.; Verbiest, T.; Persoons, A.; Samyn, C. *Tetrahedron*, **2005**, *61*(3), 687-691.
- (74) Evenson, S.J.; Mumm, M.J.; Pokhodnya, K.I.; Rasmussen, S.C. *Macromolecules*, **2011**, *44*(4), 835-841.
- (75) Usta, H.; Lu, G.; Facchetti, A.; Marks, T.J. *J. Am. Chem. Soc.*, **2006**, *128*(28), 9034-9035.
- (76) Ohshita, J.; Nodono, M.; Watanabe, T.; Ueno, Y.; Kunai, A.; Harima, Y.; Yamashita, K.; Ishikawa, M. *Journal of Organometallic Chemistry*, **1998**, *553*(1-2), 487-491.
- (77) Liao, L.; Dai, L.; Smith, A.; Durstock, M.; Lu, J.; Ding, J.; Tao, Y. *Macromolecules*, **2007**, *40*(26), 9406-9412.
- (78) Huo, L.; Chen, H.-Y.; Hou, J.; Chen, T.L.; Yang, Y. *Chemical Communications*, **2009**(37), 5570-5572.
- (79) Carsten, B.; He, F.; Son, H.J.; Xu, T.; Yu, L. *Chemical Reviews*, **2011**, *111*(3), 1493-1528.

- (80) Atkins, P.; Paula, J.D. *Physical Chemistry* W H Freeman & Co: **2006** p.
- (81) Jenekhe, S.A.; Osaheni, J.A. *Science*, **1994**, 265(5173), 765-768.
- (82) Lim, E.; Jung, B.-J.; Lee, J.; Shim, H.-K.; Lee, J.-I.; Yang, Y.S.; Do, L.-M. *Macromolecules*, **2005**, 38(10), 4531-4535.
- (83) Kawana, S.; Durrell, M.; Lu, J.; Macdonald, J.E.; Grell, M.; Bradley, D.D.C.; Jukes, P.C.; Jones, R.A.L.; Bennett, S.L. *Polymer*, **2002**, 43(6), 1907-1913.
- (84) Cardona, C.M.; Li, W.; Kaifer, A.E.; Stockdale, D.; Bazan, G.C. *Advanced Materials*, **2011**, 23(20), 2367-2371.
- (85) Wienk, M.M.; Kroon, J.M.; Verhees, W.J.H.; Knol, J.; Hummelen, J.C.; van Hal, P.A.; Janssen, R.A.J. *Angewandte Chemie International Edition*, **2003**, 42(29), 3371-3375.
- (86) Zhou, H.; Yang, L.; Xiao, S.; Liu, S.; You, W. *Macromolecules*, **2009**, 43(2), 811-820.
- (87) Lee, S.K.; Cho, S.; Tong, M.; Hwa Seo, J.; Heeger, A.J. *Journal of Polymer Science Part A: Polymer Chemistry*, **2011**, 49(8), 1821-1829.
- (88) Szarko, J.M.; Guo, J.; Liang, Y.; Lee, B.; Rolczynski, B.S.; Strzalka, J.; Xu, T.; Loser, S.; Marks, T.J.; Yu, L.; Chen, L.X. *Advanced Materials*, **2010**, 22(48), 5468-5472.
- (89) Tashiro, K.; Yoshino, J.; Kitagawa, T.; Murase, H.; Yabuki, K. *Macromolecules*, **1998**, 31(16), 5430-5440.
- (90) Khor, E.; Ng, S.C.; Li, H.C.; Chai, S. *Heterocycles*, **1991**, 32(9), 1805-1812.

7.8 SUPPORTING INFORMATION

Figure S1. Current-Voltage Curves.

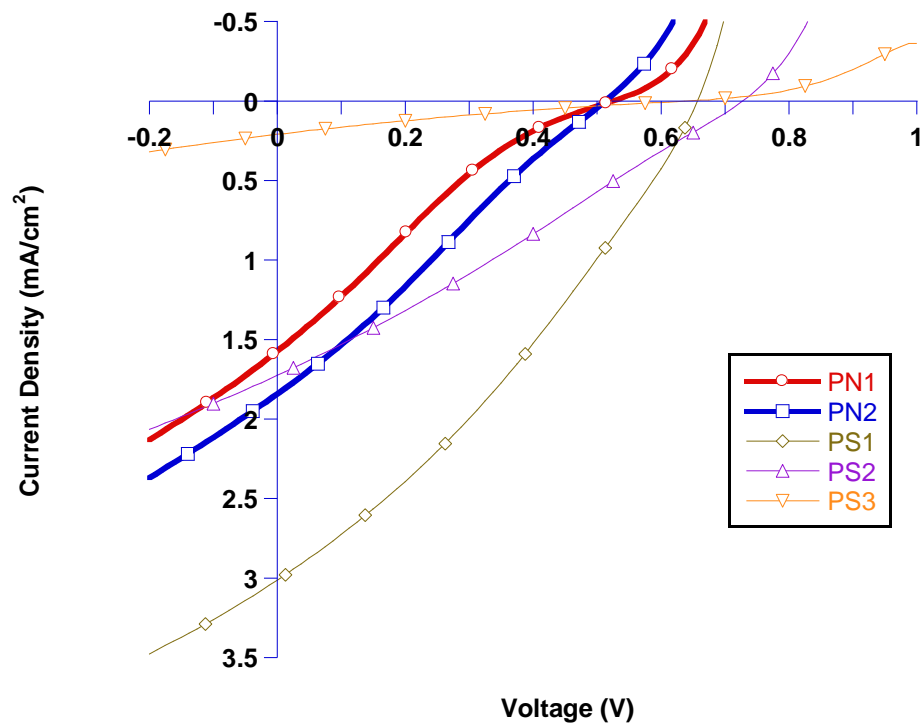


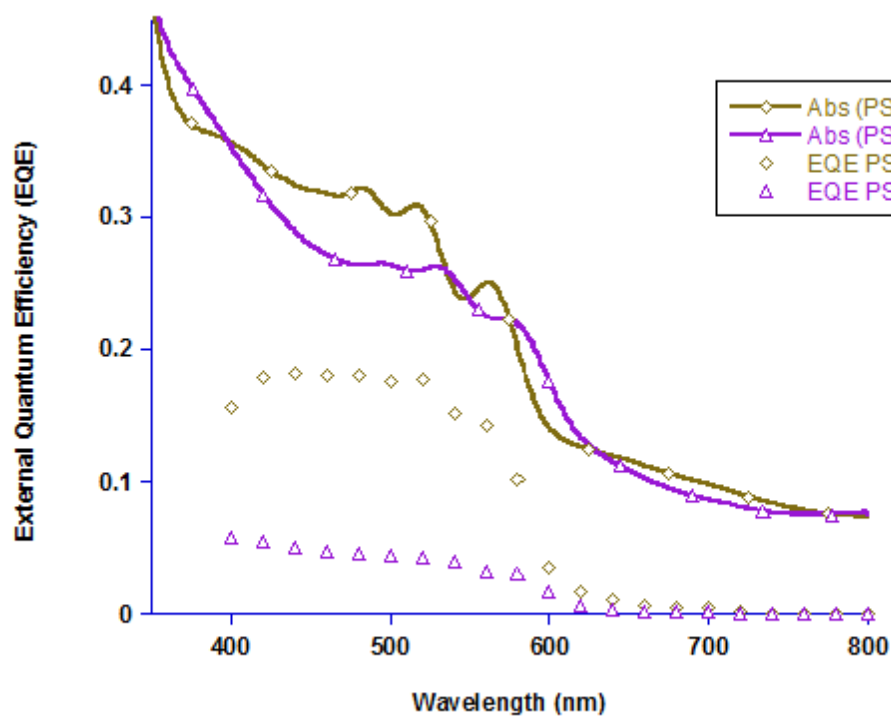
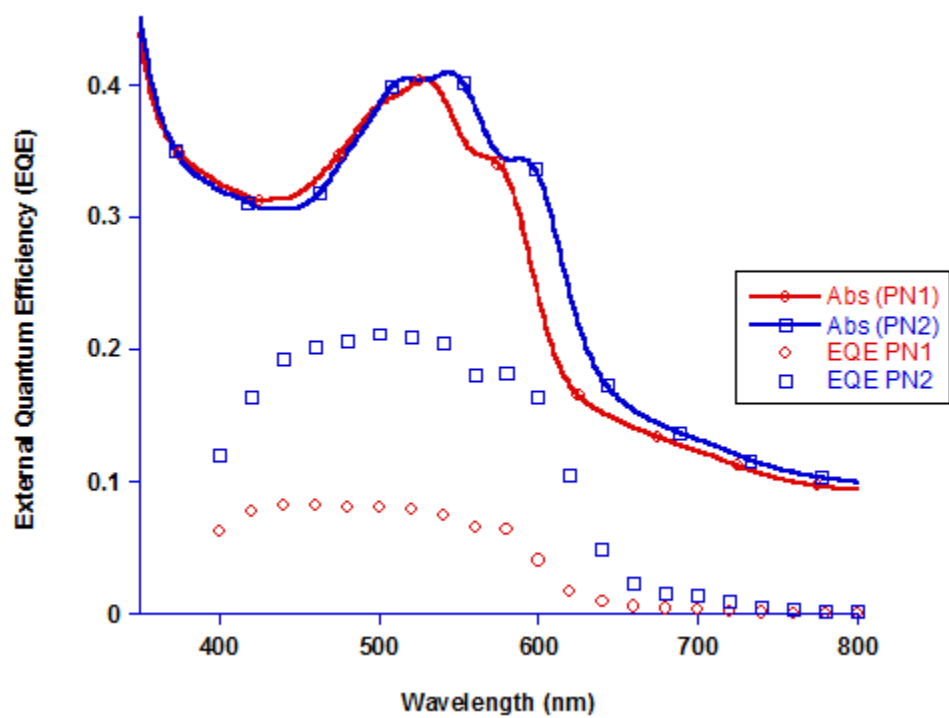
Figure S2. Absolute EQE with Absorbance Overlaid.

Figure S3. EQE was taken for both a device with no bias and a device with a -1 V applied bias. The ratio of the two devices indicates how much the extra electric field aids the separation of charges.

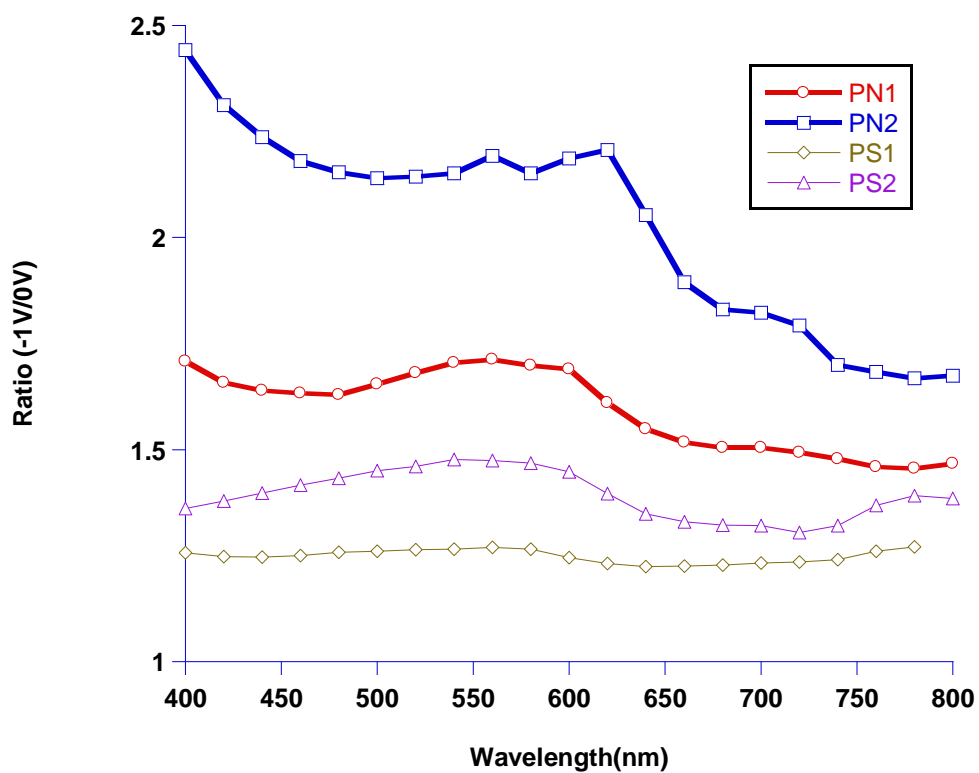


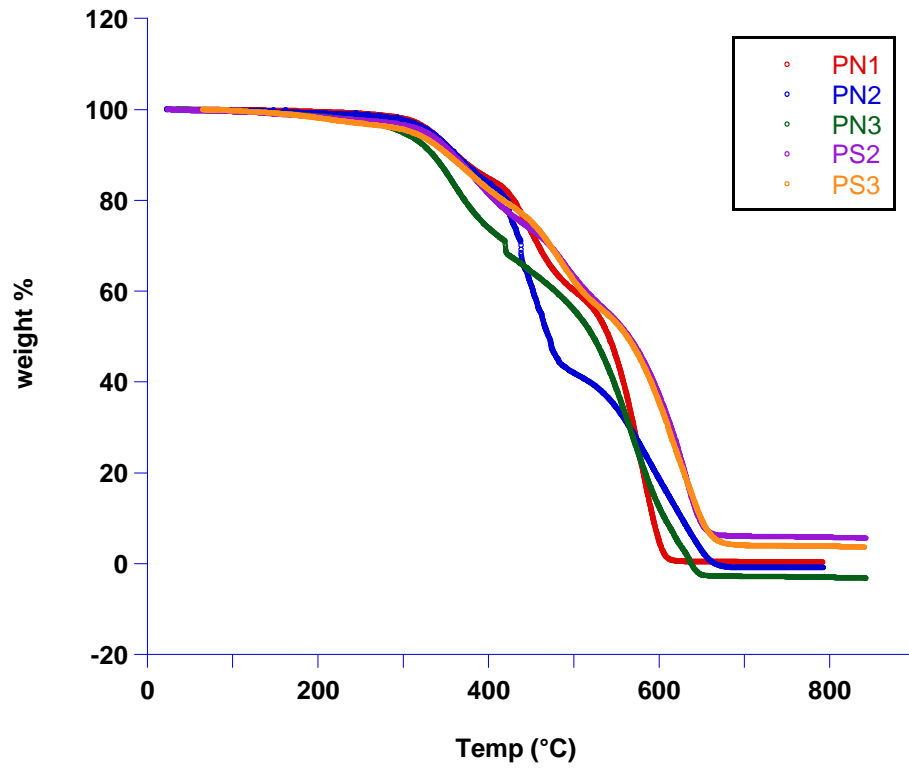
Figure S4. TGA Curves.

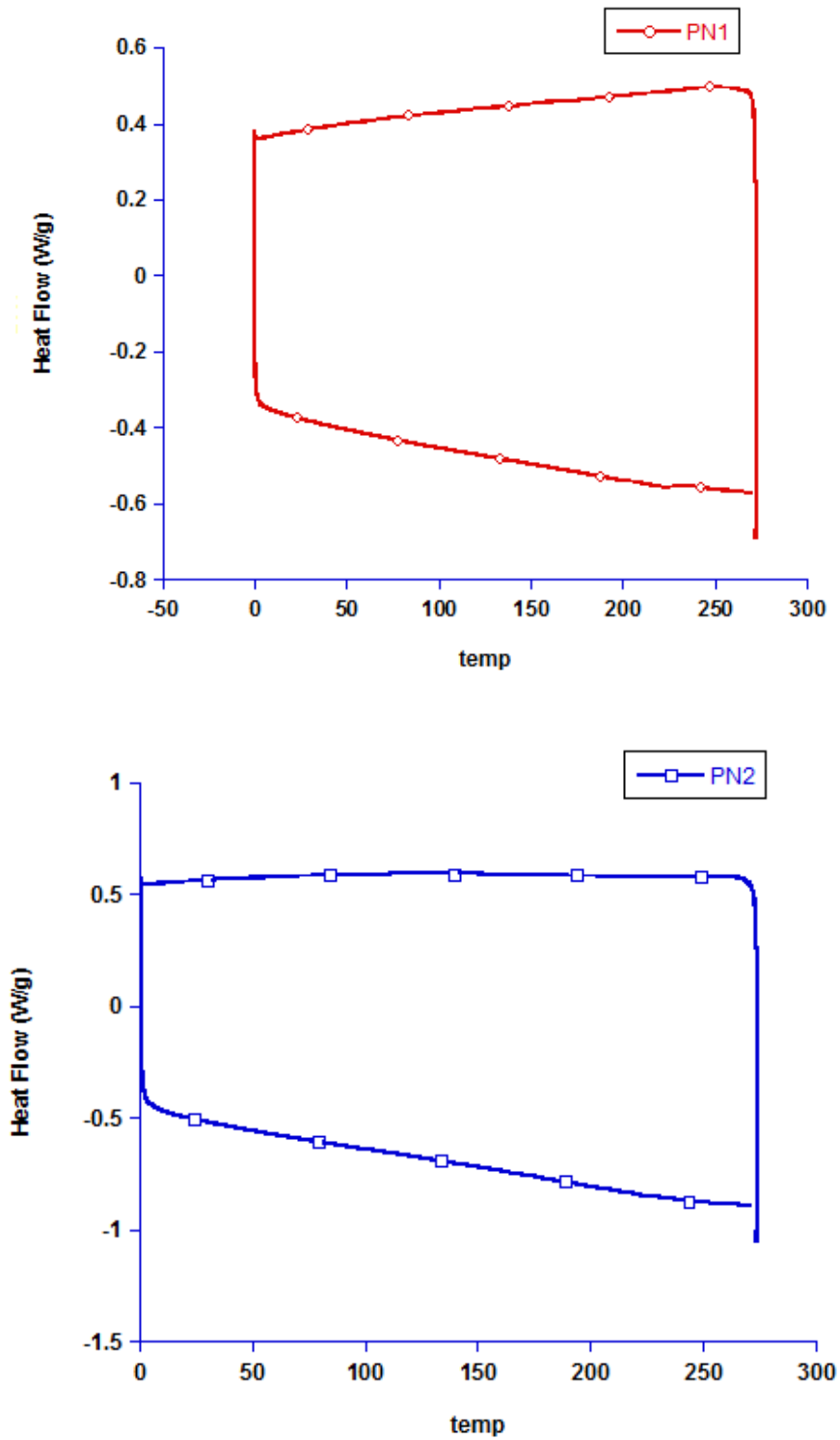
Figure S5. DSC Curves.

Figure S5 (cont.).

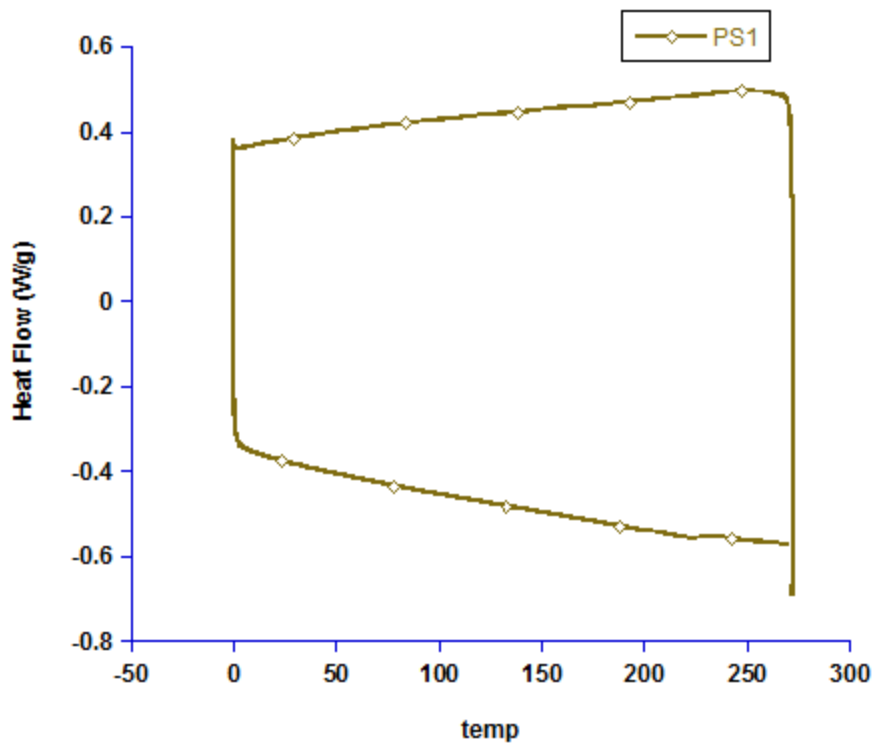
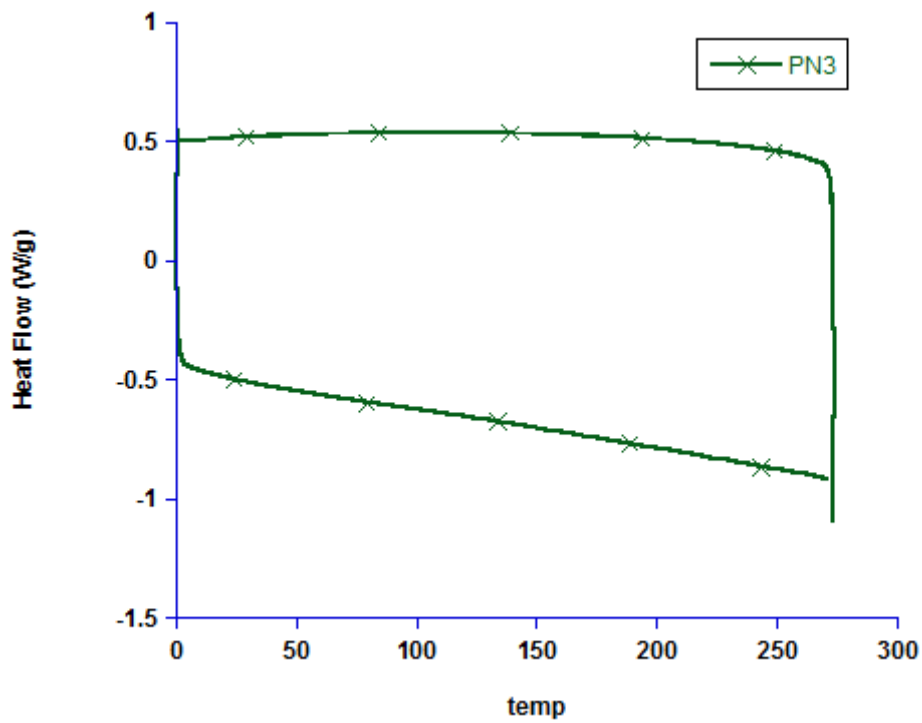


Figure S5 (cont.).

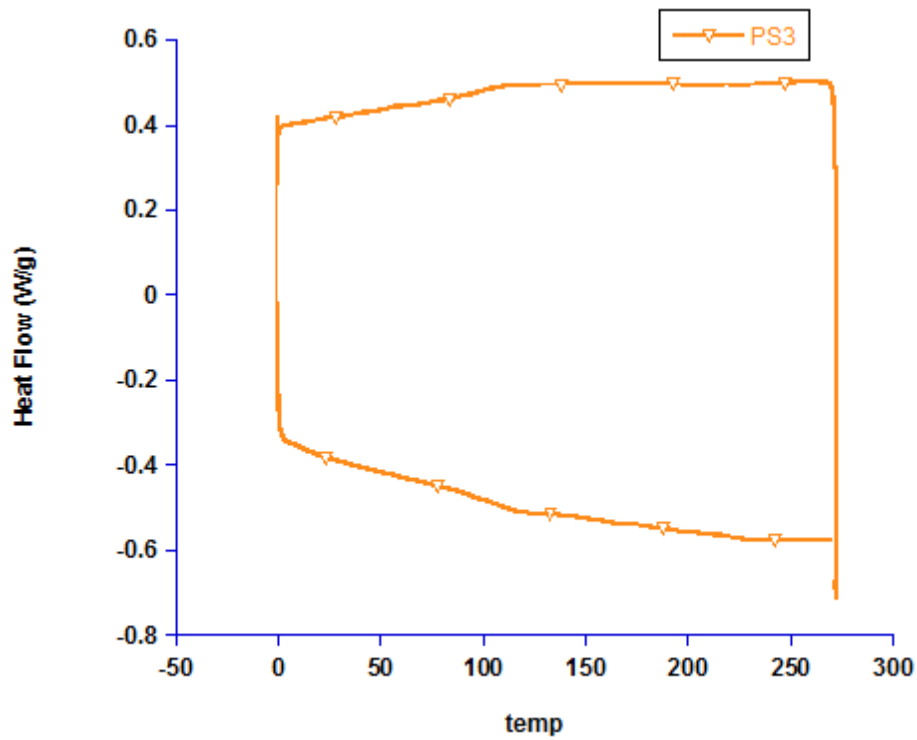
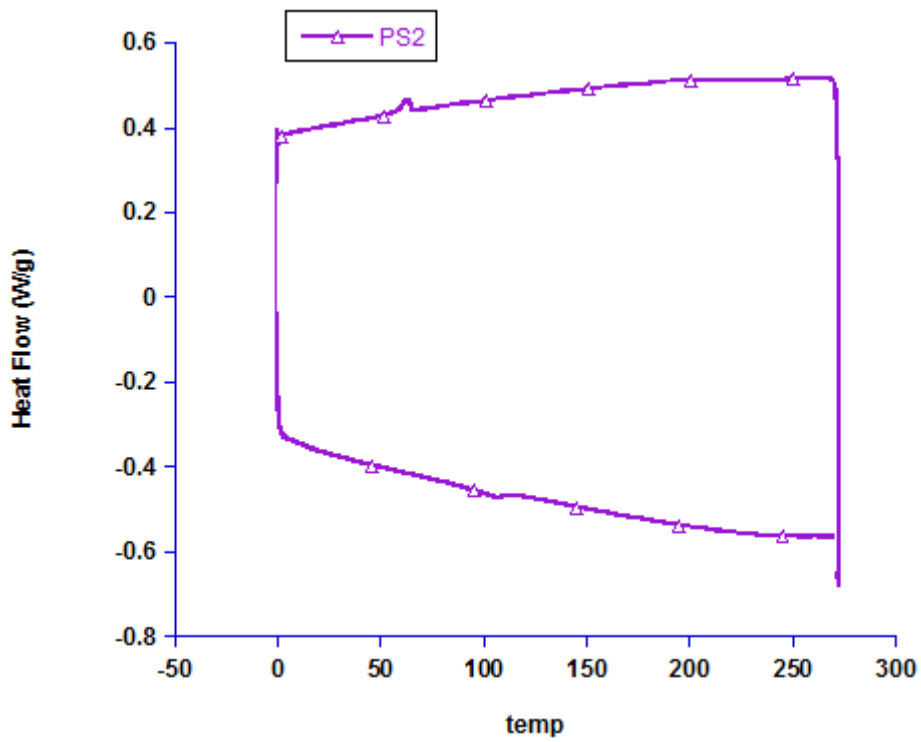
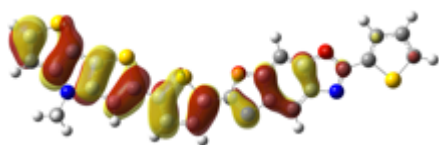


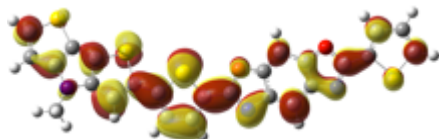
Figure S6. All of the calculations on the model oligomers were studied using the Gaussian 03W program package with the GaussView 4 GUI interface program package. Electrostatic potential maps were created using a coarse setting and an isovalue of 0.03. The calculations were performed on one repeat unit of **PN1** and **PN2**.

PN1

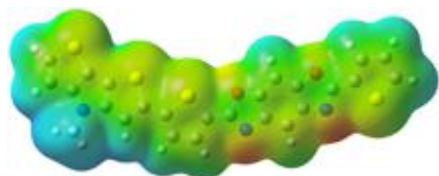
HOMO:



LUMO:



Electron Density Map:

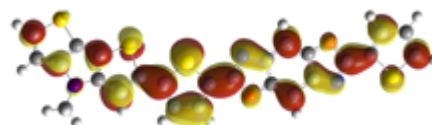


PN2

HOMO:



LUMO:



Electron Density Map:

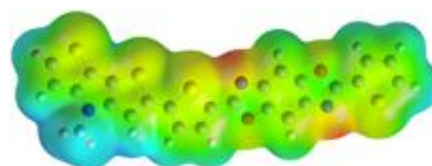


Figure S7. NMR Spectra

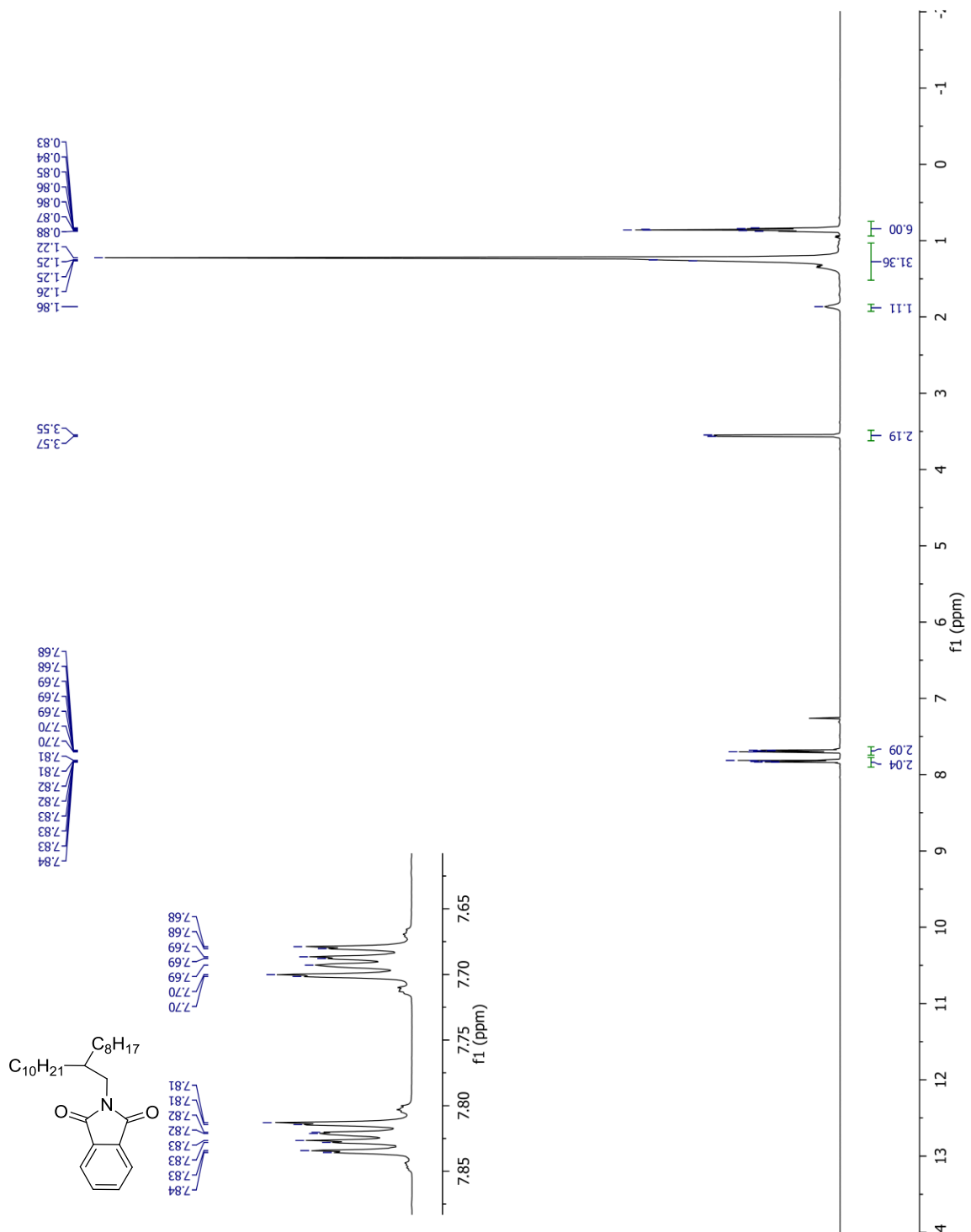


Figure S7 (cont.).

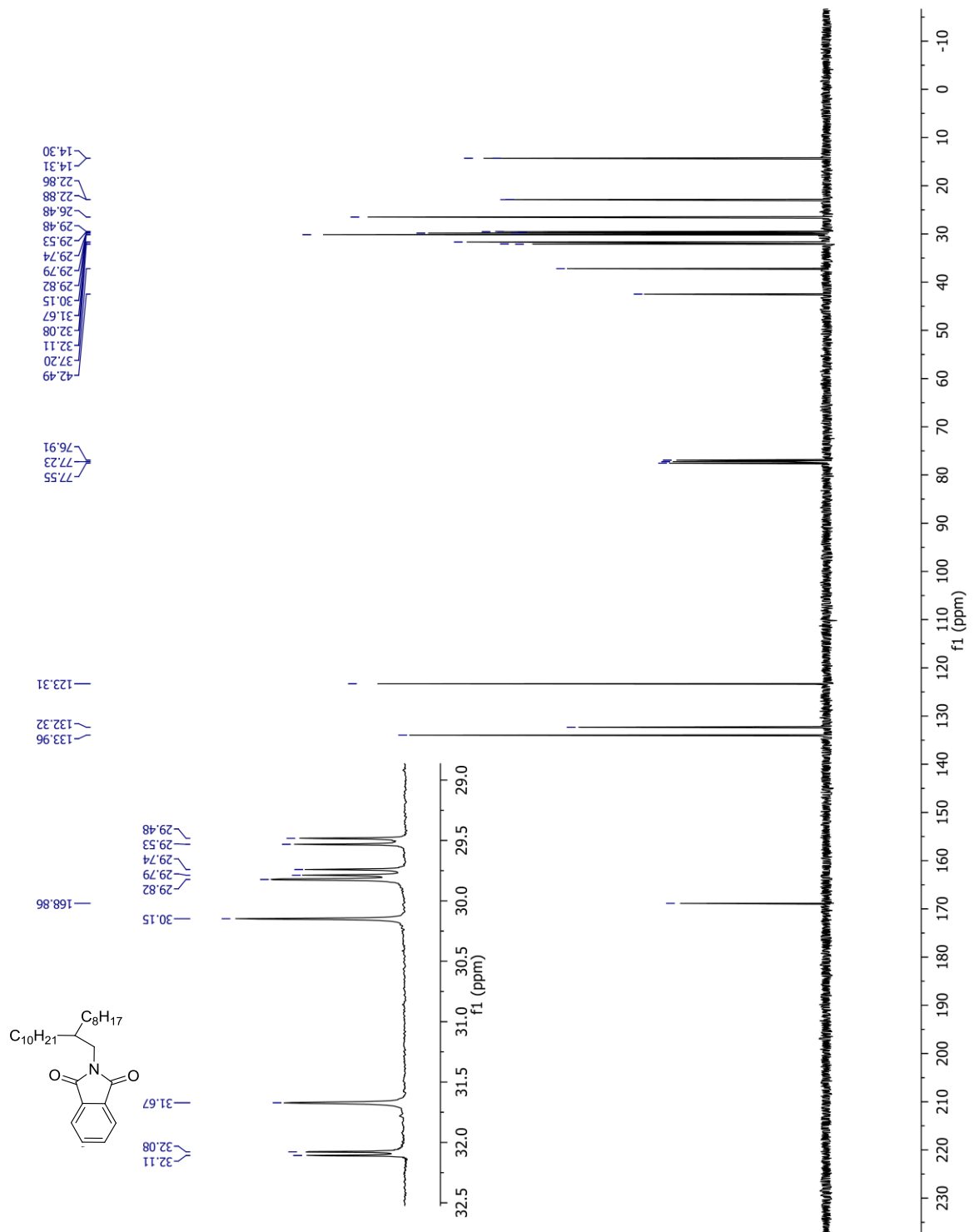


Figure S7 (cont.).

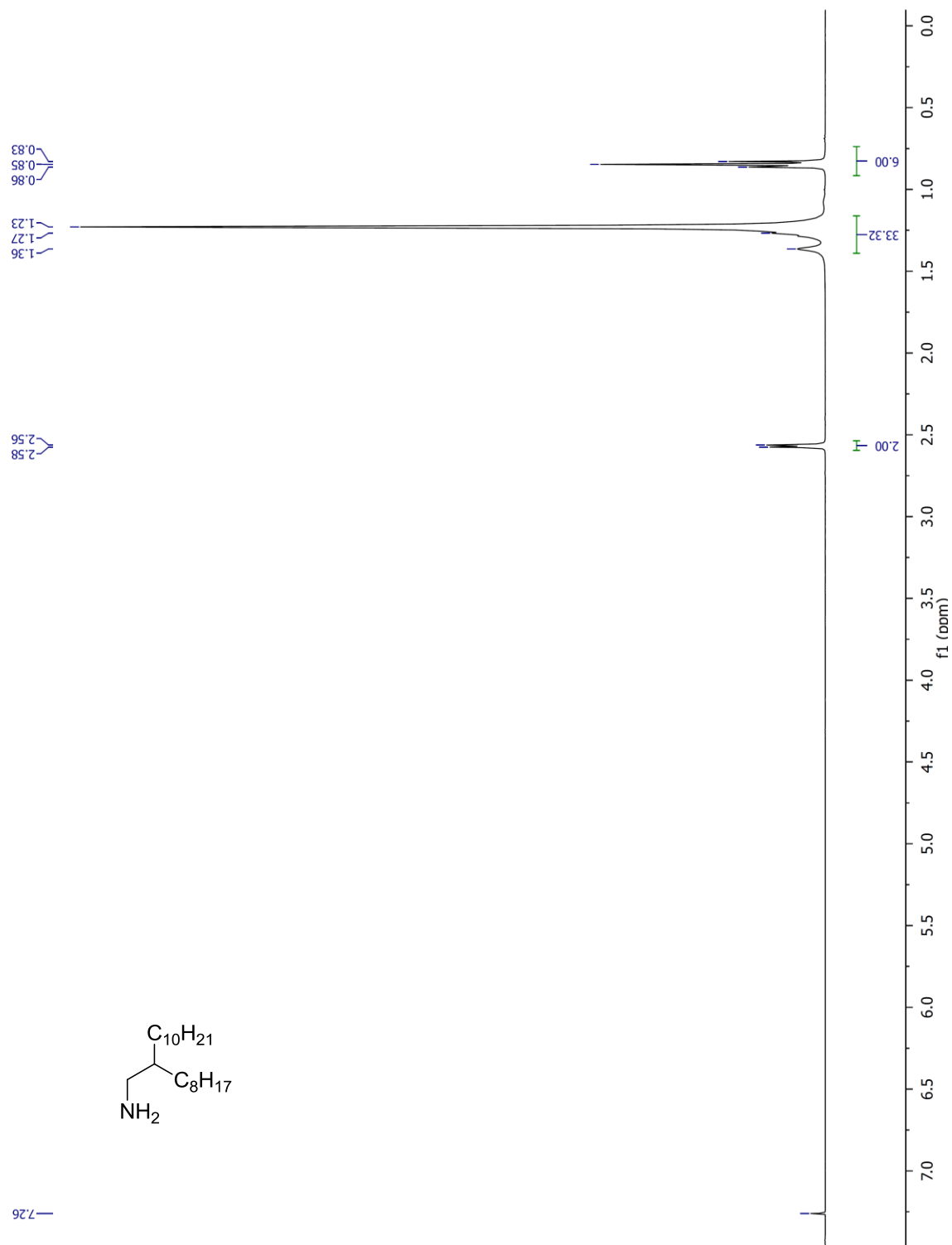


Figure S7 (cont.).

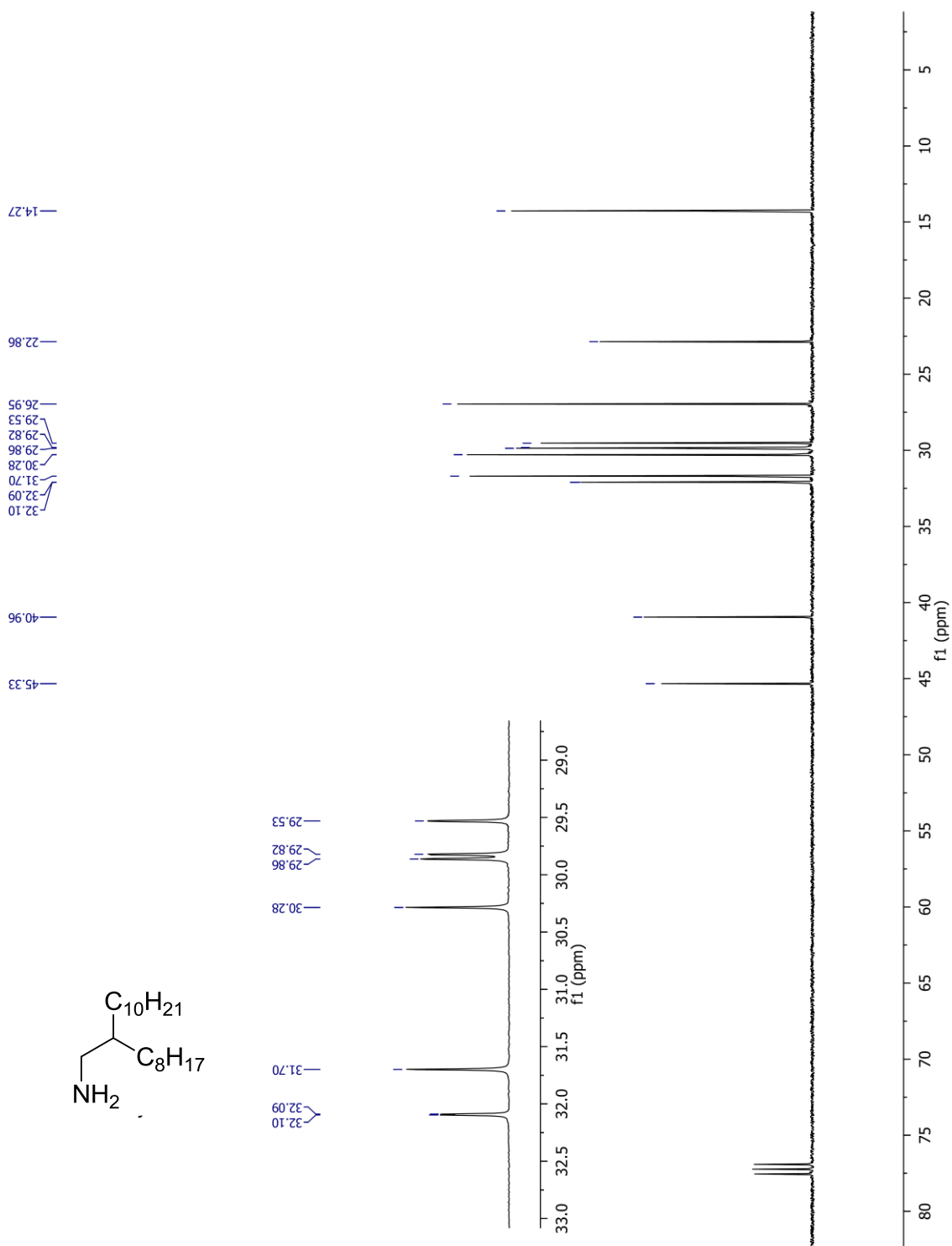


Figure S7 (cont.).

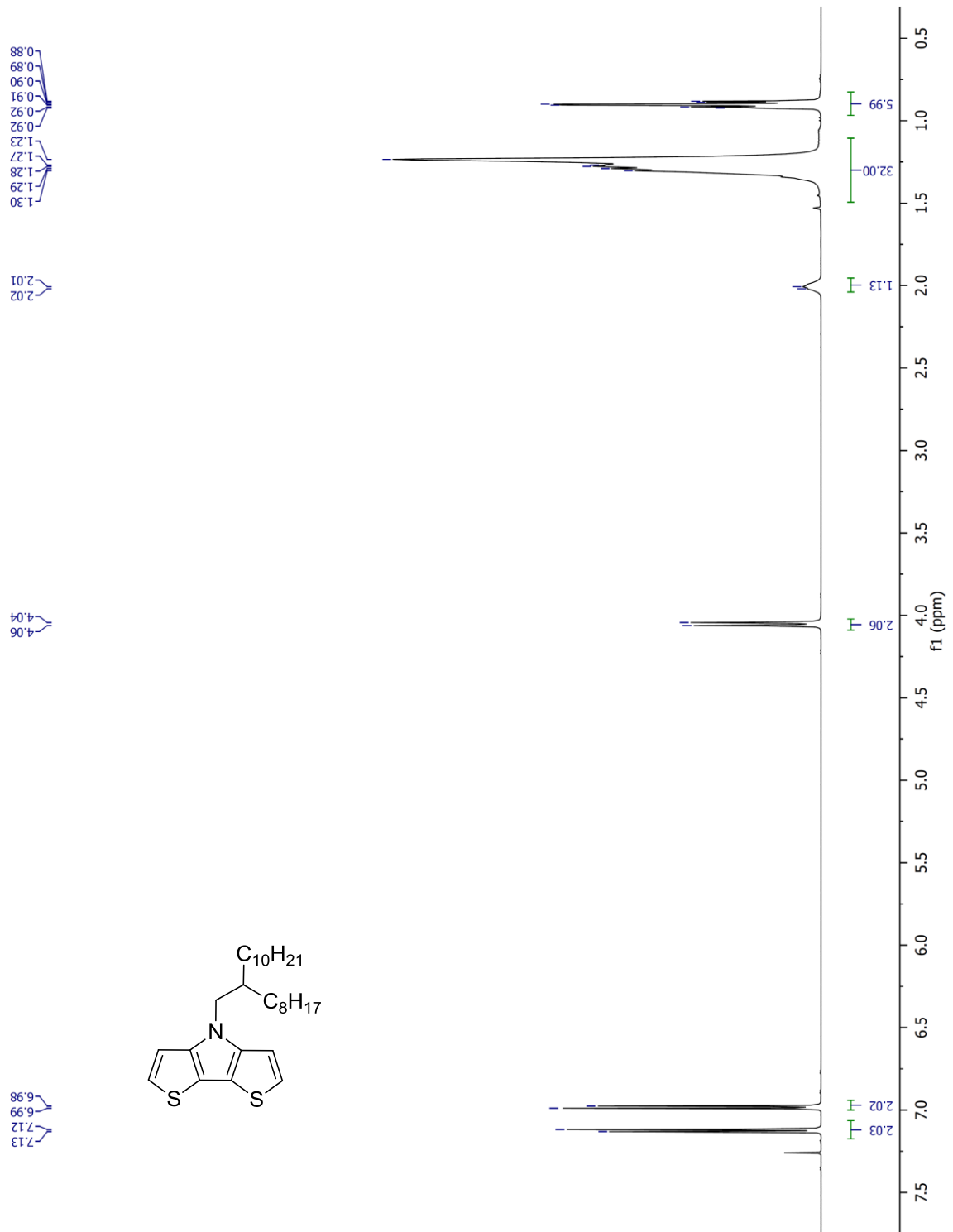


Figure S7 (cont.).

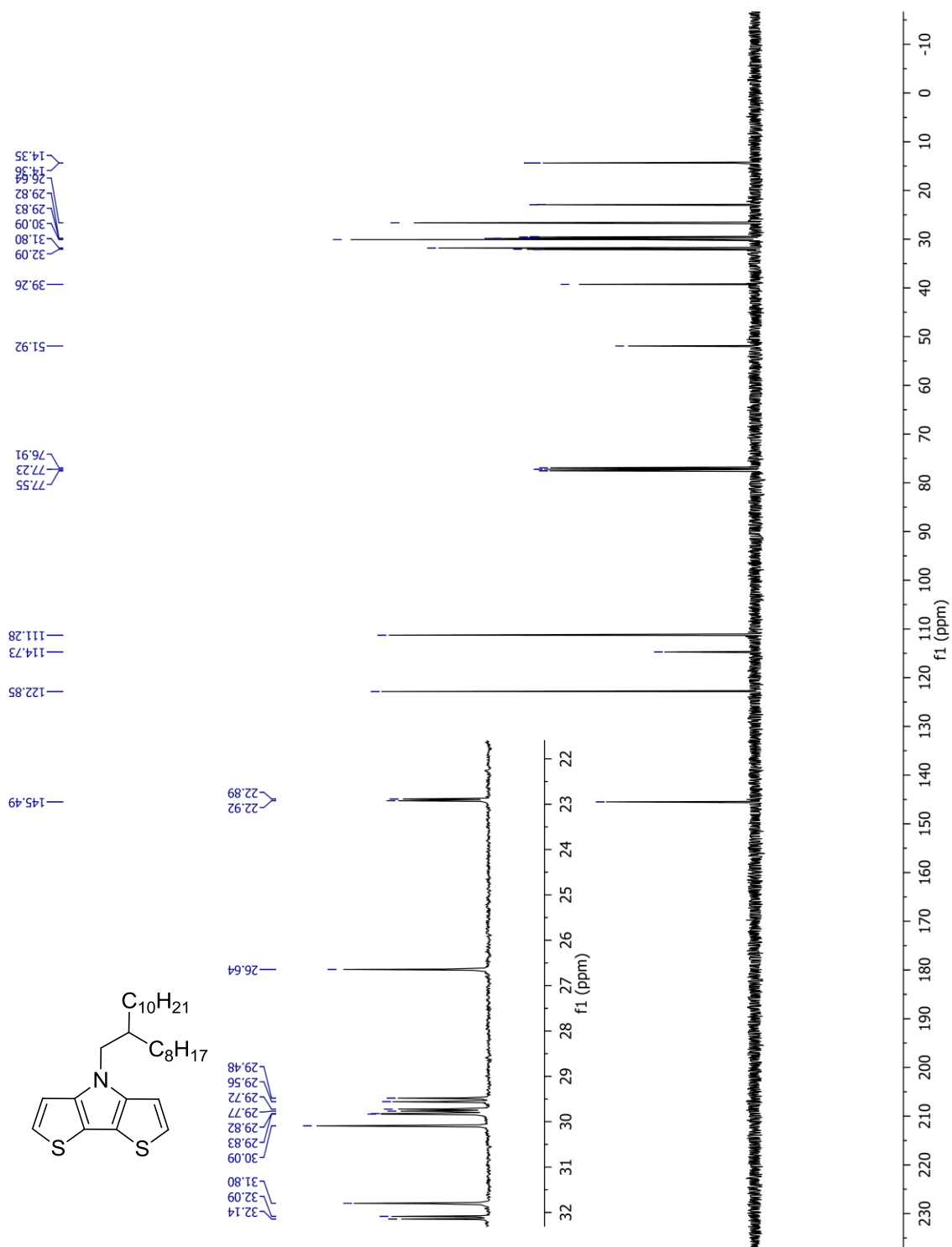


Figure S7 (cont.).

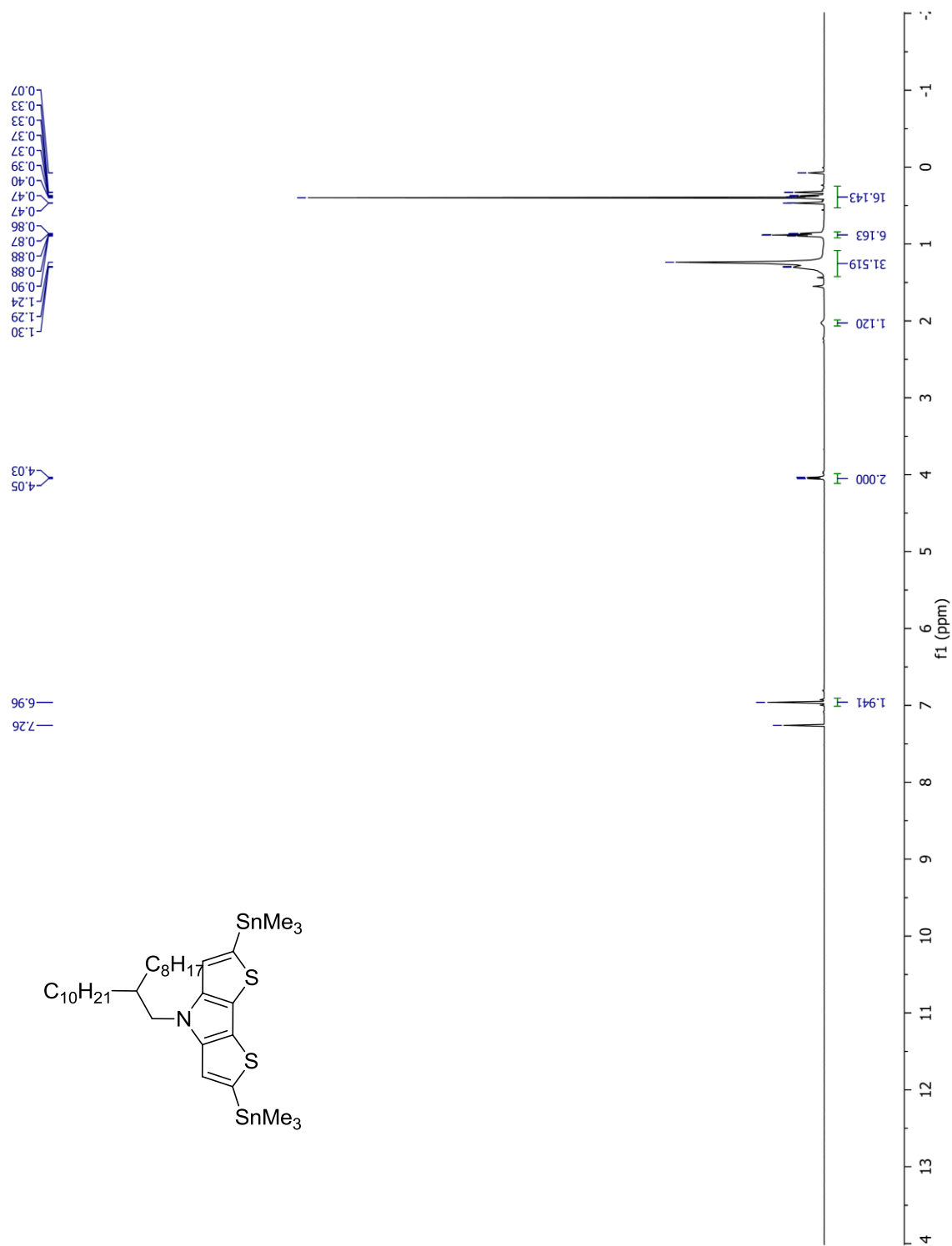


Figure S7 (cont.).

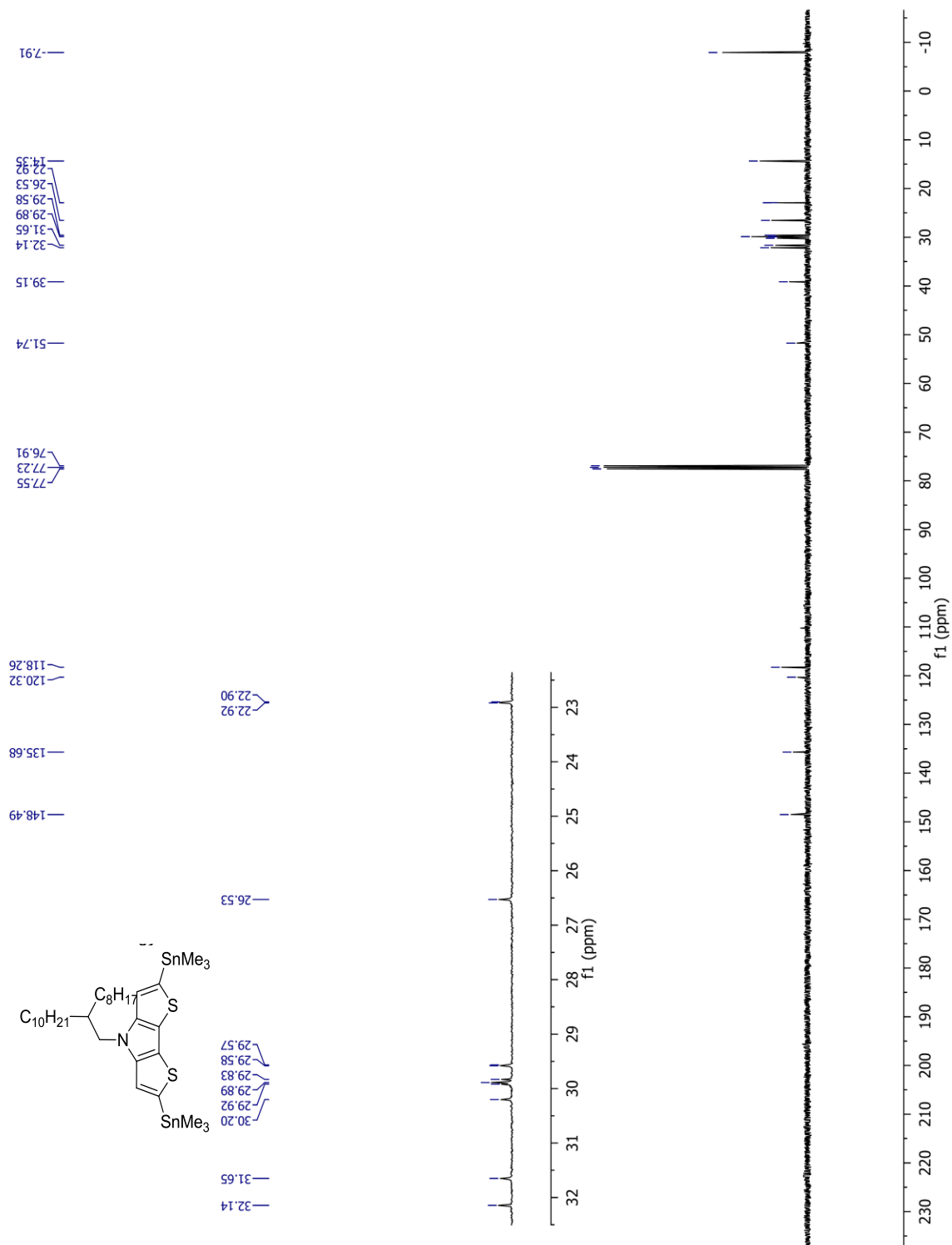


Figure S7 (cont.).

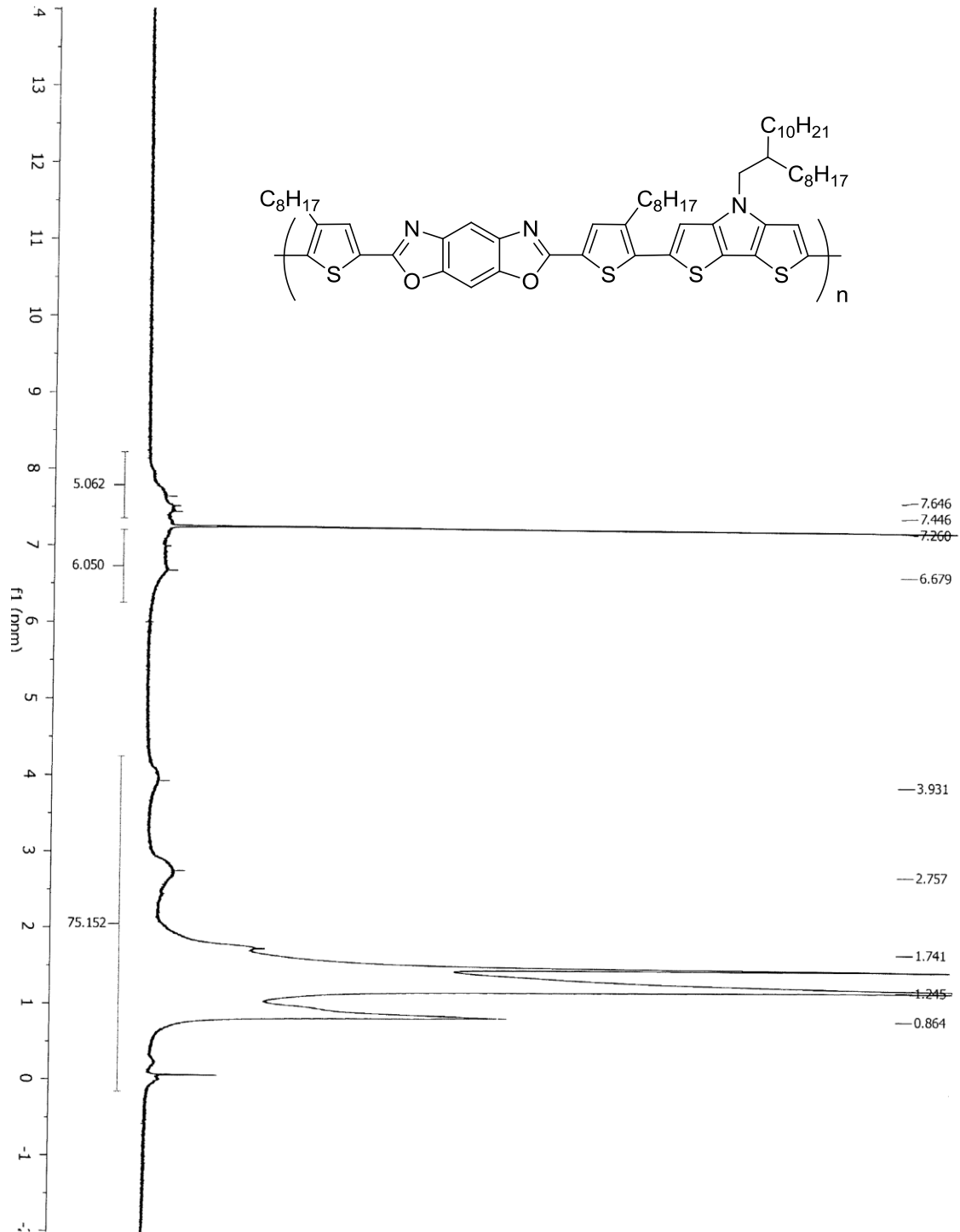


Figure S7 (cont.).

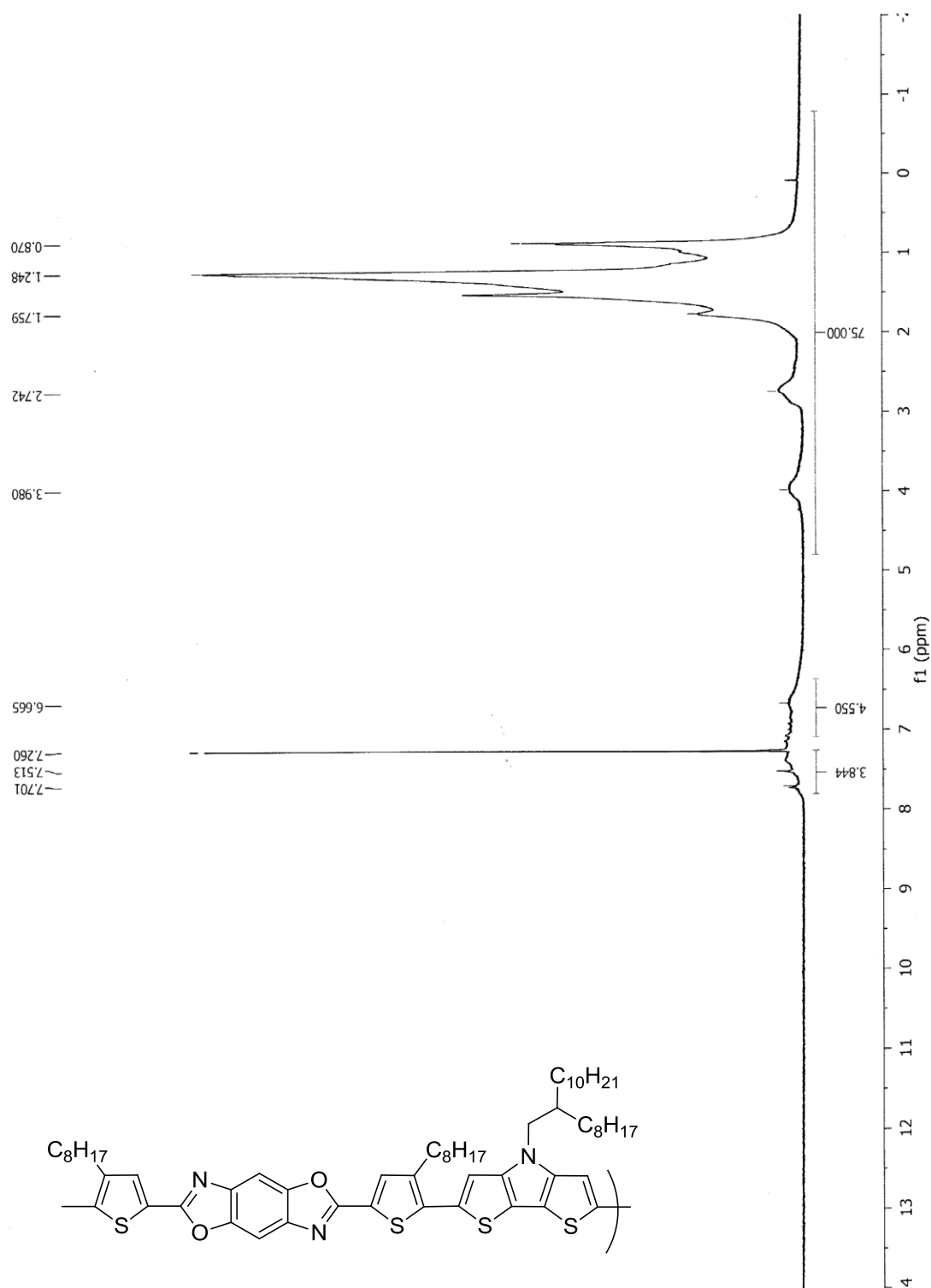


Figure S7 (cont.).

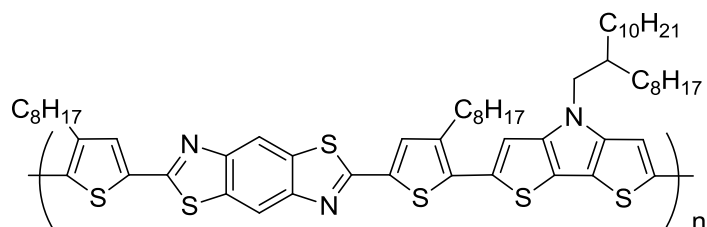


Figure S7 (cont.).

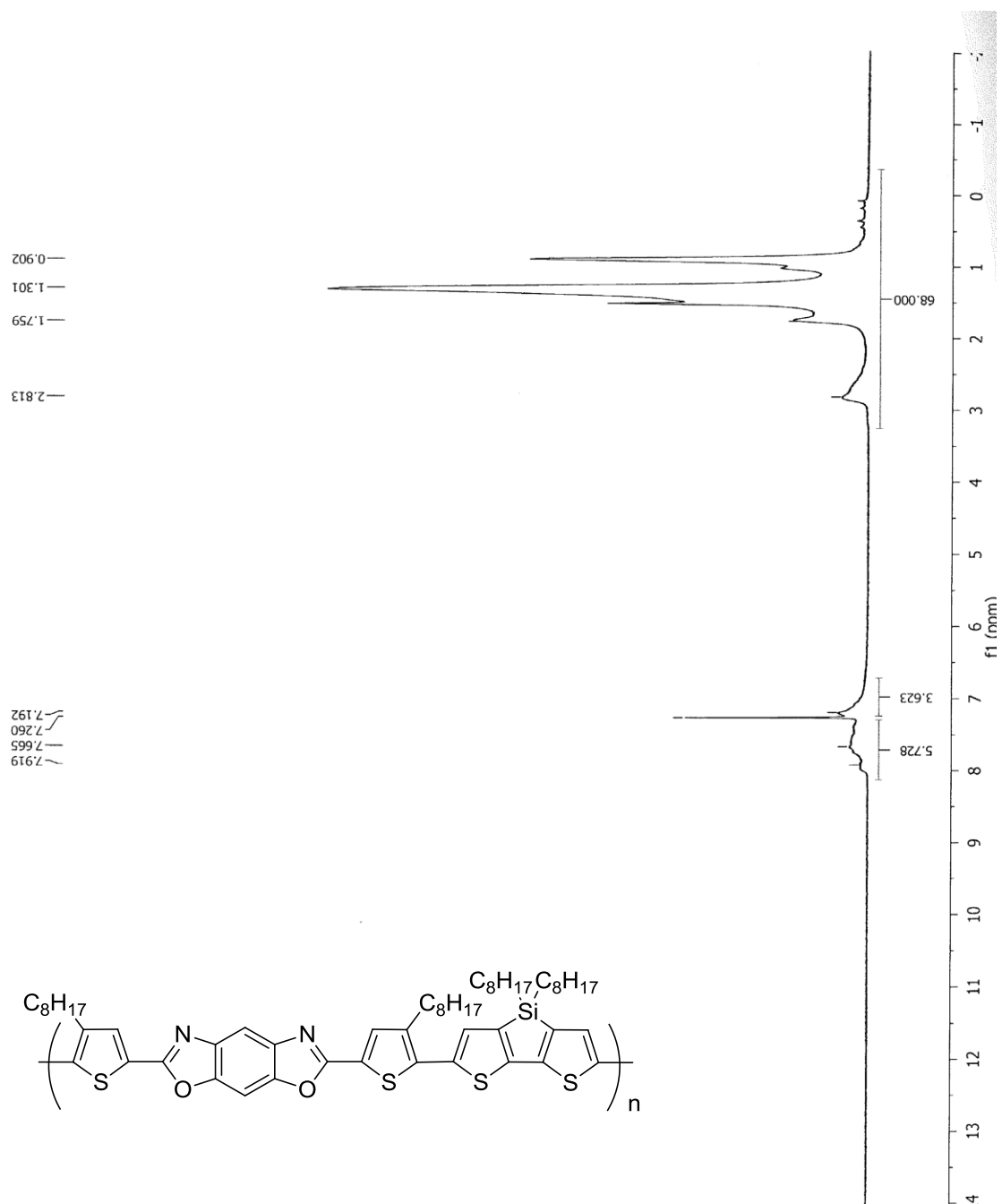


Figure S7 (cont.).

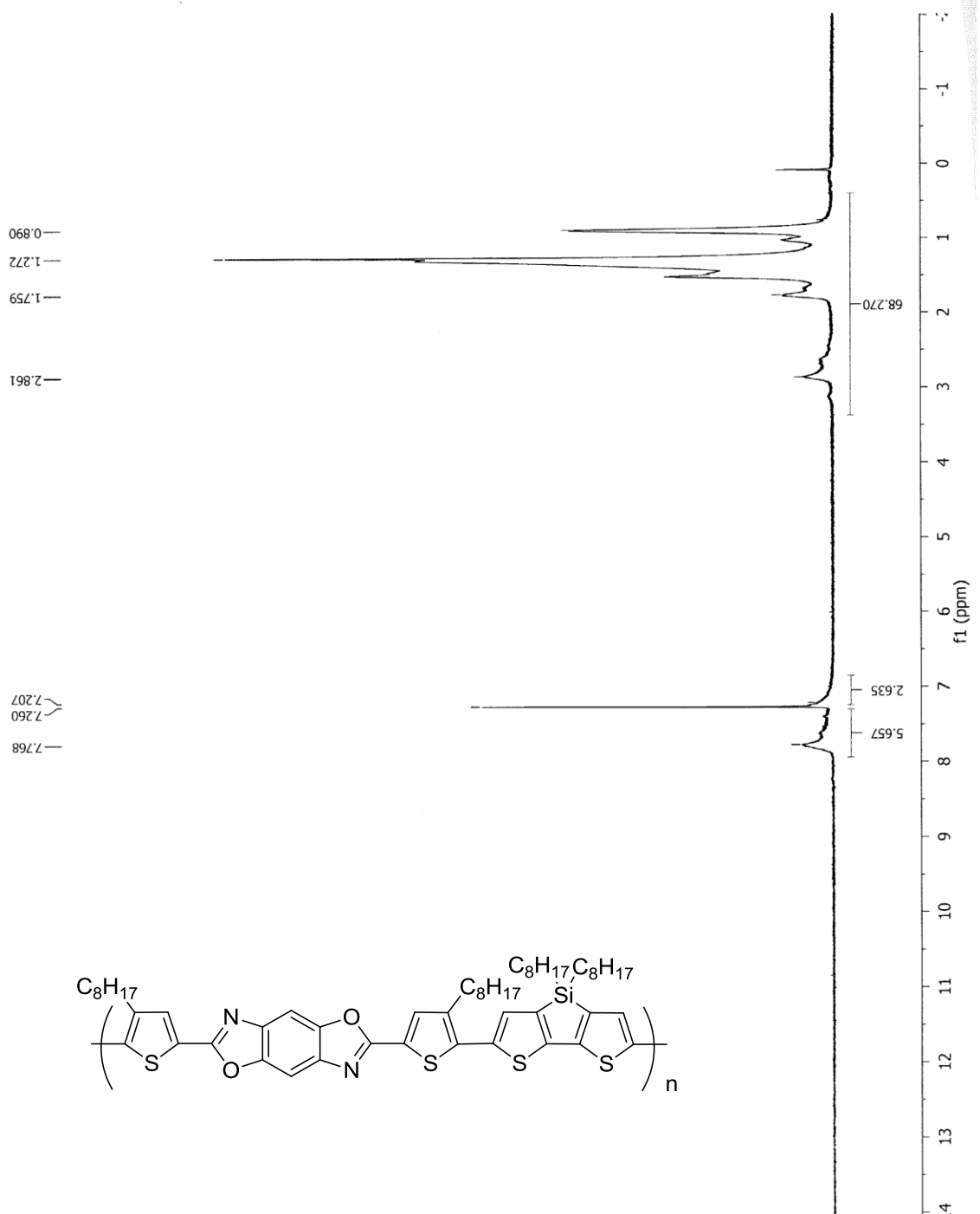
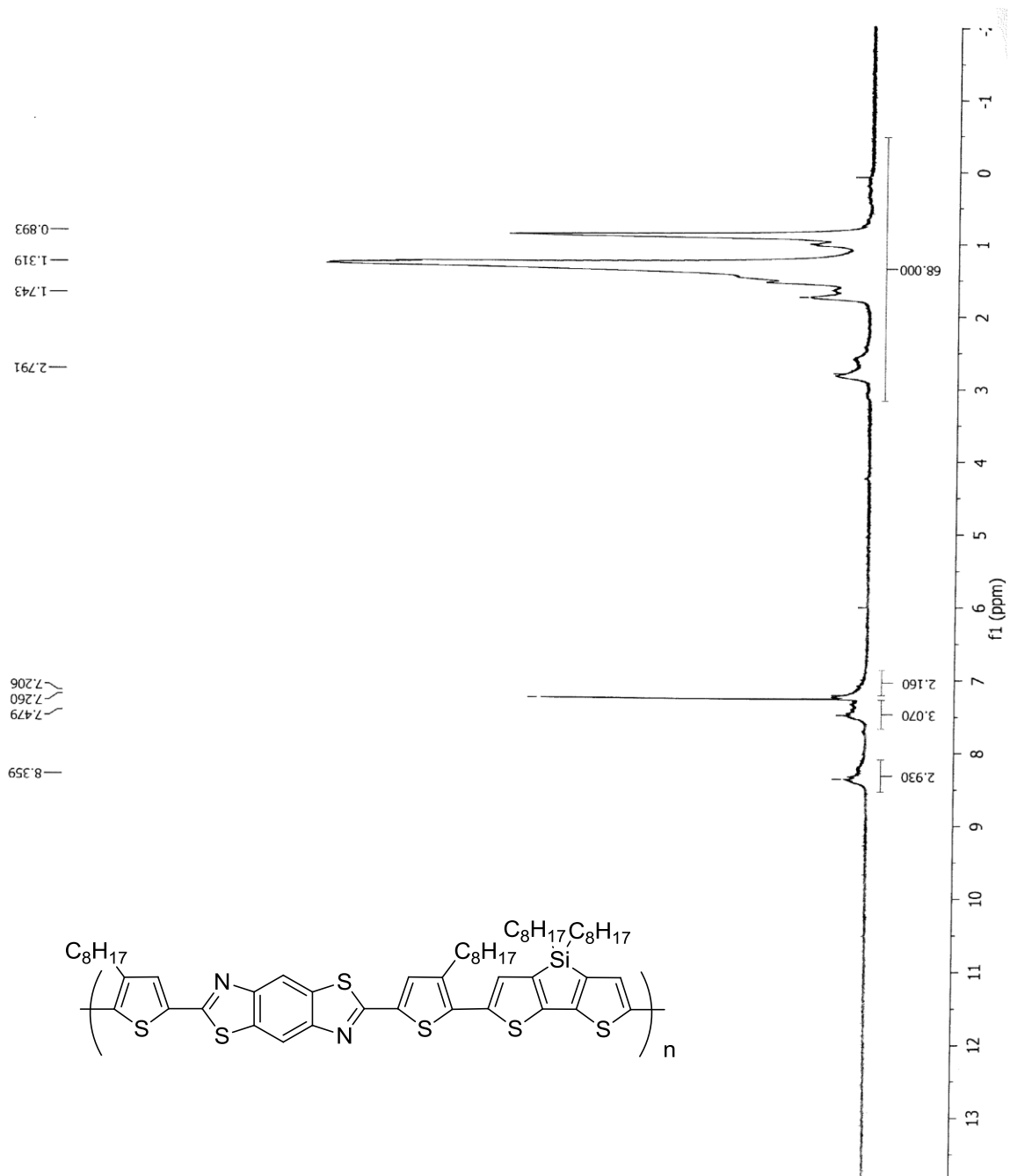


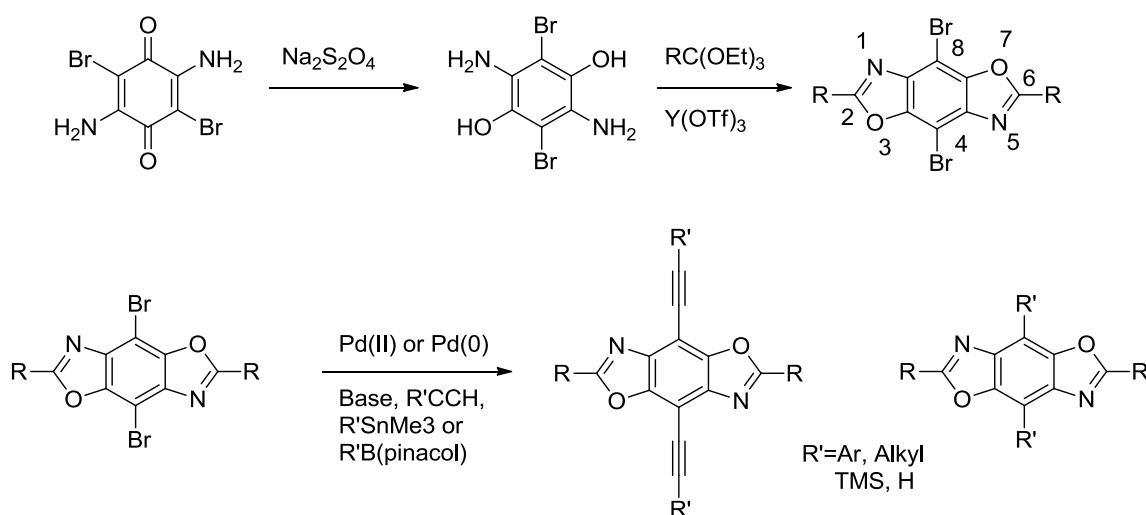
Figure S7 (cont.).



Chapter 8

General Conclusions

8.1 POSITIONAL FUNCTIONALIZATION

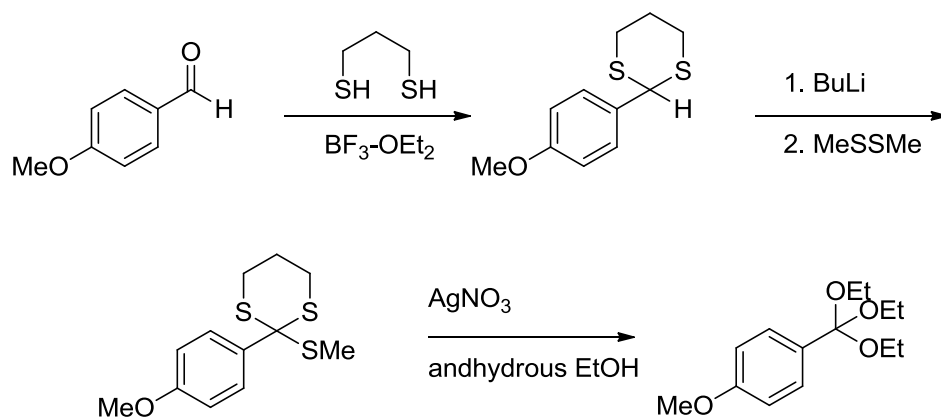


Scheme 1. Functionalization of the 4,8 positions on benzobis[1,2-*d*;4,5-*d'*]oxazole.

One of the major issues facing the synthesis of these benzobisazole polymers has been poor solubility. If alkyl chains could be added to the benzobisazole unit, then solubility and molecular weights could be improved. There is currently ongoing research in our group emphasizing functionalization of the 4,8 position of benzobis[1,2-*d*;4,5-*d'*]oxazole (Scheme 1). With bromine handles, the position has been functionalized with aryl groups and alkynyl groups using Suzuki and Sonogashira couplings. These groups can bear alkyl chains for improving solubility. The added functionality and variety of potential aryl and alkynyl groups also allows for electronic tuning. In addition to this, polymerization can be done along the 4,8-axis as opposed to the traditional 2,6-axis. This is also an excellent example of tuning electronic material properties using organic synthesis. Preliminary results are very promising and publication is forthwith.

Our other efforts to functionalize benzobisazoles focus on new orthoesters in order to

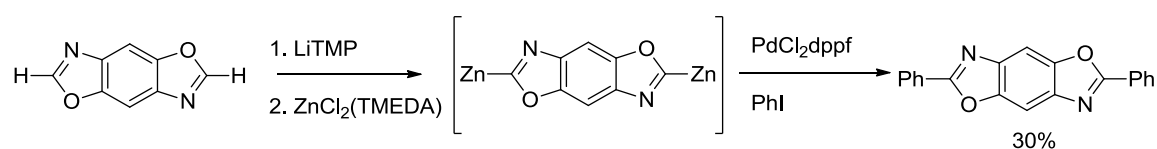
substitute at the 2,6-position beyond what has already been published. Unfortunately, the synthesis and subsequent purification of orthoesters is not a trivial matter. The primary route to functional orthoesters that we have already used in published work involves the reaction of a Grignard reagent with tetraethyl orthocarbonate. Unfortunately, producing Grignard reagents from some heterocycles works poorly or not at all, nor does this method produce pure enough product to use outright. Purification of orthoesters is difficult to perform as the orthoesters functionality is acid and moisture sensitive. Purification on an untreated silica column results in decomposition; even when the column is treated with triethylamine, some decomposition occurs. Alumina columns work, but so far produce inconsistent low to mediocre yields. The only reliable way to purify these orthoesters so far has been vacuum distillation. In this way, high yields of orthoesters have been produced. Unfortunately, the size of molecule that can be distilled even under vacuum is limited.



Scheme 2. Alternative synthesis of an orthoesters.

For this reason, new methods for orthoesters synthesis and functionalization are being developed in our labs (Scheme 2). Starting from aldehydes, 1,3-propanedithiol (or a similar dithiol) may be used to produce a cyclic dithiane. The dithiane can then be deprotonated with a lithium base and reacted with a disulfide nucleophile to produce the thioorthoester. The thioethers can then be exchanged with ethanol in a complexation reaction with collidine and silver ions to form the triethyl orthoesters. The advantages of

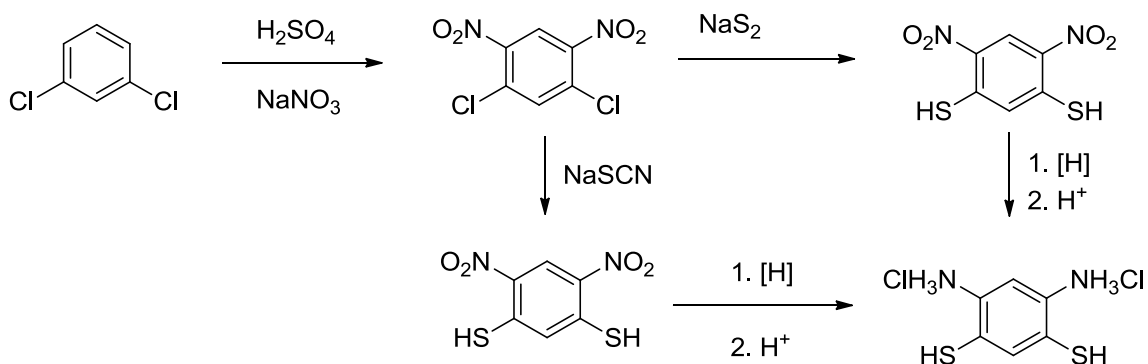
this method are the very mild conditions, allowing for synthesis of a large number of orthoesters from materials that normally don't metallate well.



Scheme 3. Zincation and cross-coupling of benzobis[1,2-*d*;4,5-*d'*]oxazole.

Another promising method of 2,6-functionalization involves direct C-H activation of the benzobisazole. Several experiments have been tried using copper and/or palladium and any number of different bases, but success has been nonexistent. However, the most promising method involves zincation of the 2,6-position using a mixture of lithium tetramethyl piperidine and zinc chloride tetramethyl ethylenediamine (Scheme 3). The metallated benzobisoxazole was then reacted with phenyl iodide using palladium in Negishi-type coupling. The 30% yield of product is low, but perhaps conditions could be improved. The advantage of this method is the lack of a need for orthoesters and the sheer number of possible metal-catalyzed cross-couplings with aryl halides, with the potential for direct polymerization as well.

8.2 SYNTHESIS OF BENZO[1,2-*D*;5,4-*D'*] BISTHIAZOLE

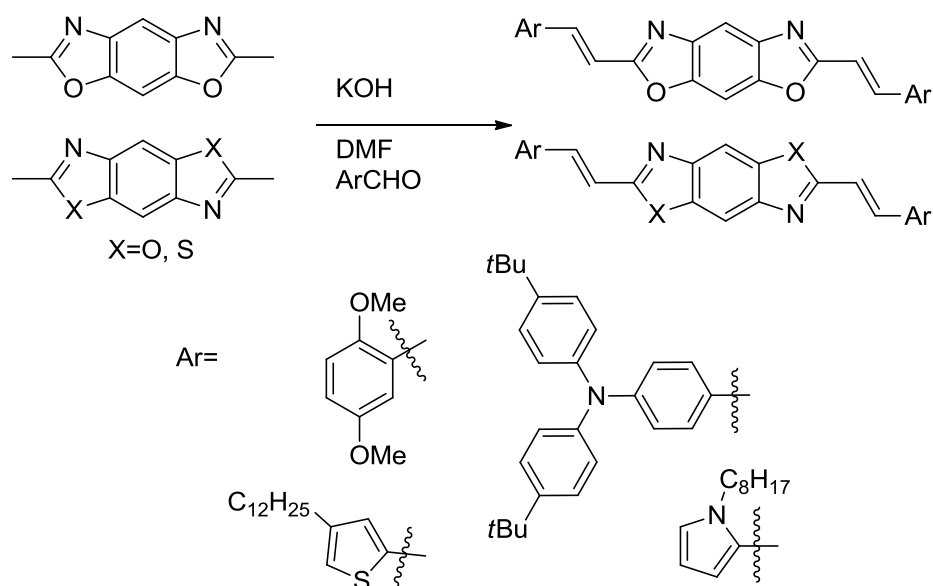


Scheme 4. Possible synthetic routes to 4,6-diamino-1,3-benzenedithiol bishydrochloride.

The unprotonated compound is most likely very unstable.

The two benzobisoxazole units, benzo[1,2-*d*;5,4-*d'*] bisoxazole and benzo[1,2-*d*;4,5-*d'*] bisoxazole are both easy to make and comparisons can be made between the two to see how positional isomerism affects the electronic properties. However, only benzo[1,2-*d*;4,5-*d'*] bisoxazole has an analogous sulfur analogue that can be synthesized currently. The sulfur analogue of benzo[1,2-*d*;5,4-*d'*] bisoxazole, benzo[1,2-*d*;5,4-*d'*] bithiazole, has posed a major challenge to synthesize. Past efforts undertaken in our labs to synthesize the diaminodithiobenzene precursor are highlighted in Scheme 4, but all have failed to produce results. Unfortunately, there are very few literature reports on this compound, they are all very old, and new synthetic routes will most likely have to be devised. The routes highlighted above are by no means exhaustive, and

8.3 SMALL MOLECULES



Scheme 5. The synthesis of various dyes using “aldol” condensation with an aldehyde.

In addition to being able to craft polymers from benzobisazoles, our group has explored the synthesis of small molecule dyes (Scheme 5). Work is currently focused on producing both simple dyes without much functionality to asymmetric dyes possessing added functionality in order to bind a metal or provide a handle for post-translational modification. The monomer units discussed in Chapters 6 and 7 are examples of small

molecule dyes. By altering the 4,8- and/or 2,6- substitution pattern on benzobisazoles, basic conclusions can be drawn about how different functionalities affect the properties of a material. These conclusions provide guidance for future molecular designs. Many dyes are also easier to fabricate and purify than conjugated polymers. Although there are no immediate plans to incorporate these dyes into devices, they are promising materials for monomers, sensors, sensitizers, and non-linear optics.

In conclusion, benzobisazoles have been proven useful synthons for incorporation into organic molecules for semiconducting applications. Red shifts in the absorbance and fluorescence spectra can be seen on going from *cis*BBO to *trans*BBO to BBZT containing polymers. The same general trend can be observed in decreasing LUMO levels for these systems. Another general trend that has been observed going from *cis*BBO to *trans*BBO to BBZT is the increase in solid state order. Benzobisazoles are weak acceptors, but their charge transport properties and stable structures make them promising for future applications. The work on these moieties, although it is backed up by three decades of research, is still in its early phases. Continued research on benzobisazoles will undoubtedly yield interesting, if not useful, results into dynamic structure-function relationships.

8.4 ACKNOWLEDGEMENT

The complicated and sometimes harrowing fabrication of this thesis has been made easier primarily through the persistence of my love, Kimberly Topp, whose efforts to watch our son and keep me sane (no easy task) through her love and companionship have filled me with gratitude. Her ability to be there with me through my worst moments and help me pull myself out of them has made me stronger for the experience. Malika Jeffries-EL, my advisor, has played no small role in keeping me motivated and inspired. I would like to thank her for keeping me positive and pushing me to do my best. I would also like to thank Sumit Chaudhary and his students for scientific discussions, collaboration, and showing me the engineering side of this research. I would like to thank the Jeffries-EL group for their continued support and fantastic sense of humor. They have managed to put up with my social deficiencies and have made coming to work a joyful experience. I would like to thank Achala Bhuwarka in particular for making me smile on the worst of days.

I would also like to thank Randy Benedict who lives just down the hall from my lab, and Robert Roggers, who lives in another building. Our occasional breaks away from work have filled me with excellent new ideas (some of which have appeared in this thesis), laughter, and wonder. I would like to thank The Doctor Jesse Waldo (and his wife, Sami Waldo) whose aptitude for organic synthesis, passion for life and ridiculous personality have aided me immensely in both my graduate career and life. I thank Drew Makowski for keeping my spirit alive, dragging me outside, and telling me the truth even if I didn't want to hear it. I would like to also thank Donald Rogness for philosophical discussion and new music, as well as the occasional journey outside and bike ride. I'll miss you all when I move.

I would also like to thank New Glarus Brewing of Wisconsin for their delicious beverage-based inspiration. Frito-Lay has also played a role through providing me with necessary sustenance, specifically hot cheese dip and Tostitos. Why I should desire to eat so much junk while writing is beyond me, but it certainly got the job done. I would also like to thank Anderson Erickson and their lovely dairy cattle because I do so enjoy the

occasional bite of cheese. Some days, all I was able to drink was milk, and so it sustained my writing efforts. I would also like to thank pig farmers everywhere for Bacon. Bacon is so delicious. The wonderful owners of Thai Kitchen deserve particular appreciation. Their food and attitudes have provided me with an indescribable quantity of sustenance and joy over the past six years,

Lastly, I would like to thank those many people I have encountered over the past six years who have helped me to grow both as a person and as a researcher. Specifically, I would like to thank Grandmaster Yong Chin Pak for teaching me Taekwondo and the philosophy of courtesy, integrity, perseverance, self-control, and indomitable spirit. I would like to thank many individuals in the chemistry department, and indeed all over Iowa State, just for being friendly. Last, but certainly not least, I would like to thank George Clinton, Les Claypool and especially Jerry Garcia for their music that has lifted my spirits in both happy and troubled times. This has been quite a journey, and I am ready to move on. These moments are so bittersweet. As my thesis comes to a close, it occurs to me, what a long, strange trip it's been. To any reading these writings: work hard, follow your dreams, and you can succeed.